PERFORMANCE OF GEOTEXTILE SEPARATORS, BUCODA TEST SITE – PHASE II

WA-RD 440.1

Final Report
July 1997

Washington State Department of Transportation

Washington State Transportation Commission
Planning and Programming Service Center
in cooperation with the U.S. Department of Transportation
Federal Highway Administration

TECHNICAL REPORT STANDARD TITLE PAGE

1. REPORT NO.	2. GOVERNMENT ACCESSION NO.	3. RECIPIENT'S CATALOG NO.
WA-RD 440.1		

4. TITLE AND SUBTITLE	5. REPORT DATE
Performance of Geotextile Separators, Bucoda Test Site—Phase II	July 1997
	6. PERFORMING ORGANIZATION CODE
7. AUTHOR(S)	8. PERFORMING ORGANIZATION REPORT NO.
Peter Jason Black and Robert D. Holtz	
9. PERFORMING ORGANIZATION NAME AND ADDRESS	10. WORK UNIT NO.
Washington State Transportation Center (TRAC) University of Washington, Bx 354802 University District Building; 1107 NE 45th Street, Suite 535 Seattle, Washington 98105-4631	11. CONTRACT OR GRANT NO. T9903, Task 66
12. SPONSORING AGENCY NAME AND ADDRESS	13. TYPE OF REPORT AND PERIOD COVERED
Washington State Department of Transportation Transportation Building, MS 7370 Olympia, Washington 98504-7370	Final Research Report
	14. SPONSORING AGENCY CODE

15. SUPPLEMENTARY NOTES

This study was conducted in cooperation with the U.S. Department of Transportation, Federal Highway Administration.

16. ABSTRACT

A full-scale field study was conducted to investigate the influence of five different geotextile separators on the performance of a pavement system. Five years after the geotextiles had been installed, the site was excavated to evaluate the soil and geotextile conditions, collect representative samples for laboratory testing, and perform a series of in-situ tests.

The fine-grained subgrade soils appeared to have consolidated since the geotextiles were installed. Density tests suggested that the subgrade in sections containing geotextiles consolidated more than in the test sections without geotextiles. Evidence of subgrade fines migration into the base course aggregates was found at some of the explorations where geotextiles were installed. However, the fines migration did not appear to adversely affect the performance of the pavement system.

Permittivity testing suggested that heat-bonded geotextiles are more susceptible to clogging than needle-punched or slit-film geotextiles. Initial base course layer thickness was found to significantly affect the strength and elongation at failure of the geotextiles. The lighter-weight geotextiles contained more construction damage; however, the damage was not reflected in the results of the strength tests.

Evaluation of current filtration and survivability criteria indicated that the FHWA filtration design criteria produce reasonable predictions of filtration performance, whereas the maximum AOS values specified by Task Force 25 and WSDOT may not always be effective in preventing fines migration. The Task Force 25 survivability criteria for geotextile separators appear reasonable, whereas the WSDOT survivability criteria may be too restrictive for some conditions.

17. KEY WORDS	18. DISTRIBUTION STATEMENT
Geotextiles, geotextile separators	No restrictions. This document is available to the public through the National Technical Information Service, Springfield, VA 22616

19. SECURITY CLASSIF. (of this report)	20. SECURITY CLASSIF. (of this page)	21. NO. OF PAGES	22. PRICE
None	None	210	

Final Research Report
Research Project T9903, Task 66
Bucoda Test II

PERFORMANCE OF GEOTEXTILE SEPARATORS BUCODA TEST SITE—PHASE II

by

Peter Jason Black
Research Assistant

Robert D. Holtz
Professor of Civil Engineering

Department of Civil Engineering
University of Washington, Box 352700
Seattle, Washington 98195

Washington State Transportation Center (TRAC)
University of Washington, Box 354802
University District Building
1107 NE 45th Street, Suite 535
Seattle, Washington 98105-4631

Washington State Department of Transportation
Technical Monitor
Tony Allen, State Geotechnical Engineer
Materials Laboratory

Prepared for

Washington State Transportation Commission
Department of Transportation
and in cooperation with
U.S. Department of Transportation
Federal Highway Administration

July 1997

DISCLAIMER

TABLE OF CONTENTS

List of Figures

Number | Page

Number	Page

Number Page

LIST OF TABLES

Number Page

ACKNOWLEDGMENTS

The author wishes to express sincere appreciation to the members who served on the exam committee, Professors Robert D. Holtz, Steven L. Kramer, and Joe P. Mahoney for their assistance in preparation of this document by providing helpful discussions and recommendations. In particular thanks is extended to Professor Robert D. Holtz who always made time for assistance and guidance.

Sincere gratitude is also extended to Mr. Tony Allen of WSDOT for his support throughout this project. Mr. Don Chadbourne's assistance throughout the field investigation was also valuable. The field investigation would not have been successful without the outstanding effort of my fellow graduate students Wei Lee and Erik Andersen. The help offered by Mr. Kenneth B. Knowlan, Mr. Richard W. Terry, and Mr. Lynn N. Gmeiner saved considerable time during the laboratory testing.

Funding for the project was provided by WSDOT.

1.0 INTRODUCTION

Geotextiles are becoming more commonly used in roadway construction due to their versatility, construction efficiency, and most importantly cost effectiveness. Geotextiles can improve the performance of a pavement system primarily by separating the aggregate base course from a weaker, finer-grained subgrade. Geotextiles also perform secondary functions which include filtration, drainage, and reinforcement. To perform effectively, the geotextile must survive the construction process as well as accommodate the intended long-term (vehicle) loading conditions.

Although geotextiles have been used as separators in roadways for many years, only recently have state and federal agencies attempted to specify guidelines for their use (Holtz, 1996). Many of these agencies, including the Washington Department of Transportation (WSDOT), have developed construction specifications for geotextile separators based on the American Association of State Highway and Transportation Officials, the Associated General Contractors, and the American Road and Transportation Builders Association (AASHTO-AGC-ARTBA) Task Force 25 (1989) recommendations. Current information establishing the performance of geotextile separators using this criteria is limited, warranting the need for further research.

This report represents the second phase of a full scale field and laboratory study conducted to investigate the influence of different geotextiles on the long-term performance of a pavement system. Specifically, the study examines the influence of five different geotextiles installed in a test road section. Although the primary purpose of the study was to investigate the long-term geotextile performance, some conclusions about the short-term performance are also made. The findings of the study are compared with current WSDOT and Federal Highway Administration (FHWA) specifications and design methods for geotextile separators.

2.0 PROJECT BACKGROUND

The test site is located approximately 32 km south of Olympia on SR-507 in Bucoda, Washington, as shown in Figure 2.1. The test road section consists of a two-lane highway with asphalt pavement. At the test location, the highway runs in the northeast-southwest direction, however the highway generally runs north-south, thus the traffic lanes are termed northbound and southbound in this study. The topography of the roadway generally slopes down at a gradient of 4.4 percent in the northeast (northbound) direction.

The Phase I study (Tsai et al., 1993) was coordinated with reconstruction performed at the test site by WSDOT in June, 1991. Prior to the roadway repairs, the test site had a long history of poor pavement performance which included significant rutting and fatigue (alligator) cracking. The poor pavement performance in conjunction with the soft subgrade soils and seasonally high groundwater table made the site ideal for application of geotextile separators.

As part of the study, five different geotextiles and a control section were installed in each lane. The length of each test section was 7.62 m, as shown in Figure 2.2. The properties of the geotextiles used in the study are summarized in Table 2.1. The initial thickness of aggregate placed over the geotextiles was designed to be 150 mm in the northbound lane, and 300 mm in the southbound lane. The total thickness of aggregate was designed to be 450 and 600 mm, respectively, in the north and southbound lanes, although these thicknesses were found to vary as much as 150 mm throughout the test section. A large steel drum roller was used without vibration for compaction. Also, water was sprayed on the base course by a water truck to aid in obtaining better compaction results.

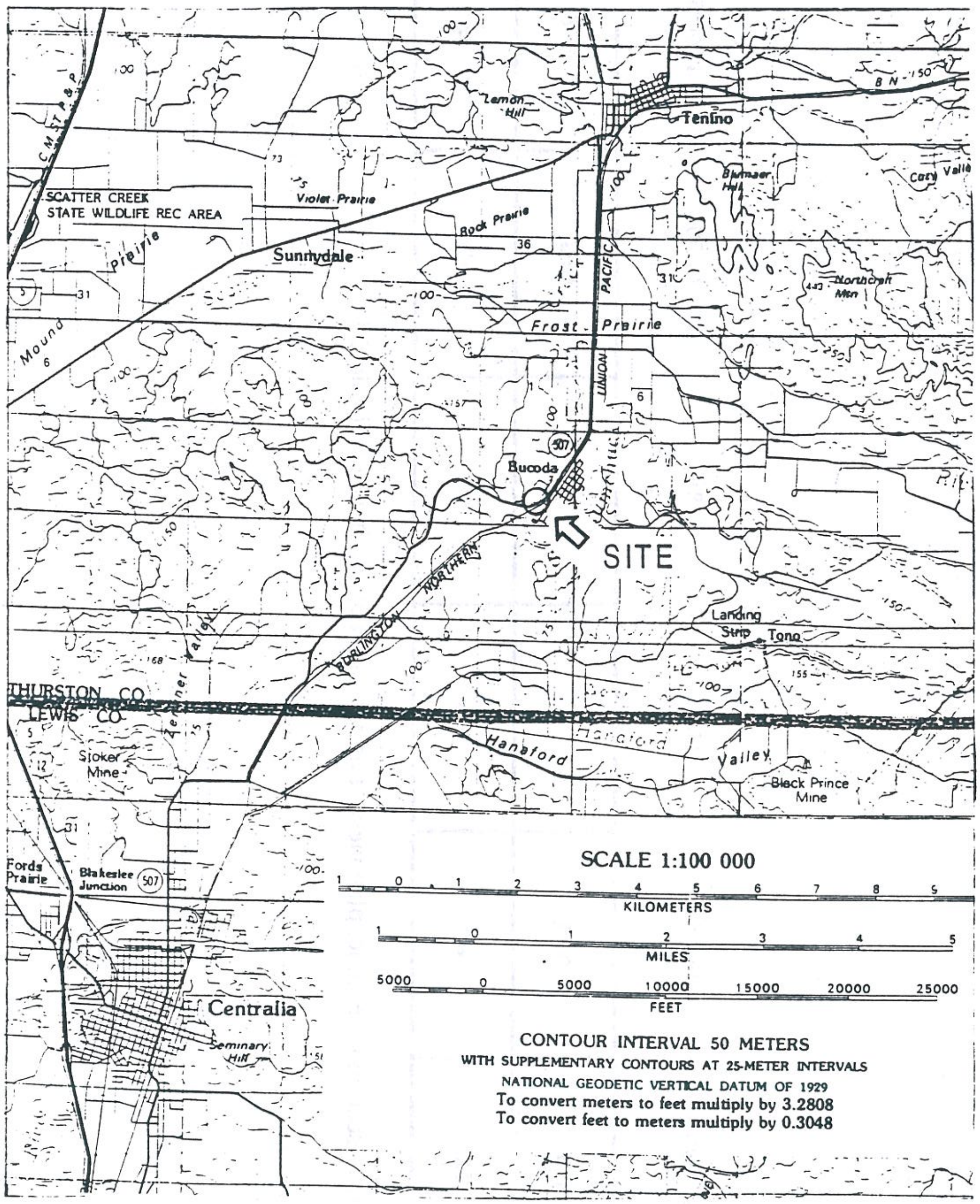

Figure 2.1 - Test site location map.

Station	177+70	177+95	178+20	178+45	178+70	178+95
SB Lane	**HB**	**NP4**	**SF**	**Soil**	**NP8**	**NP6**
NB Lane	**HB**	**NP4**	**NP6**	**Soil**	**NP8**	**SF**

Figure 2.2 - Test road section schematic, plan view. For definition of symbols, see Table 2.1.

Table 2.1 - Geotextile properties. Source: Geotextile Fabrics Report (GFR), December 1990.

Geotextile	Structure	Polymer Type	Thickness mm (mils)	Mass per Unit Area g/m^2 (oz/yd^2)	Permitt. (sec^{-1})	AOS mm (US Sieve)
HB - Reemay Inc. 3401	nonwoven	PP	0.4 (17)[91]	132 (3.9)	0.1	0.21 (70)
NP4 - Polyfelt TS500	nonwoven	PP	1.5 (60)*	152 (4.5)*	2.7	0.18-.30 (80-50)
NP6 - Polyfelt TS600	nonwoven	PP	2.0 (80)*	214 (6.3)*	2.1	0.15-.21 (100-70)
NP8 - Polyfelt TS700	nonwoven	PP	2.6 (105)*	280 (8.3)*	1.6	0.125-.18 (120-80)
SF - Exxon GTF 300	woven	PP	0.5 (19.5)	240 (7.1)++	0.1*	0.30 (50)

Geotextile	Wide Width Strength/Elongation MD kN/m (lb/in.)/%	Wide Width Strength/Elongation XD kN/m (lb/in.)/%	Grab Tensile/ Elongation kN (lb)/%	Puncture kN (lb)	Trapez. Tear Strength kN (lb)
HB	6.1 (35)/45	7.0 (40)/50	0.578 (130)/60	0.178 (40)	0.267 (60)
NP4	8.8 (50)/80*	7.0 (40)/50*	0.489 (110)/50	0.267 (60)	0.222 (50)
NP6	12.3 (70)/95*	10.5 (60)/50*	0.667 (150)/50	0.335 (75)	0.311 (70)
NP8	15.8 (90)/95*	14.0 (80)/50*	0.911 (205)/50	0.445 (100)	0.380 (85)
SF	30.6 (175)/15[92]	30.6 (175)/15[92]	1.334 (300)/20	0.645 (145)	0.511 (115)

All values reported as minimum average roll values (MARV) unless noted

* Typical values
PP = polypropylene
[91] Source: December 1991 GFR -- Data not reported in December 1990 GFR
[92] Source: December 1992 GFR -- Data not reported in December 1990 GFR
++ From packaging label

To investigate the soil and groundwater conditions at the test site prior to the remediations, WSDOT performed several subsurface explorations along the test road section in April and May of 1991. The explorations consisted of borings with standard penetration tests in addition to portable penetrometer tests that were performed using hand-operated equipment. The penetrometer test data was correlated to standard penetration test values. The field logs from these explorations in addition to some laboratory testing results from WSDOT are provided in Appendix A. According to the field logs, piezometers were also installed in three borings. However, the only piezometer (plastic standpipe) encountered during the field investigation for this study was adjacent to the northbound lane at station 178+00, as discussed later.

3.0 Objective and Scope of Work

3.1 Objective of the Study

The primary objective of the study was to investigate the influence of different geotextiles on the long-term performance of the test road pavement system. The results are intended to aid WSDOT in the cost-effective selection and specification of these products. This research represents the first post-construction investigation to be carried out at the Bucoda Test Site. The overall approach was primarily forensic in nature.

3.2 Scope of Work

To accomplish the research objective, the project was separated into seven tasks:

1. Literature review
2. Field work plans
3. FWD and pavement condition survey
4. Field investigation
5. Laboratory testing
6. Evaluation of field and laboratory results
7. Report

In Task 1, the previous work on the Bucoda Test Site was reviewed (Savage, 1991, Tsai and Savage, 1992, and Tsai et al., 1993) in addition to other geotextile separator studies, particularly those performed by Holtz and Page (1991) and Metcalfe and

Holtz (1994). A search of other relevant publications was also conducted and is summarized in Section 4.0.

Task 2 included developing the field investigation procedures. Investigation procedures used by Holtz and Page (1991) and Metcalfe and Holtz (1994) were reviewed so that the field investigation could be as efficient as possible. The planned field work was coordinated with the WSDOT maintenance crew, which provided the materials and services necessary for the pavement cutting, soil excavation, and backfill and patching operations, as well as traffic control services.

For Task 3, WSDOT crews performed FWD tests at each different geotextile location in the test section for comparison with previous FWD tests in the test section. The pavement condition survey was performed during the field investigations.

The field investigations were carried out in Task 4. The field procedures included establishing the test pit locations, cutting the pavement, exhuming and replacing the geotextiles, performing in-situ soil tests, collecting representative soil samples, taking photographs, backfilling the excavations, and patching the pavement. The exhumed samples were taken to the University of Washington laboratories for further testing, Task 5.

Task 6 included analyzing the results of the field and laboratory tests in the context of the results developed in Task 1 (literature review) and the original objectives of the Bucoda Test Site research. The findings, conclusions, and recommendations of the study are presented in this report, Task 7.

4.0 STATE OF THE ART AND PRACTICE

This section presents the results of the literature review and summarizes the results of the Phase I research. Current WSDOT and FHWA specifications and design methods are also presented.

4.1 Literature Review Results

The following sections outline the functions of geotextiles used in roadway applications including separation, filtration and drainage, and reinforcement. Case studies describing fines migration and subgrade consolidation observations are described. Survivability and durability issues are also discussed. The literature review mainly focuses on research literature published since the completion of the reports of Metcalfe and Holtz (1994), Holtz and Page (1991), and Tsai (1995). Metcalfe and Holtz (1994) and Tsai (1995), in particular, provide fairly comprehensive reviews of research literature published prior to their studies.

4.1.1 Separation

Koerner (1994) defines geotextile separation as "the introduction of a flexible, porous textile placed between dissimilar materials so that the integrity and functioning of both materials can remain intact or be improved". In other words, geotextile separators prevent intrusion of fine-grained subgrade soils up into the base course soils. This is important because the strength of the base course soil can be significantly decreased by only a small amount of fines (Holtz et al., 1995). Thus, geotextile separators improve the performance of a pavement system by maintaining the design thickness of the pavement system. As such, the primary function of geotextiles used in roadway applications is separation.

Several full scale field studies have been performed to evaluate the performance of geotextile separators (Brorsson and Eriksson, 1986; Bonaparte et al., 1988; Holtz and Page, 1991; Metcalfe and Holtz, 1994; to name a few). By and large, researchers have concluded that geotextile separators have performed effectively throughout a variety of subgrade soil and construction conditions. Some researchers were even pleasantly surprised by the effectiveness of some geotextile separators after discovering that significant amounts of damage occurred to the geotextiles during construction. In fact, no documented case history involving the complete failure of a pavement system due to the poor performance of a geotextile separator could be found.

4.1.2 Filtration/Drainage

Filtration and drainage are secondary functions of geotextile separators. The geotextile must act as a filter by preventing subgrade soils from migrating up into the base course due to the high pore pressures induced by wheel loads. It must also act as a drain, allowing the excess pore pressures to dissipate through the geotextile and the subgrade soils to gain strength by consolidating (Holtz et al., 1995).

Filtration and drainage can be impeded by blinding, clogging, and caking, as illustrated in Figure 4.1. Blinding is defined as the blockage of pore openings on the bottom surface of the geotextile, and can occur immediately when the geotextiles are placed on the subgrade. Clogging is defined as the entrapment of soil particles within the pore structure of the geotextile. Caking is the deposition of soil particles on the top surface of the geotextile. Blinding and clogging are primarily attributed to the subgrade soil particles, while caking may result from the migration of subgrade fines through the geotextile or the settling of fines from the base course soils. Similar definitions of blinding, clogging, and caking were used by Metcalfe and Holtz (1994).

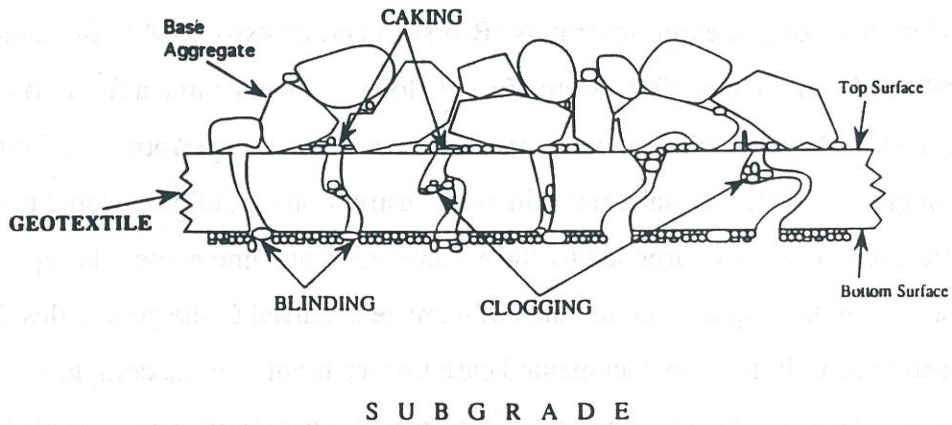

Figure 4.1 - Illustration of blinding, clogging, and caking (reproduced from Metcalfe and Holtz, 1994).

4.1.3 Migration of Fines Into Base Course Soils

A variety of field studies have generally found no evidence of significant migration of subgrade fines through geotextiles into the base course soils (Brorsson and Eriksson, 1986; Bonaparte et al., 1988; Holtz and Page, 1991; Metcalfe and Holtz, 1994). Conversely, laboratory tests and numerical analyses by Alobaidi and Hoare (1996) indicates that geotextiles may not be effective in controlling the migration of fines under dynamic loading conditions; they cite other research that supports their findings (Ayres, 1986; Bell et al., 1981; Yang and Yu, 1989).

Metcalfe and Holtz (1994) exhumed geotextile separators at fourteen different sites in western Washington. Three of the six exhumed woven slit-film geotextiles were found to contain some caked fines on the surface of the geotextile; however, it could not be determined if the fines had migrated through the geotextile, or if the fines had settled from the base course aggregate. It is interesting to note that only one of the three geotextiles containing the caked fines failed the Task Force 25 (1989) and FHWA (Holtz et al., 1995) retention criteria for apparent opening size (AOS). Several of the other geotextiles also failed the retention criteria, but no evidence of caked fines was observed at these locations.

Rowe and Badv (1996) performed laboratory tests to compare the retention capabilities of an exhumed nonwoven geotextile, granular graded filter, and no filter at all. They found that the geotextile and graded granular filter were about equally efficient in minimizing the intrusion of a clayey till into a uniformly graded gravel. In the absence of a filter-separator, a significant amount of fines intruded into the stone layer. However, their tests probably do not accurately model the conditions of a realistic pavement structure because the tests did not include dynamic loading effects. The loading conditions consisted of a static force applied for one to two weeks.

As indicated above, Alobaidi and Hoare (1996) performed laboratory tests and numerical analyses to evaluate the migration of fines through geotextiles into a base course layer; pore water pressures were also examined. They concluded that geotextiles do not reduce the cyclic deformation and cyclic pore pressures within a subgrade. By contrast, they found that geotextiles allow for quick dissipation of the cyclic pore pressure during the time of a loading cycle, thereby causing erosion of the subgrade surface and an upward movement of the eroded particles. In addition, they concluded that high permeability geotextiles cause more pumping because they allow quicker dissipation of cyclic pore pressure. Also, thick geotextiles reduced the critical hydraulic gradient at the boundary of the contact area between a base particle and subgrade soil and therefore reduced fines migration.

Some of the conclusions of Alobaidi and Hoare (1996) may be questionable because it appears their numerical model used to predict pore pressures did not realistically model the geosynthetic. The subgrade and geotextile were assigned the same elastic moduli; therefore, the geotextile would have little influence on the response of the subgrade soil. If a higher modulus was assigned to the geotextile, the stress distribution in the subgrade would presumably change, altering the pore water pressures. It should be noted, however, that their paper did not include details of their numerical analysis (e.g. it is unknown if failure criteria were assigned to the soil or geotextile).

Tsai (1995) found no evidence of fines migration through geotextiles subjected to dynamic loading in a laboratory model. He also provides an excellent summary of other laboratory tests conducted to evaluate fines migration.

4.1.4 Consolidation of Subgrade

The literature review revealed that information concerning the consolidation of the subgrade underlying geotextile separators is very limited. Detailed examinations of the rate and/or magnitude of subgrade consolidation were not reported in any of the full scale field studies reviewed.

General observances of subgrade consolidation for a full scale study were made by Brorsson and Eriksson (1986) who state that during installation of nine different geotextiles "it was impossible to walk on the subgrade material without sinking down half the height of one's wellingtons". In excavations made five and ten years later, the subgrade was found to be firm, dry and well consolidated at all the test pit locations. Bonaparte et al. (1988) also found that the subgrade underlying geotextile separators at seven different sites had compressed or consolidated since the geotextiles were installed, 1 to 12 years prior.

Evidence of subgrade consolidation was also found by Metcalfe and Holtz (1994). At the time of their field investigation, the subgrades were generally found to be firm at all test pit locations. However, construction records at several of the test sites indicated that soft subgrade conditions existed at the time the geotextiles were installed. During their exhumations, ruts in some of the subgrades were also observed indicating that soft soil conditions preexisted.

4.1.5 Reinforcement

Reinforcement is also a secondary function of geotextile separators. The reinforcing effects are most pronounced in weak subgrades where loading causes deformations (rutting) in the subgrade to develop the tensile strength of the geosynthetic. Holtz et al. (1995) state that geogrids and geotextiles provide reinforcement through three possible mechanisms:

1. Lateral restraint of the base and subgrade through friction and interlock between the aggregate, soil, and the geosynthetic.
2. Increase in the system bearing capacity by forcing the potential bearing capacity failure surface to develop along alternative, higher shear strength surfaces.
3. Membrane support of the wheel loads. In this case, the wheel load stresses must be great enough to cause plastic deformation and ruts in the subgrade. To mobilize the tensile stresses in the geosynthetic, the wheel path rutting must be in excess of 100 mm.

Holtz et al. (1995) state that geosynthetics provide reinforcing functions when the subgrade CBR< 1, and possibly provide reinforcement when the CBR ranges from 1 to 2. The geosynthetics do not provide reinforcing functions when the CBR is greater than 2 to 3. Further, they suggest that geosynthetics are not effective in most highway construction cases where the subgrade CBR exceeds a value of 3.

Geogrids are used in roadway applications where soft subgrade soils are present almost solely for their reinforcing capabilities. Collin et al. (1996) performed a full scale load test to evaluate the reinforcing effects of two different geogrids. They concluded that it was conservative to estimate that the geogrids tested would increase the pavement life 2 to 4 times with respect to unreinforced pavements, and for flexible pavements constructed on subgrades with a CBR of 3 and with base course thicknesses between 175 and 300 mm.

A similar study was performed by Austin and Coleman (1993) who conducted a full scale field test on an unpaved haul road to evaluate the effectiveness of six geosynthetics (1 woven, 4 geogrids, and 1 nonwoven/geogrid combination) as the primary reinforcement in aggregate layers placed over very soft subgrades (CBR<1). Trafficking tests indicated that the reinforced sections could sustain 2 to 3 times more equivalent single axle loads (ESAL) than the unreinforced sections, based on rutting criteria. The combined use of a geogrid and nonwoven geotextile was found to have the best performance.

Similar results were found by Fannin and Sigurdsson (1996) who also conducted a full scale field test on an unpaved road with a subgrade CBR ranging from 1 to 2. Geotextiles outperformed geogrids when very thin base course layers were used, and separation was critical. Geogrids, on the other hand, outperformed geotextiles when thicker base course layers were used. From laboratory tests, Nishida and Nishigata (1994) also concluded that reinforcement is a primary function when the ratio of the applied stress on the subgrade soil to the shear strength of subgrade soil (σ/c_u) is high; separation is most important when the ratio is low.

4.1.6 Numerical Modeling of Reinforcement

The reinforcement mechanism has been examined by some researchers using numerical formulations. However, assumptions of the constitutive relations, failure criterion, stress distributions, and geotextile anchorage and membrane effects incorporated into the models vary considerably. A few numerical models are summarized below to illustrate this point.

Table 4.1 - Summary of numerical model parameters.

Model	Purpose of Development	Numerical Scheme	Soil Models (Constitutive Relat.)	Geosynthetic Models
Bourdeau (1991)	Eval. membrane effect of 2 layer soil system	FD Iteration, 2D plane strain	Base: Theory of stochastic stress distrib. in particulate media. Subgrade: Winkler Model	Elastic, unbounded strength; Full & partial anchorage consid. w/ M-C slip criteria
Dondi (1994)	Eval. reinf. effect in paved system w/ single reinf. layer	FE, 3D field	Bituminous: Elastic Base: Drucker-Prager Subgrade: Cam-clay	Elastic; friction at interface M-C elasto-plastic
Helwany and Wu (1995)	Long term eval. of GRS struct.; can be used for walls	Time marching FE, 2D	All soils: Sekiguchi-Ohta (mod. anisotropic Cam-clay)	Nonlinear visco-elastic; no slippage at soil/geosynthetic interface

Note: FD = Finite difference, FE = Finite element, M-C = Mohr-Coulomb

The literature search indicates that rather sophisticated models have been developed to investigate the reinforcement mechanism. However, a model evaluating the effect that the redistribution of stress (due to the presence of a geosynthetic) has on the consolidation of a soft subgrade could not be found.

4.1.7 Survivability

Survivability is the ability of geosynthetics to resist damage during installation, road construction, and initial operations. To perform its intended function, the geotextile must survive the construction operations (Holtz et al., 1995). The stresses applied to the geotextile during initial construction are likely the highest mechanical stresses the geotextile will be exposed to. Therefore, survivability is one of the most important design and selection considerations.

The level of damage a geosynthetic incurs during installation is largely a function of the severity of the stresses imposed on the geosynthetic from the elements of construction (i.e. weight and type of compaction equipment, initial lift thickness, aggregate characteristics, subgrade preparation, and subgrade shear strength). Task Force 25 (1989) provides a rating system of construction survivability based on anticipated construction conditions, discussed in more detail in Section 4.4.

After exhuming 75 geosynthetics from 48 different sites, Koerner and Koerner (1990) found that as the survivability condition (rating) became more severe, the installation damage to the geotextiles increased yielding greater reductions in the retained strength. They also found that low mass per unit area geotextiles suffered the greatest strength reductions and number of holes.

As one might expect, the degree of geosynthetic damage increases with increasing intensity of compaction effort (Watts and Brady, 1994). Several researchers (Metcalfe and Holtz, 1994; Paulson, 1990; Sandri et al., 1993; Rainey and Barksdale, 1993) have found that base course aggregate type has a significant influence on the degree of installation damage, maybe more so than the initial lift thickness.

For consideration of installation damage in design, Allen and Bathurst (1994) provide a summary of more than 3500 index tensile load-strain tests performed on 55 different geosynthetic reinforcement products in site damaged and undamaged condition. The study compares the peak strength, strain at failure, and modulus of control and damaged specimens. The compilation of data can be used as a preliminary guide to reconstruct index load-strain curves for damaged specimens at a pre-selected level of strength loss using index load-strain curves for undamaged specimens. Strength loss criteria can be related to survivability conditions as described by Allen (1991) to establish the preselected strength loss level.

4.1.8 Durability

Ingold (1988) indicates the definition of durability "is generally understood to mean the ability of the geotextile to maintain its integrity, and a high degree of initial mechanical performance, over a long period of time when subjected to its operational environment". Potential degradational processes affecting geosynthetics are outlined by Koerner (1994); these include temperature, oxidation, hydrolysis, chemical, radioactive, biological, and sunlight (ultraviolet) degradation. Allen (1991) also provides a comprehensive review of current durability issues.

After installation, reductions in the strength and stiffness of geotextiles are not directly affected by temperatures in most geotextile applications, as generally only extreme temperatures influence the geotextile properties. The melting points of polyethylene, polypropylene, and polyester are 125, 165, and 250 °C, respectively. Temperatures indirectly affect the geotextile properties by helping to accelerate other degradation processes such as oxidation, hydrolysis, chemical, biological, etc.

Thermo-oxidation of polymers causes a deterioration of physical properties including decreased molecular weight, discoloration of the polymer, and decreased mechanical strength (Kelen, 1983). Polyolefins (which include polypropylene and polyethylene) are considered to be the most susceptible to oxidation, although oxygen can react with all types of polymers causing degradation. In short, the oxidation process occurs through a series of consecutive free radical reactions. Hydroperoxides are formed which branch into free radicals which produce further radical reactions (Kelen, 1983). The rate of the oxidation reaction is significantly affected by temperature. The Arrhenius relationship, used by many researchers, indicates that higher temperatures increase the rate of the oxidation reaction exponentially (Allen, 1991). The presence of certain transfer metals, such as iron, manganese, and copper has a catalyzing effect on the oxidation reaction by allowing the branching reactions to occur at lower temperatures (Wisse, 1988). To mitigate oxidation, antioxidants can be added to the polymers during their manufacturing.

Hydrolysis is the scission of long chain linear molecules by "absorption" of water molecules resulting in a decrease in molecular weight (Risseeuw and Schmidt, 1990; den Hoedt, 1989). Polyester geotextiles are most susceptible to hydrolysis, particularly when exposed to high levels of acidity or alkalinity (Koerner, 1994). Hydrolysis in high alkaline media however, is considered to be more severe than in highly acidic environments (Risseeuw and Schmidt, 1990). Polypropylene is considered highly stable against hydrolysis (Schneider, 1989; Mathur et al., 1994).

Information regarding polymer reactions with specific chemicals can generally be obtained from the manufacturers, although ASTM D 543 does provide a method to evaluate the resistance of plastics to chemical reagents. Koerner (1994) also states that ASTM Committee D-35 has developed a protocol for laboratory (ASTM D5322) and field (ASTM D5496) chemical degradation assessments by immersion procedures. Radioactive degradation is considered to be of concern only where geosynthetics are exposed to very high levels radiation, such as nuclear waste sites, although this concern is somewhat speculative due to the lack of research in this area (Koerner, 1994).

Where present, biological forms may degrade filtration and drainage characteristics of geotextiles by growing within the geotextile structure. The polymer filaments may be jeopardized if microorganisms, bacteria, or fungi use the polymers as feedstock, although this is considered to be very unlikely (Koerner, 1994). Allen's (1991) research suggests that biological degradation (by consummation) is not a problem for high molecular weight polymers commonly used for geosynthetics, although low molecular weight polymers and some polymer additives may be susceptible.

Geosynthetics, particularly polypropylene products, lose significant strength and stiffness when exposed to ultraviolet (UV) light via photo-oxidation. More specifically, UV-B causes severe polymer degradation, while UV-A causes less damage. The intensity of the UV light depends on the season, temperature, geographic location, cloud cover, and moisture (Koerner, 1994). The best way to mitigate UV degradation is to limit exposure. Photostabilizers, such as carbon black, can also be added during manufacturing to the protect the polymers (polyolefins). When assessing UV resistance, Cazzuffi et al. (1994) indicate that the geometrical properties of geosynthetics, such as fiber diameter for geotextiles, rib thickness for geogrids, and sheet thickness for geomembranes are also important since weathering usually affects only a thin surficial thickness of the polymer elements.

ASTM D4355 and ASTM D5208 are testing standards that allow the evaluation of geosynthetic degradation due to UV light. Koerner (1994) indicates however, that these tests can be challenged on grounds of technical relevancy because of uncertainties associated with the artificial simulation of sunlight by laboratory lamps.

The photo-oxidation process is well illustrated by several field studies. Although quite a few studies evaluating the influence of UV degradation have been performed, the literature review focused on recently published papers.

Tisinger et al. (1993) evaluated a polypropylene nonwoven geotextile exposed to UV degradation over a period of seven months during the construction of a landfill. At the end of the observation period, holes ranging from 20 to 200 mm in size had formed in areas of the geotextile. On average, geotextile samples between the holes retained 77 percent of their grab strength. The study also attributed some of the geotextile degradation to heat.

McGown et al. (1995) performed wide width tensile tests and sustained load (creep) tests on four types of geosynthetics (a woven polypropylene, nonwoven polypropylene/polyester, and polypropylene and high density polyethylene geogrids) exposed up to 12 months of natural weathering. The woven polypropylene geotextile had the worst performance, retaining only 24 percent of its wide width tensile strength after about 200 days of exposure to the Kuwait sun. The nonwoven polypropylene/polyester geotextile retained about 73 percent of it wide width strength in the same time interval. The geogrids were found to have no significant changes in strength. In a related study, Cazzuffi et al. (1994) found that geogrids and geomembranes generally sustained less strength and stiffness degradation than geotextiles when exposed to weathering.

Cassady and Bright (1995) evaluated several polyolefin geosynthetics exposed to natural weathering over a nine year period. The geotextiles contained various types and amounts of stabilizing additives. Carbon black, at 2.5 percent by weight, was determined to be the most effective means of retarding the deteriorative effects of UV light.

The uncertainties involved with the synergism of the above described degradational processes make it difficult to account for multiple degradational issues in design. In particular, complexities arise when two or more processes are interactive. For example, a particular chemical or pH level may adversely effect the structure of a polymer in addition to influencing a certain degradational bio-organism. Clearly, the synergism of degradational processes is site-specific and would be difficult to evaluate in the laboratory in many cases. Much research is needed in this area to understand the synergism of degradational mechanisms.

4.1.9 Similar Studies

Holtz (1996) summarizes a two part study performed by Holtz and Page (1991) and Metcalfe and Holtz (1994) that evaluates the properties and overall performance of geotextile separators. Holtz and Page (1991) exhumed geotextile separators for eight sites in eastern and central Washington, and Metcalfe and Holtz (1994) exhumed geotextiles from 14 sites in western Washington. The study included field evaluations and laboratory testing of the geotextiles, base course, and subgrade soils.

Their study found that all of the geotextile separators adequately performed their intended function of separation, however, the geotextiles experienced very different levels of damage during construction. Base course aggregate type appeared to have to more influence on the level of damage than the initial aggregate lift thickness. The woven slit-film and nonwoven needle-punched geotextiles survived the installation conditions reasonably well, the nonwoven heat-bondeds did not although they were installed under some of the more severe site survivability conditions. Testing indicated the permittivity of the slit-film and needle-punched geotextiles increased by similar percentages after being washed. The heat-bonded geotextiles had the highest percentage increases in permittivity, suggesting that they clog more than other geotextiles. There was evidence that the slit-films experienced much more blinding than the other geotextiles, and that iron staining and caking may also have affected their drainage performance adversely. The presence of caked fines on the upper surface of three slit-films suggested that their pore openings were too large for the intended filtration function, and they might be subject to fines migration although evidence on this point was inconclusive. Metcalfe and Holtz (1994) recommended that WSDOT require a maximum AOS of 0.3 mm for geotextiles used in separation applications. All of the pavements examined were in good condition, except one which showed signs of premature failure; however, the failure could not be attributed to the performance of the geotextile separator.

In addition to the Phase I study (summarized in Section 4.2), Tsai (1995) conducted a laboratory study evaluating the effect of dynamic loading on the separator system. The study examined the influence that different geotextiles and subgrade strengths had on the rut depths and subgrade pore pressures as a function of the number of loading cycles. The nonwoven geotextiles used were the same (manufacturer and type) as those used in the Bucoda Test Site, but the woven geotextile was different.

Tsai found that the rut depth was significantly affected by the aggregate base thickness, subgrade soil type and strength, and the presence of a geotextile, but not the geotextile type and weight. The geotextiles were found to perform as well as granular graded filters, however the granular filters were found to be easily displaced. Peak pore pressures in the subgrade were found to be influenced by aggregate base thickness, subgrade soil type and strength, but not by the geotextile type and weight.

No significant amount of fines were observed to migrate through the geotextiles as a result of the dynamic tests. He concluded that geotextiles may not be needed for good subgrades (CBR>7) and where thick aggregate bases (>300 mm) are used.

4.1.10 Summary of Literature Research

By and large, full scale field studies have found that geotextiles perform effectively as separators throughout a variety of subgrade soil and construction conditions. Researchers have come to contradictory conclusions of the ability of geotextile separators to prevent subgrade fines migration; however, the majority of the field studies reviewed suggest that geotextiles prevent fines migration in most soil conditions. Information concerning the consolidation of the subgrade underlying geotextile separators is very limited. Three field studies noting subgrade consolidation were found; however the influence geotextiles had on the rate or magnitude of consolidation was not examined in detail.

Field and laboratory studies indicate that the reinforcement mechanisms of geosynthetics can significantly improve the performance of a roadway constructed over a soft soil. Short-term studies performed on soft subgrade soils indicate the reinforcement function of a geosynthetic appears to dominate the separation function where relatively thick base courses are used; separation dominates where thinner base courses are installed. Rather sophisticated numerical models have been developed to investigate the reinforcement mechanism; however, an existing model evaluating the effect that the redistribution of stress (due to the presence of a geosynthetic) has on the consolidation of a soft subgrade could not be found.

Geosynthetics are subject to degradation from a variety of sources. Their mechanical properties (strength, filtration and drainage characteristics, etc.) can be adversely affected by short-term degradation such as installation damage, or long-term degradation such as thermo-oxidation, hydrolysis, biological, or chemical degradation.

4.2 Summary of Phase I Research Findings

The Phase I research summary is based on review of Savage (1991), Tsai and Savage (1992), and Tsai et al. (1993). A copy of the latter reference is included in Appendix A.

The purpose of the Phase I study was to evaluate and compare the performance of five different geotextile separators under two different initial base course lift thicknesses so that constructability and installation requirements could be assessed. Instrumentation was installed to monitor vertical strains throughout the cross section, deformations in the geotextiles, and changes of water content and temperature. Rut depths were measured during trafficking tests.

The following conclusions were made after the field investigations and laboratory testing was complete:

- Geotextiles were found to eliminate base/subgrade intermixing if they survived the installation and placement operations.

- The presence of geotextiles led to more uniform rut depths, if the geotextiles survived the installation and placement operations.

- Rut depth was reduced by geotextiles if the subgrade had a modest shear strength.

- Based on visual observations and rut depths, the NP8 geotextile had the best overall performance in comparison to the other geotextiles used in the study.

- Strains in the subgrade soil appeared to be reduced by the SF geotextile; however, some pumping of the subgrade may have influenced the results.

- The observations indicated that during construction the needle-punched nonwoven geotextiles allowed unrestricted drainage of the subgrade while the other types tended to retard drainage. The heavier weight needle-punched nonwoven geotextiles appeared to enhance drainage.

4.3 Current WSDOT Design Methods

Two sources are presently used by WSDOT for specification and design of geotextile separators, the WSDOT Design Manual (1994) and the WSDOT 1996 Standard Specifications for Road, Bridge, and Municipal Construction.

4.3.1 Definitions: Separation and Soil Stabilization Applications

The WSDOT Design Manual and the WSDOT 1996 Standard Specifications divide the use of geotextile separators into two applications: separation and soil stabilization. The primary difference between these applications is the function the geotextiles are intended to perform. Geotextiles used in separator applications are intended to function as separators between two dissimilar soils. The basic function of geotextiles used in soil stabilization applications is to reinforce soft subgrade soils.

These functions are defined in detail in Chapter 530.04 of the WSDOT Design Manual. Separation is defined as "the prevention of two dissimilar materials from mixing. This is a primary function of geotextiles placed between a fine-grained subgrade and a granular base course beneath a roadway." Reinforcement is defined as "the strengthening of a soil mass by the inclusion into the soil mass of elements (i.e., geosynthetics) which have tensile strength. This is the primary function of high strength geotextiles and geogrids in geosynthetic reinforced wall or slope applications, or roadways placed over very soft subgrade soils which are inadequate to support the weight of the construction equipment or even the embankment itself."

The application for which the geotextile is used depends on the subgrade conditions. These conditions are defined in Chapter 530.05 which states that the need for soil stabilization geotextiles should be anticipated if the subgrade resilient modulus is less than or equal to 40,000 kPa, or if a saturated fine sandy, silty or clayey subgrade is likely to be present. Separation geotextiles are expected to be feasible if the subgrade resilient modulus is greater than 40,000 kPa and if a saturated fine sandy, silty or clayey subgrade is not likely to be present. In general, separation geotextiles should not be required if the subgrade is dense and granular and/or if the subgrade resilient modulus is greater than 105,000 kPa.

The WSDOT Pavement Guide (1995) correlates subgrade moduli to CBR values using the following relationship, which is considered valid for fine-grained soils with a CBR of 10 or less:

$$E_{SG}\ (\text{MPa}) = 10\ (\text{CBR}) \qquad \text{(Eq. 4-1)}$$

Therefore, a subgrade resilient modulus of 40,000 kPa would correlate to a CBR of 4, and a resilient modulus of 105,000 kPa would roughly correlate to a CBR of 10 or 11. According to a correlation chart provided by Koerner (1994, p.173), a

CBR of 4 roughly correlates to a undrained shear strength of 120 kPa, and a CBR of 10 correlates to a undrained shear strength of about 300 kPa.

Geosynthetics used for separation and soil stabilization applications must meet filtration, drainage, and durability criteria, described in more detail in Section 4.3.3. Geosynthetics used specifically for filtration or drainage applications must meet different criteria depending on the survivability conditions and soil to be filtered, outlined by the WSDOT Design Manual and the WSDOT 1996 Standard Specifications.

4.3.2 Construction Requirements

The 1996 Standard Specifications Section 2-12.3 requires the subgrade beneath the area to be covered by the geotextile to be graded to a smooth, uniform condition free from ruts, potholes, and protruding objects. The geotextiles must be laid smooth without excessive wrinkles. For separation and soil stabilization applications, the overlap distance must be a minimum of 600 mm at all longitudinal and transverse seams, or the seams can be sewn together. Where observed, damage incurred to the geotextiles during construction must be repaired by replacing the damaged portion of the geotextile with a patch. The patch must overlap the adjacent undamaged portions of the geotextile the minimum distance stated above. The geotextiles cannot be exposed to sunlight during installation more than 14 calendar days.

The initial lift thickness must be at least 150 mm for geotextiles used for separation applications, and 300 mm for geotextiles used in soil stabilization applications. In addition, for soil stabilization applications, the first lift should be compacted by loaded haul equipment, without the use of vibratory compaction. In all cases, the construction vehicles must be limited in size and weight to reduce rutting in the initial lift to not greater than 80 mm deep to prevent overstressing of the geotextile. Also, turning of vehicles directly on the first lift is not permitted.

4.3.3 Required Geotextile Properties

The WSDOT 1996 Standard Specifications Section 9-33 (p. 9-186) summarizes the required properties for geotextiles used for separation and soil stabilization applications, reproduced in Table 4.2.

Table 4.2 - WSDOT geotextile test methods and property requirements (after WSDOT 1996 Standard Specifications).

		Geotextile Property Requirements[1]	
Geotextile Property	Test Method[2]	Separation Woven/Nonwoven	Soil Stabilization Woven/Nonwoven
AOS	ASTM D4751	0.60 mm max. (#30 sieve)	0.43 mm max. (#40 sieve)
Water Permittivity	ASTM D4491	0.02 sec^{-1} min.	0.10 sec^{-1} min.*
Grab Tensile Strength, min. in machine and x-machine direction	ASTM D4632	1100 N/700 N min.	1400 N/900 N min.
Grab Failure Strain, in machine and x-machine direction	ASTM D4632	< 50%/≥50%	< 50%/≥50%
Seam Breaking Strength	ASTM D4632[3]	990 N/630 N min.	1200 N/800 N min.
Puncture Resistance	ASTM D4833	350 N/220 N min.	500 N/350 N min.
Tear Strength, min. in machine and x-machine direction	ASTM D4533	350 N/220 N min.	500 N/350 N min.
Ultraviolet (UV) Radiation stability	ASTM D4355	50% strength retained min., after 500 hrs. in weatherometer	50% strength retained min., after 500 hrs. in weatherometer

* Number changed from value shown on p. 9-186 (1996 Standard Specifications) per T. Allen.

[1] Minimum average roll values (MARV).

[2] Test procedures used are essentially in conformance with the most recently approved ASTM geotextile test procedures, except for geotextile sampling and specimen conditioning, which are in accordance with WSDOT Test Methods 914 and 915, respectively.

[3] With seam located in center of 200 mm long specimen oriented parallel to grip faces.

4.4 FHWA Design Methods

The FHWA geotextile design methods are included in the *Geosynthetic Design and Construction Guidelines* (Holtz et al., 1995). For the filtration design methodology outlined by FHWA, the test road section was considered to be less critical in nature, and contain less severe soil and hydraulic conditions.

For silt and clay subgrade soils (with more than 50% passing the 0.075 mm sieve) with steady state flow conditions, the following criteria should be used for filtration design of geotextile separators:

Retention Criteria:

$$AOS \leq B\, D_{85(soil)} \leq 0.3 \text{ mm}$$

Where: AOS = apparent opening size
B = 1.0 for woven geotextiles
B = 1.8 for nonwoven geotextiles
D_{85} = soil particle size for which 85% are smaller (mm)

Permeability/Permittivity Criteria:

$$k_{geotextile} \geq k_{soil}$$

$$\psi \geq 0.1 \text{ sec}^{-1} \quad \text{for} > 50\% \text{ passing } 0.075 \text{ mm}$$

Clogging Resistance:

$$AOS \geq 3\, D_{15(soil)} \quad \text{for } C_u > 3$$

The recommended FHWA survivability criteria summarized in Tables 4.3 and 4.4 are based on the AASHTO-AGC-ARTBA Task Force 25 guidelines (1989). The Task Force 25 filtration design requirements are also provided in Table 4.4.

Table 4.3 - Construction survivability ratings (after Task Force 25, 1989).

Site Soil CBR at Installation	<1		1-2		>2	
Equipment Ground (kPa) Contact Pressure	>350	<350	>350	<350	>350	<350
Cover Thickness[1] (Compacted, mm)						
100[2,3]	NR	NR	H	H	M	M
150	NR	NR	H	H	M	M
300	NR	H	M	M	M	M
450	H	M	M	M	M	M

H=High, M=Medium, NR=Not Recommended

[1] Maximum aggregate size not to exceed one half the compacted cover thickness.
[2] For low volume unpaved roads (ADT < 200 vehicles).
[3] The 100 mm minimum cover is limited to existing road bases and is not intended for use in new construction.

The properties of the geotextiles used at the test site are compared with FHWA, Task Force 25, and WSDOT criteria in Section 8.3.

Table 4.4 - Physical property requirements of Task Force 25 (1989).

Survivability Level	Grab Strength (N) ASTM D 4632		Puncture Resistance (N) ASTM D 4833		Tear Strength ASTM D 4533	
	< 50% Geotextile Elongation	> 50% Geotextile Elongation	< 50% Geotextile Elongation	> 50% Geotextile Elongation	< 50% Geotextile Elongation	> 50% Geotextile Elongation
Moderate	801	512	311	178	311	178
High	1201	801	445	334	445	334

Additional Requirements	Test Method
Apparent Opening Size (AOS) 1. < 50 % soil passing 0.075 mm sieve, AOS < 0.6 mm 2. > 50 % soil passing 0.075 mm sieve, AOS < 0.3 mm	ASTM D 4751
Permeability k of the geotextile > k of the soil (permittivity times the nominal geotextile thickness	ASTM D 4491
Ultraviolet Degradation At 150 hours of exposure, 70 % strength retained	ASTM D 4355
Geotextile Acceptance	ASTM D 4759

Note: Values shown are minimum average roll values. Strength values are in the weakest principal direction. The values of the geotextile elongation do not imply the allowable consolidation properties of the subgrade soil. These must be determined by a separate investigation. Numeric values are hard conversions of English units.

5.0 FIELD EXPLORATIONS AND IN-SITU TESTING

The field investigation was conducted on June 17 through June 19, 1996. A total of twelve test pits were excavated throughout the test section. Soil samples were collected throughout the excavated profiles, tests were performed on the subgrade soils, and geotextile samples were exhumed. Observations of the soil and groundwater conditions were also made. WSDOT personnel have performed FWD tests on the test section on several occasions since their installation in 1991. The most recent FWD tests were performed on March 25, 1996.

The weather conditions during the three day period of field investigations ranged from cloudy with periods of rain on the first day, to mostly sunny on the following days. Daily precipitation measurements made for the National Oceanic and Atmospheric Administration (NOAA) at the Centralia station for the month of June, 1996 are provided in Table A.7, in Appendix A. Monthly precipitation data dating back to January 1990 are provided in Table A.8 and Figure A.1. The Centralia station is located approximately 10 to 12 km southwest of the test site, and is the closest NOAA station to the site. As can be seen in Table A.8 and Figure A.1, the amount of precipitation in the months prior to the field investigation was "normal" in comparison to the average based on the previous seven years.

Exploratory excavations were made at the HB, NP4, NP6, and SOIL test sections in the northbound lane on the first day (June 17) of the field investigations. All of the test pits in the southbound lane were excavated on the second day, and excavations at the two remaining northbound lane test pit locations were made on the last day of the field investigation.

5.1 Investigation Procedures

The University of Washington research team on-site throughout the field investigation consisted of three graduate research assistants. Dr. R.D. Holtz, the University of Washington research supervisor, was also periodically on-site to observe the investigation. WSDOT maintenance crews provided the materials and services necessary for the pavement cutting, soil excavation, and backfilling and patching operations, in addition to the traffic control services.

To examine the different geotextiles and soil control sections at the test site, six exploratory excavations were made on the inside wheel paths of each traffic lane at approximately 7.62 m intervals. The center of the test pits were located at stations 177+65, 177+90, 178+15, 178+40, 178+65, and 178+90, as shown in Figure 5.1. The excavations were approximately 1.8 m by 1.2 m in size, with the length being oriented in the direction parallel to the centerline. The center of the excavations were located 0.9 m from the centerline to position the excavations over the inside wheel path. Excavations were not made in the outside wheel paths to avoid instrumentation that was installed in these areas during the Phase I study.

After the locations of the excavations were established, the asphalt concrete surface was removed with a grinding machine adapted to a backhoe, shown in Figure 5.2. The compacted base course material overlying the geotextiles was loosened by hand using shovels and steel prying bars. The loose soil was removed from the excavation using a vacuum operated pump truck (Vactor 2100 Series), shown in Figure 5.3. The vacuum truck greatly expedited the excavation and reduced the amount of hand shoveling that would have been required.

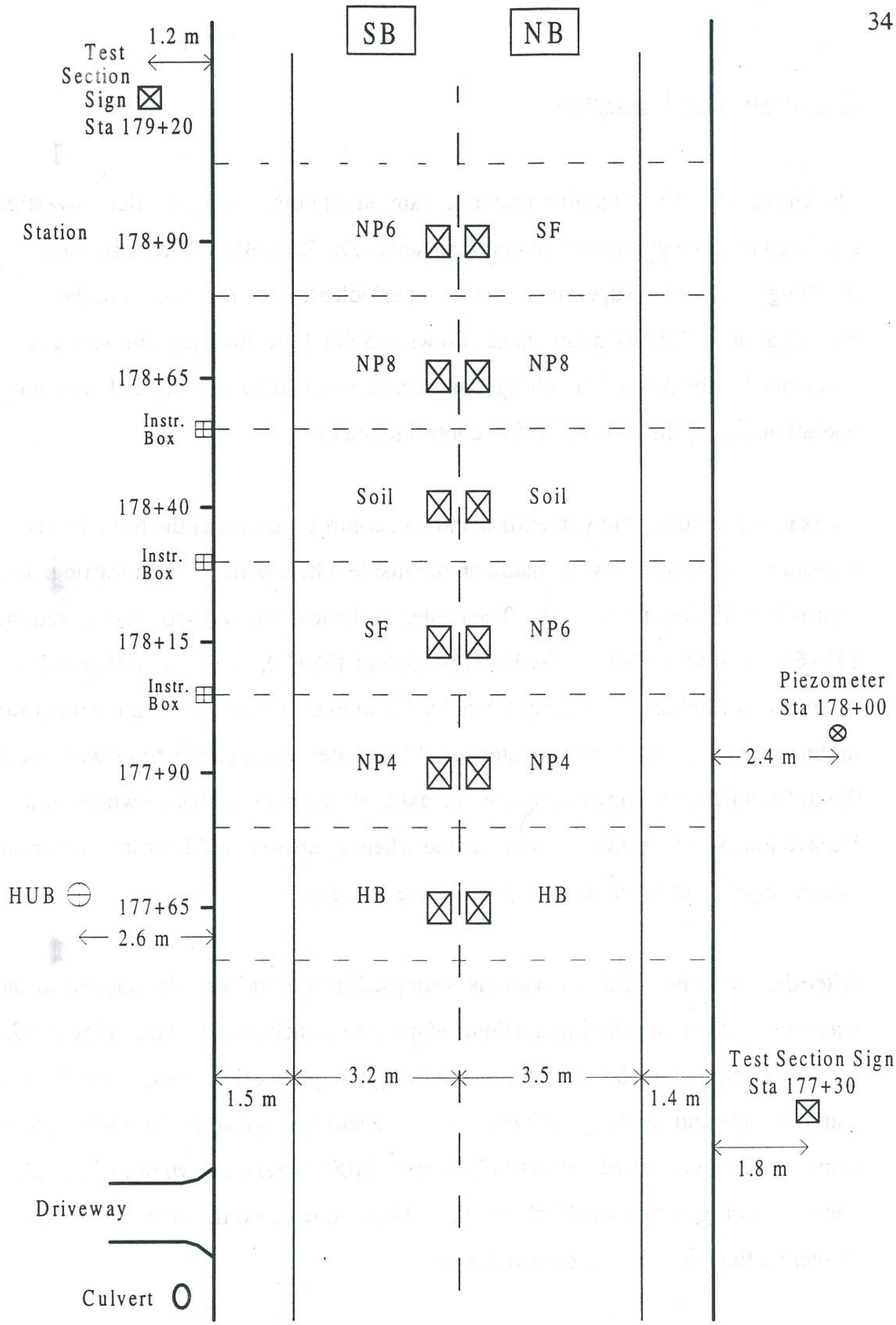

Figure 5.1 - Schematic of test road section, plan view.

Figure 5.2 - Pavement grinding operations.

Figure 5.3 - Vacuum truck.

Figure 5.4 - Patching operations.

Once the excavation depth was within about 150 mm of the anticipated geotextile location, careful excavations were made by hand to find the geotextile. Once the geotextile was found, the last 100 to 150 mm of base course material overlying the geotextile was removed by hand. The vacuum truck was not used in this area of the excavation because the suction might have changed the properties (i.e. permittivity) of the geotextile by removing some of the soil particles possibly clogging and blinding the geotextile.

Typically, three samples of the base course material were collected at each test pit site so that a profile of the soil properties could be established by laboratory tests. The uppermost soil sample was taken within the first 300 mm of excavated soil, the next at approximately 150 mm above the geotextile. In most of the excavations, a soil sample was also taken immediately above the geotextile, typically within 20 mm of geotextile. The sample taken at this location is termed "mudcake" in the remaining portions of this report because some of the samples appeared to contain a higher content of fine soil particles, as discussed later.

After the base course soils were removed, a utility knife was used to cut the perimeter of the exposed geotextiles in the test pits. The geotextile samples were carefully removed and visual observations were recorded. The samples were then photographed and stored in a sealed plastic bag. For ease of transportation and storage, the samples were typically folded two to three times before they were placed in the bags.

For the most part, the geotextiles appeared relatively undamaged by the excavation procedures although some damage was unavoidable in a few cases. Where incurred, the damage to the geotextiles was largely due to the shovels and steel bars used to loosen the base course aggregates. Also, efforts were made not to stand on the geotextiles after they were exposed. If it was necessary to stand in the excavation prior to exhuming the geotextiles, the research team members stood near the outside perimeter of the excavation.

After the geotextiles were removed, observations of the subgrade soil conditions were recorded and a series of in-situ tests were performed. The in-situ tests consisted of the pocket penetrometer, torvane, and nuclear densometer tests, the results of which are discussed in detail in the following sections. Subgrade samples were also collected for later laboratory tests.

Prior to the backfilling operations, new geotextiles (same type and manufacturer) were installed to replace the exhumed geotextiles. The edges of the replacement geotextiles overlapped the edges of the existing geotextiles 30 to 50 mm. WSDOT backfilled the test holes with imported aggregate compacted in 200 to 300 mm lifts with a small, vibratory steel-drum roller. The asphalt patches were at least 150 mm thick and consisted of hot-mix asphalt concrete. Figure 5.4 shows several test pits prepared for asphalt patches.

To avoid complications with the station locations during future research on the test road section, a hub (No. 4 rebar) was driven at the edge of the southbound lane 7.3 m from the centerline at Station 177+70. The locations of other landmarks and the dimensions of the test road section were recorded and are shown in Figure 5.1.

It should also be noted that three yellow, plastic instrumentation boxes installed during the Phase I study were encountered at the edge of the southbound lane at Stations 178+57.5, 178+32.5, and 178+07.5, as shown in Figure 5.1. Some of the boxes contained up to about 50 mm of water because the lids were cracked, but otherwise the boxes were in good condition. The boxes contained wires and cables that led to some of the sensors. As discussed in the Phase I study, the electronic instrumentation consisted of moisture/temperature meters, bison coils, and tensiometers.

Attempts were not made to reconnect and take readings from the instrumentation because meaningful information could probably not be obtained. This is because the moisture/temperature meters could not be calibrated during their installation so their readings would not be relevant; the tensiometers were never connected due to complications with the data logger. Also, the main purpose of the bison coils was to evaluate the subgrade strains due to the initial (short-term) installation stresses.

5.2 Exploration Observations

The soil and geotextile conditions encountered in the explorations are summarized in Table 5.1. Figure 5.5 profiles the northbound and southbound lanes, by showing the elevations of the roadway surface and native subgrade stratum. Figures 5.6 through 5.39 are photographs that were taken in the field and laboratory of the soil and geotextile conditions encountered.

The elevations referenced in the Table 5.1 and Figure 5.5 are based on an assumed elevation of 100.00 m for the invert of the culvert shown in Figure 5.1. The elevations were measured by the University of Washington research team with a tripod mounted level. The roadway surface throughout the test section slopes down in the northbound direction at an average slope of 4.4 percent.

At the time of the field investigation, the asphalt pavement in the test road section was in good condition. Pavement distress, such as rutting or fatigue (alligator) cracking was not observed in the asphalt pavement at any location in the test section. As shown in Table 5.1, the asphalt pavement thickness ranged from 152 to 165 mm.

Table 5.1 - Summary of the field exploration data, northbound lane.

Test Section	Station	Surface Elevation (m)	Pavement Thickness (mm)	Depth to Subgrade from Surface (mm)	Mudcake (mm)	Comments:
HB	177+65	101.20	165	510 to 560	10 to 20	Subgrade soil heavily iron stained to a depth of 10 to 30 mm. Organics in subgrade soil to a depth of approx. 80 mm, subgrade soil contains irregular structure. Geotextile heavily iron stained.
NP4	177+90	100.88	165	430 to 610	Trace	Subgrade soil heavily iron stained to a depth of 10 to 20 mm. Trace organics in subgrade soil; subgrade soil contains irregular structure. Subgrade severely rutted along the east edge of test pit. The rut depth appeared to be in excess of 100 mm. Geotextile heavily iron stained.
NP6	178+15	100.52	165	580 to 610	10 to 20	Subgrade soil mottled to a depth of 300+ mm, containing heavy iron stains in the upper 20 to 30 mm. Geotextile heavily iron stained.
Soil	178+40	100.19	165	610	N/A	Subgrade soil mottled to a depth of 100 mm. Intermixing of base course and subgrade soil less than 30 to 50 mm.
NP8	178+65	99.87	165	530	Trace	Subgrade soil heavily mottled to a depth of 300+ mm. No iron staining on top of geotextile, minimal iron staining on bottom of geotextile.
SF	178+90	99.54	165	510 to 530	40 to 50	Subgrade soil iron stained in isolated areas to a depth of 10 mm. No iron staining on top of geotextile, minimal iron staining on bottom of geotextile.

Note: Elevations based on an assumed elevation of 100.00 m for the invert of the culvert shown in Figure 5.1.

Table 5.1 (continued) - Summary of the field exploration data, southbound lane.

Test Section	Station	Surface Elevation (m)	Pavement Thickness (mm)	Depth to Subgrade from Surface (mm)	Mudcake (mm)	Comments:
HB	177+65	101.20	152	860 to 890	Trace*	Subgrade soil mottled to a depth of 100 mm, containing heavy iron stains in the upper 10 mm. Trace organics in subgrade soil; subgrade soil somewhat irregular in structure. Wetted zone of base course soil 30 to 50 mm above geotextile. Aggregate in wetted zone iron stained. Geotextile heavily iron stained.
NP4	177+90	100.88	152	790 to 810	Trace	Subgrade soil mottled to a depth of 50 mm, containing heavy iron stains in the upper 10 to 30 mm. Trace organics (rootlets) in subgrade soil; subgrade soil somewhat irregular in structure. Geotextile heavily iron stained.
SF	178+15	100.52	165	740 to 760	Trace*	Subgrade soil mottled to a depth of 250+ mm, containing heavy iron stains in the upper 10 mm. Wetted zone of base course soil 30 mm above geotextile. Minor to moderate iron staining on geotextile.
Soil	178+40	100.19	165	840	N/A	Heavy groundwater seepage encountered in test pit a depth of 810 mm. Slight mottling of native soil. Intermixing of base course/subgrade soil could not be seen due to water.
NP8	178+65	99.87	165	690	10 to 40	Subgrade soil iron stained in upper 10 mm. Multicolored iron staining of subgrade soil. Wetted zone of base course soil 50 mm above geotextile. Minor to moderate iron staining on geotextile.
NP6	178+90	99.54	165	640 to 690	50	Subgrade soil iron stained in isolated areas to a depth of 10 to 30 mm. Wetted zone of base course soil 50 mm above geotextile. Minor to moderate iron staining on geotextile.

* No significant evidence of migrated fines in the base course, but caked fines on the geotextile.
Note: Elevations based on an assumed elevation of 100.00 m for the invert of the culvert shown in Figure 5.1.

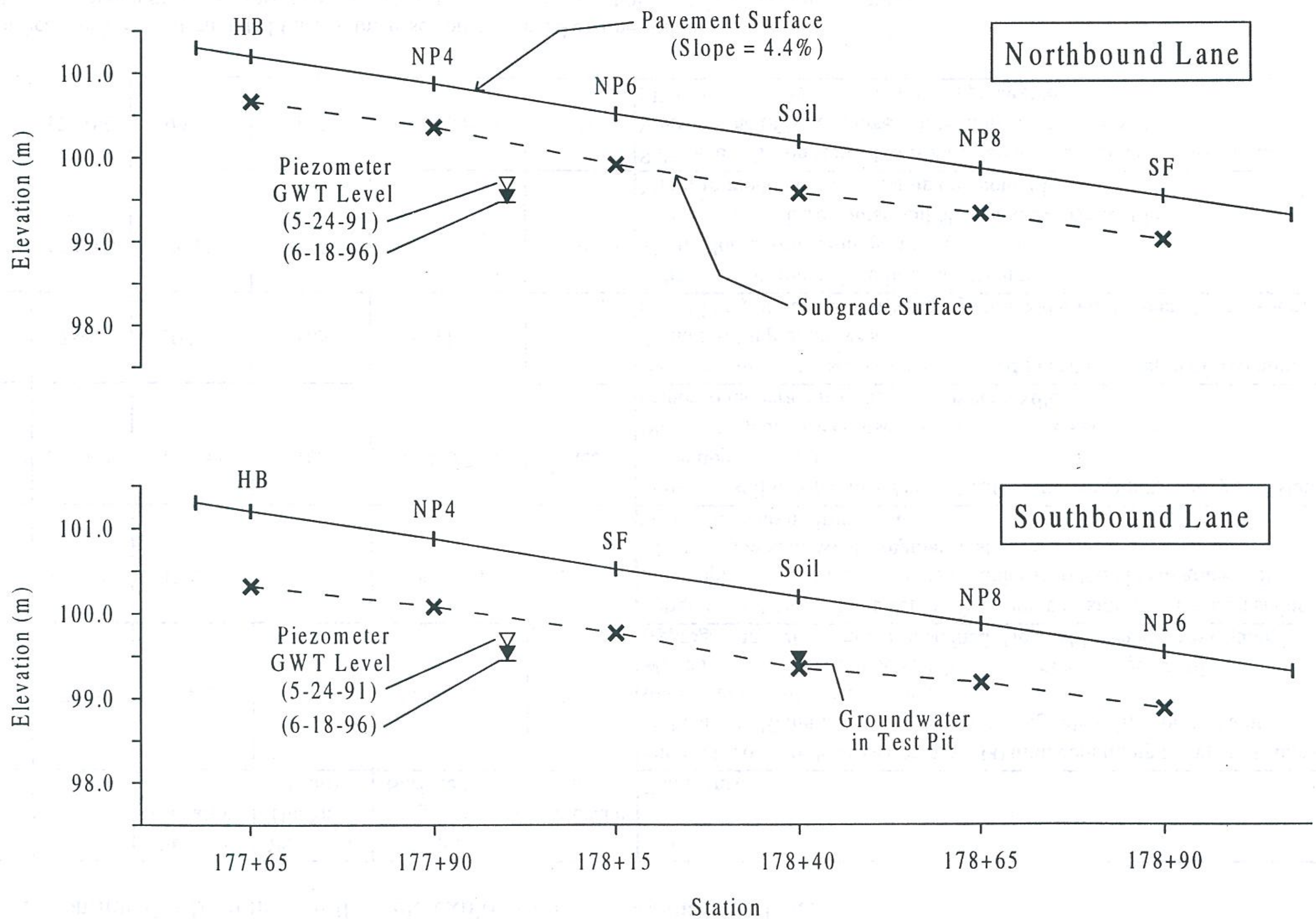

Figure 5.5 - Profile of test section.

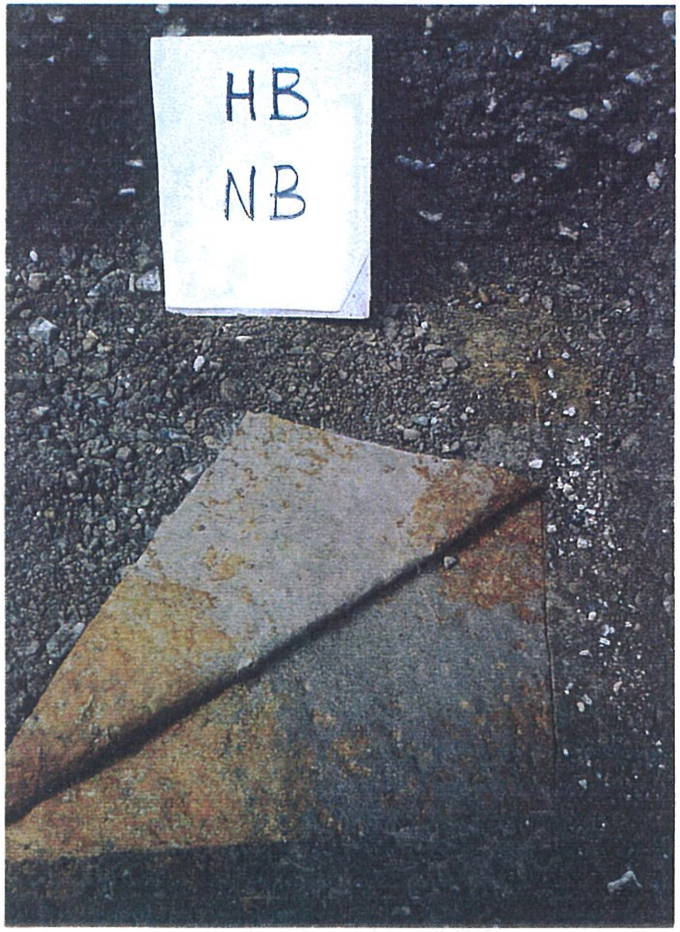

Figure 5.6 - HB-NB geotextile before removal, with corner peeled back

Figure 5.7 - HB-NB geotextile after removal, top face shown.

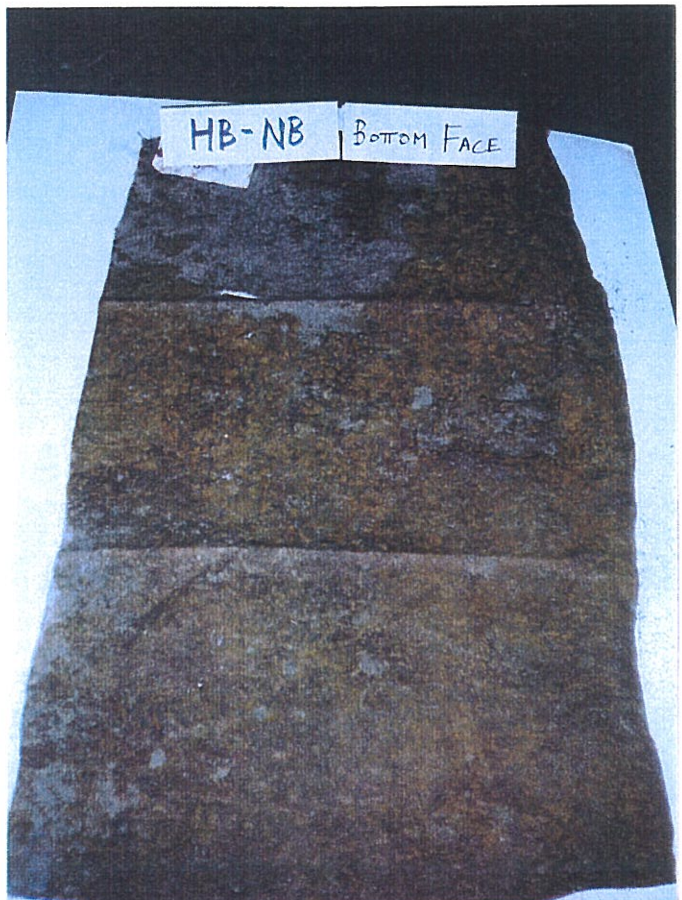

Figure 5.8 (top) - Bottom face of HB-NB, laboratory photograph. Figure 5.9 (bottom) - Bottom face of HB-NB, laboratory photograph showing iron staining.

Figure 5.10 - NP4-NB geotextile after removal, top face shown.

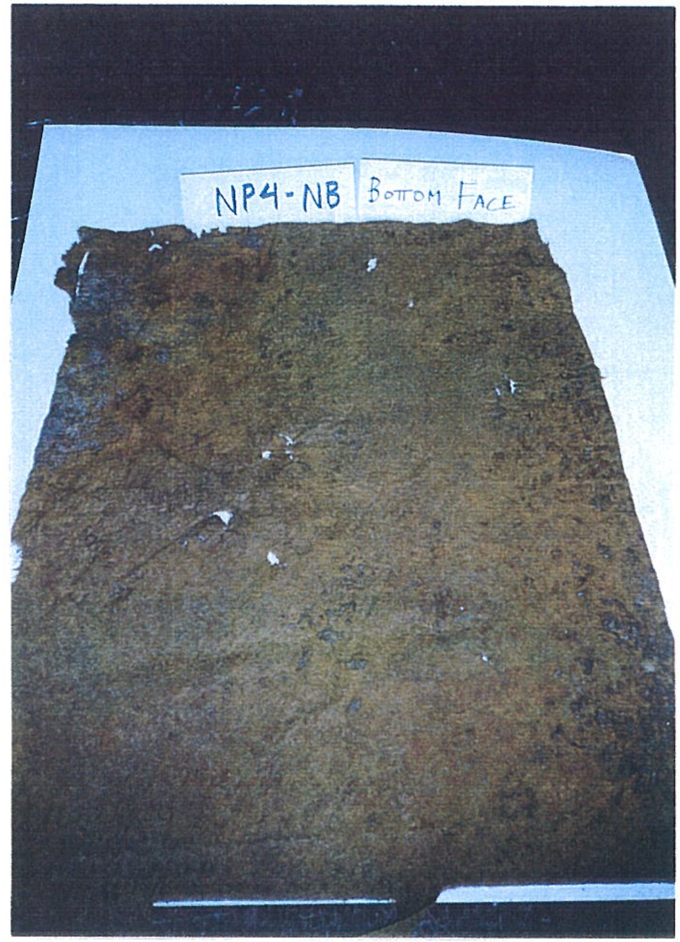

Figure 5.11 - Bottom face of NP4-NB geotextile, lab. photo.

Figure 5.12 (top) - Bottom of NP4-NB wide width specimen, lab. photo. showing iron staining. Arrow indicates machine direction. Figure 5.13 (bottom) - NP6-NB geotextile before removal, with corner peeled back.

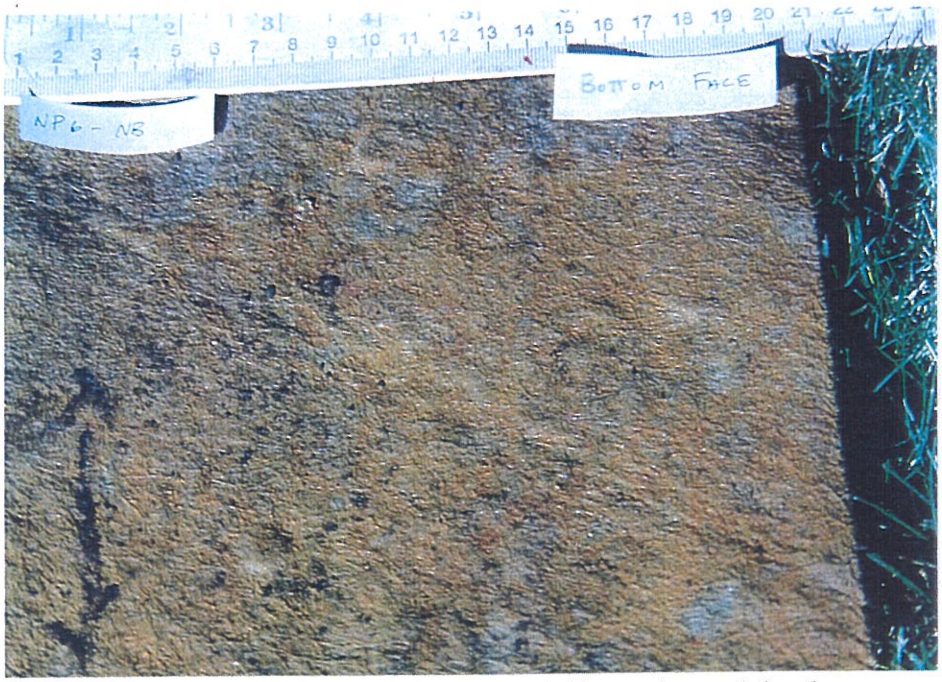

Figure 5.14 - Bottom of NP6-NB wide width specimen, lab. photo. showing iron staining. Arrow indicates machine direction.

Figure 5.15 - Soil-NB section interface between base course and subgrade soils.

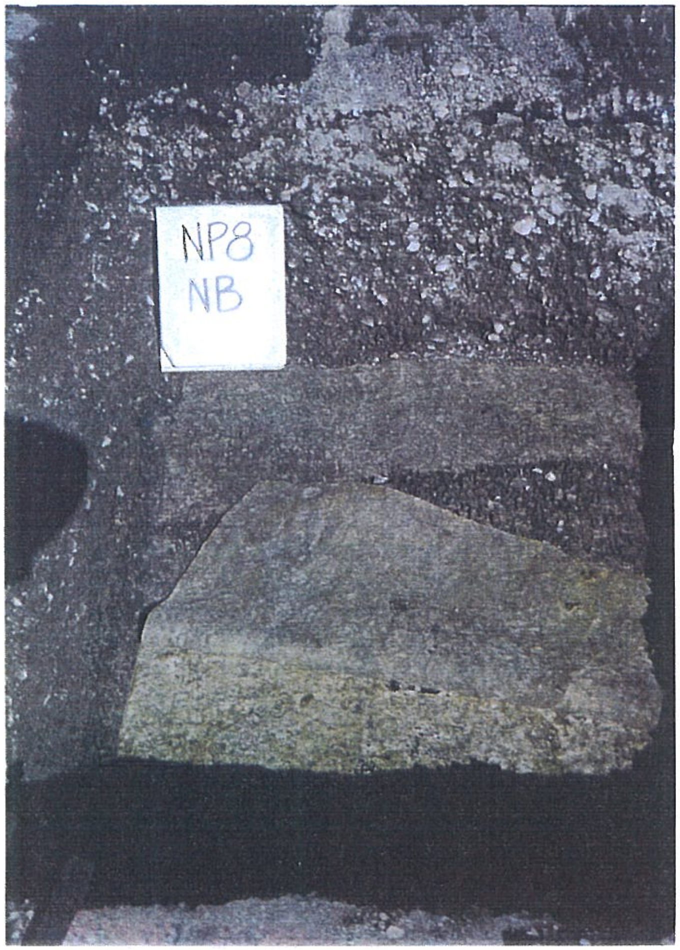

Figure 5.16 - NP8-NB geotextile before removal, with corner peeled back.

Figure 5.17 - NP8-NB subgrade soil, after removal of the samples.

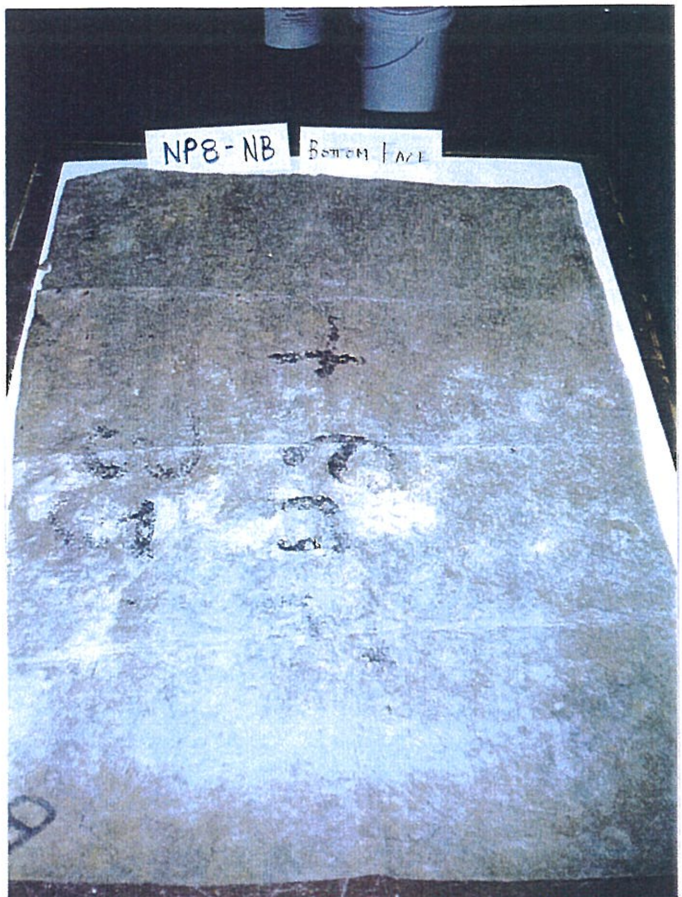

Figure 5.18 (top) - Bottom of NP8-NB geotextile, lab. photo. Figure 5.19 (bottom) - Bottom of NP8-NB wide width specimen, laboratory photograph showing iron staining and indentations from aggregate. Arrow indicates machine direction.

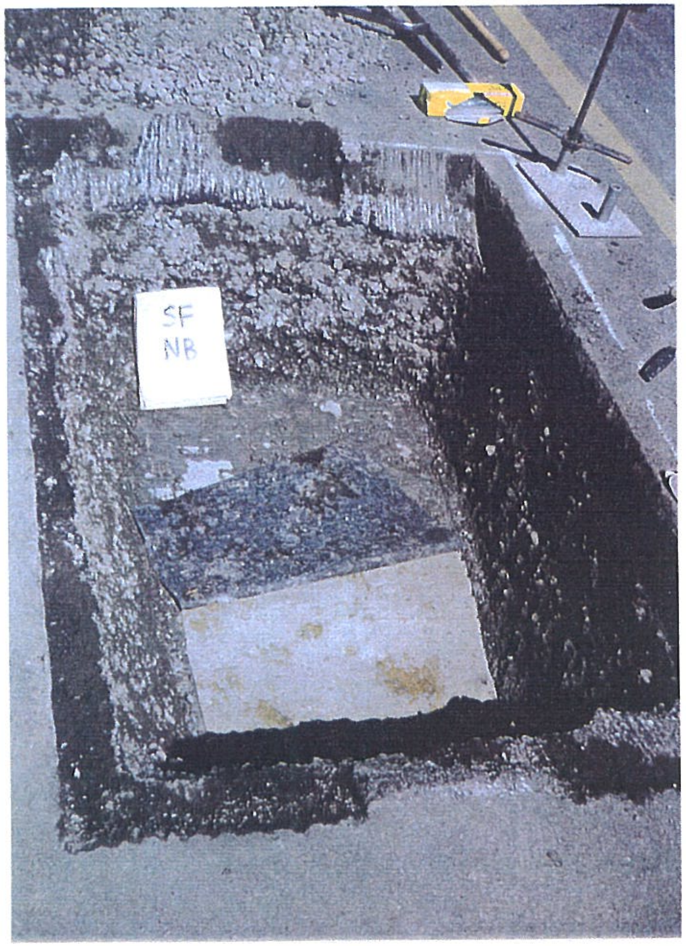

Figure 5.20 - SF-NB geotextile before removal, with corner peeled back.

Figure 5.21 - SF-NB geotextile after removal, bottom face shown.

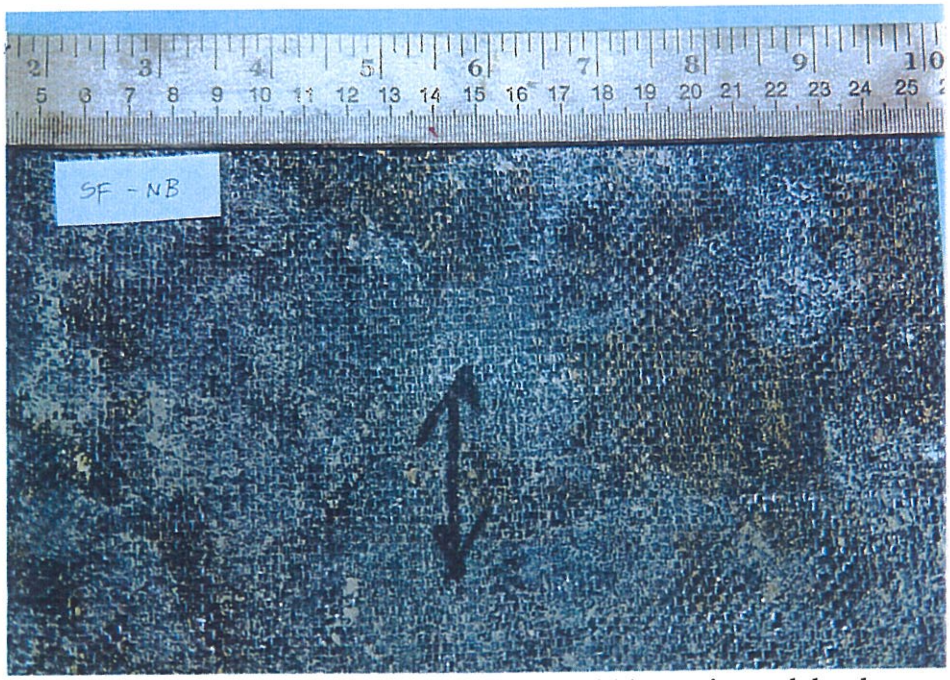

Figure 5.22 - Bottom of SF-NB wide width specimen, lab. photo. showing iron staining. Arrow indicates machine direction.

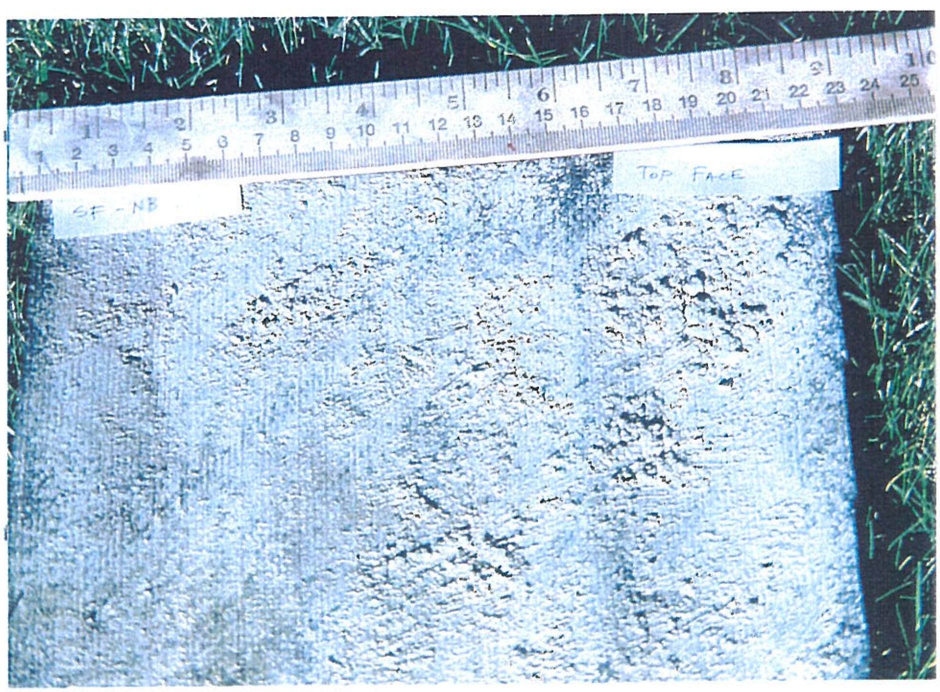

Figure 5.23 - Top of SF-NB wide width specimen, lab. photo. Soil on geotextile is dry.

Figure 5.24 (top) - HB-SB geotextile before removal, with corner peeled back. Figure 5.25 (bottom) - HB-SB geotextile after removal, top face shown.

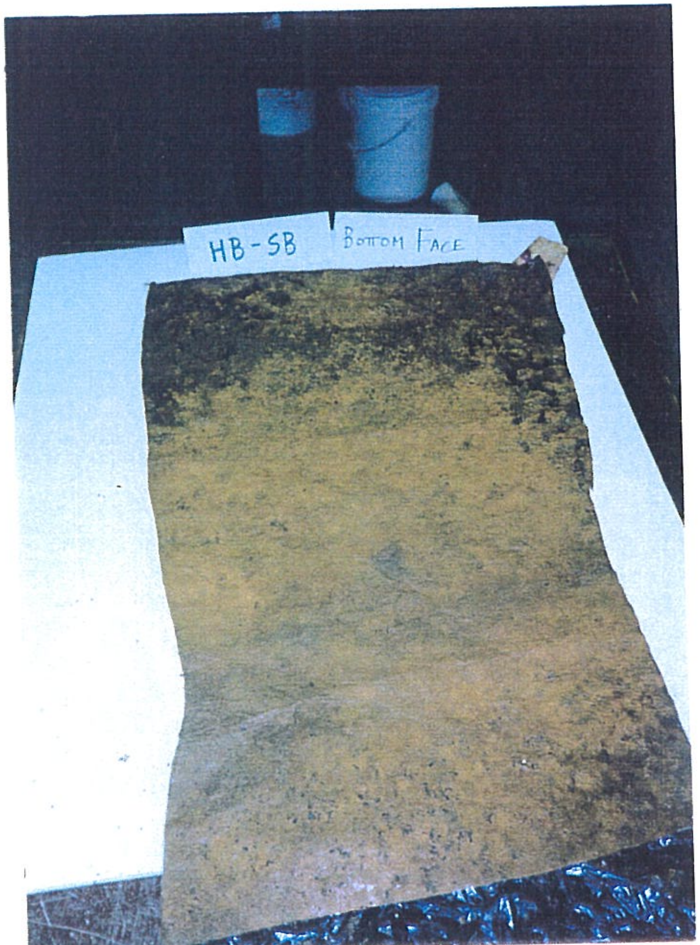

Figure 5.26 - Bottom of HB-SB geotextile, laboratory photograph.

Figure 5.27 - NP4-SB geotextile before removal, with corner peeled back.

Figure 5.28 (top) - Bottom of NP4-SB geotextile, lab. photograph. Figure 5.29 (bottom) - Top of NP4-SB wide width specimen, lab. photograph.

Figure 5.30 - SF-SB geotextile before removal, with corners peeled back.

Figure 5.31 - SF-SB geotextile after removal, top face shown.

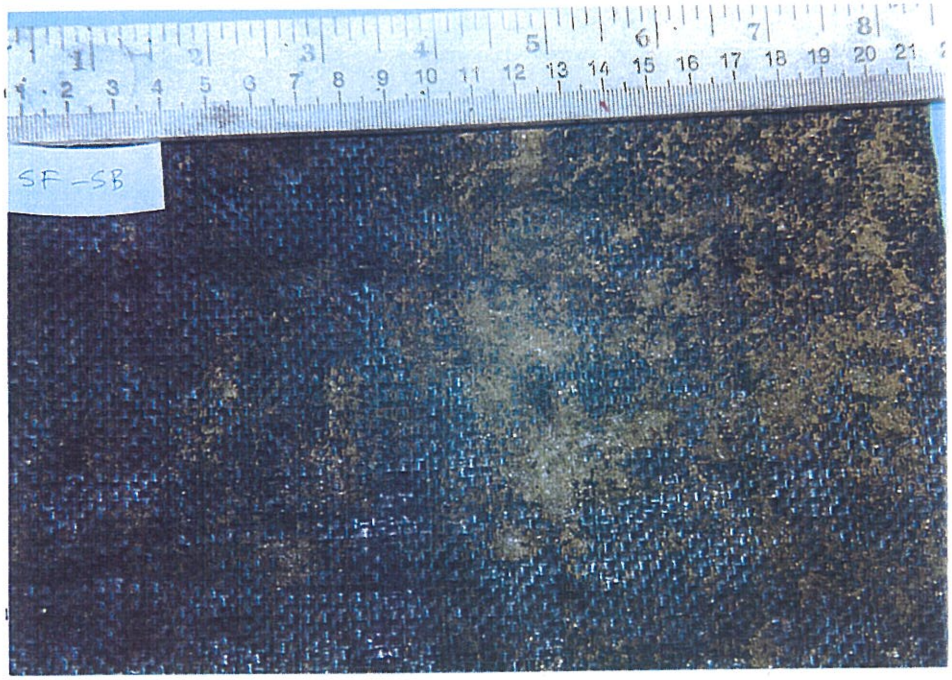

Figure 5.32 - Bottom of SF-SB geotextile,
laboratory photograph showing blinding.

Figure 5.33 - Top of SF-SB wide width specimen,
laboratory photograph showing caking.

Figure 5.34 - Groundwater seepage in Soil-SB excavation.

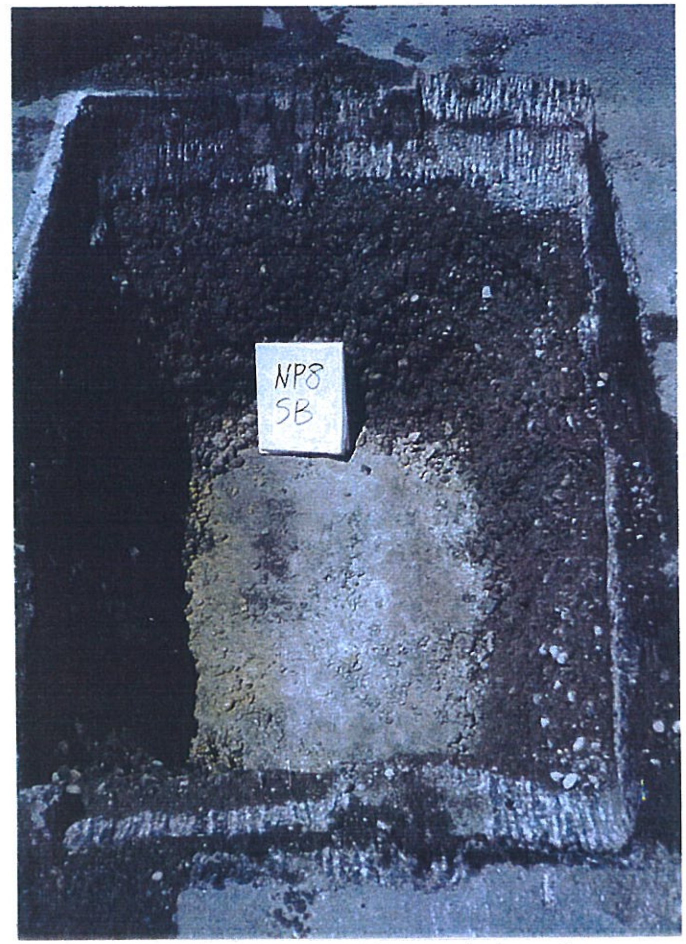

Figure 5.35 - Multicolored iron staining of subgrade soil in NP8-SB excavation after removal of the geotextile.

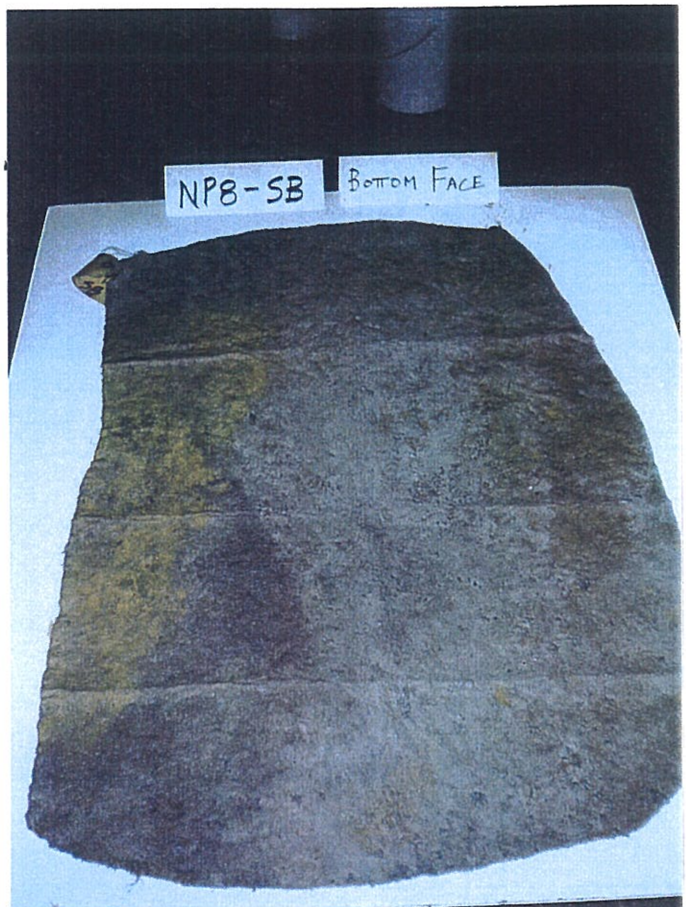

Figure 5.36 (top) - Bottom of NP8-SB geotextile, laboratory photograph showing multicolored iron staining. Figure 5.37 (bottom) - Top face of NP8-SB wide width specimen, laboratory photograph showing caking.

Figure 5.38 (top) - NP6-SB geotextile before removal, with corner peeled back.
Figure 5.39 (bottom) - Bottom of NP6-SB geotextile, laboratory photograph showing iron staining and clogging.

5.2.1 Base Course and Subgrade Soil Observations

The crushed rock base course soils encountered in the excavations were generally dense to very dense, well to poorly graded gravels with sand and some silt. The shape of the majority of the aggregate was subangular to angular. Most of the subgrade soils consisted of medium stiff to stiff, silty clay. However, the subgrade soils were observed to be highly variable in composition, color, moisture condition, and plasticity. Laboratory tests also showed this variability, as discussed later. Portions of the HB and NP4 subgrade soils in both lanes may have contained fill or even colluvium, as suggested by the irregular structure of the soil samples and the organic debris observed in these sections, noted in Table 5.1.

The somewhat inhomogeneous subgrade soils encountered in the NP6-NB, NP8-NB, and SF-SB excavations were probably residual deposits formed by weathering of a sandstone bedrock. Sampling excavations revealed that these soils were heavily mottled to depths in excess of 300 mm. The mottling is likely due to the combination of the soil mineralogy and seasonal fluctuation of the groundwater table. Although the subgrade soils encountered at other locations may have originated from the same residual deposits, they typically had a more homogeneous texture and were not as deeply mottled.

Although deep mottling conditions were not observed in all subgrade soils, iron staining was observed on the surface of the subgrade soils at all exploratory locations once the geotextile was removed, as shown in Figures 5.6, 5.13, 5.17, 5.20, 5.24, 5.27, 5.30, 5.35, and 5.38. Where observed, the iron staining appeared to penetrate 10 to 30 mm into the soil stratum, as indicated in Table 5.1. It is interesting to note the variety of stain colors shown in the photographs, particularly the multicolored staining at the NP8-SB location, Figure 5.35. (It should be noted that the observed rust colorations are referred to as iron stains or iron oxide precipitates throughout this report. These colorations may be due to other minerals; however, testing to determine the soil mineralogy was beyond the scope of this project.)

The general subgrade conditions during the installation of the geotextiles were noted to be soft and saturated in the Phase I study. During the trafficking tests for the Phase I study, the rut depths in the initial layer of fill after ten passes of a loaded dump truck ranged from 19 to 264 mm in the northbound lane, and 3 to 38 mm in the southbound lane. The most severe rutting (264 mm) was located in the outside wheel path of the NP4-NB section. The subgrade soils at all explorations were generally observed to be firm and consolidated during the field investigation performed for this study, even at the NP4-NB section where the subgrade was found to be rutted in excess of 100 mm on the eastern edge of the test pit. Tsai and Savage (1992) indicate that ruts up to 160 mm in depth were measured in the inside wheel path of this section during the trafficking tests. It should be noted that subgrade observations could not be made at the Soil-SB section due to the groundwater encountered, as discussed in the following section.

5.2.2 Groundwater Observations

As noted in Table 5.1 and shown in Figure 5.34, heavy groundwater seepage was encountered approximately 30 mm above the subgrade soil in the Soil-SB excavation. Groundwater seepage was not encountered in any of the other excavations. It is not clear why groundwater was retained at the Soil-SB location. A possible explanation is that the geotextiles in the other sections provided some lateral drainage. Another possibility is that groundwater at the Soil-SB location may have been perched in a low area of the subgrade, although this is difficult to ascertain from the subgrade profile shown in Figure 5.5. A wetted zone of base course aggregate was also observed approximately 30 to 50 mm above all the geotextiles in the southbound lane, except at the NP4-SB location. This wetted zone suggests the groundwater table may have temporarily risen due to the rain events that occurred in the previous weeks, or possibly after the rain on the first day of the field investigations.

As mentioned in Section 2.0, a plastic standpipe piezometer was installed adjacent to the northbound lane (shown in Figure 5.1) by WSDOT during an exploratory boring in May, 1991. Measurements taken on June 18, 1996 indicated the water level was 0.91 m below the ground surface at the piezometer location. The boring log (Appendix A) indicates that the water level was at a depth of 0.76 m on May 24, 1991. The elevations of the piezometer water levels are shown in the test section profile, Figure 5.5. As shown in the figure, the groundwater elevation observed in the Soil-SB excavation roughly coincides with the water level measured in the piezometer.

5.2.3 Fines Migration Observations

Varying amounts of fines from the subgrade soils appeared to have migrated through the geotextiles into the base course. This zone of intermixed base course and migrated fines above the geotextile is termed "mudcake" in this report. The maximum penetration of the migrated fines into the base course soils was observed to be 50 mm above the geotextiles at the SF-NB and NP6-SB locations, as indicated in Table 5.1. In general, the fines in the mudcake soils were the same color as the underlying subgrade soils. Even in cases where heavy iron stains were present in the subgrade soils, the fines in the mudcake soils were stained similar colors.

As indicated in Table 5.1, significant evidence of subgrade fines migration into the base course aggregate was not observed at the HB-SB and SF-SB locations, but caked fines were observed on the geotextiles. The lack of mudcake at these locations suggests that a majority of the caked fines on these geotextiles probably originated from the base course. However, it cannot be ruled out that a portion of the caked fines may have migrated from the subgrade.

Figure 5.15 shows the interface between the base course and subgrade soils in the Soil-NB location. The zone of intermixing was observed to be about 30 to 50 mm thick. The zone of intermixing could not be seen in the Soil-SB location due to the heavy groundwater seepage discussed above.

5.2.4 Geotextile Observations

Figures 5.6 through 5.39 show that the geotextiles contained various amounts of iron staining. (It should be mentioned the geotextiles samples in the photographs are damp/wet, unless otherwise noted.) The iron staining on the woven geotextiles was in the form of iron oxide precipitates deposited on the surface of the geotextiles. The iron oxides did not appear to be deposited on the surface of the nonwoven geotextiles, rather the oxide precipitates tended to be distributed throughout the geotextile structure, discoloring the geotextile. As in the subgrade soil observations, it is interesting to note the variety of stain colors on the geotextiles, particularly the multicolored staining on the NP8-SB geotextile sample, Figure 5.36. A close-up photograph of the iron staining on a portion of the HB-NB geotextile is also shown in Figure 5.9.

The geotextile samples exhumed from the southbound lane were generally wetter than the geotextile samples from the northbound lane. This may have been due to a temporary rise in the ground water table which also contributed to the wetted zone of aggregate observed above the geotextiles in the southbound lane, discussed in Section 5.2.2.

In general, the geotextiles contained a minimal amount of damage due to aggregate puncture. However, angular aggregates did partially penetrate isolated areas of the lighter-weight nonwoven geotextiles, particularly the NP4 geotextile. The holes created by the partially penetrated aggregates varied in size but were generally less than 1 to 2 mm in diameter. Aggregate indentations were commonly observed on all of the geotextile samples, as shown in Figures 5.6, 5.14, 5.19, 5.21, and 5.24. A more detailed description of the damage to the geotextiles is provided in Section 6.2. It should be noted that most of the relatively large tears and holes in the geotextiles shown in Figures 5.7, 5.8, and 5.10 occurred during the excavation process.

As discussed earlier, the subgrade soil at the NP4-NB exploration location was found to be rutted in excess of 100 mm on the eastern edge of the test pit. Due to the excessive deformations, the geotextile was torn along the edge of the rut.

5.3 In-Situ Soil Test Results

The in-situ tests performed on the subgrade soils consisted of pocket penetrometer, torvane and density tests. Similar tests were performed on the subgrade soils during the Phase I study. Comparisons between the results are presented in Section 8.0.

5.3.1 Strength Tests

Pocket penetrometer and torvane tests were performed on the surface of the subgrade soil immediately after the geotextile was removed. The results of the tests are presented in Tables 5.2 and 5.3, and in Figures 5.40 and 5.41. Note that tests were not performed on the subgrade soils in the Soil-SB section due to the groundwater encountered.

Even though the pocket penetrometer and torvane tests produce reasonable estimates of the undrained shear strength, it is important to recognize the uncertainties associated with these in-situ tests, particularly those related to the shallow depths and small areas of soil tested by these instruments. The strength measured by the pocket penetrometer is derived by depressing a 6.4 mm diameter probe into a soil stratum. The depth of influence is 13 mm at most (twice the diameter). The torvane measures the strength required to shear a 18.8 mm diameter shear vane plate depressed approximately 3.6 mm into soil. Also, the potential for variability is increased when these tests are performed on inhomogeneous soils, such as some of the residual soils encountered at this site. These factors likely contribute to the high standard deviation values shown in Tables 5.2 and 5.3.

The pocket penetrometer and torvane tests produced similar trends in shear strength for the subgrade soils in the southbound lane, shown in Figure 5.41. The pocket penetrometer and torvane results did not agree with each other for the northbound lane, as shown in Figure 5.40. However, the difference between the values produced by the two tests appear to be within a tolerable range considering the uncertainty associated with the test methods, as discussed above. The lines connecting the data points in Figures 5.40 and 5.41 are intended to aid in presenting

Table 5.2 - Results of pocket penetrometer tests, shear strength (kPa).

Section	HB-NB	NP4-NB	NP6-NB	Soil-NB	NP8-NB	SF-NB	HB-SB	NP4-SB	SF-SB	Soil-SB	NP8-SB	NP6-SB
	105.3	47.9	114.9	57.5	119.7	33.5	162.8	47.9	129.3	N/A	19.2	57.5
		110.1	86.2	38.3	158.0	57.5	158.0	38.3	114.9		33.5	43.1
		43.1	124.5	47.9	143.6	33.5	158.0	57.5	129.3		28.7	62.2
		81.4	47.9	62.2	114.9	33.5	< 215.5	81.4	100.5		38.3	38.3
		57.5	71.8	57.5	153.2	33.5	< 215.5	57.5	91.0		33.5	43.1
		81.4	114.9		< 215.5	52.7	158.0	33.5	114.9			43.1
		81.4	91.0		< 215.5	33.5	< 215.5	76.6	114.9			52.7
			95.8		138.9		< 215.5	38.3				43.1
					134.1			33.5				
								43.1				
Average	105.3	71.8	93.4	52.7	154.8	39.7	187.3	50.8	113.5	N/A	30.6	47.9
Std. Dev.	--	23.6	25.3	9.6	37.1	10.6	30.1	17.2	14.0	N/A	7.3	8.5

Table 5.3 - Results of torvane tests, shear strength (kPa).

Section	HB-NB	NP4-NB	NP6-NB	Soil-NB	NP8-NB	SF-NB	HB-SB	NP4-SB	SF-SB	Soil-SB	NP8-SB	NP6-SB
	83.8	100.5	69.4	93.4	102.9	76.6	177.2	69.4	62.2	N/A	71.8	79.0
	100.5	98.2	93.4	83.8	110.1	79.0	126.9	67.0	95.8		67.0	69.4
	114.9	155.6	105.3	95.8	98.2	57.5	134.1	74.2	126.9		79.0	76.6
	91.0	98.2	148.4	105.3	110.1	59.9	179.6	74.2	126.9		62.2	88.6
			129.3		74.2	57.5			107.7		59.9	79.0
			83.8		79.0	50.3			100.5		86.2	
					119.7				119.7		67.0	
Average	97.6	113.1	104.9	94.6	99.2	63.4	154.4	71.2	105.7	N/A	70.5	78.5
Std. Dev.	13.5	28.4	29.4	8.9	16.9	11.6	27.8	3.6	22.8	N/A	9.4	6.9

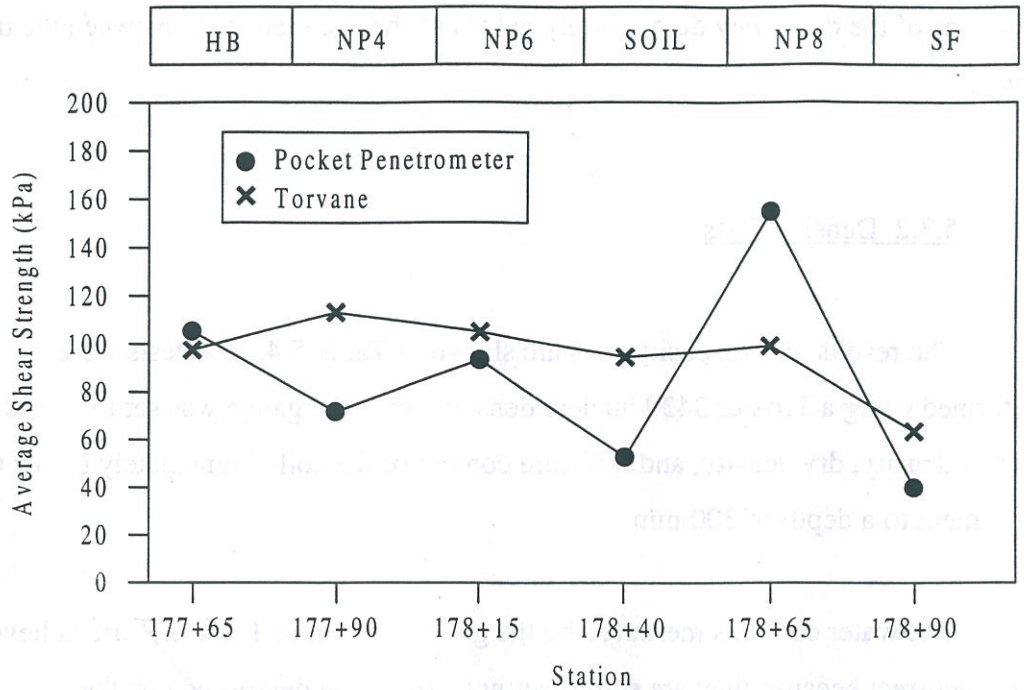

Figure 5.40 - Pocket penetrometer and torvane test results, northbound lane.

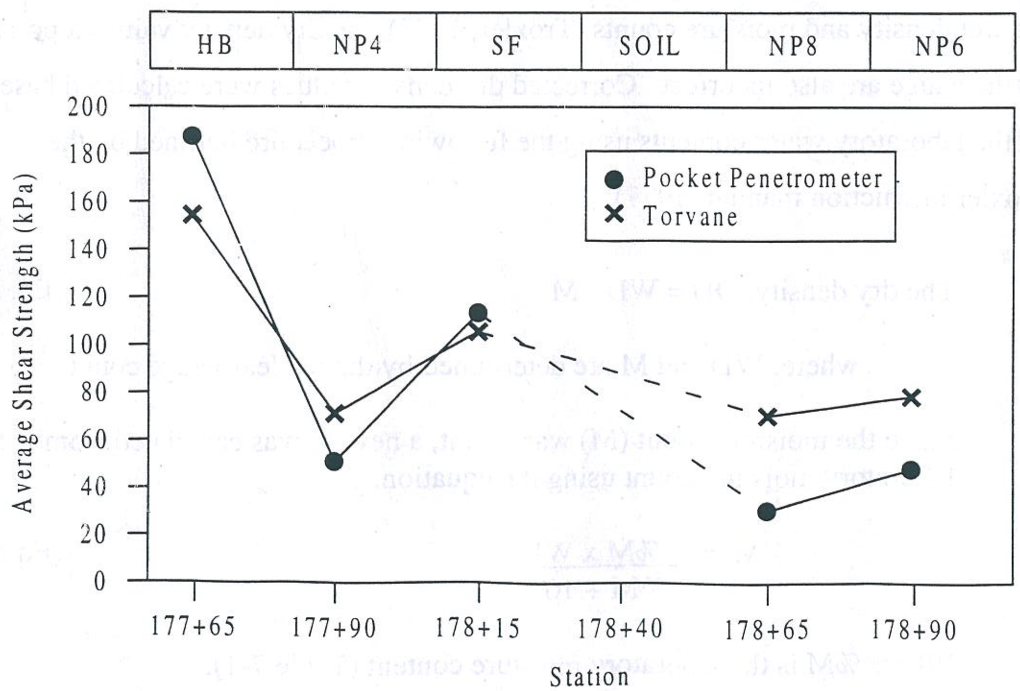

Figure 5.41 - Pocket penetrometer and torvane test results, southbound lane.

the trends of the data; they do not imply values of the shear strength between the data points.

5.3.2 Density Tests

The results of the density tests are shown in Table 5.4. The tests were performed using a Troxler 3430 nuclear densometer. The gauge was set to measure the wet density, dry density, and moisture content of the soils immediately below the instrument to a depth of 300 mm.

The water contents measured by the gauge (shown in Table 5.4) are believed to be incorrect because they are significantly below those determined by the laboratory tests, shown later in Section 7.2.1 (Table 7.1). The reason for the discrepancy is not clear. However, because the gauge determines the dry density from the wet density and moisture counts (Troxler, 1977), the dry density values reported by the gauge are also incorrect. Corrected dry density values were calculated based on the laboratory water contents using the following procedure outlined by the Troxler instruction manual (1977):

The dry density, $DD = WD - M$ (Eq. 5-1)

where, WD and M are determined by the nuclear gauge count.

Since the moisture count (M) was errant, a new M was calculated from the laboratory moisture count using the equation:

$$M = \frac{\%M \times WD}{\%M + 100} \qquad \text{(Eq. 5-2)}$$

Where %M is the laboratory moisture content (Table 7-1).

Table 5.4 - Results of density tests with corrected values.

Section	Station	WD (Mg/m^3)	Gauge DD (Mg/m^3)	Gauge Moisture (%)	Corrected M (Mg/m^3)	Corrected DD (Mg/m^3)
HB - NB	177+65	1.86	1.74	6.8	0.44	1.43
NP4 - NB	177+90	1.90	1.76	7.8	0.42	1.48
NP6 - NB	178+15	1.87	1.72	8.3	0.46	1.41
Soil - NB	178+40	1.67	1.53	8.9	0.62	1.05
NP8 - NB	178+65	1.83	1.67	9.7	0.54	1.29
SF - NB	178+90	1.83	1.67	9.3	0.51	1.32
HB - SB	177+65	1.99	1.88	5.8	0.36	1.63
NP4 - SB	177+90	1.78	1.62	10.0	0.58	1.20
SF - SB	178+15	1.90	1.76	8.3	0.44	1.46
Soil - SB	178+40	1.79	1.58	13.6	0.52	1.28
NP8 - SB	178+65	1.81	1.64	10.3	0.55	1.26
NP6 - SB	178+90	1.84	1.68	9.4	0.53	1.31

Notation: WD = Wet Density
DD = Dry Density
M = Moisture Count

5.4 FWD Tests

Falling weight deflectometer (FWD) tests were performed on the test section by WSDOT personnel on April 29, 1991, just before the installation of the geotextiles in June 1991. Tests were subsequently conducted on July 24, 1991, November 25, 1991, and March 25, 1996.

5.4.1 Discussion of the FWD Test Method

FWD tests are nondestructive tests used to evaluate the elastic moduli of various pavement components. The FWD testing equipment delivers a transient force impulse to the pavement surface and measures the resulting deflections with up to seven velocity transducers placed at various distances from the applied load. The major advantage of this type of device is its ability to accurately model a moving wheel load in both magnitude and duration and the use of a relatively small static load compared to the impulse loading (Huang, 1993).

The Dynatest Model 8000 FWD system applies an impulse load ranging from 6.7 to 107 kN by dropping a weight ranging from 50 to 300 kg from a height of 20 to 381 mm. The duration of the load pulse is about 25 to 30 ms. The load is transmitted to the pavement system by a 300 mm diameter loading plate. The seven velocity transducers used to measure the deflections can be raised and lowered hydraulically with the loading plate. One of the transducers is located in the center of the loading plate. The testing equipment is trailer-mounted for ease of transportation and rapid testing.

The output summary values provided by WSDOT include maximum pavement deflections, area values, and estimated subgrade moduli. The maximum pavement deflections were determined from the sensor at the center of the loading plate. The area values were formulated by combining the deflection measurements from four of the transducers. The theoretical minimum and maximum area values are 280 and 915 mm, respectively. Low area values suggest the pavement structure is similar to the underlying subgrade material (which is not necessary bad if the if the subgrade is extremely stiff). High area values indicate the pavement system is extremely stiff (WSDOT Pavement Guide, 1995). Note that the units of the area value are mm not mm^2 because they are normalized by the surface deflection at the center of the test load.

5.4.2 FWD Test Results

The results of the FWD tests performed on March 25, 1996 are presented in Tables 5.5 and 5.6. The results of the tests performed in 1991 are presented in Tables A.1 through A.6 in Appendix A. Comparisons between the test results are provided in Section 8.1.1.

The output summary values in Tables 5.5 and 5.6 were normalized by WSDOT to a 40 kN load adjusted for pavement thickness and temperature. The area values were normalized to a 103.4 MPa subgrade modulus. The moduli determinations were based on deflections at the fourth sensor, 0.61 m from the load plate.

Table 5.5 - Results of FWD tests in northbound lane, March 25, 1996.

Station	Geotextile	Deflection (mm)	Area Value (mm)	Subgrade Modulus (kPa)
177+68	HB-NB	0.52	518	97213
178+13	NP6-NB	0.46	551	99254
178+38	Soil-NB	0.51	521	97344
178+63	NP8-NB	0.54	528	86905
178+88	SF-NB	0.73	470	77893
179+13		0.78	455	78851

Table 5.6 - Results of FWD tests in southbound lane, March 25, 1996.

Station	Geotextile	Deflection (mm)	Area Value (mm)	Subgrade Modulus (kPa)
177+68	HB-SB	0.59	483	96902
178+13	SF-SB	0.56	505	90587
178+38	SF-SB	0.65	488	81375
178+63	Soil-SB	0.52	528	89821
178+88	NP6-SB	0.68	503	71122
179+13		1.26	401	54967

6.0 Laboratory Geotextile Observations

The exhumed geotextile samples were brought back to the laboratory for detailed examination. The evaluation included assessing the damage to the geotextiles caused by the installation operations and the exhumation procedures. The degree of blinding and clogging, and the iron staining the geotextiles experienced was also evaluated. The geotextiles were also examined under a microscope with photographic capability.

6.1 Discussion of Observation Techniques

The geotextiles were placed over a light table so that the damage could be more easily assessed. Geotextile damage from aggregate puncture was interpreted to be due to the construction procedures. Aggregate puncture damage typically seemed to fray the polymer filaments in the nonwoven geotextiles, and break or separate the tapes of the woven geotextiles. Damage consisting of sharp tears or cuts of the filaments or tapes was assumed to be due to the exhumation procedures.

During the laboratory observations, blinding was interpreted as the blockage of pore openings on the bottom surface of the geotextile. Clogging was defined as the entrapment of soil particles within the pore structure of the geotextile, while caking was defined as the deposition of soil particles on the top surface of the geotextile, as illustrated in Figure 4.1. These definitions are consistent with Metcalfe and Holtz (1994). Detailed definitions of blinding, clogging, and caking are discussed further in Section 4.1.2.

Observations of the iron staining were also made. As previously mentioned, the observed rust colorations on the geotextiles are referred to as iron stains or iron oxide precipitates throughout this report, although these colorations may be due to other minerals. Testing to determine the soil chemistry and mineralogy was beyond the scope of this project.

6.2 Results of the Laboratory Observations

The results of the laboratory observations of the geotextiles are presented in Table 6.1. Holes or tears in the geotextiles less than 2 mm in size were not recorded. Recording the number and size of holes less than 2 mm would have been difficult because of the high degree of blinding, clogging, and caking of some of the specimens. Attempts to do so would have also been very time consuming.

As shown in Table 6.1, the northbound lane geotextile samples contained more construction damage than the southbound lane samples. This is most likely because the initial lift of base course was approximately 150 mm thick in the northbound lane, as opposed to 300 mm thick in the southbound lane. The high level of damage to the NP4-NB sample may be related to the large geotextile deformations incurred during the traffic tests performed for the Phase I study, and discussed in Section 5.2.4.

In general, the exhumed nonwoven geotextiles contained various degrees of clogging, but did not appear to be significantly blinded. Conversely, the woven geotextiles appeared to be more affected by blinding than clogging. Similar trends involving the blinding and clogging of woven and nonwoven geotextiles were observed by Metcalfe and Holtz (1994).

Iron oxide precipitates deposited on the surface of the woven geotextiles (discussed in Section 5.2.4) covered some of the pore openings. The iron oxides tended to discolor the nonwoven geotextiles by being distributed throughout their structure.

Table 6.1 - Results of geotextile laboratory observations.

Geotextile	Sample Size (cm x cm)	Holes ≥ 2 mm in Size Caused by Aggregate Puncture	Tears ≥ 2 mm in Size Caused by Excavation Procedures	Percent Blinding/ Clogging	Percent Iron Staining	Comments
HB-NB	61 by 91	5 mm	15, 50 mm	65 to 80	55 to 65	Slight to moderate caking.
NP4-NB	61 by 112	3 mm , 3 mm, 3 mm, 4 mm, 4 mm, 7 mm 8 mm, 13 mm, 22 mm	6 mm, 19 mm, 19 mm 21 mm, 30 mm, 42 mm 52 mm, 55 mm	60 to 80	90 to 95	Slight to moderate caking.
NP6-NB	58 by 91	3 mm, 3 mm		65 to 80	90	Minimal caking (< 5%).
NP8-NB	76 by 107	8 mm	8 mm, 10 mm, 15 mm 19 mm, 20 mm, 29 mm	50 to 65	< 5	Black writing on bottom face, from Phase I study. Minimal caking (< 5%).
SF-NB	66 by 102	7 mm	20 mm, 23 mm	15 to 30	5 to 10	Sporadic iron oxide deposits. Heavy caking.
HB-SB	56 by 97			85 to 95	95	Slight to moderate caking.
NP4-SB	66 by 112	3 mm, 3 mm		90 to 95	90	Moderate caking.
NP6-SB	76 by 99		4 mm	80 to 90	10 to 25	Moderate to heavy caking.
NP8-SB	64 by 86			95	25 to 30	Multicolored staining. Heavy caking.
SF-SB	84 by 137		4 mm	15 to 25	20 to 30	Sporadic iron oxide deposits. Moderate to heavy caking.

Note: The lighter-weight geotextiles (HB and NP4) contained the most damage due to partially penetrated aggregates. The majority of the holes were less than 1 to 2 mm in size.

The visual estimates of blinding and clogging in Table 6.1 include the effects of both soil particles and chemical precipitates. Discerning the influence of each on the permittivity characteristics was beyond the scope of this study.

It was found that the soil particles blinding the bottom and caked on the top of the woven slit-film geotextiles easily flaked off, especially after a small amount of drying. The actual amount of soil particles (or iron oxide precipitates) blinding the slit-film geotextiles in-situ is probably higher than that observed in the laboratory, as some of the blinding soil particles likely became dislodged when the geotextiles were removed from the subgrade. These problems were not associated with the nonwoven geotextiles because they were more susceptible to clogging than blinding, discussed above. Little material was lost in handling the nonwoven geotextiles because the particles clogging them were trapped within the fibers of the geotextiles.

On the whole, the nonwoven geotextiles in the southbound lane contained higher percentages of clogging than the northbound lane samples, as indicated in Table 6.1. The north and southbound slit-film geotextiles contained about the same amount of blinding. Also, there does not appear to be trends of increased or decreased iron staining between any of the geotextiles.

A significant amount of caking was observed on the NP6-NB, SF-NB, HB-SB, SF-SB, NP8-SB, and NP6-SB geotextiles samples. Photographs illustrate the caking in Figures 5.13, 5.23, 5.25, 5.31, 5.33, 5.37, and 5.38. As discussed in Section 5.2.3, it appears that a significant amount of the caked fines migrated through the geotextiles from the underlying subgrade, except at the HB-SB and SF-SB locations where the lack of mudcake suggests that the caked fines on the geotextiles may have more likely originated from the base course. The results of the hydrometer test performed on the SF-NB mudcake fines support the observation that the caked fines migrated from the subgrade soils, as discussed in Section 7.2.2.

6.3 Microscope Observations

A microscope with photographic capability was used to examine the geotextiles. Figures 6.1 through 6.8 show photographs of the specimens. Figures 6.1, 6.3, 6.4, and 6.7 show photographs of the specimens in antecedent and dry moisture conditions. Figures 6.2, 6.5, 6.6, and 6.8 are photographs of permittivity specimens after the washing procedures. The scale in the photographs was determined by taking a duplicate of each picture with a ruler inserted into the field of view.

Figure 6.1 shows the bottom of a severely blinded and clogged portion of a heat-bonded geotextile. As shown in the figure, the dry soil particles and iron oxides appear to cling to portions of the geotextile filaments. Figure 6.2 shows a heat-bonded specimen after the washing procedures used for the permittivity tests, discussed in Section 7.1.4. The soil particles and iron oxide precipitates were difficult to wash from the specimen using the washing techniques, as evidenced by clogging of some of the smaller pore spaces. Based on observations at this magnification level, the geotextile filaments appear to be intact and undamaged. Note that the magnification used in Figure 6.2 is about the highest level attainable by the optical microscope.

Figures 6.3 and 6.4 show the antecedent and dry moisture conditions, respectively, of two needle-punched geotextile samples. As shown in Figure 6.3, the soil particles and iron oxide precipitates appear to be suspended in solution. However, when allowed to dry, some of the particles cling to the filaments as observed in the heat-bonded samples. Figures 6.5 and 6.6 show needle-punched specimens after the washing procedures used for the permittivity test. Small areas of red colorations (possibly iron oxide precipitates) can be seen on the filaments in Figure 6.5. Figure

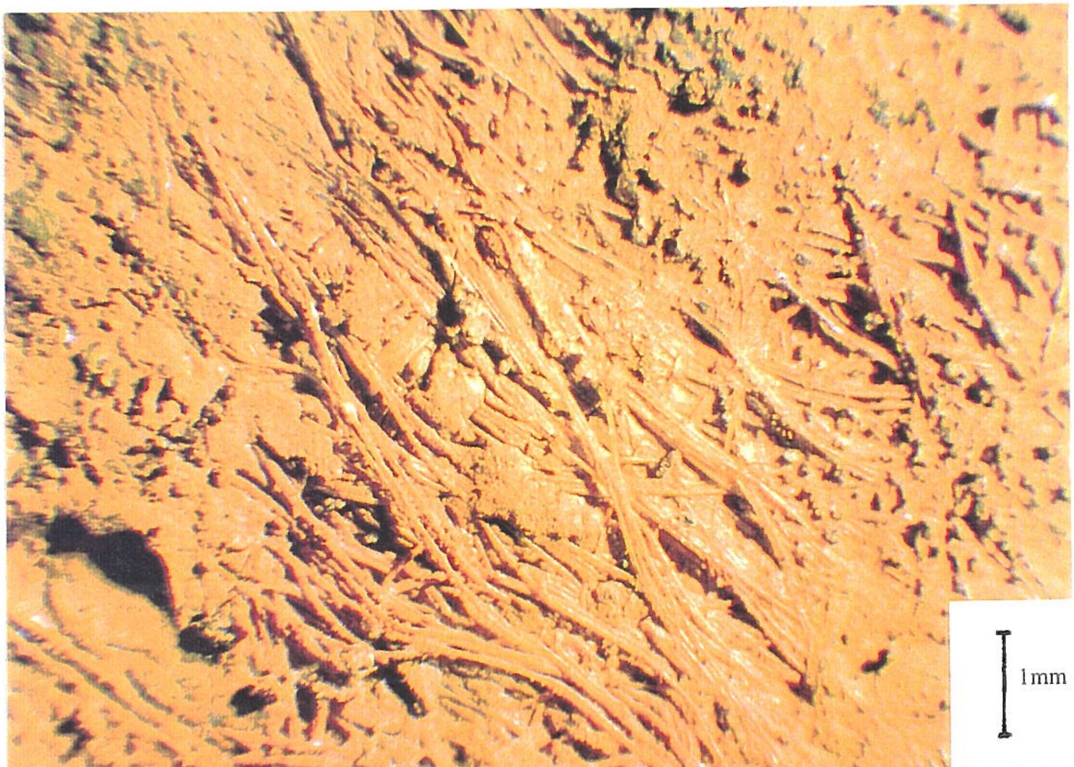

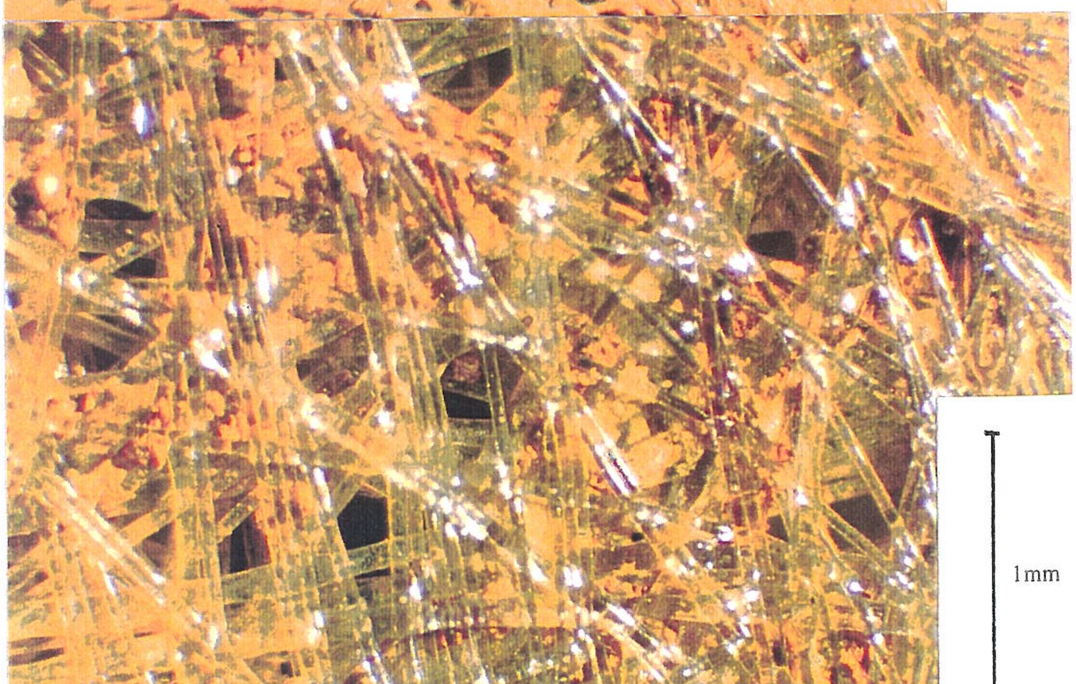

Figure 6.1 (top) - Dry HB-SB geotextile, bottom face shown. Figure 6.2 (bottom) - HB-SB geotextile after washing for permittivity test, bottom face shown.

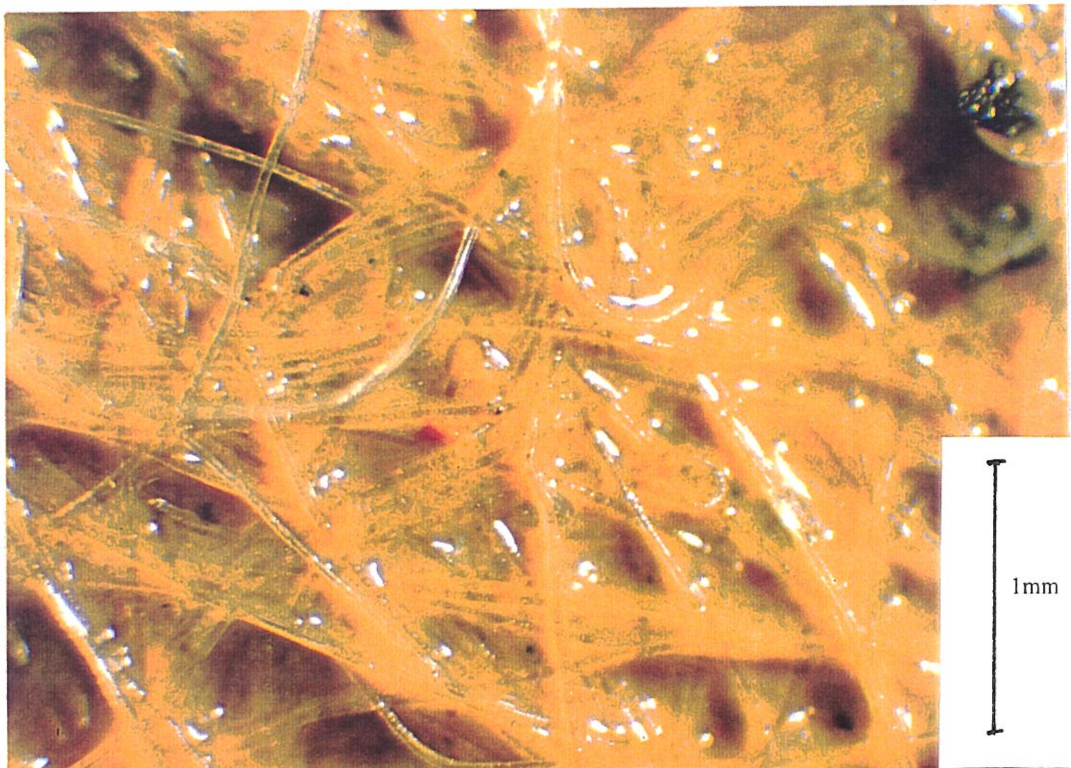

Figure 6.3 (top) - NP4-SB geotextile (wet), bottom face shown. Figure 6.4 (bottom) - Dry NP4-NB geotextile, top face shown.

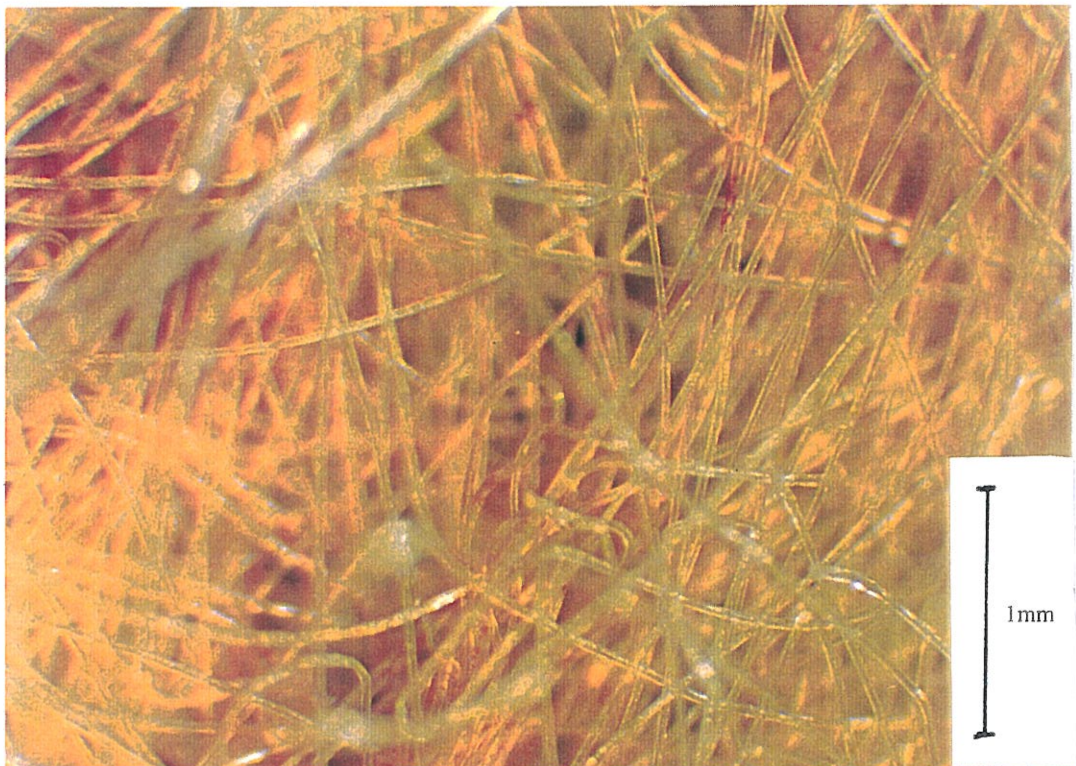

Figure 6.5 (top) - NP4-NB geotextile after washing for permitt. test, bottom shown.
Figure 6.6 (bot.) - NP4-NB geotextile after washing for permitt. test, bottom shown.

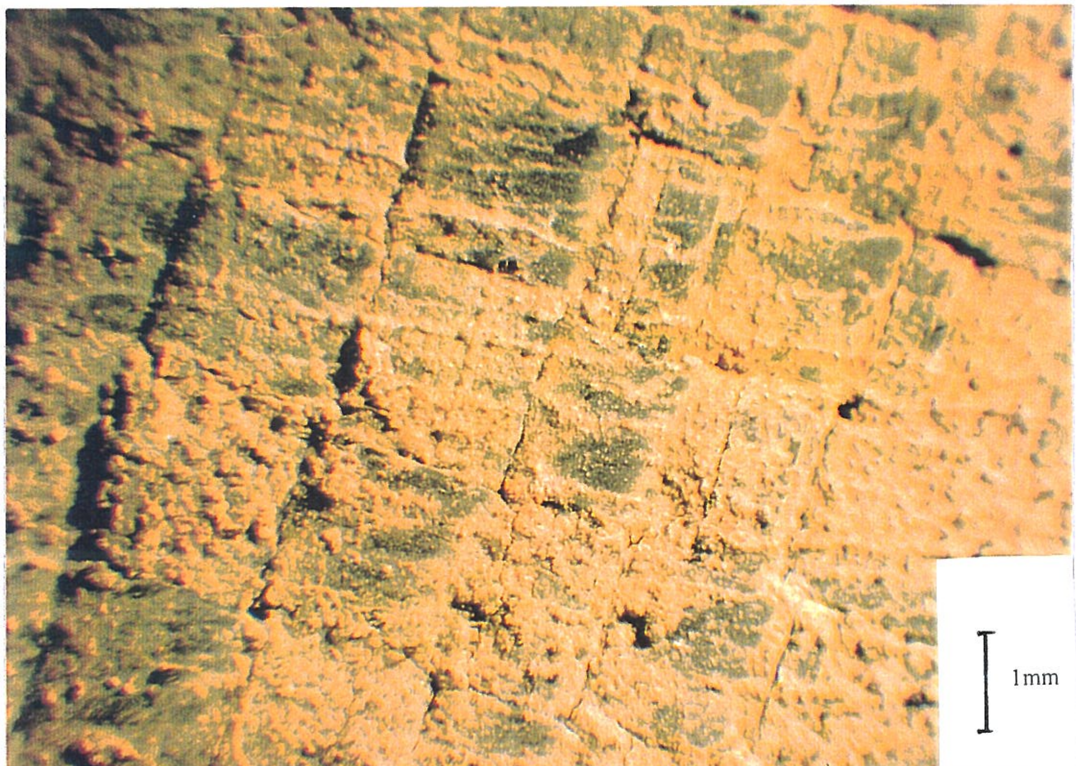

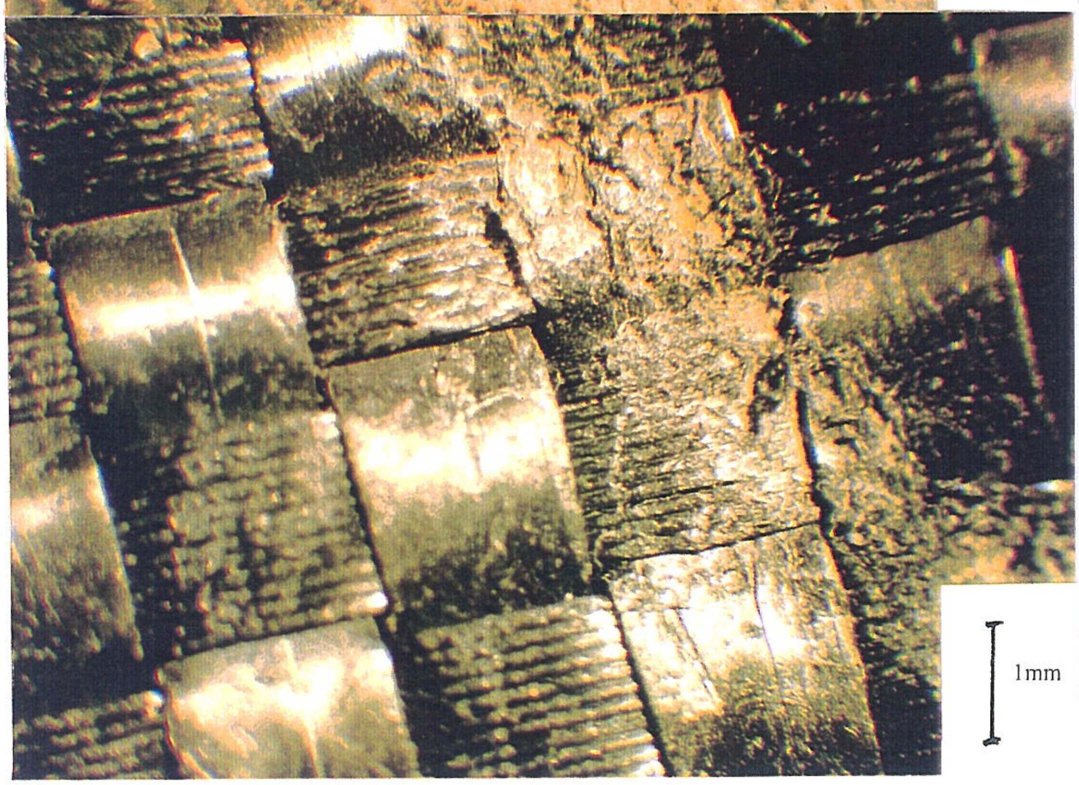

Figure 6.7 (top) - Dry SF-NB geotextile, top face shown.
Figure 6.8 (bot.) - SF-NB geotextile after washing for permitt. test, top face shown.

6.6 shows a cluster of soil particles/iron oxide precipitates lodged in the needle-punched filaments.

Figure 6.7 shows significant caking on the top surface of a slit-film geotextile sample at the northbound lane location. Figure 6.8 shows the top surface of a slit-film geotextile after the permittivity washing procedures. The damage observed in the right third of the photograph appeared to be due to aggregate indentation. It is also interesting to note the corrugated tapes.

7.0 LABORATORY TESTS

Laboratory tests were performed on the soil and geotextile samples retrieved during the field exploration. The soil tests included water content tests, grain size distribution analyses, and Atterberg limit tests. Permittivity tests and wide width strength tests were performed on the geotextile samples. All laboratory tests were performed at the University of Washington Soil Mechanics and Geosynthetic Laboratories.

7.1 Test Methods

7.1.1 Water Content Tests

Water content tests were performed on each retrieved sample to establish a profile of the water contents at each exploration location. As discussed previously, a total of three to four samples typically were taken at each test pit location. Two water content tests were performed on each sample. The water content tests were performed in accordance with ASTM D 2216.

7.1.2 Grain Size Distribution Analyses

A grain size distribution analysis was performed on all retrieved samples, primarily for classification purposes. The analysis was also performed to evaluate trends in the migration of fines though the separator system. The grain size distribution of the base course materials was determined by mechanical sieving of the coarse fraction, greater than the No. 200 sieve. The percent passing the No. 200 sieve was determined by washing the fines of the specimen through a No. 200 sieve. The mechanical sieving was performed in accordance with ASTM C 136. The soils were classified according to the Unified Soil Classification System (USCS), ASTM D 2487.

Hydrometer analyses were performed on all of the native subgrade samples. A hydrometer analysis was also performed on the fines washed from the SF-NB mudcake sample. The fines from the mudcake sample were obtained by washing the soil through a No. 200 sieve into a large bucket. The water was then evaporated in an oven. Hydrometer analyses were not performed on the fines of other base course soils because the samples typically contained less than 10 percent fines.

The hydrometer analyses were performed in general accordance with ASTM D 422. Calgon (active ingredient: hexametaphosphate) was used as the dispersing agent, prepared at 40 g/L solution. The soil used in the hydrometer tests was oven-dried and pulverized prior to soaking in 125 mL of the dispersing agent solution. The soil was allowed to soak in the solution at least 24 hours prior to hydrometer testing, and was periodically mixed using a malt mixer. De-ionized water was used in lieu of distilled or demineralized water as specified by ASTM. The de-ionized water was considered to more accurately represent the field conditions. A value of 2.70 was assumed for the specific gravity of the solids for the soil particle diameter calculations.

7.1.3 Atterberg Limits

Atterberg limit tests were conducted on the subgrade soil samples to classify the soils, and to compare the classifications with those determined in the Phase I study. The tests were performed in accordance with ASTM D 4318. The soil specimens were not oven-dried prior to testing.

7.1.4 Permittivity Tests

The permittivity tests were performed using a permeameter that was designed and constructed based on the "STS geotextile permeameter" design, Christopher (1983). A photograph of the permeameter is shown in Figure 7.1. The STS permeameter design differs from the apparatus detailed in the ASTM D 4491 standard; however the apparatus and the basic principles of the permeameter test conform to the ASTM requirements. Deaired water was used for the permittivity tests to minimize the amount of entrained air bubbles which could accumulate in the geotextile during the test and errantly decrease the permittivity. Details of the testing procedure are presented in Appendix C.

Permittivity tests were performed on four specimens from each exhumed geotextile under a constant head of 50 mm. Five tests were performed on each specimen to verify that the geotextile permittivity was increasing with each test due to the washing of the soil particles from the specimen. After the five tests were completed, the specimen was removed from the apparatus and massaged under swiftly moving tap water to remove nearly all of the soil particles remaining in the geotextile. To evaluate the increase in permittivity, each washed specimen was tested five more times to establish an average permittivity value. The permittivity of the washed specimens was not expected to increase with each test because most of the fines were already washed from the specimen.

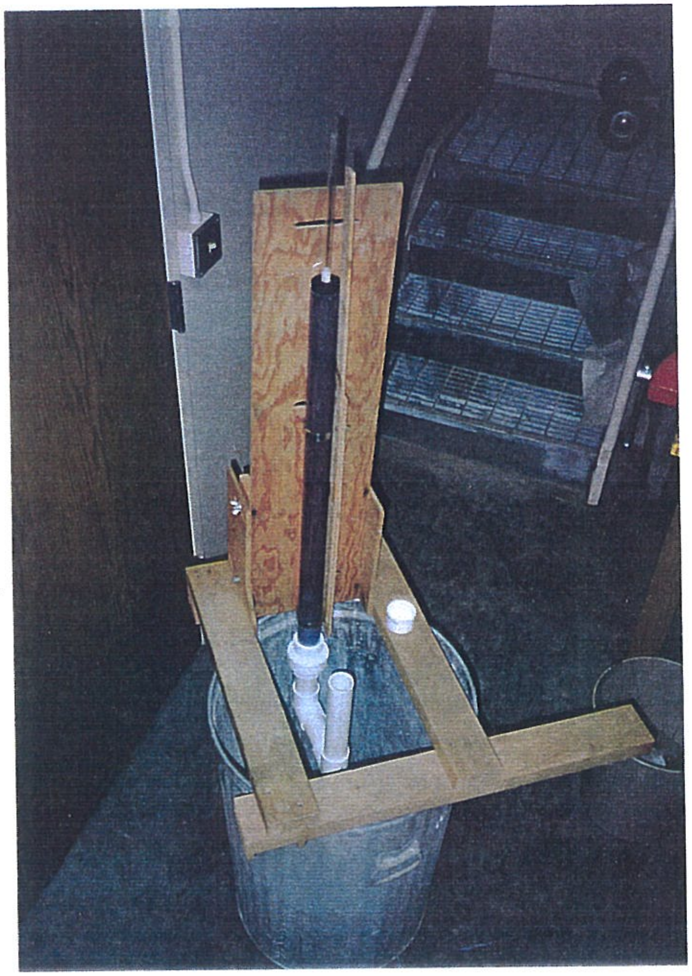

Figure 7.1 - Permeameter apparatus.

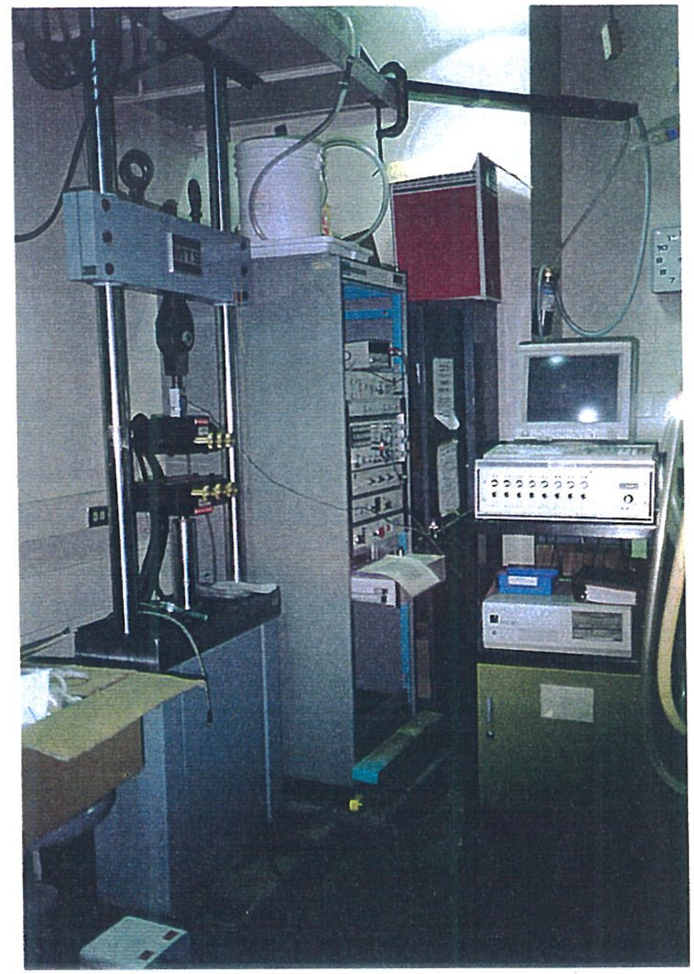

Figure 7.2 - Wide width tensile testing apparatus.

The constant head test method was used instead of the falling head method due to the high heads required to facilitate falling head tests using the STS permeameter. The higher heads would be required because of the rapid drop of the water column for high permittivity geotextiles. A constant, low head test was also advantageous because it caused less washing of the geotextile specimens.

The permittivity and permeability of the geotextile was determined by using Darcy's Law:

$$\text{Permittivity, } \psi = \frac{Q\, R_t}{A\, h} \qquad \text{(Eq. 7-1)}$$

$$\text{Permeability, } k = \psi\, t \qquad \text{(Eq. 7-2)}$$

where:

ψ = permittivity (sec^{-1})
k = permeability (cm/sec)
t = thickness of geotextile (cm)
A = cross sectional area of specimen (cm^2)
h = head of water on specimen (cm)

Q = flow rate (cm^3/s), $Q = \frac{d\,(a_{out} - a_{in})}{T}$ (Eq. 7-3)

d = drop of water level in permeameter during test (cm)
a_{out} = inside area of standpipe (cm^2)
a_{in} = area within outside perimeter of air supply tube (cm^2)
T = time for flow (sec)

R_t = temperature correction factor, $R_t = \frac{u_t}{u_{20^\circ}}$ (Eq. 7-4)

u_t = water viscosity at test temperature (millipoises)
u_{20° = water viscosity at 20° C (millipoises)

As shown in Equation 7-1, the permittivity of the specimens was standardized to a water temperature of 20° C. The temperature of the water during the tests ranged from 15° to 18° C. The cross sectional area of the test specimens subjected to flow was 11.40 cm^2.

There are several sources of error that could influence the reported permittivity values. As described in Appendix C, the time interval of the test is recorded by manually starting a stopwatch while simultaneously initiating flow by removing a finger from the air supply tube. The stopwatch is stopped when a finger is placed over the air supply tube to terminate flow. Due to human error, the stopwatch is not likely started and stopped simultaneously at the initiation and termination of flow. The error in the time measurement for this procedure is estimated to be as much as 0.2 seconds for each test.

Error could also be introduced when reading the water level measurements. Because the values were read to the nearest millimeter, each time a reading was taken an error up to 0.5 mm could be introduced. Since the water level in the standpipe was read twice during a test, the total error for each test could be up to 1 mm. The possible errors associated with the time and water level measurements could account for ± 3 percent of the typical permittivity calculation. This error decreases as the permittivity of the geotextile decreases due to the longer time required for the water level in the standpipe to drop.

7.1.5 Wide Width Strength Tests

The wide width strength tests were performed using a MTS 810 testing device, which was hydraulically driven and controlled by a MTS 442 Controller. The geotextile clamping system consisted of "Geo" Grip clamps, manufactured by Curtis "Sure-Grip", Inc. The clamps were operated by a hydraulic pump controlled by foot switches. The pump was adjusted to apply a total pressure of approximately 13,100 kPa to the clamps when testing nonwoven specimens, and 20,700 kPa when testing woven specimens. Labtech Notebook computer software was used for automatic data acquisition during the test. A photograph of the wide width testing apparatus in shown in Figure 7.2.

A total of six specimens from each exhumed geotextile were tested, in addition to the tests performed on the control geotextiles. All specimens were tested in the machine direction and inundated for at least 24 hours prior to testing. The number and size of any holes lying between the testing grips were also recorded. The wide width tests were performed in accordance with ASTM D 4595. Details of the testing procedures are described in Appendix D.

7.2 Summary of Test Results

7.2.1 Water Content Tests

The results of the water content tests are presented in Table 7.1. As discussed previously, two water content tests were performed on each retrieved soil sample. The average value of these two tests are used in the analyses throughout the remainder of this report. The tests indicate the water contents of the base course soils (excluding the mudcake samples) ranged from 3.1 to 9.6 percent. The water contents of the mudcake samples ranged from 4.4 to 9.8 percent, and the water contents of the subgrade soils ranged from 22.2 to 59.0 percent.

Table 7.1 - Water content test results.

Northbound Lane			
Section	low m%	high m%	Average
HB - 300	4.4	4.8	4.6
HB + 150	3.0	3.6	3.3
HB - Mud	4.3	4.4	4.4
HB - Nat	30.4	30.6	30.5
NP4 - 300	4.8	4.9	4.9
NP4 + 150	5.0	5.4	5.2
NP4 - Mud	4.9	--	4.9
NP4 - Nat	27.3	29.0	28.2
NP6 - 300	3.7	4.5	4.1
NP6 + 150	5.8	7.0	6.4
NP6 - Mud	4.8	--	4.8
NP6 - Nat	32.1	33.2	32.7
Soil - 300	3.5	4.1	3.8
Soil + 0-100	4.2	5.5	4.9
Soil +100-200	3.6	4.5	4.1
Soil - Nat	58.3	59.7	59.0
NP8 - 300	3.5	4.0	3.8
NP8 + 150	4.7	4.9	4.8
NP8 - Mud	3.9	5.3	4.6
NP8 - Nat	41.8	41.8	41.8
SF - 300	3.4	4.2	3.8
SF + 150	4.1	4.3	4.2
SF - Mud	7.2	8.2	7.7
SF - Nat	38.3	38.7	38.5

Southbound Lane			
Section	low m%	high m%	Average
HB - 300	3.4	3.8	3.6
HB + 150	3.5	4.9	4.2
HB - Nat	21.4	22.9	22.2
NP4 - 300	3.3	3.8	3.6
NP4 + 150	3.3	4.2	3.8
NP4 - Mud	3.9	8.6	6.3
NP4 - Nat	47.5	48.9	48.2
SF - 300	3.4	3.9	3.7
SF + 150	4.6	5.1	4.9
SF - Nat	29.9	30.0	30.0
Soil - 300	3.5	4.0	3.8
Soil + 150	4.5	4.8	4.7
Soil - Nat	37.7	43.4	40.6
NP8 - 300	2.8	3.3	3.1
NP8 + 150	9.3	9.9	9.6
NP8 - Mud	6.7	9.4	8.1
NP8 - Nat	43.0	44.5	43.8
NP6 - 300	3.6	4.1	3.9
NP6 + 150	4.9	5.0	5.0
NP6 - Mud	9.5	10.1	9.8
NP6 - Nat	39.2	41.3	40.3

Notation:
- \- 300 = Sample within top 300 mm of fill
- \+ 150 = Sample approximately 150 mm above geotextile
- \+ 0-100 = Sample within 0-100 mm above fill/subgrade interface
- \+ 100-200 = Sample within 100-200 mm above fill/subgrade interface
- Nat = Native soil
- Mud = "Mudcake" above geotextile

It was anticipated that the water content of the mudcake samples would be higher than the base course samples due to the higher fines content observed in the mudcake, and the wetted zone observed in the aggregate immediately above most of the geotextiles in the southbound lane (as discussed in Section 5.2.2). As shown in Table 7.1, the water contents of the mudcake samples were higher than the base course samples only at the SF-NB, NP4-SB, and NP6-SB exploratory locations. It is not clear why the water contents of the mudcake samples are lower than the base course samples at the other locations; one reason may be because its difficult to control/measure the water content of base course aggregate. Another reason is that it was difficult to obtain a representative sample of mudcake because the mudcake layers were thin in most cases. (Note that in addition to the control sections, mudcake samples were not collected at the HB-SB and SF-SB exploratory locations due to the lack of mudcake observed in the base course aggregates.) Based on the results summarized in Table 7.1, there does not appear to be consistent trends of increasing or decreasing water content throughout the profiles of the base course soils in the exploratory excavations.

7.2.2 Grain Size Distribution Analyses Results

The results of the sieve and hydrometer analysis are presented in Appendix B, Figures B.1 through B.13. Figure B.13 presents the results of the hydrometer tests performed on the subgrade soil and the fines washed from the mudcake at the SF-NB exploration. The base course samples (excluding the mudcake samples) contained 1.8 to 8.6 percent fines. The mudcake samples contained 4.0 to 11.6 percent fines, while the fines content of the subgrade soils ranged from 57 to 100 percent.

Field observations indicated that the mudcake soils generally contained more fines than the overlying base course aggregates. However, testing indicated the fines content in the mudcake samples were higher only at the SF-NB, NP4-SB, and NP6-SB locations. (As previously noted, in addition to the control sections, mudcake samples were not collected at the HB-SB and SF-SB exploratory locations due to the lack of mudcake observed in the base course aggregates.) It is not clear why the grain size analysis contradicts the field observations at the other geotextile locations. Possible explanations include errors in the testing methods or difficulties in sampling the mudcake, discussed previously.

Based on the laboratory test results, there does not appear to be any consistent trends of increasing or decreasing fines content throughout the profile of the base course soils in the exploratory excavations. It is interesting to note, however, that the mudcake samples that contained a higher fines content than the base course samples (SF-NB, NP4-SB, and NP6-SB) were also the only samples to have higher water contents than the base course samples, discussed in Section 7.2.1.

As shown by the two grain size distribution curves in Figure B.13, the fines washed from the mudcake sample at the SF-NB location have a similar distribution slope to the underlying subgrade soil, although there is some divergence in the range of the smaller particle sizes (0.001 to 0.004 mm). Deviations between these grain size distributions should be expected however, because of the preexisting fines in the mudcake sample (from the base course).

As discussed in Section 7.1.2, a dispersing agent was used for the hydrometer tests. It should be noted that hydrometer tests were also performed on some of the subgrade soils without using a dispersing agent, so that the influence of the dispersing agent could be evaluated. The grain size distributions of these tests were found to be substantially different from tests which included a dispersing agent, probably because of soil flocculation. These tests were therefore disregarded and their results are not reported.

7.2.3 Atterberg Limit Test Results

The results of the Atterberg Limit tests are presented in Figure 7.3. As shown in the figure, all but three of the subgrade soils were high plasticity soils. The natural water contents of all the subgrade soils were higher than the plastic limits, except at the NP6-NB and SF-SB locations, where the water contents were slightly below the plastic limits. Comparisons to the Phase I tests are provided in Section 8.1.1.

7.2.4 Permittivity Test Results

The results of the permittivity tests performed on the exhumed samples are presented in Tables C.1 through C.10 in Appendix C and are summarized in Table 7.2. Permittivity tests conducted on control samples are presented in Tables C.11 through C.15. The permeability values shown in Tables C.1 through C.15 were calculated based on the geotextile thicknesses reported by the manufacturers', shown in Table 2.1. The objective of the permittivity testing was to evaluate the degree of blinding and clogging of the geotextiles by comparing the permittivity test results before and after washing.

As discussed previously, permittivity tests were conducted on four specimens from each exhumed geotextile, and each unwashed and washed specimen was tested five times. The unwashed permittivity values for each geotextile presented in Table 7.2 were determined from the first test run conducted on each of the unwashed specimens. The first test run represented the maximum amount of blinding and

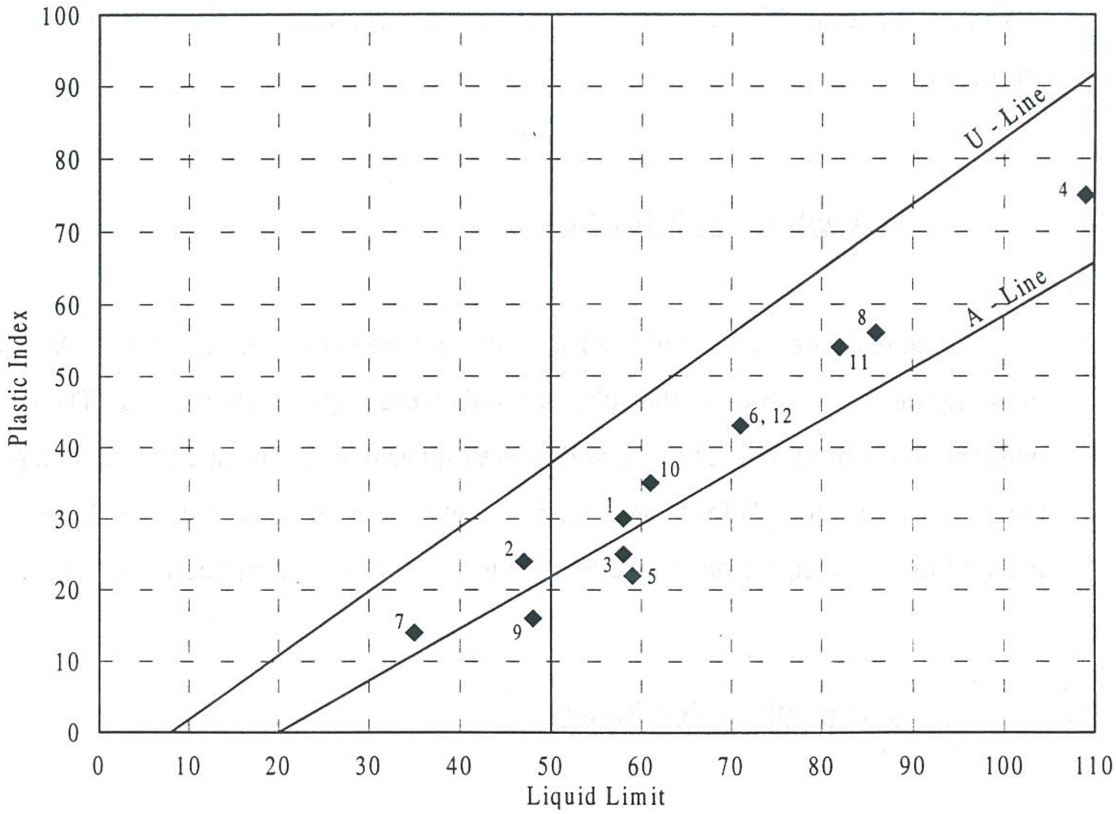

Marker	1	2	3	4	5	6
Section	HB-NB	NP4-NB	NP6-NB	Soil-NB	NP8-NB	SF-NB
LL	58	47	58	109	59	71
PL	28	23	33	34	37	28
PI	30	24	25	75	22	43
USCS	CH	CL	MH	CH	MH	CH
w_n (%)	30.5	28.2	32.7	59.0	41.8	38.5

Marker	7	8	9	10	11	12
Section	HB-SB	NP4-SB	SF-SB	Soil-SB	NP8-SB	NP6-SB
LL	35	86	48	61	82	71
PL	21	30	32	26	28	28
PI	14	56	16	35	54	43
USCS	CL	CH	ML	CH	CH	CH
w_n (%)	22.2	48.2	30.0	40.6	43.8	40.3

Figure 7.3 - Atterberg limit test results.

Table 7.2 - Summary of permittivity test results.

Geotextile	Specimen Number	Laboratory Tests: Unwashed 1st test run ψ (sec^{-1})	Laboratory Tests: Washed Average ψ (sec^{-1})	Laboratory Tests: % increase in ψ	Manufacturer's Reported Value Permittivity (sec^{-1})
HB - NB	1	0.14	2.17	1450	
	2	0.94	3.44	266	0.1
	3	0.15	2.19	1360	
	4	0.30	2.49	730	
			Average	951	
NP4 - NB	1	1.34	2.86	113	
	2	0.89	2.35	164	2.7
	3	2.06	3.95	92	
	4	1.57	2.68	71	
			Average	110	
NP6 - NB	1	2.22	3.05	37	
	2	2.19	2.95	35	2.1
	3	1.88	3.02	61	
	4	1.54	3.17	106	
			Average	60	
NP8 - NB	1	1.60	2.29	43	
	2	0.97	1.91	97	1.6
	3	1.24	2.49	101	
	4	2.04	2.83	39	
			Average	70	
SF - NB	1	0.17	0.27	59	
	2	0.12	0.20	67	0.1*
	3	0.12	0.19	58	
	4	0.14	0.23	64	
			Average	62	

* Typical value, all other manufacturer reported values are MARV.

Table 7.2 (continued) - Summary of permittivity test results.

Geotextile	Specimen Number	Laboratory Tests: Unwashed 1st test run ψ (sec^{-1})	Washed Average ψ (sec^{-1})	% increase in ψ	Manufacturer's Reported Value Permittivity (sec^{-1})
HB - SB	1	0.04	2.05	5025	
	2	0.39	1.92	392	0.1
	3	0.66	3.15	377	
	4	0.13	2.69	1969	
			Average	1941	
NP4 - SB	1	1.83	2.24	22	
	2	2.15	2.88	34	2.7
	3	1.95	2.78	43	
	4	1.75	2.78	59	
			Average	39	
NP6 - SB	1	1.83	2.82	54	
	2	2.00	3.22	61	2.1
	3	1.88	3.21	71	
	4	1.31	2.39	82	
			Average	67	
NP8 - SB	1	1.15	2.39	108	
	2	1.12	2.37	112	1.6
	3	0.71	2.51	254	
	4	1.02	2.29	125	
			Average	149	
SF - SB	1	0.08	0.14	75	
	2	0.09	0.19	111	0.1*
	3	0.09	0.18	100	
	4	0.11	0.22	100	
			Average	97	

* Typical value, all other manufacturer report values are MARV.

clogging of the geotextile. As shown in Tables C.1 through C.10, the permittivity of the unwashed specimens generally increased with each test run as the fines were washed from the specimen. The washed permittivity values presented in Table 7.2 represent the average of the five tests performed on each specimen. As can be seen in Tables C.1 through C.10, there appears to be no trend of increasing or decreasing permittivity in the five tests performed on each washed specimen. Therefore, the average of the washed test values should be a more accurate representation of the data.

The heat-bonded specimens were found to have the highest percent increase in permittivity with values ranging from 951 percent in the northbound lane specimens to 1941 percent in the southbound lane specimens. The average increase in permittivity of the needle-punched geotextile specimens ranged from 39 percent in the NP4-SB specimens to 149 percent in the NP8-SB specimens. The average increase of the slit-film geotextiles ranged from 62 percent in the southbound lane specimens to 97 percent in the northbound lane specimens.

The percent increase in permittivity was generally found to vary between specimens cut from the same geotextiles, as shown in Table 7.2. The heat-bonded permittivity increases appear to be the most variable, ranging from 392 to 5025 percent in the southbound lane specimens. By contrast, the slit-film permittivity increases appear to be the least variable, ranging from 58 to 67 percent in the northbound lane specimens.

The purpose of the permittivity testing was not to evaluate conformance with the manufacturers' reported values. However, as shown in Table 7.2, all of the washed geotextile specimens did exceed the manufacturers' reported permittivity value, except for three of the NP4 specimens which were just below the reported value. The majority of the heat-bonded and slit-film unwashed specimens exceeded the manufacturers' values, however most of needle-punched specimens did not. Discretion needs to be used when interpreting the above comparisons because the laboratory results are average values, and the manufacturers' values are reported in mean average roll values (MARV), except for the slit-film geotextile.

Permittivity tests were also performed on control specimens to evaluate the effect the washing techniques had on the structure of geotextiles. Although the control specimens contained no soil particles, the washing procedure was performed for a similar duration using the same massaging techniques used on the exhumed specimens. The results of these tests are presented in Tables C.11 through C.15 in Appendix C and are summarized in Table 7.3.

Table 7.3 - Summary of control specimen permittivity (Ψ) test results.

Control Sample	Average ψ (sec^{-1}) Unwashed	Washed	% Change in ψ After Washing
HB	1.47	1.55	+ 5.4
NP4	3.34	3.51	+ 5.1
NP6	2.65	2.70	+ 1.9
NP8	1.92	1.91	- 0.5
SF	0.12	0.12	0.0

The results of the permittivity tests on the control specimens indicate that the effects of the washing process are relatively minor in comparison to the percent increase in permittivity of the geotextiles shown in Table 7.2.

7.2.5 Wide Width Strength Test Results

The wide width strength test results performed on the exhumed samples are presented in Tables D.1 and D.2 in Appendix D, and are summarized in Tables 7.4

and 7.5. The results of wide width tests performed on control samples are presented in Tables D.3 and D.4, and are summarized in Table 7.6. The purpose of the wide width tests was to compare the exhumed geotextile test results with the results obtained from the control tests and the manufacturer's reported values. In addition, comparisons of the results were to be made between the northbound and southbound lanes to evaluate the effect of the different initial base course lift thicknesses.

As shown in Table 7.4, the average wide width strength retained by the needle-punched geotextile samples ranged from 83 to 121 percent compared to the control tests, and 80 to 104 percent compared to the manufacturer's reported values. The average strength retained by the heat-bonded samples ranged from 94 to 120 percent compared to the control tests, the slit-film samples ranged from 77 to 84 percent compared to the control tests. Although they are tabulated in Tables 7.4 and 7.5, the results of the heat-bonded and slit-film geotextile wide width tests cannot be directly compared with the manufacturers' values, because the manufacturers' reported their data in MARV. The wide width test results presented in Tables 7.4 and 7.5 are average values. The six wide width tests performed on the specimens of each exhumed sample were not enough to establish a statistical data base from which reliable MARV values could be determined.

As shown in Table 7.5, the average elongation at failure retained by the needle-punched samples ranged from 28 to 42 percent compared to the control tests, and 25 to 37 percent compared to the manufacturers' reported values. The average elongation at failure retained by the heat-bonded samples ranged from 49 to 64 percent compared to the control tests, the slit-film samples ranged from 64 to 67 percent compared to the control tests. On the whole, the average retained elongation at failure values were notably less than the average retained strength values.

Table 7.4 - Summary of wide width test results - Strength.

Geotextile	Average Strength - Typical Values Exhumed Test Results (kN/m)	Control Test Results (kN/m)	Control Percent Retained	Manufacturers' Reported Values (kN/m)	Manuf. Percent Retained
HB - NB	5.7	6.1	94	6.1*	94
NP4 - NB	7.3	7.5	98	8.8	84
NP6 - NB	9.7	10.9	90	12.3	80
NP8 - NB	13	15.6	83	15.8	82
SF - NB	29	37.6	77	30.6*	95
HB - SB	7.4	6.1	120	6.1*	120
NP4 - SB	9	7.5	121	8.8	104
NP6 - SB	11.9	10.9	110	12.3	97
NP8 - SB	14.4	15.6	92	15.8	91
SF- SB	31.7	37.6	84	30.6*	103

* Reported as MARV

Table 7.5 - Summary of wide width test results - Elongation at failure.

Geotextile	Average Elongation at Failure - Typical Values Exhumed Test Results (%)	Control Test Results (%)	Control Percent Retained	Manufacturers' Reported Values (%)	Manuf. Percent Retained
HB - NB	27	55	49	45*	60
NP4 - NB	22	79	28	80	28
NP6 - NB	24	84	29	95	25
NP8 - NB	28	96	29	95	29
SF - NB	12	21	57	15*	80
HB - SB	35	55	64	45*	78
NP4 - SB	28	79	35	80	35
NP6 - SB	35	84	42	95	37
NP8 - SB	31	96	32	95	33
SF- SB	14	21	67	15*	93

* Reported as MARV

Table 7.6 - Results of wide width strength tests on control specimens.

Geotextile	Jaw Type	Number Tested	Ave. Wide Width Str. (kN/m)	Strength Std. Dev. (kN/m)	Average Elong. at Fail. (%)	Elongation Std. Dev. (%)
HB	Knurled	6	6.1	0.4	55	3.0
HB	Roughened	4	5.6	5.6	69	12.1
NP4	Knurled	6	7.5	0.5	79	4.1
NP4	Roughened	2	8.2	0.5	95	5.7
NP6	Knurled	6	10.9	0.7	84	5.8
NP6	Roughened	3	12.1	0.6	113	11.8
NP8	Knurled	6	15.6	0.4	96	8.3
SF	Knurled-NP	3	34.7	0.6	18	1.0
SF	Knurled-DT	6	37.6	1.3	21	1.9
SF	Knurled-EP	3	39.1	0.6	24	1.5

All specimens tested in the machine direction (MD)
NP = No protection at jaw face
DT = Specimen protected at jaw face by duct tape
EP = Specimen protected at jaw face by epoxy

Non-Shaded Results: Used for comparison with exhumed specimens
Shaded Results: Not used for comparison with exhumed specimens

Comparisons between the northbound and southbound lane test results are made in Section 8.2.3. Comparisons between the test results and the WSDOT and FHWA requirements could not be made because a wide width test strength requirement is not specified by WSDOT or FHWA, as indicated in Sections 4.3 or 4.4.

Wide width tests were performed on control samples to determine their strength and elongation at failure for comparative purposes. To evaluate the effect of different types of clamping jaws on nonwoven specimens, tests were performed with knurled face jaws and roughened face jaws. The knurled surface consisted of a symmetric diamond pattern. The texture of the roughened face was similar to 60 grit sand paper, and was created by coarse sandblasting.

As shown in Table 7.6, the average elongation at failure for the nonwoven geotextile specimens was markedly higher when the roughened surface jaw type was used rather than the knurled face jaws. This is because the roughened surface allowed significantly more geotextile slip between the clamping jaws during testing, even when high clamping pressures were applied. The different jaw types did not appear to have as dramatic an effect on the strength characteristics. The knurled face jaws produced somewhat higher average strengths than the roughened surface jaws in the NP4 and NP6 specimens, but slightly lower average strengths in the HB specimens.

The knurled face jaw strength and elongation at failure results more closely agreed with the manufacturers' reported values shown in Table 2.1 for the nonwoven geotextiles. Therefore, the knurled face jaws were used to test the nonwoven exhumed specimens.

Due to the relatively high loads required for testing the woven (slit-film) geotextiles, the knurled face jaws were used with a high clamping pressure to minimize slip during testing. However, this clamping procedure produced some damage to the geotextile. To help protect the geotextile, duct tape was placed on each side of the geotextile prior to clamping. Tests were also performed on samples protected by epoxy. The results tabulated in Table 7.6 show that specimens protected by duct tape yielded higher strengths and elongations at failure than those with no protection at all, but the specimens protected by epoxy produced the highest strengths and elongations at failure. However, because the duct tape protection was easier and much faster to apply than epoxy, duct tape was used to protect the exhumed slit-film geotextiles during testing.

The results of the wide width tests could not be directly compared with the slit-film geotextile values in Table 2.1 because the manufacturer's values were reported in MARV. The values presented in Table 7.6 are average values. Due to time constraints, there were not enough tests performed on the control samples to establish a statistical data base from which reliable MARV values could be determined.

It should be noted that the wide width test results were supposed to be compared with the results of tests performed on the same geotextile lots as those actually installed at the site. These tests were performed by Polyfelt, Inc. but the data has since been lost.

8.0 Analysis of Results

The analysis of the results of the field and laboratory observations and tests are discussed in this section. The findings are also compared with the Phase I study.

8.1 Soil and Groundwater Conditions

The subgrade soils throughout the test section were observed to be highly variable in composition, color, moisture condition, and plasticity during the field investigation. The water content and Atterberg limits test results, shown in Table 7.1 and Figure 7.3, respectively, also illustrate this variability. The subgrade soils were found to contain more than 58 percent fines and consisted mainly of medium stiff to stiff, silty clays. The base course soils were generally dense to very dense, well to poorly graded gravels with sand and some silt. The shape of the majority of the aggregates was subangular to angular.

The groundwater table at the test section fluctuates seasonally. The level of the groundwater table appears to rise significantly after rain events, as evidenced by a wetted zone of base course aggregate observed above the geotextiles in the southbound lane during the field investigation. The wetted zone was presumably due to precipitation that occurred in the previous weeks, or possibly the rain on the previous day. Heavy groundwater seepage was encountered above the subgrade in the Soil-SB test pit excavation, but seepage was not encountered at any of the other explorations. Piezometer measurements indicated the water table was 0.76 to 0.91 m below the ground surface at the piezometer location, as discussed in Section 5.2.2.

8.1.1 Comparisons to Phase I Study

The water content test results are compared to the Phase I study in Figures 8.1 and 8.2. As shown in the figures, the water contents are similar to those determined in the Phase I study, except at the Soil-NB and NP4-SB locations where the water contents were found to be much higher than in the Phase I study. The water content test results from both studies are consistent in showing trends of a general subgrade water content increase in the northern direction throughout the test section profile.

As shown in Figure 8.3, the Atterberg limit test results do not compare well with the Phase I study. The test results are similar to the Phase I study only at the NP4-NB, NP8-NB, HB-SB, and NP6-SB test locations. These results further illustrate the variability of the soil conditions throughout the test section.

The results of the torvane and pocket penetrometer tests are compared to the Phase I study in Figures 8.4 through 8.7. As shown in Figures 8.4 and 8.5, the torvane tests indicate there has been a general increase in subgrade shear strength in both lanes since the geotextiles were installed. In general, the pocket penetrometer tests shown in Figures 8.6 and 8.7 contradict the torvane test results, however. The reasons for these contradictions probably are associated with the highly variable results these tests produce, discussed in Section 5.3.1.

The density test results are compared to the Phase I study in Figures 8.8 and 8.9. The results indicate a general increase in density (wet and dry density) at all test locations except at the Soil-NB and Soil-SB sections where the densities were at or below the densities recorded during the Phase I study. The increases in dry density in the sections containing geotextiles ranged from 0.7 percent at the HB-NB location to 39.0 percent at the SF-SB location. These results suggest the subgrade has

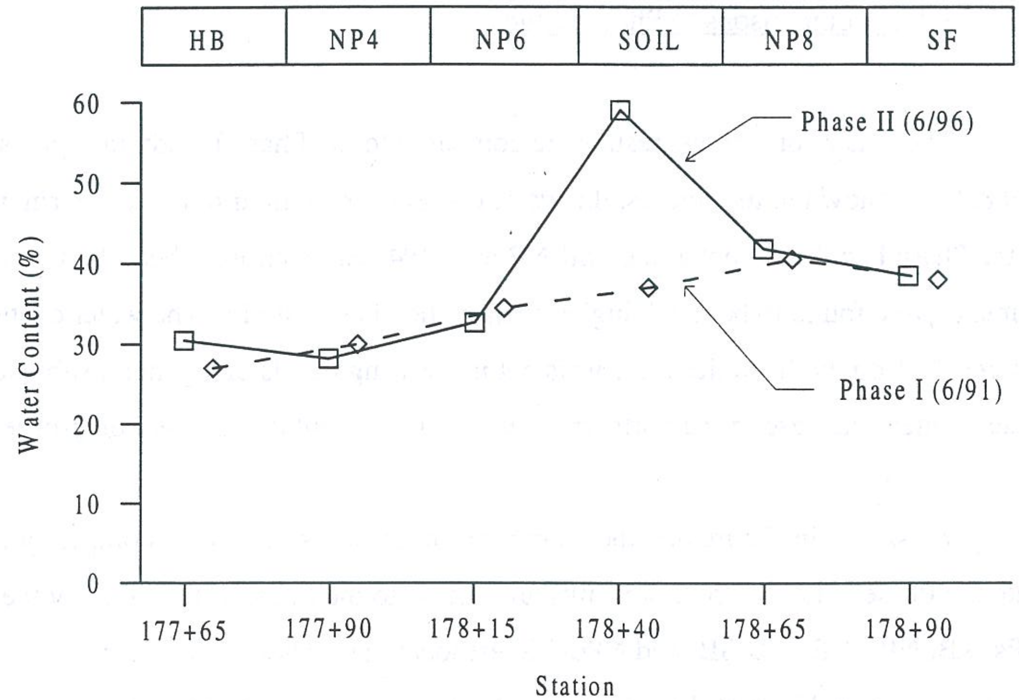

Figure 8.1 - Comparison of water content test results, northbound lane.

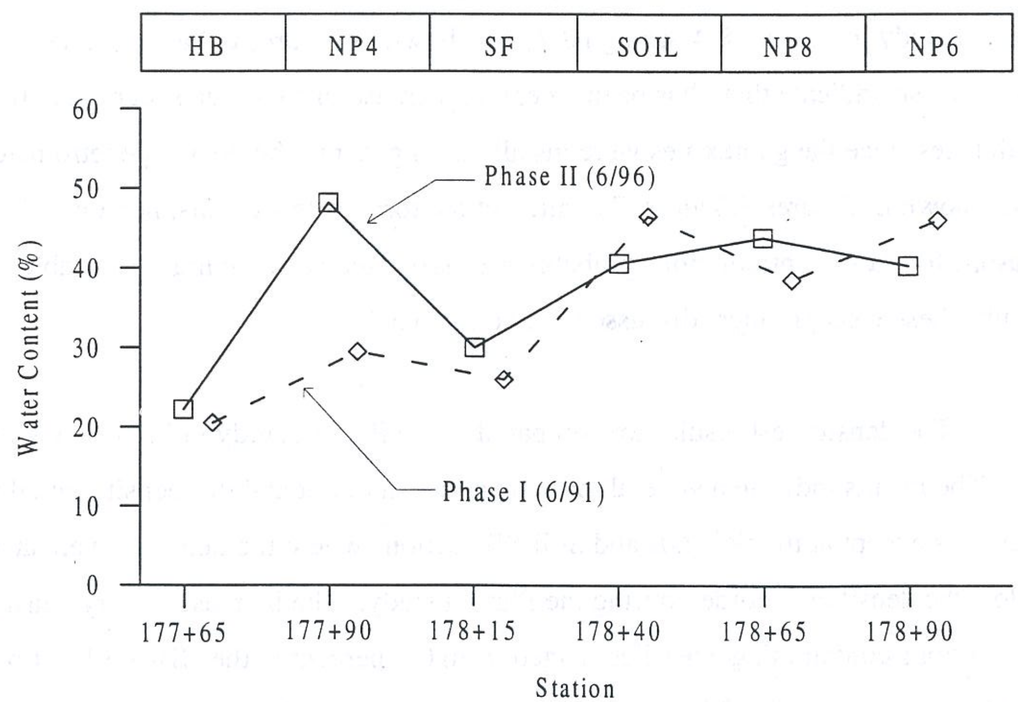

Figure 8.2 - Comparison of water content test results, southbound lane.

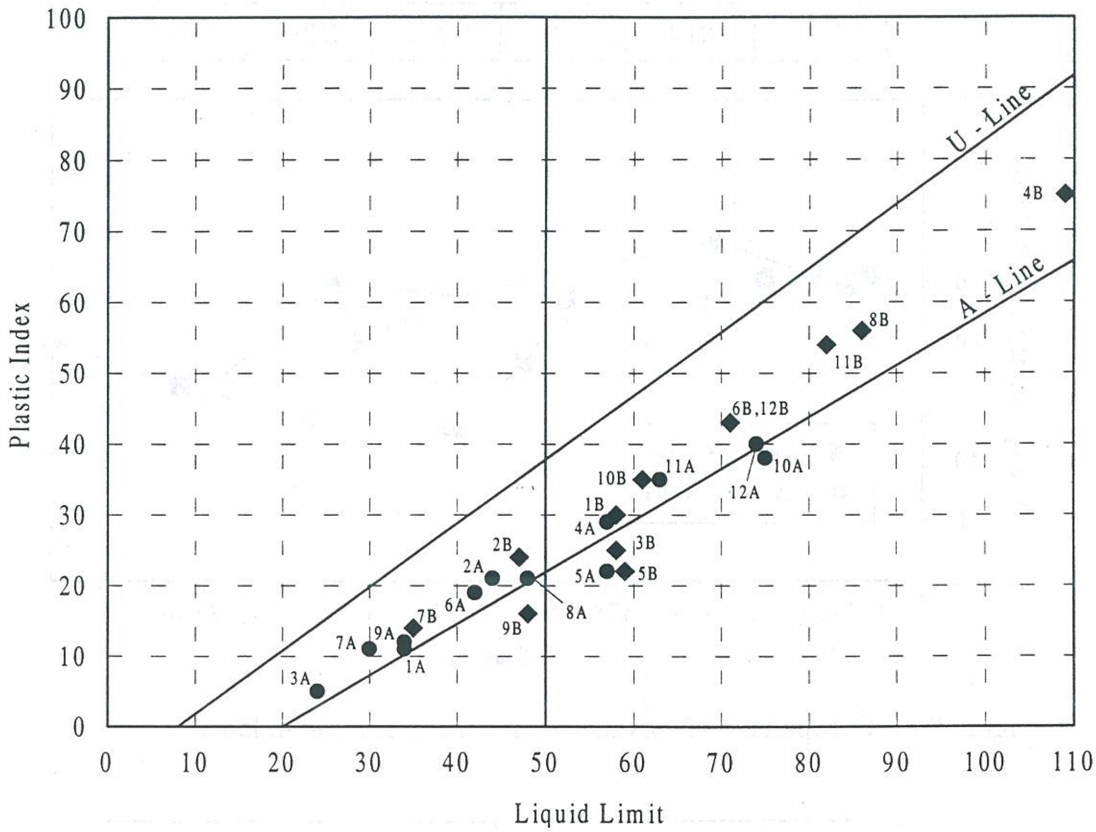

Legend

Phase I - Marker	Phase II - Marker	Section
1A	1B	HB - NB
2A	2B	NP4 - NB
3A	3B	NP6 - NB
4A	4B	SOIL - NB
5A	5B	NP8 - NB
6A	6B	SF - NB
7A	7B	HB - SB
8A	8B	NP4 - SB
9A	9B	SF - SB
10A	10B	SOIL - SB
11A	11B	NP8-SB
12A	12B	NP6 - SB

Figure 8.3 - Comparison of Atterberg limits test results.

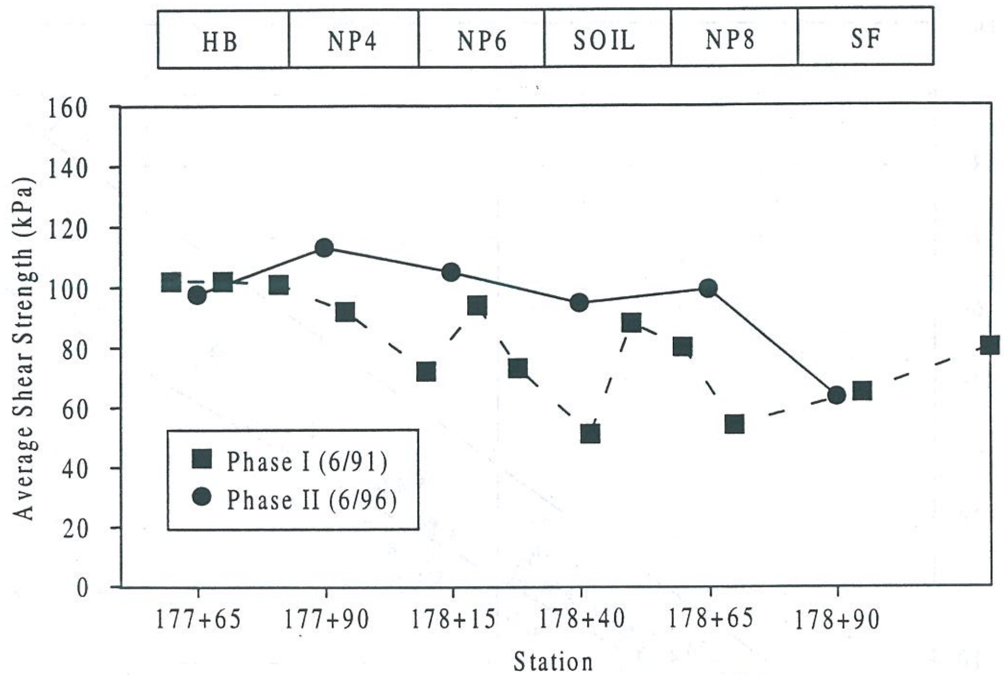

Figure 8.4 - Comparison of torvane test results, northbound lane.

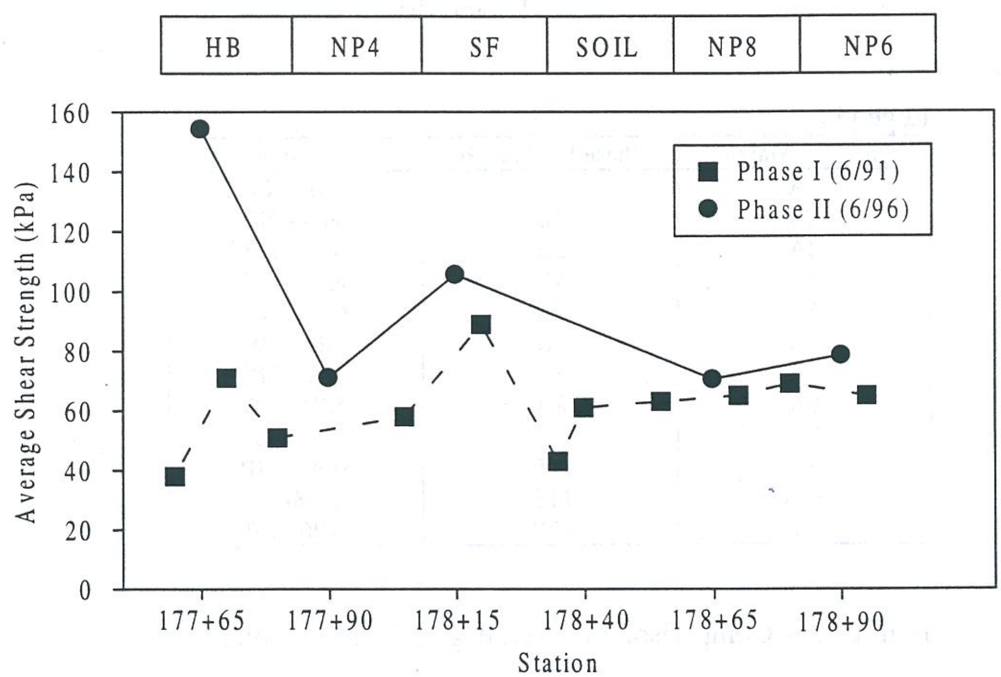

Figure 8.5 - Comparison of torvane test results, southbound lane.

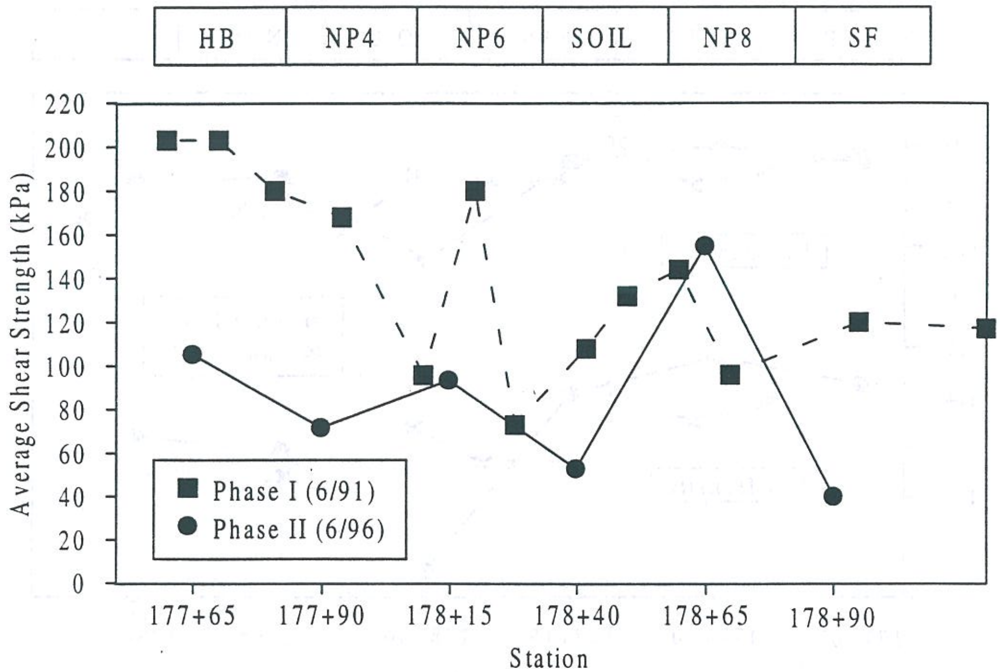

Figure 8.6 - Comparison of pocket penetrometer tests, northbound lane.

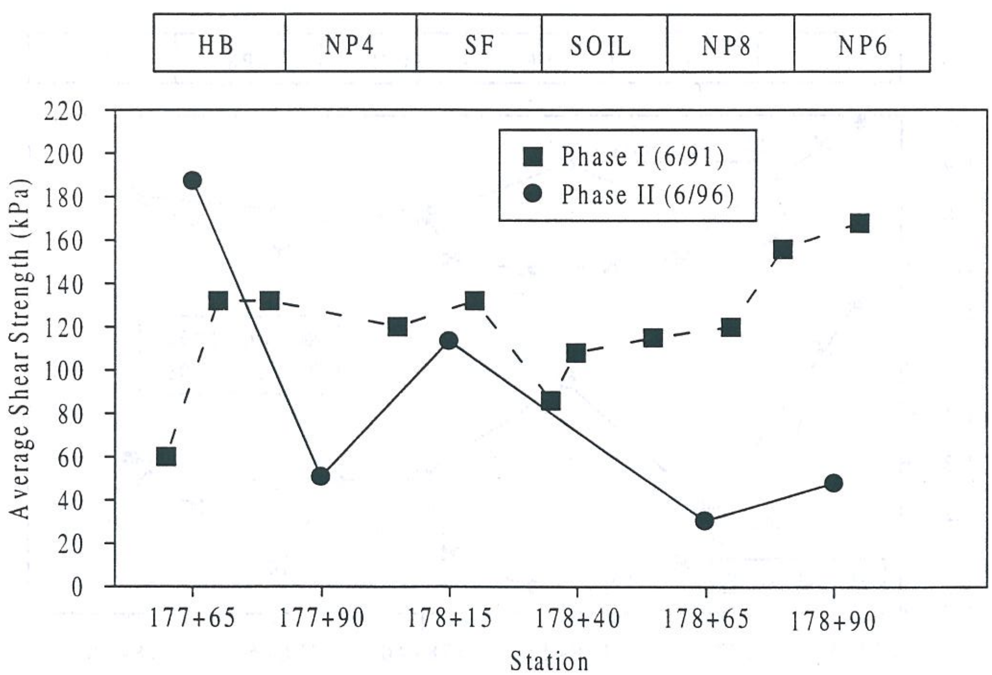

Figure 8.7 - Comparison of pocket penetrometer tests, southbound lane.

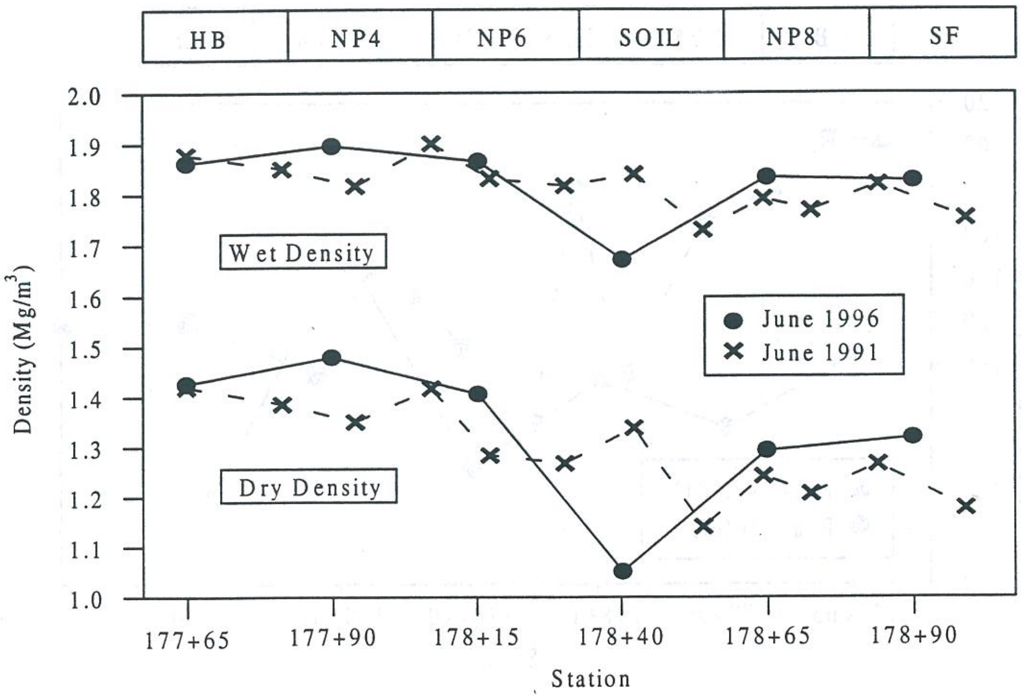

Figure 8.8 - Comparison of density tests, northbound lane.

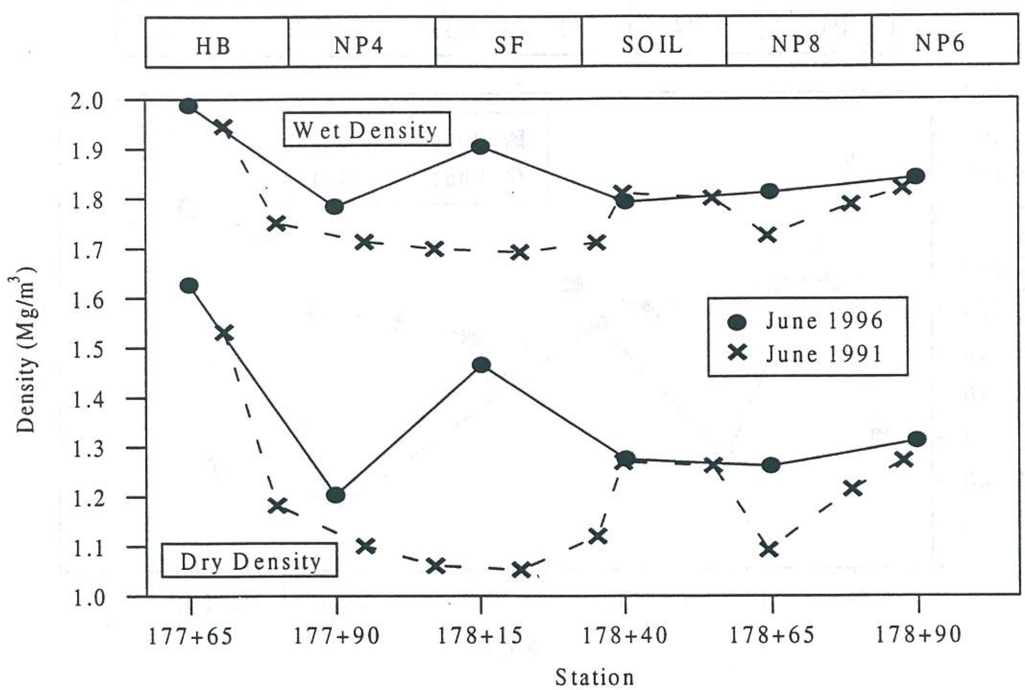

Figure 8.9 - Comparison of density tests, southbound lane.

consolidated more in the areas containing geotextiles than in the areas without geotextiles (control sections).

The subgrade moduli determined from the FWD tests are presented in Figures 8.10 and 8.11. The results indicate there has generally been a steady increase in the subgrade modulus throughout the test section since April 1991, even at the sections without the geotextiles.

8.1.2 Consolidation of Subgrade

The general subgrade conditions during the installation of the geotextiles were noted to be soft and saturated in the Phase I study. In fact, ruts up to 264 mm were observed during the trafficking tests, as discussed in Section 5.2.1. In the field investigations performed for this study the subgrade conditions were generally observed to be firm and consolidated at all explorations, except at the Soil-SB location where observations could not be made due to heavy groundwater seepage.

The density and torvane test results support the consolidation observations, the pocket penetrometer tests do not. However, the torvane and pocket penetrometer tests are less reliable than the density tests because of the high variability associated with the torvane and pocket penetrometer tests, discussed in Section 5.3.1. The FWD tests indicate there has been a general increase in the subgrade modulus throughout the test section; therefore, it can be inferred that the subgrade soils have consolidated.

As discussed previously, the density tests suggest the subgrade in the sections containing geotextiles consolidated more than the subgrade in the control sections.

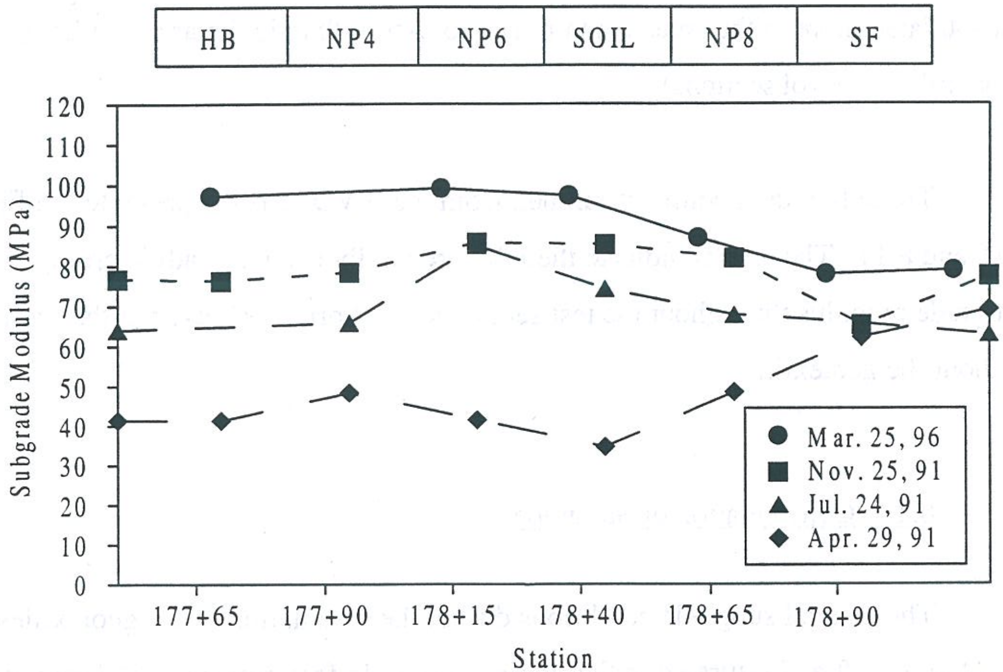

Figure 8.10 - Comparison of FWD test results, northbound lane.

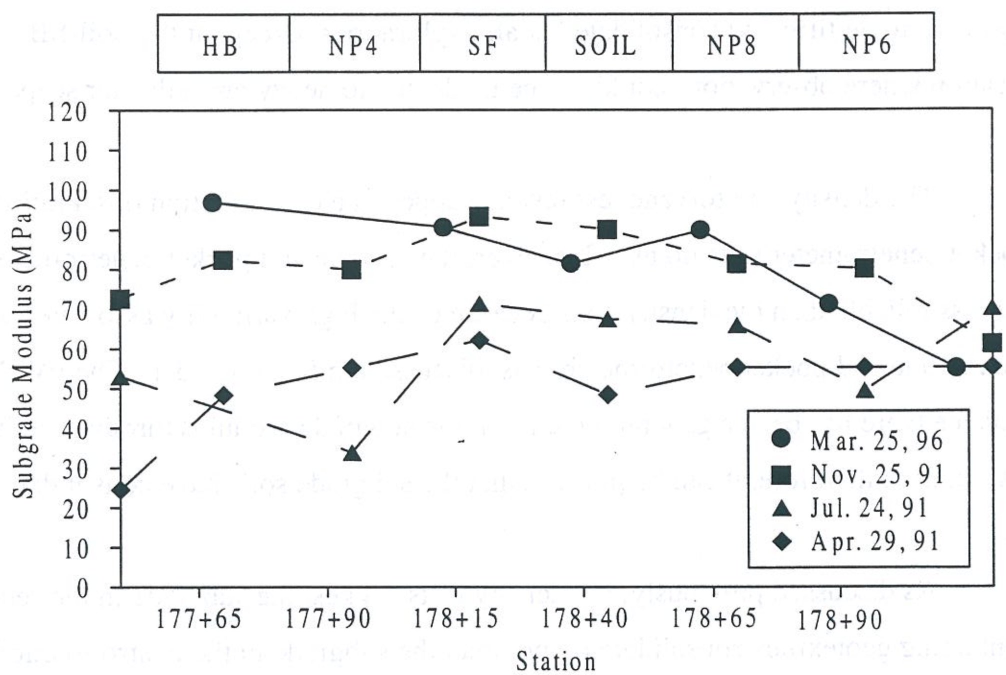

Figure 8.11 - Comparison of FWD test results, southbound lane.

8.2 Geotextile Performance

The geotextiles were evaluated in terms of their filtration and drainage characteristics, separation performance, and capability to retain strength and elongation at failure. Their ability to resist installation damage and long-term degradation was also examined.

8.2.1 Filtration and Drainage

In general, the exhumed nonwoven geotextiles contained various degrees of clogging, but did not appear to be significantly blinded. Conversely, the woven geotextiles appeared to be more affected by blinding than clogging. Similar trends involving the blinding and clogging of woven and nonwoven geotextiles were observed by Metcalfe and Holtz (1994).

As indicated in Figure 8.12, the heat-bonded geotextiles had the largest average increases in permittivity after washing, compared to the needle-punched and slit-film geotextiles which had similar increases in permittivity. The large increases in permittivity of the heat-bonded specimens indicates that these geotextiles experienced significantly more clogging than the other geotextiles. The slit-film permittivity values may be less representative of the in-situ conditions than the other geotextiles because the soil particles blinding the bottom and caked on the top of the slit-films flaked off easily with only minimal handling, especially after a small amount of drying. Also, it is likely that some particles blinding the geotextile were dissociated when the geotextiles were removed from the subgrade. These problems were not associated with the nonwoven geotextiles because the particles clogging the geotextiles were trapped within the fibers of the geotextiles. The above findings are consistent with those of Metcalfe and Holtz (1994).

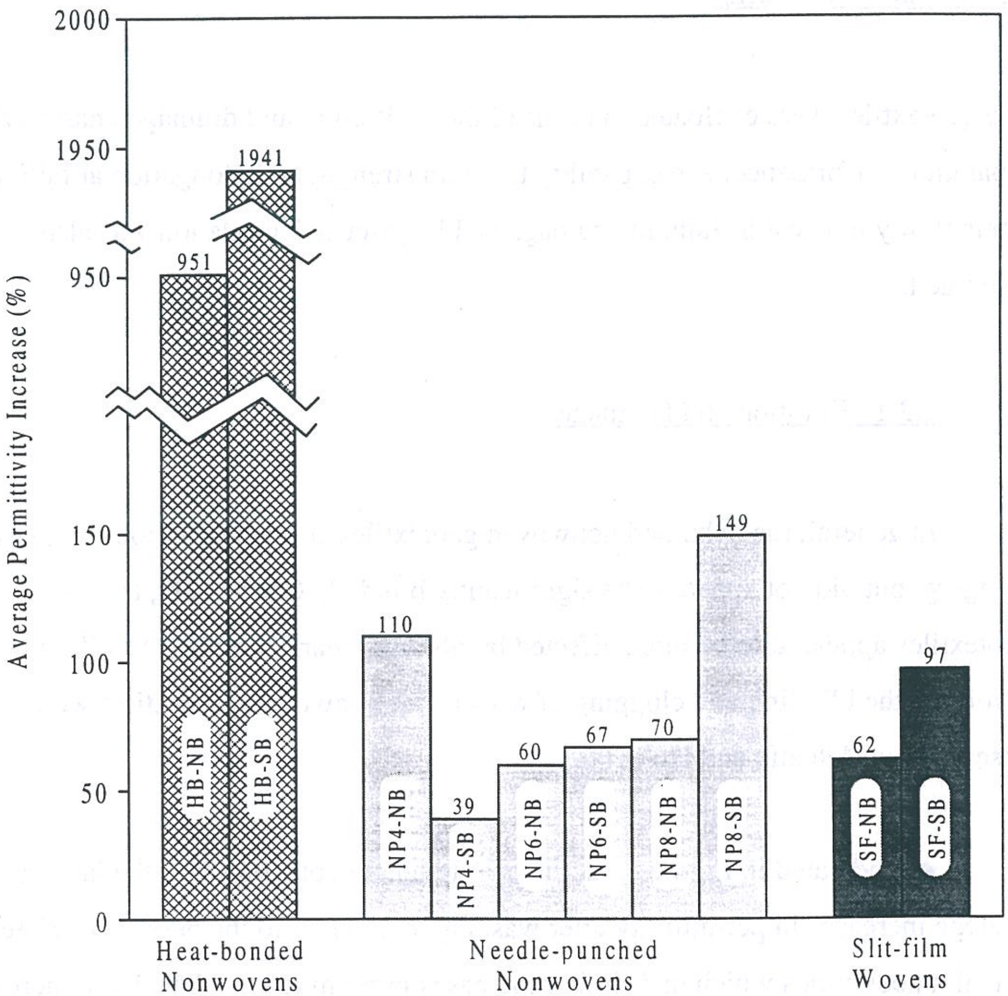

Figure 8.12 - Average permittivity increase (after washing) vs. geotextile type.

Except for the NP4 geotextile, the average permittivity increases were higher in the southbound lane than the northbound lane, as shown in Figure 8.12. This trend is consistent with the laboratory observations, discussed in Section 6.2. In general, the southbound lane geotextiles may have experienced more blinding and clogging because they may have been subjected to a higher number of groundwater fluctuation cycles due to their greater depth. However, evidence to support this hypothesis is lacking.

Some of the geotextile blinding and clogging was due to iron oxide precipitates. The permittivity tests and blinding/clogging observations made for this study included the effects of both soil particles and chemical precipitates. The iron staining on the woven slit-film geotextiles was in the form of iron oxide precipitates deposited on the surface of the geotextiles. The iron oxides did not appear to be deposited on the surface of the nonwoven geotextiles, rather the oxide precipitates tended to be distributed throughout the geotextile structure, discoloring the geotextile.

Based on laboratory observations, there does not appear to be trends of increased or decreased iron staining between any of the geotextiles. This suggests that iron staining may be more dependent on the subgrade soil composition (chemistry, mineralogy, etc.) than the type of geotextile. Also, the amount of iron staining may not be particularly sensitive to the amount of groundwater fluctuation cycles, although undoubtedly some cyclic or dynamic action must occur to promote the movement of the stained particles.

As discussed previously, caking was observed on some of the geotextiles. Metcalfe and Holtz (1994) concluded from their permittivity test results that caking on the geotextiles probably prevented the flow of water through the pores, even though the geotextiles were placed in the permeameter in such a way as to simulate upward flow from the subgrade through the geotextiles (as in this study). For the geotextiles tested in this study, it was difficult to evaluate the affect the caked fines had on the permittivity values because the specimens that contained caking were also blinded and/or clogged. To directly evaluate the influence of caking, specimens that contained only caking would need to be examined.

As discussed in Section 8.1, heavy groundwater seepage was encountered above the subgrade in the Soil-SB test pit excavation, but not in any of the other explorations. Therefore, it appears that the geotextiles are providing lateral drainage since the conditions (i.e. depth to subgrade, soil type, etc.) at the Soil-SB location were not radically different than the conditions at the other southbound lane explorations.

8.2.2 Fines Migration/Separation

As shown in Table 8.1, significant fines were observed to have migrated into the base course aggregates at the HB-NB, NP6-NB, SF-NB, NP6-SB, and NP8-SB exploratory locations. The most severe migration was measured to be up to 50 mm at the SF-NB and NP6-SB sections. Possible mechanisms for fines migration are the fluctuating groundwater table and pumping action from the vehicle loading.

Table 8.1 - Summary of mudcake observations.

Geotextile	Mudcake Thickness (mm)	Geotextile	Mudcake Thickness (mm)
HB-NB	10 to 20	HB-SB	Trace*
NP4-NB	Trace	NP4-SB	Trace
NP6-NB	10 to 20	NP6-SB	50
NP8-NB	Trace	NP8-SB	10 to 40
SF-NB	40 to 50	SF-SB	Trace*

* No significant evidence of migrated fines in the base course, but caked fines on the geotextile.

The migrated fines in the base course aggregates were generally the same color as the subgrade soils. Even in cases where heavy iron stains were present in the subgrade soils, the migrated fines were similar colors. To confirm the grain size distribution of the migrated fines was similar to the subgrade soil, a hydrometer analysis was performed on the fines washed from the SF-NB mudcake sample, as discussed in Section 7.1.2. As shown in Figure 8.13 (and Figure B.13), the fines washed from the mudcake sample have a similar distribution slope to the underlying subgrade soil, although there is some divergence in the range of the smaller particles sizes (0.001 to 0.004 mm). Deviations between these grain size distributions should be expected however, because of the preexisting fines in the mudcake sample (from the base course).

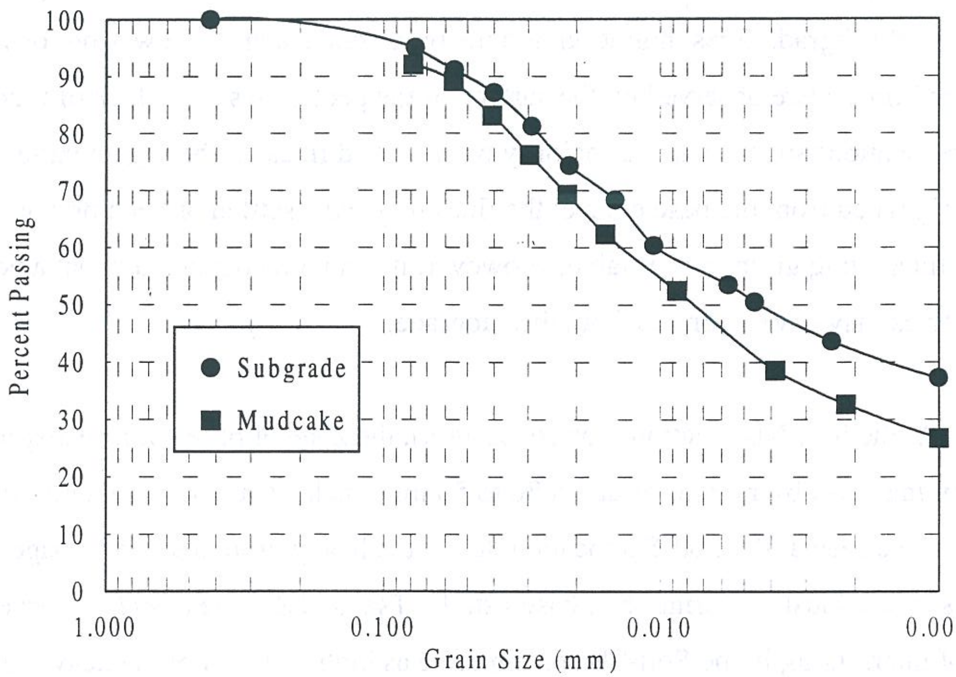

Figure 8.13 - Hydrometer test results for subgrade soil and mudcake fines, SF-NB.

The sieve analyses indicated that the mudcake samples contained more fines than the overlying base course only at the SF-NB, NP4-SB, and NP6-SB locations. It is not clear why the grain size testing did not reflect the increased level of fines observed in the mudcake at the other locations. The most likely possibility is associated with the difficulties in obtaining representative samples of the thin mudcake layers.

Grain size distributions of all the subgrade soils are provided in Figures 8.14 and 8.15. However, it is difficult to correlate trends in the observed fines migration with the grain size distribution curves. Trends involving fines migration are better addressed by the FHWA filtration design criteria, discussed later.

Also, as indicated in Table 8.1, at the HB-SB and SF-SB locations significant evidence of subgrade fines migration into the base course aggregate was not observed, but caked fines were observed on the surface of the geotextiles. The lack of mudcake at these locations suggests that a majority of the caked fines on these geotextiles may have originated from the base course; the fines may have settled or been drawn down by the fluctuating groundwater table. However, it cannot be discounted that a portion of the fines may have migrated from the subgrade.

At the Soil-NB location (control section), the zone of base course/subgrade intermixing was observed to be about 30 to 50 mm thick. The zone of intermixing could not be seen at the Soil-SB location due to the heavy groundwater seepage discussed previously. During the Phase I study, Tsai and Savage (1992) observed the zone of intermixing in the Soil-SB section to be as high as 130 mm in excavations made after the second layer of base course soil was placed (about 600 mm total base course thickness). Other than construction traffic, loading on the southbound lane prior to the excavations consisted of ten passes of a loaded dump truck for the trafficking tests and about a day and a half of normal vehicle traffic.

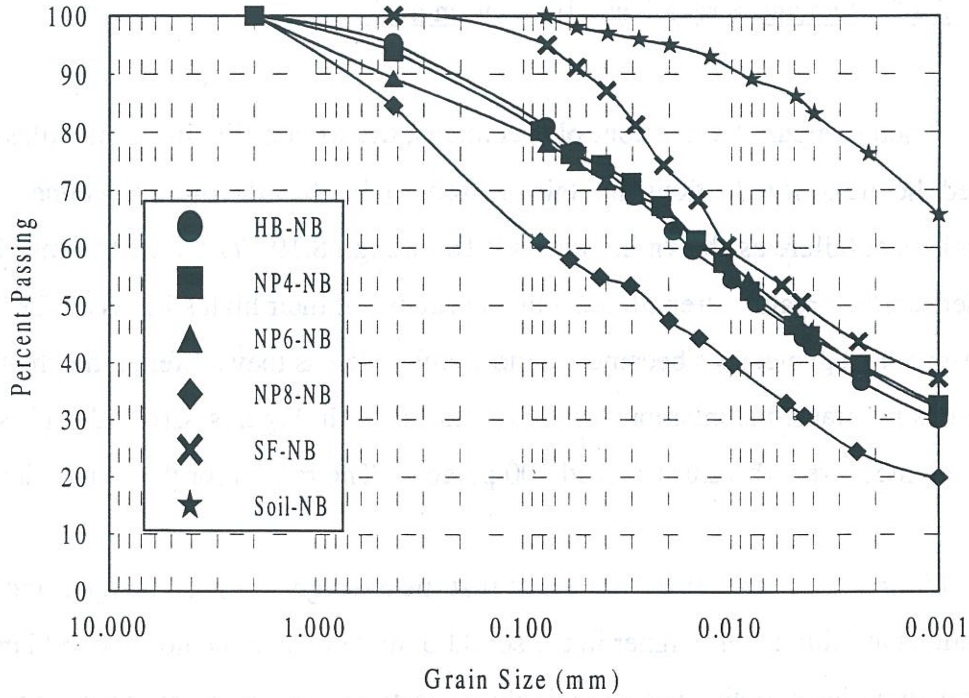

Figure 8.14 - Hydrometer test results for subgrade soils, northbound lane.

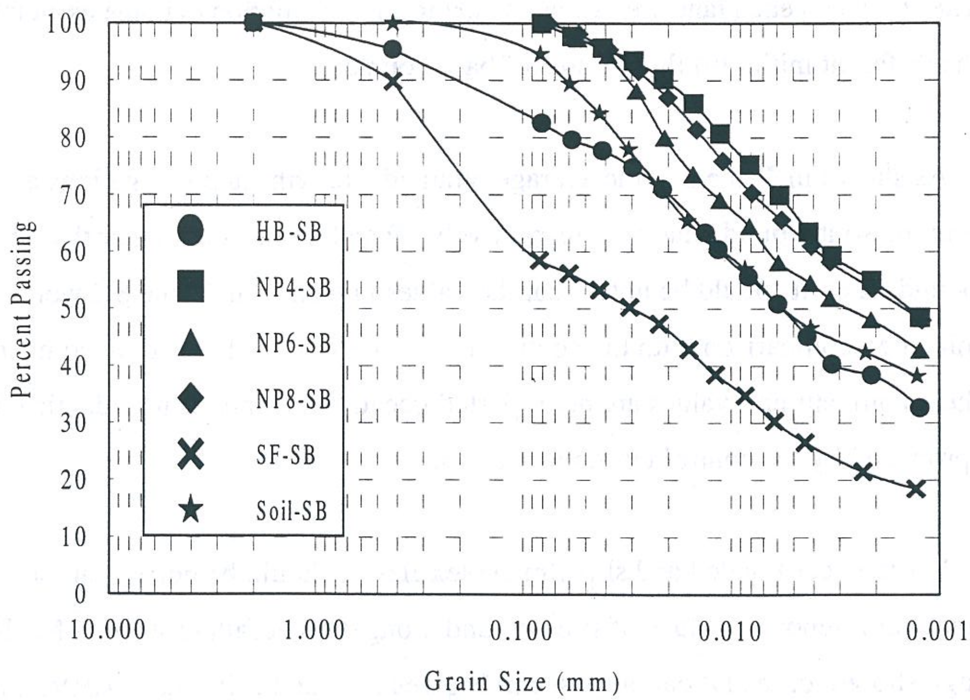

Figure 8.15 - Hydrometer test results for subgrade soils, southbound lane.

8.2.3 Retained Strength and Elongation at Failure

When compared to the control specimens, the woven slit-film geotextiles suffered the greatest reductions in retained strength, but had the highest retained elongations at failure as shown in Figures 8.16 through 8.19. The slit-films may have experienced the greatest strength reductions because of their high stiffness. The needle-punched geotextiles became the most embrittled as they suffered the greatest reductions in retained elongation at failure. As shown in Figures 8.16 and 8.17, some of the retained strength values exceed 100 percent. The reason for this is not clear.

Figures 8.16 through 8.19 indicate that the average retained strengths and elongations at failure were higher in the southbound lane than the northbound lane. As the geotextiles in both lanes were likely subjected to the same amount of long-term degradational factors (i.e. thermo-oxidation, etc.), the differences in the retained properties between each lane are primarily due to the installation damage associated with the different initial lift thicknesses of base course.

As shown in Table 8.2, the average retained strengths and elongations at failure in the southbound lane were respectively 19 and 25 percent higher than the northbound lane. It should be noted that the values presented in Table 8.2 were determined by comparison with the control tests. The values obtained by comparison with the manufacturers' values are not reported because they are nearly identical to those produced by the control test comparisons.

For the heat-bonded and slit-film geotextiles, it should be noted that the manufacturers' reported values of strength and elongation at failure were in MARV. Although shown for analytical purposes in Figures 8.17 and 8.19, the MARVs should

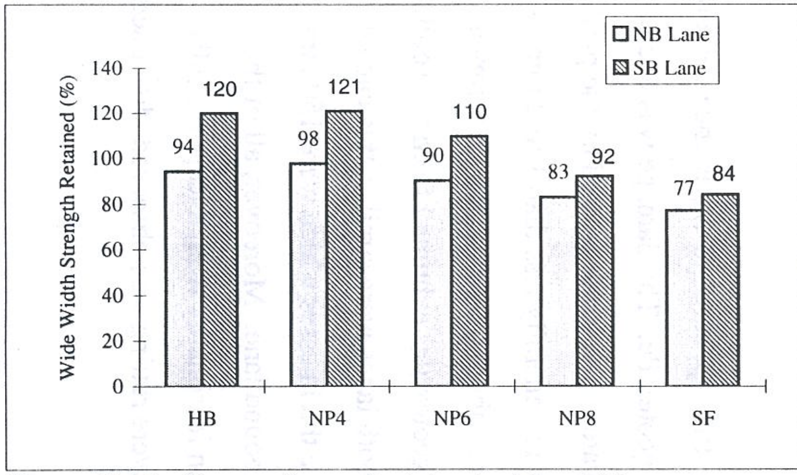

Figure 8.16 - Comparison of retained wide width strength determined by the control tests.

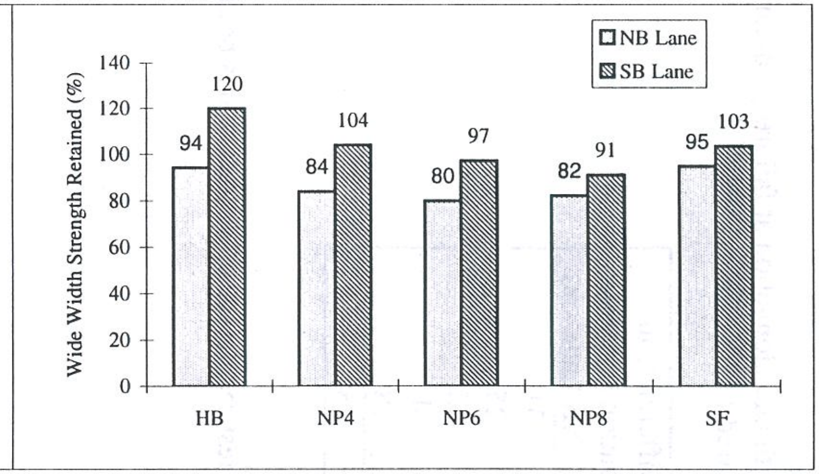

Figure 8.17 - Comparison of retained wide width strength determined by the manufacturers' reported values.

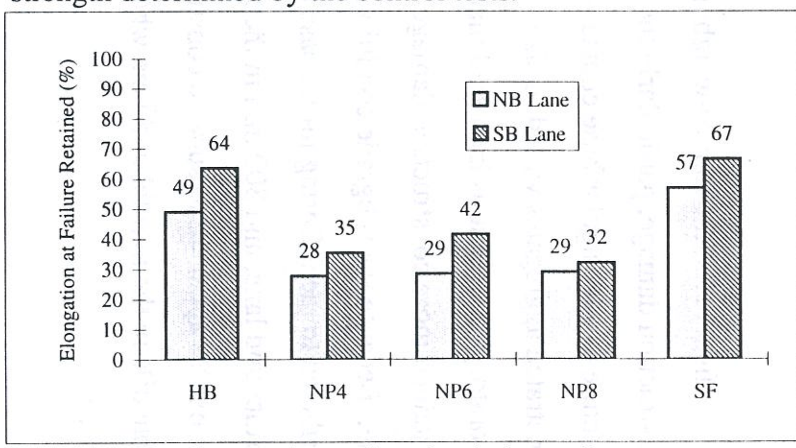

Figure 8.18 - Comparison of retained elongation at failure determined by the control tests.

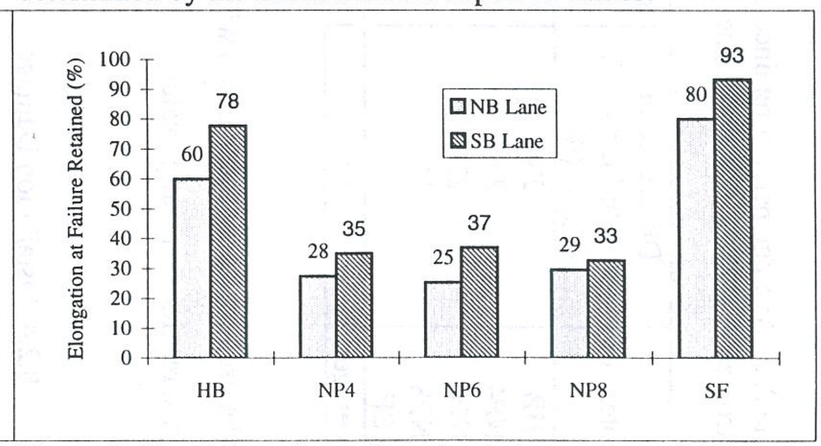

Figure 8.19 - Comparison of retained elongation at failure determined by the manufacturers' reported values.

Table 8.2 - Average percent retained strength and elongation at failure (compared to control tests) of the southbound lane compared to northbound lane.

Geotextile	Difference in Strength SB vs. NB Lane (%)	Difference in Elongation at Failure SB vs. NB Lane (%)
HB	28	31
NP4	23	25
NP6	22	45
NP8	11	4
SF	9	18
Average	19	25

not be used for direct comparison with the test results for these geotextiles because the test results are average values.

8.2.4 Installation Damage

In general, the lighter-weight geotextiles appeared to experience the most construction damage, particularly the NP4 geotextile. The damage was due to puncture by the angular base course aggregates. The holes created by the partially penetrated aggregates varied in size, but were generally less than 1 to 2 mm. Also, laboratory observations indicated that the northbound lane geotextile samples contained more construction damage than geotextiles exhumed from the southbound lane. Because the subgrade conditions in both lanes were similar, this can be attributed to the differing initial base course thicknesses which were 150 mm in the northbound lane, and 300 mm in the southbound lane. Moreover, all of the geotextiles appeared to survive construction reasonably well, except the NP4 geotextile in the northbound lane where severe rutting was observed, discussed earlier.

It is interesting to note that the level of installation damage observed on the lighter weight geotextiles is not reflected in Figures 8.16 through 8.19. Figures 8.16 and 8.17 indicate that the HB and NP4 geotextile specimens had the highest values of average retained strength. These findings partially contradict Koerner and Koerner (1990) who found that the low mass per unit area geotextiles suffered the greatest strength reductions and number of holes.

8.2.5 Long-Term Degradation

It is difficult to distinguish between the effects of installation damage and long-term degradation in the reductions in retained strength and elongation at failure. However, of all the long-term degradational mechanisms, the geotextiles at this site appear to be the most susceptible to thermo-oxidation which can cause embrittlement and reductions in strength (Section 4.1.8). Some of the transfer metals like iron, manganese, and copper which increase the potential for thermo-oxidation degradation, are likely included in the precipitates causing the staining discolorations on the geotextiles. The effects of long-term degradation could be better evaluated by comparing the results of these wide width tests with those in a future study, say 5 to 10 years from now.

Visual examinations of the geotextile fibers under a microscope did not reveal evidence of biological growth.

8.3 FHWA, Task Force 25, and WSDOT Criteria

The geotextile filtration performance is compared to the FHWA, Task Force 25, and WSDOT design criteria in Table 8.3. For the FHWA design criteria, the grain size

Table 8.3 - Subgrade and geotextile characteristics vs. filtration design criteria.

Geotextile	Subgrade Soil	Percent Pass. No. 200	C_u	D_{85} (mm)	D_{15} (mm)
HB-NB	Fat clay w/sand (CH)	81	200	0.12	0.00018
HB-SB	Lean clay w/sand (CL)	82	69	0.10	0.00027
NP4-NB	Lean clay w/sand (CL)	78	186	0.13	0.00013
NP4-SB	Fat clay (CH)	99	31	0.014	0.00015
NP6-NB	Elast. silt w/sand (MH)	78	217	0.20	0.00011
NP6-SB	Fat clay (CH)	100	81	0.025	0.00012
NP8-NB	Sand elastic silt (MH)	60	554	0.42	0.0002
NP8-SB	Fat clay (CH)	100	65	0.017	0.00008
SF-NB	Fat clay (CH)	95	286	0.034	0.00007
SF-SB	Sandy silt (ML)	57	235	0.33	0.0008

				FHWA		TF 25	WSDOT	
Geotextile	Subgrade Soil	Mudcake Thickness (mm)	Manufact. Reported AOS (mm)	Req'd max. AOS-Rentent. (mm)	Req'd min. AOS-Clogging (mm)	AOS<0.3 mm for >50% pass No. 200 sieve	Separator AOS≤0.60 (mm)	Soil Stab. AOS≤0.43 (mm)
HB-NB	CH	10 to 20	0.21	0.22 - OK	0.0005 - OK	OK	OK	OK
HB-SB	CL	Trace*	0.21	0.18 - NG	0.0008 - OK	OK	OK	OK
NP4-NB	CL	Trace	0.18 - 0.30	0.23 ~ OK	0.0004 - OK	~ OK	OK	OK
NP4-SB	CH	Trace	0.18 - 0.30	0.03 - NG	0.0005 - OK	~ OK	OK	OK
NP6-NB	MH	10 to 20	0.15 - 0.21	0.30 - OK	0.0003 - OK	OK	OK	OK
NP6-SB	CH	64 to 69	0.15 - 0.21	0.05 - NG	0.0004 - OK	OK	OK	OK
NP8-NB	MH	Trace	0.125 - 0.18	0.30 - OK	0.0006 - OK	OK	OK	OK
NP8-SB	CH	10 to 40	0.125 - 0.18	0.03 - NG	0.0002 - OK	OK	OK	OK
SF-NB	CH	40 to 50	0.30	0.03 - NG	0.0002 - OK	~ OK	OK	OK
SF-SB	ML	Trace*	0.30	0.30 ~ OK	0.0002 - OK	~ OK	OK	OK

* No significant evidence of migrated fines in base course, but caked fines on geotextile.

Table 8.3 (continued) - Subgrade and geotextile characteristics vs. filtration design criteria.

	FHWA		Task Force 25	WSDOT-Separation	WSDOT-Soil Stab.
Geotextile	Min. Permeability of Unwashed Geot. Specimens (cm/s)	ψ of Unwashed Geotext. Specimens ≥ 0.1 (sec^{-1})	Min. Permeability of Unwashed Geot. Specimens (cm/s)	ψ of Unwashed Geotext. Specimens ≥ 0.02 (sec^{-1})	ψ of Unwashed Geotext. Specimens ≥ 0.10 (sec^{-1})
HB-NB	0.006 - OK	All 4 tests OK	0.006 - OK	All 4 tests OK	All 4 tests OK
HB-SB	0.001 - OK	3 OK, 1 NG	0.001 - OK	All 4 tests OK	3 OK, 1 NG
NP4-NB	0.1 - OK	All 4 tests OK	0.1 - OK	All 4 tests OK	All 4 tests OK
NP4-SB	0.3 - OK	All 4 tests OK	0.3 - OK	All 4 tests OK	All 4 tests OK
NP6-NB	0.3 - OK	All 4 tests OK	0.3 - OK	All 4 tests OK	All 4 tests OK
NP6-SB	0.3 - OK	All 4 tests OK	0.3 - OK	All 4 tests OK	All 4 tests OK
NP8-NB	0.3 - OK	All 4 tests OK	0.3 - OK	All 4 tests OK	All 4 tests OK
NP8-SB	0.2 - OK	All 4 tests OK	0.2 - OK	All 4 tests OK	All 4 tests OK
SF-NB	0.006 - OK	All 4 tests OK	0.006 - OK	All 4 tests OK	All 4 tests OK
SF-SB	0.004 - OK	1 OK, 3 NG	0.004 - OK	All 4 tests OK	1 OK, 3 NG

Note: All washed geotextile specimens meet permeability and permittivity criteria for FHWA, Task Force 25, and WSDOT requirements.

Table 8.4 - Required index strength properties of WSDOT and Task Force 25 compared to manufacturers' values.

	WSDOT - Separation Application			Task Force 25 Moderate Survivability Rating			Task Force 25 High Survivability Rating		
Geotextile	Grab	Puncture	Tear	Grab	Puncture	Tear	Grab	Puncture	Tear
HB	NG	NG	NG	OK	OK	OK	NG	NG	NG
NP4	NG	OK	OK	OK	OK	OK	NG	NG	NG
NP6	NG	OK	OK	OK	OK	OK	NG	OK	NG
NP8	OK	OK	OK	OK	OK	OK	OK	OK	OK
SF	OK	OK	OK	OK	OK	OK	OK	OK	OK

Note: For Task Force 25 criteria, all nonwovens assumed >50% geotextile elongation; wovens <50% elongation (see Table 4.4).

distribution of the subgrade soils was determined from Figures B.1 through B.12. Where there was a high percentage of very small soil particles in the subgrade soils, the hydrometer tests did not yield D_{15} values. In these instances, the D_{15} values had to be extrapolated from the grain size curve produced by the hydrometer tests.

As shown in Table 8.3, the FHWA criteria provided reasonable predictions of filtration performance for most of the geotextiles. However, the FHWA criteria did not predict retention failure at the HB-NB and NP6-NB locations where mudcake was observed. Also, the FHWA criteria predicted a retention failure for the HB-SB and NP4-SB geotextiles, but no mudcake was observed at these locations. However, caked fines were observed on the HB-SB geotextile, as discussed in Section 8.2.2.

As seen in Table 8.3, both the Task Force 25 and WSDOT criteria for the maximum AOS were not effective at half (five cases) of the explorations containing geotextiles, as subgrade fines migration into the base course was observed. At three of these locations (SF-NB, NP6-SB, and NP8-SB) the subgrade soil particle sizes were very small ($D_{85} \leq 0.034$ mm). The criteria may have also failed at the HB-SB and SF-SB locations if some of the fines caked on the geotextiles migrated from the subgrade.

Table 8.3 indicates that all of the geotextile specimens meet the FHWA and Task Force 25 geotextile permeability requirements. Also, all of the specimens meet the permittivity requirements for geotextiles used in WSDOT separation applications. All but one heat-bonded and three slit-film unwashed specimens meet the FHWA and WSDOT soil stabilization applications permittivity requirements.

Comparisons between the manufactures' reported index strength values and the WSDOT and Task Force 25 requirements are presented in Table 8.4. For the Task Force 25 criteria (outlined in Table 4.4), the nonwoven geotextiles used in the study were assumed to have greater than 50 percent geotextile elongation, and the woven geotextiles were assumed to have less than 50 percent elongation. These assumptions appear reasonable based on the manufacturers' reported values, shown in Table 2.1.

Based on the Task Force 25 survivability criteria outlined in Table 4.3, the geotextiles installed in the southbound lane would have a moderate construction survivability rating, and the geotextiles in the northbound lane would have a moderate to high survivability rating. It should be noted that WSDOT does not incorporate different levels of survivability into the 1996 Standard Specifications for geotextiles used in separation applications. However, WSDOT does include different levels of survivability criteria for geotextiles used in underground drainage and permanent erosion control applications.

As shown in Table 8.4, according to the WSDOT required strength criteria for geotextile separators, only the NP8 and SF geotextiles would be allowed to be used at the test site. For the Task Force 25 criteria, all of the geotextiles would be allowed in moderate survivability conditions, while only the NP8 and SF geotextiles would be allowed in high survivability conditions.

As discussed in Section 8.2.4, all of the geotextiles at the test site survived construction reasonably well, except the NP4 geotextile in the northbound lane where severe rutting occurred. The lighter-weight geotextiles appeared to experience the most construction damage, however this damage was not reflected in the results of the strength tests. Based on the above information, it appears the index strength properties required by Task Force 25 for moderate and high survivability conditions are reasonable. The WSDOT strength requirements for geotextile separators may be too restrictive in conditions of moderate survivability (as defined by Task Force 25).

9.0 SUMMARY, CONCLUSIONS, AND RECOMMENDATIONS

9.1 Summary

A full scale field study has been conducted to investigate the influence of different geotextiles on the performance of a pavement system. The test road section is located on SR-507 in Bucoda, Washington and consists of a two-lane highway with asphalt pavement. Five different geotextiles and a control section were installed in each lane, in conjunction with WSDOT repair operations in 1991. Prior to the installation of the geotextiles, the site had a long history of poor pavement performance and contained soft subgrade soils and a seasonally high groundwater table, which made the site ideal for application of geotextile separators. In June, 1996, excavations were made at each test section (12 in total) to evaluate the soil and geotextile conditions, collect representative samples, and perform a series of in-situ tests.

In general, the subgrade soils appeared to have consolidated since the geotextiles were installed. Density tests suggest that the subgrade in sections containing geotextiles consolidated more than in the sections without geotextiles (control sections).

Permittivity testing indicated that the needle-punched and slit-film geotextiles experienced similar increases in permittivity after washing. The heat-bonded geotextiles had the highest increases in permittivity after washing, which implies they experienced the most clogging. The permittivity values of the slit-film geotextiles are less representative of the in-situ conditions than the other geotextiles because particles blinding the slit-films may have been dislodged when they were removed from the subgrade or in handling. Soil particles as well as chemical precipitates (iron oxides) contributed to the blinding and clogging observed on the geotextiles.

Evidence of subgrade fines migration into the base course aggregates was found at half (five cases) of the explorations where geotextiles were installed. Fines migration may also have occurred at two other locations, as fines were found to be caked on the surface of the geotextiles. The FHWA filter design predictions correlated reasonably well with these observances.

The slit-film geotextiles had the greatest reductions in retained strength, but became the least embrittled as they had the highest retained elongations at failure. The needle-punched geotextiles became the most embrittled as they suffered the greatest reductions in elongation at failure. The geotextiles in the northbound lane suffered greater reductions in retained strength and elongation at failure than the geotextiles in the southbound lane, most likely due to the differing initial base course layer thicknesses. The geotextiles in the northbound lane also contained more construction damage (aggregate puncture). The lighter-weight geotextiles contained the greatest number of holes due to aggregate puncture; however, this damage was not reflected in the strength testing, as the HB and NP4 geotextiles retained the most strength.

It appears the index strength properties required by Task Force 25 for moderate and high survivability conditions are reasonable. The WSDOT strength requirements for geotextile separators may be too restrictive in conditions of moderate survivability (as defined by Task Force 25).

The asphalt pavement at the test site was in good condition at the time of the field investigation. Therefore, the observed fines migration into the base course and the damage incurred by the geotextiles did not appear to adversely impact the performance of the pavement system since construction.

9.2 Conclusions

1. At a site with a history of poor pavement performance, various types of geotextile separators have been effective in preserving the integrity of the pavement system since construction.

2. From permittivity testing, it appeared that heat-bonded geotextiles were significantly more susceptible to clogging than needle-punched or slit-film geotextiles.

3. The FHWA filtration design criteria produced reasonable predictions of filtration performance. The maximum AOS values specified by WSDOT and Task Force 25 were not always effective in preventing fines migration, particularly for saturated, fine-grained subgrades consisting of very small particles ($D_{85} \leq 0.034$ mm).

4. The initial lift thickness of base course had a significant effect on the strength and elongation at failure of geotextiles. Elongation at failure (i.e. modulus) appeared to be more affected than strength.

5. More geotextile damage due to aggregate puncture generally appeared to occur under thinner initial base course lifts. Visual examinations indicated the lighter-weight (HB and NP4) geotextiles sustained more construction damage; however, this damage was not reflected in the results of the strength tests. Moreover, all of the geotextiles at the test site appeared to survive construction reasonably well, except the NP4 geotextile in the northbound lane where severe rutting occurred.

6. The index strength properties required by Task Force 25 for moderate and high survivability conditions appear reasonable. The WSDOT strength requirements for geotextile separators may be too restrictive in conditions of moderate survivability (as defined by Task Force 25).

7. The subgrade soils in the test section appeared to have consolidated since the geotextiles were installed. Density tests suggested that the subgrade in the sections containing geotextiles consolidated more than the subgrade in the sections without geotextiles.

8. Geotextiles may provide lateral drainage. However, the effect that lateral drainage has on subgrade consolidation and pavement performance is unclear.

9. The long-term performance of geotextile separators may not be critical in many cases because of increased subgrade strength and reduced compressibility due to consolidation. In these cases, long-term degradational issues are of less importance.

9.3 Evaluation of WSDOT Specifications

Based on the observations of fines migration, the maximum allowable AOS value of 0.60 mm for geotextiles used in separation applications may be too large. However, it should be noted that a maximum AOS of 0.30 mm as specified by Task Force 25 and recommended by Metcalfe and Holtz (1994) would not have restricted the use of any of the geotextiles at the test site.

As shown in Table 8.3, the fine-grained subgrade soil at four locations consisted of very small particles with $D_{85} \leq 0.034$ mm. Fines migration was observed at three of these locations. The FHWA filter design criteria for these soils specify maximum AOS values ranging from 0.03 to 0.05 mm. According to GFR (1996), LINQ Industrial Fabrics produces a geotextile (Typar 3801) with an AOS value as low as 0.07 mm. However, no other manufacturers produce geotextiles with AOS values reasonably close to 0.03 mm. Based on the above information, currently available geotextiles may not be able to completely prevent fines migration in saturated, fine-grained subgrades consisting of very small particles (say $D_{85} \leq 0.034$ mm). In these cases it may be necessary to compensate for some fines migration in the design of the pavement system by increasing the thickness of the asphalt concrete and/or the base course. Graded granular filters could also be considered.

As discussed in Section 8.3, the WSDOT strength requirements for geotextile separators may be too restrictive in conditions of moderate survivability (as defined by Task Force 25). Based on the performance of the geotextile separators at the test site, it appears that the strength requirements in the 1996 Standard Specifications could be reduced so that lighter-weight geotextile separators could be used in some conditions. These conditions should be the same or better than those in the southbound lane of the test site where the subgrade was saturated and relatively soft, and the initial thickness of base course was at least 300 mm.

Implementing different strength requirements for geotextile separators based on different levels of survivability appears viable, as it already exists for geotextiles used in underground drainage and permanent erosion control applications (Section 9-33.2, 1996 Standard Specifications). In fact, the strength requirements for geotextiles used in low survivability (as defined by WSDOT) underground drainage applications appear reasonable for geotextile separators used in conditions equal to or better than the southbound lane of the test site, discussed above. As shown in Table 9.1, the WSDOT strength specifications for low survivability are essentially the same as the Task Force 25 requirements for moderate survivability. Comparisons between the manufacturers' reported values and the WSDOT requirements for low survivability conditions are presented in Table 9.2.

Table 9.1 - Comparison of WSDOT and Task Force 25 strength requirements.

	WSDOT Low Surviv. Underground Drainage	Task Force 25 Moderate Survivability
Strength Test	Woven/Nonwoven	Woven/Nonwoven
Grab Tensile - Strength	800 N/500 N min.	801 N/512 N min.
Grab Tensile - Failure Strain	<50%/≥50%	<50%/>50%
Puncture	300 N/180 N	300 N/178 N
Trapezoid Tear	300 N/180 N	300 N/178 N

Note: For Task Force 25, geotextiles with <50% failure strain are assumed to be woven, geotextiles with >50% failure strain are assumed to nonwoven.

Table 9.2 - Comparison of manufacturers' reported strength values with WSDOT requirements for low survivability conditions.

	WSDOT - Low Survivability Underground Drainage Applications		
Geotextile	Grab	Puncture	Tear
HB	578 N - OK	178 N - OK	267 N - OK
NP4	489 N - OK	267 N - OK	222 N - OK
NP6	667 N - OK	335 N - OK	311 N - OK
NP8	911 N - OK	445 N - OK	380 N - OK
SF	1334 N - OK	645 N - OK	511 N - OK

Similar implementation of different levels of survivability criteria might also be considered for geotextiles used in reinforcement applications, although additional research may be necessary to evaluate the required strength properties.

The permittivity testing from this study and Metcalfe and Holtz (1994) indicate that heat-bonded geotextiles are more susceptible to clogging than needle-punched or slit-film geotextiles. These findings should be considered by WSDOT when geotextiles are selected for filtration and drainage applications.

9.4 Recommendations for Future Research

Observations of long-term pavement performance at the test site should be made. In particular, at the onset of pavement failure (i.e. rutting, fatigue cracking, etc.) valuable information could be obtained by reexamining the soil and groundwater conditions, fines migration, subgrade densities, etc. The reevaluation would provide insight on how these conditions affect failure.

The effects of long-term degradation on the geotextiles at the test site could be studied in greater detail. The study could compare the results of strength tests in the present research with those in a future study, say 5 to 10 years from now. Also, the different types of degradational mechanisms could be examined in detail by scanning electron microscopy (SEM) and chemical structural analysis techniques such as differential scanning calorimetry (DSC) and Fourier transform infrared spectroscopy (FTIR). Although long-term degradational issues may not be critical in many separation applications as stated in the above conclusions, the information obtained from such research could be applied to other geotextile applications such as reinforced walls or slopes where long-term performance can be important.

More detailed examination of the FWD data could also be performed by employing the back-calculation techniques used by WSDOT. The back-calculations produce better estimates of the subgrade moduli based on the actual thicknesses of the pavement components. FWD tests could also be correlated with long-term pavement performance.

As previously discussed, the density tests suggest that the subgrade in the sections containing geotextiles consolidated more than in the control sections. To develop a possible explanation for this observation, the relation between mechanical stresses and pore pressures within the subgrade could be evaluated by using numerical modeling techniques, such as the computer software FLAC (Fast Lagrangian Analysis of Continua). Also, the influence that chemical reactions (i.e. oxidation involving transfer metals) and their subsequent thermal effects have on subgrade consolidation should be investigated.

The findings of this study should be compared to the AASHTO M-288 requirements once they are published.

List of References

Allen, T.M. (1991). "Determination of Long-Term Tensile Strength of Geosynthetics: A State-of-the-Art Review", *Proceedings Geosynthetics '91 Conference*, Altanta, USA. Vol. 1, pp. 351-379.

Allen, T.M. and Bathurst, R.J. (1994). "Characterization of Geosynthetic Load-Strain Behavior After Installation Damage", *Geosynthetics International,* Vol. 1, No. 2, pp. 181-199.

Alobaidi, I. and Hoare, D.J. (1996). "The Development of Pore Water Pressure at the Subgrade-Subbase Interface of a Highway Pavement and its Effect on Pumping of Fines", *Geotextiles and Geomembranes,* Elsevier Science Limited, Vol. 14, No. 2, pp. 111-135.

Austin, D.N. and Colemen, D.M. (1993). "A Field Evaluation of Geosynthetic-Reinforced Haul Roads Over Soft Foundation Soils", *Proceedings Geosynthetics '93 Conference*, Vancouver, Canada. Vol. 1, pp. 65-80.

Ayres, D. (1986). "Geotextiles or Geomembranes in Track - British Railway Experience", *Geotextiles and Geomembranes*, Vol. 3, pp. 129-142. (cited reference)

Bell, A.L., McCullough, L.M., and Gregory, B.J. (1981). "Clay Contamination in Crushed Rock Highway Sub-bases", *Proceedings of the Conference on Engineering Materials,* Sydney, New South Wales, Australia, pp. 355-365. (cited reference)

Bonaparte, R., Ah-Line, C., Charron, R., and Tisinger, L. (1988). "Survivability and Durability of a Nonwoven Geotextile", *Geosynthetics for Soil Improvement,* Geotechnical Special Publication No. 18, ASCE, pp. 68-91.

Bourdeau, P.L. (1991). "Membrane Action in a Two-Layer Soil System Reinforced By Geotextile", *Proceedings Geosynthetics '91 Conference*, Altanta, USA, Vol. 1, pp. 439-453.

Brorsson, I. and Eriksson, L. (1986). "Long-Term Properties of Geotextiles and Their Function as a Separator in Road Construction", *Proceedings 3rd International Conference on Geotextiles*, Vienna, Austria. Vol. 1, pp. 93-98.

Cassady, L. and Bright, D.G. (1995). "Durability of Geosynthetics Exposed to Nine Years of Natural Weathering", *Proceedings Geosynthetics '95 Conference*, Nashville, USA, Vol. 3, pp. 841-851.

Cazzuffi, D.A., Fede, L., Montanelli, F., and Rimoldi, P. (1994). "Outdoor and UV-B Laboratory Weathering Resistance of Geosynthetics", *Proceedings 5th International Conference on Geotextiles, Geomembranes, and Related Products,* Singapore, Sept. 1994, Vol. 3, pp. 1195-1198.

Christopher, B.R. (1983). "Evaluation of Two Geotextile Installations in Excess of a Decade Old", *Transportation Research Record 916*, Transportation Research Board, pp. 79-88.

Collin, J.G., Kinney, T.C., Fu, X. (1996). "Full Scale Highway Load Test of Flexible Pavement Systems With Geogrid Reinforced Base Courses", *Geosynthetics International,* Vol. 3, No. 4, pp. 537-549.

den Hoedt, G. (1989) "Durability Experience in the Netherlands 1958-1988", *Durability and Aging of Geosynthetics,* edited by R. M. Koerner, Elsevier Applied Science, pp. 82-94.

Dondi, G. (1994). "Three-Dimensional Finite Element Analysis of a Reinforced Paved Road", *Proceedings 5th International Conference on Geotextiles, Geomembranes, and Related Products*, Singapore, Sept. 1994, Vol.1, pp. 95-100.

Fannin, R.J. and Sigurdsson, O. (1996). "Field Observations on Stabilization of Unpaved Roads with Geosynthetics", *Journal of Geotechnical Engineering*, ASCE, Vol. 122, No. 7, July 1996. Paper No. 10806, pp. 544-553.

Geotechnical Fabrics Report, (December 1990). Volume 8, Number 7.

Geotechnical Fabrics Report, (December 1991). Volume 9, Number 9.

Geotechnical Fabrics Report, (December 1992). Volume 10, Number 9.

Geotechnical Fabrics Report, (December 1996). Volume 14, Number 9.

Helwany, M.B. and Wu, J.T.H. (1995). "A Numerical Model for Analyzing Long-Term Performance of Geosynthetic-Reinforced Soil Structures", *Geosynthetics International*, Vol. 2, pp. 429-453.

Holtz, R.D. (1996). *Performance of Geotextile Separators,* Report No. WA-RD 321.2, Research Project T9233, Task 13, WSDOT, 55 pp.

Holtz, R.D., Christopher, B.R., and Berg, R.R. (1995). *Geosynthetic Design and Construction Guidelines,* Publication No. FHWA HI-95-038, US Dept. of Transportation, FHWA, 395 pp.

Holtz, R.D. and Page, M.W. (1991). *Performance of Geotextile Separators,* Report No. WA-RD 280.1, Final Technical Report, Research Project GC 8719, Task 14, WSDOT, pp. 136.

Huang, Y.H. (1993). *Pavement Analysis and Design,* Prentice-Hall, Inc., 805 pp.

Ingold, T.S. (1988). "Civil Engineering Requirements For Long-Term Behaviour of Geotextiles", *Durability of Geotextiles,* Chapman and Hall Ltd., pp. 20-29.

Kelen, T. (1983). *Polymer Degradation*, Van Nostrand Reinhold Company Inc., 211 pp.

Koerner, R.M. (1994). *Designing with Geosythetics*, Third Edition, Prentice-Hall, Inc., 783 pp.

Koerner, G.R., and Koerner, R.M. (1990). "The Installation Survivability of Geotextiles and Geogrids", *Proceedings 4th International Conference on Geotextiles, Geomembranes, and Related Products,* The Hague, Netherlands, Vol. 2, pp. 597-602.

Mathur, A., Netravali, A.N., and O'Rourke, T.D. (1994). "Chemical Aging Effects on the Physio-Mechanical Properties of Polyester and Polypropylene Geotextiles", *Geotextiles and Geomembranes*, Elsevier Science Limited, Vol. 13, No. 9, pp. 591-626.

McGown, A., Andrawes, K.Z., and Al-Mudhaf, H.F. (1995). "Assessment of the Effects of Long-Term Exposure on the Strength of Geotextiles and Geogrids", *Proceedings Geosynthetics '95 Conference,* Nashville, USA, Vol. 3, pp. 939-949.

Metcalfe, Robert C. and Holtz, Robert D. (1994). *Performance of Geotextile Separators in Western Washington,* Report No. WA-RD 321.1, Final Technical Report, Research Project T9233, Task 13, WSDOT, 257 pp.

National Oceanic and Atmospheric Administration, *Climatological Data*, Washington, January, 1990 through June, 1996. Volumes 94 No. 1 through 100 No. 6, U.S. Department of Commerce.

Nishida, K. and Nishigata, T. (1994). "The Evaluation of Separation Function for Geotextiles", *Proceedings 5th International Conference on Geotextiles, Geomembranes, and Related Products,* Singapore, Sept. 1994, Vol. 1, pp. 139-142.

Paulson, J.N. (1990). "Summary and Evaluation of Construction Related Damage to Geotextiles in Reinforcing Applications", *Proceedings 4th International Conference on Geotextiles, Geomembranes, and Related Products,* The Hague, Netherlands. Vol. 2, pp. 615-619.

Rainey, T., and Barksdale, R. (1993). "Construction Induced Reduction in Tensile Strength of Polymer Geogrids", *Proceedings Geosynthetics '93 Conference*, Vancouver, Canada, Vol. 2, pp. 729-742.

Risseeuw, P. and Schmidt, H.M. (1990). "Hydrolysis of HT Polyester Yarns in Water at Moderate Temperatures", *Proceedings 4th International Conference on Geotextiles, Geomembranes, and Related Products*, The Hague, Netherlands. Vol. 2, pp. 691-696.

Rowe, R. Kerry and Badv, K. (1996). "Use of a Geotextile Separator to Minimize Intrusion of Clay into a Coarse Stone Layer", *Geotextiles and Geomembranes*, Elsevier Science Limited, Vol. 14, No. 2, pp. 73-93.

Sandri, D., Martin, J.S., Vann, C.W., Ferrer, M., and Zeppenfeldt, I. (1993). "Installation Damage Testing of Four Polyester Geogrids in Three Soil Types", *Proceedings Geosynthetics '93 Conference,* Vancouver, Canada, Vol. 2, pp. 743-755.

Savage, B.M. (1991). "Field Activities Report", Bucoda, Washington, Field Research Project, June 25, 1991, unpublished, 29 pp.

Schneider, H. (1989) "Long-Term Performance of Polypropylene Geosynthetics", *Durability and Aging of Geosynthetics,* edited by R. M. Koerner, Elsevier Applied Science, pp. 95-109.

Task Force 25 of the AASHTO-AGC-ARTBA Joint Committee (1989). "Guide specification for geotextiles in separation applications," March 1989, revised.

Tisinger, L.G., Clark, B.S., Giroud, J.P., and Christopher, B.R. (1993). "Analysis of an Exposed Polypropylene Geotextile", *Proceedings Geosynthetics '93 Conference*, Vancouver, Canada, Vol. 2, pp. 757-771.

Troxler Electronic Laboratories, Inc. and Subsidiary Troxler International, Ltd. (1977). *3400 Series Instruction Manual, 2nd Edit.*, Troxler Electronic Laboratories, Inc.

Tsai, W.-S., and Savage, B.M., (1992). "Evaluation of Geotextiles as Separators in Roadway Construction", Bucoda, Washington, prepared for Polyfelt, Inc., unpublished. Prepared for Polyfelt, Inc., 80 pp.

Tsai, W.-S., Savage, B.M., Holtz, R.D., Christopher, B.R., and Allen, T.M. (1993) "Evaluation of Geotextiles as Separators in a Full-Scale Road Test", *Proceedings of the Geosynthetics '93 Conference,* Vancouver, Canada, Vol. 1, pp. 35-48.

Tsai, W.-S. (1995). "Evaluation of Geotextiles as Separators in Roadways", Doctoral Thesis, University of Washington, 172 pp.

Watts, G.R.A, and Brady, K.C. (1994). "Geosynthetics: Installation Damage and the Measurement of Tensile Strength", *Proceedings 5th International Conference on Geotextiles, Geomembranes, and Related Products,* Singapore, Sept. 1994, Vol. 3, pp. 1159-1164.

Wisse, J.D.M. (1988). "The Role of Thermo-Oxidative Ageing in the Long-Term Behaviour of Geotextiles", *Durability of Geotextiles*, Chapman and Hall Ltd., pp. 207-216.

WSDOT 1996 Standard Specifications for Road, Bridge, and Municipal Construction. Washington State Department of Transportation and Amercian Public Works Association.

WSDOT Design Manual, unpublished (November 1, 1994 Draft). Manual No. M22-01, pp. 530-1--530-23.

WSDOT Pavement Guide (February 1995). pp. 7-70--7-104.

Yang, C. and Yu, X. (1989). "Mud-Pumping Prevention of Railway Subgrade by Using Geotextile", *Proceedings of the 12th International Conference on Soil Mechanics and Foundation Engineering,* Rio de Janeiro, Vol. 3, pp. 1693-1695. (cited reference)

APPENDIX A

DATA FROM PREVIOUS STUDIES

APPENDIX A

DATA FROM PREVIOUS STUDIES

FWD results from tests performed in 1991 are presented in Tables A.1 through A.6. Precipitation data is provided in Tables A.7 and A.8, and Figure A.1. The logs of explorations performed at the test section by WSDOT are included along with the results of their laboratory tests. A copy of Tsai et al. (1993) is also included.

Table A.1 - FWD test results in northbound lane, April 29, 1991.

Station	Geotextile	Deflection (mm)	Area Value (mm)	Subgrade Modulus (kPa)
177+50		1.4	457	41400
177+70	HB-NB	1.8	432	41400
177+95	NP4-NB	1.5	508	48300
178+20	NP6-NB	2.1	406	41400
178+45	Soil-NB	2.0	432	34500
178+70	NP8-NB	1.3	432	48300
178+95	SF-NB	1.0	457	62100
179+20		1.2	406	69000

Table A.2 - FWD test results in southbound lane, April 29, 1991.

Station	Geotextile	Deflection (mm)	Area Value (mm)	Subgrade Modulus (kPa)
177+50		1.7	483	24500
177+70	HB-SB	2.2	330	48300
177+95	NP4-SB	2.0	381	55200
178+20	SF-SB	1.0	457	62100
178+45	Soil-SB	1.5	457	48300
178+70	NP8-SB	0.7	635	55200
178+95	NP6-SB	0.9	533	55200
179+20		1.3	432	55200

Table A.3 - FWD test results in northbound lane, July 24, 1991.

Station	Geotextile	Deflection (mm)	Area Value (mm)	Subgrade Modulus (kPa)
177+50		0.81	503	64048
177+95	NP4-NB	0.88	475	65813
178+20	NP6-NB	0.70	467	85105
178+45	Soil-NB	0.75	483	74183
178+70	NP8-NB	0.76	505	67688
178+95	SF-NB	0.80	500	65606
179+20		0.89	485	62751

Table A.4 - FWD test results in southbound lane, July 24, 1991.

Station	Geotextile	Deflection (mm)	Area Value (mm)	Subgrade Modulus (kPa)
177+50		0.94	516	53002
177+95	NP4-SB	1.41	518	33854
178+20	SF-SB	0.78	488	71329
178+45	Soil-SB	0.83	483	67378
178+70	NP8-SB	0.91	470	65833
178+95	NP6-SB	1.21	470	49423
179+20		1.68	361	70150

Table A.5 - FWD test results in northbound lane, November 25, 1991.

Station	Geotextile	Deflection (mm)	Area Value (mm)	Subgrade Modulus (kPa)
177+50		0.62	544	76769
177+70	HB-NB	0.65	531	76300
177+95	NP4-NB	0.61	541	78444
178+20	NP6-NB	0.57	531	85808
178+45	Soil-NB	0.57	536	85208
178+70	NP8-NB	0.62	521	81871
178+95	SF-NB	0.78	521	65116
179+20		1.06	417	77348

Table A.6 - FWD test results in southbound lane, November 25, 1991.

Station	Geotextile	Deflection (mm)	Area Value (mm)	Subgrade Modulus (kPa)
177+50		0.66	541	72715
177+70	HB-SB	0.62	518	82402
177+95	NP4-SB	0.65	518	79989
178+20	SF-SB	0.56	516	93269
178+45	Soil-SB	0.55	531	90035
178+70	NP8-SB	0.59	544	81278
178+95	NP6-SB	0.60	541	80154
179+20		1.34	391	61083

Table A.7 - Daily precipitation data at Centralia station for month of June, 1996.

Day	Precip. (mm)	Day	Precip. (mm)	Day	Precip. (mm)
1		11		21	
2		12		22	
3		13		23	8.9
4	1.3	14		24	3.0
5		15		25	
6	T	16		26	
7		17	8.1	27	T
8		18	T	28	
9	0.5	19		29	
10	T	20		30	

T = Trace

June (1996) Total = 21.8 mm

Table A.8 - Monthly precipitation data at Centralia station, since January 1990.

	Yearly Precipitation (mm)							
Month	1990	1991	1992	1993	1994	1995	1996	Average
Jan.	371.6	127.5	205.2	90.4	105.2	127.5	161.3	169.8
Feb.	211.6	149.4	96.0	4.3	166.9	118.6	258.3	143.6
Mar.	87.9	110.0	39.9	85.9	108.0	153.4	82.6	95.4
Apr.	99.3	173.0	122.2	154.2	38.6	126.2	195.3	129.8
May	61.7	78.2	8.6	128.8	40.9	38.6	96.8	64.8
June	73.4	42.7	23.6	75.2	53.3	36.8	21.8	46.7
July	8.9	4.8	8.9	34.8	4.1	49.8	N.A.	18.5
Aug.	49.5	37.6	27.2	5.6	25.7	32.5	N.A.	29.7
Sept.	0.0	0.3	55.6	0.5	21.6	66.5	N.A.	24.1
Oct.	181.4	56.6	74.2	48.5	183.4	M	N.A.	108.8
Nov.	269.7	179.6	167.9	56.9	189.7	326.1	N.A.	198.3
Dec.	140.7	114.8	165.6	176.5	241.0	240.5	N.A.	179.9
Totals	1555.8	1074.4	994.9	861.6	1178.3	1316.7	---	1209.4

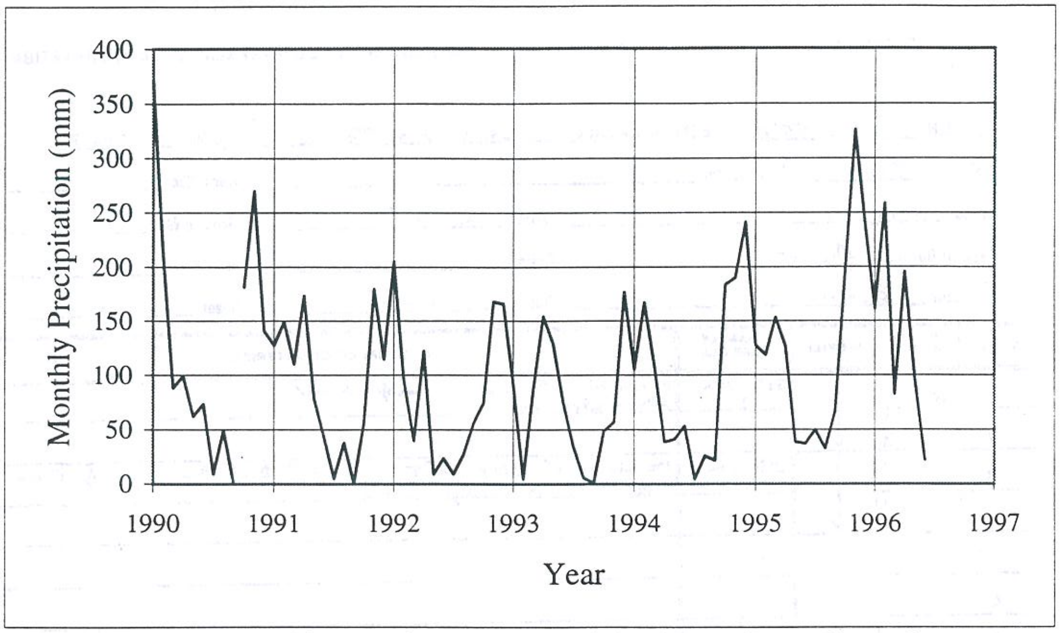

Figure A.1 - Six year history of monthly precipitation at Centralia station.

TEST BORING

WASHINGTON STATE DEPARTMENT OF TRANSPORTATION

___ S.H. ___ S.R. 507 SECTION Lewis County Line to Tenino Job No. C 3883

Hole No. C-1 Sub Section ___ Cont. Sec. ___

Station 179+11 Offset L 16' Ground El. ___

Type of Boring Auger Casing ___ W.T. El. ___

Inspector Evans Date 5-16-91 Sheet 1 of 1

DEPTH	BLOWS PER FT.		PROFILE	SAMPLE TUBE NOS.	DESCRIPTION OF MATERIAL
1	5	5 3	↓	STD Pen 1	retained 6" Loose Sandy Gravel Hit water at 1'
2		2 3			
3	2	1 1	↓	STD Pen 2	retained 1' very soft. Top 2" Dark Brown Sandy Gravel. The rest is Gray Clay
4		1 1			
5					
6					
7					
8	3	1 1	↓	STD Pen 3	retained 1½' Soft, Gray Clay, Brown at top of Sampler
9		2 3			
10	6	2 2	↓	STD Pen 4	retained 1' Medium Stiff Light Bluish gray Clay
11		4 4			
12					
13					Piezometer Installed to 11'
14					5/24/91 → depth to W.T. = 2.5 ft

DOT FORM 351-003 REVISED 12/79

Original to Materials Engineer
Copy to Bridge Engineer
Copy to District Administrator

Copy to ___

LOG OF TEST BORING — **WASHINGTON STATE DEPARTMENT OF TRANSPORTATION**

___ S.H. ___ S.R. 507 SECTION Lewis County Line to Tenino Job No. C 3883

Hole No. C-2 Sub Section ______ Cont. Sec. ______

Station 178 Offset L 14' Ground El. ______

Type of Boring Auger Casing ______ W.T. El. ______

Inspector Evans Date 5-16-91 Sheet 1 of 1

DEPTH	BLOWS PER FT.	PROFILE	SAMPLE TUBE NOS.	DESCRIPTION OF MATERIAL
1	6 (5, 3)		STD Pen 1	retained 6" Medium Stiff Light Brown Clay. Top 2" Dark Brown Gravel
2	(3, 5)			
3	15 (4, 7)		STD Pen 2	retained 1' Stiff Light Brown clay.
4	(8, 8)			
5				
6				
7				
8	3 (1, 1)		STD Pen 3	retained 1½' Soft, Tan Clay. Top 2" reddish Brown.
9	(2, 3)			
10	4 (1, 2)		STD Pen 4	retained 2' Soft, Dark Gray Clay.
11	(2, 3)			
12				No Water
13				Piezometer installed to 11'
14				
				5/24/91 → depth to W.T. = 0.5 ft

DOT FORM 351-003 REVISED 12/79

Original to Materials Engineer
Copy to Bridge Engineer
Copy to District Administrator

Copy to ______

ᴇST BORING   WASHINGTON STATE DEPARTMENT OF TR...

___ S.H. ___ S.R. 507 SECTION Lewis County line to Tenino Job No. C-3883

Hole No. C-3 Sub Section ___ Cont. Sec. ___

Station 178 Offset R 25' Ground El. ___

Type of Boring Auger Casing ___ W.T. El. ___

Inspector Evans Date 5-16-91 Sheet 1 of 1

DEPTH	BLOWS PER FT.		PROFILE	SAMPLE TUBE NOS.	DESCRIPTION OF MATERIAL
1	5	4 3	↓	STD Pen 1	retained 6" Medium Stiff Dark Brown clay. Top 2" are Dark Brown Top Soil.
2		2 3			
3	13	4 6	↓	STD Pen 2	retained 6" stiff reddish Brown Clay. Top 2" are sandy.
4		7 9			
5					
6					
7					
8	5	1 2	↓	STD Pen 3	retained 6" Medium stiff Light Brown Clay. At Top of Sample 1½" are a dark Brown rooty Soil with sandy clay right under the Soil.
9		3 4			
10	9	2 4	↓	STD Pen 4	retained 2" Stiff Greenish Gray clay with sandy clay at the Top.
11		5 6			
12					No water
13					Piezometer Installed to 11'
14					5/24/91 - depth to W.T. = 2.5 ft

DOT FORM 351-003 REVISED 12/79

Original to Materials Engineer
Copy to Bridge Engineer
Copy to District Administrator

Copy to ___

LOG OF TEST BORING

WASHINGTON STATE DEPARTMENT OF TRANSPORTATION

S.H. ____ S.R. 507 SECTION Lewis Co. Line to Vic. Tenino SCL Job No. 3856

Hole No. P-1 Sub Section ____ Cont. Sec. ____

Station 179+00 Offset 17' Lt. Ground El. -0.8' from ℄ El.

Type of Boring Portable Penetrometer Casing None W.T. El. -1.3' from ℄ Elc

Inspector ____ Date 4-18-91 Sheet 1 of 1

DEPTH	BLOWS PER FT.	PROFILE	SAMPLE TUBE NOS.	DESCRIPTION OF MATERIAL
	10		11, 12, 9	Br. Wet Slightly silty Sandy Gravel
			4, 4, 4, 5	Sample Wet Brownish Red Slightly Sandy Clay with traces of gravel
	3			
			8, 8, 10, 13, 13	Orangish Red Clay with traces of gravel
	8			

Test drilling stopped 6' below ground elevation. The blow counts per ft. shown are equivalent to standard penetrometer blow counts. Soil descriptions are based on field identification.

DOT FORM 351-003 REVISED 12/79

Original to Materials Engineer
Copy to Bridge Engineer
Copy to District Administrator

Copy to ____

LOG OF TEST BORING | **WASHINGTON STATE DEPARTMENT OF TRANSPORTATION**

___ S.H. ___ S.R. 507 SECTION Lewis Co Line to Vic. Tenino SCL Job No. 3856

Hole No. P-2 Sub Section ___ Cont. Sec. ___

Station 175+50 Offset 20' Rt. Ground El. -2.0' from ℄ El.

Type of Boring Portable Penetrometer Casing None W.T. El. N.A.

Inspector ___ Date 4-18-91 Sheet 1 of 1

DEPTH	BLOWS PER FT.	PROFILE	SAMPLE TUBE NOS.	DESCRIPTION OF MATERIAL
	5		5, 8, 7	Gray Silty Clay (SAMPLE 1) Reddish Weathered [redacted])
			7	
	5		6, 7, 7	Gray Slighty Sandy Clay
			9	
				Test drilling stopped 4' below ground elevation. The blow counts per ft. shown are equivalent to standard penetrometer blow counts. Soil descriptions are based on field identification.

DOT FORM 351-003 REVISED 12/79

Original to Materials Engineer
Copy to Bridge Engineer
Copy to District Administrator

Copy to ___

LOG OF TEST BORING

WASHINGTON STATE DEPARTMENT OF TRANSPORTATION

____ S.H. ______ S.R. 507 SECTION Lewis Co. Line to Vic Tenino SCL Job No. 3856

Hole No. P-3 Sub Section ______ Cont. Sec. ______

Station 173+00 Offset 20' Lt. Ground El. ______

Type of Boring Portable Penetrometer Casing None W.T. El. -0.4' from ℄ Elev.

Inspector ______ Date 4-18-91 Sheet 1 of 1

DEPTH	BLOWS PER FT.	PROFILE	SAMPLE TUBE NOS.	DESCRIPTION OF MATERIAL
	11		4 5 6 8	Brown Wet Slightly Silty Sandy Gravel
				Gray Moist Sandy Silt- Clayish Like
	11		11 16 18	
				Test drilling stopped 5.5' below ground elevation.
				The blow counts per ft. shown are equivalent to standard penetrometer blow counts.
				Soil descriptions are based on field identification.

DOT FORM 351-003 REVISED 12/79

Original to Materials Engineer
Copy to Bridge Engineer
Copy to District Administrator

Copy to ______

WASHINGTON STATE
DEPARTMENT OF TRANSPORTATION

MATERIALS ENGINEER
Materials Laboratory
P. O. Box 167, Olympia, WA 98504 (Mailing Address)
1655 So. 2nd Ave.
Tumwater, Washington 98504 (Shipping Address)

Place Tumwater, WA.
Date 04-23-'91

Dear Sir:

I have forwarded by today's Delivery the following Foundation Samples.

Contract or Job No. C-3856 Section LEWIS CO. LINE TO VICINITY TENINO SCL SR No. 507 Sub-Section

Station & Offset 175+50 20'RT Hole # PP-2

E-9419 Lab No.	Drive #	Depth	Tube Position in Sampler	Clas.	Description
-1	D-1	0'0" 0'8"	M.C.= 32.5%	CL	
-2	D-2	0'8" 1'0"	M.C.= 33.0%	ML	

1 copy with samples
1 copy to addressee

Yours very truly,

Inspector.

DOT FORM 351-002 REVISED 2 80

SOIL CLASSIFICATION AND IDENTIFICATION WORKSHEET

JOB NO.:	C-3856
SAMPLE NO.:	E-9419-1
HOLE NO.:	PP-2
DATE:	04-24-91
LAB. TECH.:	P.A.A.

SOIL FIELD IDENTIFICATION

TEST	GRAVEL	SAND	SILT	CLAY
VISUAL		✓	✓	
DRIED CAST				
DILITANCY				
BITE				
TOUGHNESS				

SIEVE ANALYSIS

DRY WT.:	59.3g.
WET WT.:	78.6g.
% H_2O:	32.5%
WT. OF SAMPLE:	416.9g.

	WT.	% PASS
-1½"	Ø	100.0
-1"	Ø	100.0
-¾"	Ø	100.0
-#4	Ø	100.0
-#10	12.6g.	100.0
-#40	139.5g.	97.0
-#200	264.8g.	63.5

GRAIN SIZE CURVE

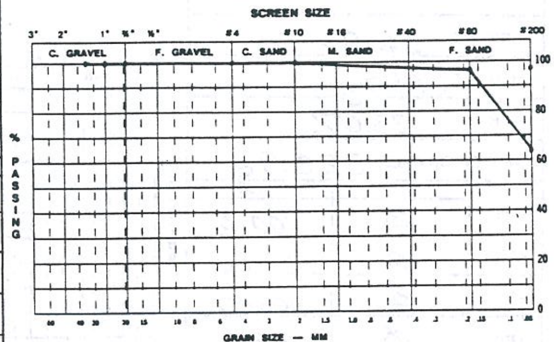

LIQUID LIMIT DETERMINATION

	LIQUID LIMIT			PLASTIC LIMIT
Can No.	110			79
Wet Wt.	23.0g.			10.0g.
Dry Wt.	16.6g.			8.2g
%H, O	38.4			PL= 22.0
Blows	24			PI= 16.4

SAMPLE DESCRIPTION

CLASS. CL LIGHT GRAY TO LIGHT BROWNISH GRAY, AND DARK BROWN TO STRONG BROWN, WET, FINE TO MEDIUM SANDY, VERY SILTY CLAY

Reference: AASHTO T-11-85

PLASTICITY CHART

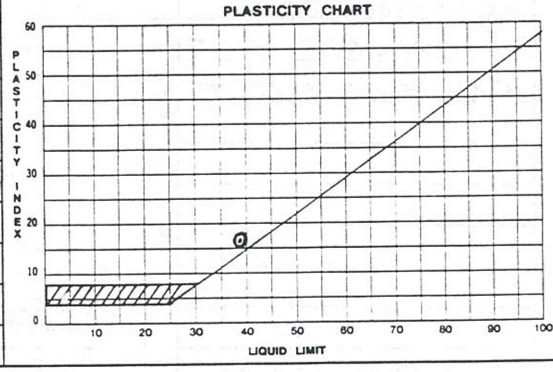

DOT FORM 351-019

SOIL CLASSIFICATION AND IDENTIFICATION WORKSHEET

JOB NO.:	C-3856
SAMPLE NO.:	E-9419-2
HOLE NO.:	PP-2
DATE:	04-24-91
LAB. TECH.:	P.A.A.

SOIL FIELD IDENTIFICATION

TEST	GRAVEL	SAND	SILT	CLAY
VISUAL		✓	✓	
DRIED CAST				
DILITANCY				
BITE				
TOUGHNESS				

SIEVE ANALYSIS

DRY WT.: 56.0g.

WET WT.: 74.5g.

% H_2O: 33.0%

WT. OF SAMPLE: 320.9g.

	WT.	% PASS
-1½"	Ø	100.0
-1"	Ø	100.0
-¾"	Ø	100.0
-#4	Ø	100.0
-#10	2.7g.	100.0
-#40	152.1	99.2
-#200	166.1	51.8

GRAIN SIZE CURVE

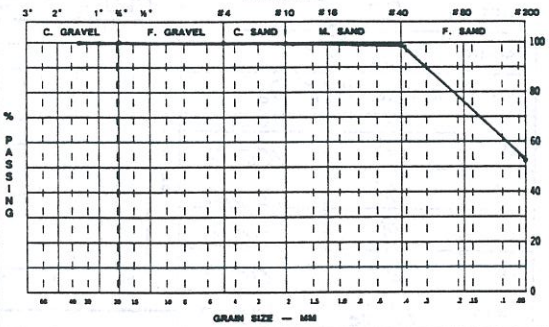

SAMPLE DESCRIPTION

CLASS.: ML

STRONG BROWN AND DARK GREY, WET, FINE SANDY SILT

Reference: AASATO T-11-85

LIQUID LIMIT DETERMINATION

	LIQUID LIMIT			PLASTIC LIMIT
Can No.				NON-PLASTIC
Wet Wt.				
Dry Wt.				
%H_2O				PL=
Blows				PI=

PLASTICITY CHART

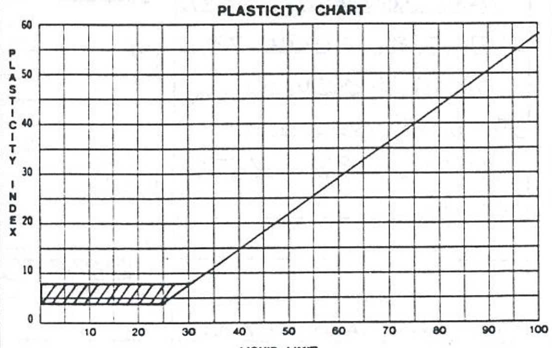

DOT FORM 351-019

Evaluation of Geotextiles as Separators in a Full-Scale Road Test

W.-S. Tsai
University of Washington, USA

B.M. Savage
University of Washington, USA

R.D. Holtz
University of Washington, USA

B.R. Christopher
Polyfelt Inc., USA

T.M. Allen
Washington State Department of Transportation, USA

ABSTRACT

To compare the ability of five different geotextiles to stabilize a soft subgrade during construction, a full scale field test was conducted on Washington state highway SR 507. Performance was compared under two different initial subbase lift thicknesses to evaluate constructibility and installation survivability. Instrumentation was installed to measure vertical strains throughout the cross section, deformations in geotextiles, and changes of water content and temperature. Rut depths were also measured in traffic tests.

The results indicated that the presence of a geotextile resulted in more uniform rut depths. The geotextiles did not however appear to reduce rut depths in test sections where the subgrades had a modest shear strength. All geotextiles had strains in the cross lane direction of less than 8%, except in one failed section. Observations indicated that subgrade drainage during construction was enhanced by the thicker needle-punched nonwoven geotextiles while some types of geotextiles tended to retard pore water dissipation.

INTRODUCTION

Although geotextiles have been widely used as separators in temporary roadways for many years, information on their long term performance in permanent roads is still quite limited. Therefore, an opportunity to investigate geotextile performance arose during the summer of 1991 in connection with the reconstruction of a state highway in Washington. A full scale field test was conducted (1) to compare the ability of different types and weights of geotextiles to stabilize a soft subgrade during construction and (2) to investigate their respective influence on the long-term performance of the pavement system. Five different geotextiles were selected. Their performance was compared under two different initial lift thicknesses (150 and 300 mm) of subbase to evaluate initial lift requirements, constructibility and installation survivability.

SITE DESCRIPTION

The test site was located approximately 32 km south of Olympia on SR 507 in Bucoda, Washington. Both lanes were included in the study.

The area chosen for the test site had a long history of poor performance and was scheduled for major maintenance when the experiment was arranged. The roadway section already contained significant ruts and alligator cracking. The subgrade consisted primarily of clayey soils, with some organic materials found in the northbound lane. The water table was high, especially in the spring, when it was within 0.3–0.6 m of the road surface. The natural water contents were higher than the plastic limits. All soils collected in the subgrades had more than 80% passing the No. 200 sieve; thus the subgrade was suitable for investigating possible soil migration.

FIELD TEST AND INSTRUMENTATION

To accomplish the research objectives, a test site 46 m long and 7 m wide was divided into six sections. One of the six sections was a control section containing no geotextile, while the other five sections each contained a different type of geotextile separator. The geotextiles installed are listed in Table 1 and their respective locations indicated in Figure 1. The geotextiles were selected based on the types of geotextiles conventionally used in stabilization applications, their estimated ability to survive construction, the diversity of filtration characteristics and the potential for lateral drainage. The length of each section was 7.6 m. Instrumentation included soil strain gages for measuring vertical strains throughout the cross section, a grid of rivet points (100 mm by 100 mm on centers) on the geotextile surfaces to measure geotextile deformations in the wheel path, and moisture temperature sensors for monitoring soil moisture and temperature changes. Schematic diagrams showing the instrumentation locations are given in Figures 1 and 2.

Table 1: Geotextiles installed.

Symbol	Type	Mass Area (g/m^2)	Survivability Rating based on AASHTO	Manufacture
Soil	no geotextile - control	-	-	-
HB	nonwoven, heat-bonded polypropylene	135	MS	Reemay
NP4	nonwoven, needle-punched polypropylene	135	LS-MS	Polyfelt
NP6	nonwoven, needle-punched polypropylene	202	MS-HS	Polyfelt
NP8	nonwoven, needle-punched polypropylene	270	HS	Polyfelt
SF	woven, slit film polypropylene	250	MS-HS	Exxon

Note:
LS - Low Survivability
MS - Moderate Survivability
HS - High Survivability

Physical Properties of Subgrade Soils. Except for a few silts of high plasticity, all soils collected in the subgrade were classified as clays of high plasticity. There was a large variation in properties of the soils at the site. For example, the initial natural water content was found to be in the range of 20 - 47 %. All soils had more than 80 % passing the No. 200 sieve. The ranges of Atterberg limits were 30 - 77 % for liquid limits, 19 - 35 % for plastic limits and 11 - 42 % for plasticity indices. Table 2 shows the representative subgrade characteristics over the length of the test section in each lane.

Table 2: Representative Characteristics of The Subgrade.

Geotextile	Soil Type	Water Content			Atterberg Limits		
		Initial	Excav 1	Excav 2	LL	PL	PI
Southbound Lane							
HB	CL	20	NA[1]	28	30	19	11
NP4	CL	31	NA[1]	NA[2]	48	27	21
SF	CL	26	NA[1]	NA[2]	34	22	12
Soil	CH	46	NA[1]	46	77	35	42
NP8	CH	38	NA[1]	42	63	28	35
NP6	CH	45	NA[1]	51	74	34	40
Northbound Lane							
HB	CL	27	30	NA[1]	34	23	11
NP4	CL	30	31	NA[1]	44	23	21
NP6	CH	35	23	NA[1]	61	31	30
Soil	CH	37	NA[2]	44	57	28	29
NP8	MH	40	42	43	57	35	22
SF	CH	47	45	50	69	30	39

Note:
1. This set of excavations was not conducted.
2. Data was lost.

Shear Strength of Subgrade. A hand vane tester and a pocket penetrometer were used to measure the in situ shear strengths of the subgrade. The measured shear strengths ranged from 31 to 127 kPa in the northbound lane and from 18 to 98 kPa in the southbound lane using a hand vane tester. The measured shear strengths were found to vary from 48 to 192 kPa in the southbound lane and from 60 to 215 kPa in the northbound lane using a pocket penetrometer. Figures 5 and 6 show the measured subgrade shear strengths using a hand vane tester.

Ground Response. In this study, three traffic tests were conducted using a loaded dump truck. One traffic test was implemented in the southbound lane and two other traffic tests were performed in the northbound lane.

Test Procedure. After removing the top layer of existing fill (0.6 m in the southbound lane and 0.45 m in the northbound lane) to reach the soft clay layer, nuclear density tests were performed on the natural subgrade. Concurrently, in situ shear strength was measured in three locations (within each lane). The locations were: close to the roadway center line and near the middle and outside of each lane, respectively, at approximately every 4.6 m along the length of the lane. Measurements were made using a pocket penetrometer and a hand vane tester. Soil samples were taken for moisture content, grain size distribution and Atterberg limits determinations. As indicated in Figure 3, moisture/temperature sensors were installed at depths of 25 mm and 200 mm below the subgrade surface in each section. A Bison strain coil was placed horizontally at a depth of 200 mm below the subgrade surface in the sections containing: SF, NPS, and the control, in the southbound lane. All instrumentation was placed under the outside wheel path and in the middle of the length of each individual section. The holes dug for the placement of the instrumentation were backfilled with clay and compacted with small hand-operated compactors.

The geotextiles were placed in such a way that the grid points ("pop" rivets) on the geotextiles were located under the outside wheel paths. After the geotextile sections were placed and overlapped 300 mm with adjacent geotextile sections, the rivet spacings were measured. Next Bison coils were attached by duct tape to geotextiles SF and NPS and a third coil placed at the top of the subgrade in the control section (Figure 3).

A first lift of base course (thickness 300 mm) in the southbound lane and a first lift (thickness 150 mm) in the northbound lane were placed over the entire length of the test section and compacted with a steel wheeled roller. The lift thicknesses were selected based on the minimum lift thickness recommendations for construction on soft subgrade by WSDOT (300 mm) and the minimum lift thickness with geotextile estimated to be required to limit rutting to less than 50 mm during construction as recommended by Steward, et. al. (1977). WSDOT personnel tested the surface of the lift for density and field moisture content using a nuclear densiometer. After the first lift of base course was compacted, samples were taken for moisture content and grain size distribution determinations.

A traffic test was performed (referred to as Traffic 1) on the base course surface using a loaded dump truck weighing 350 kN, having rear tandem axle with dual tires, passing over the entire 46 m experimental zone. A total of 10 passes were made to simulate typical construction traffic. Following passes 1, 2, 5 and 10, readings of the Bison gages and moisture/temperature sensors were taken and rut depths measured. Ground response observations were recorded for each of the intermediate passes. Two rut-depth measurements (one at the north side and one at the south side) were made in both wheel paths in each test section except for the control (soil only) sections. In the control section, only one rut depth measurement was made at the center in both wheel paths as this was the location of the largest rut depth.

After the traffic test, a small test pit was excavated (referred to as Excav 1) down to the geotextile, or to the top of the subgrade in the control section. Grid patterns were measured and visual observations of the geotextiles and subgrade conditions were recorded. Geotextile samples, 0.9 m by 0.9 m, were removed for laboratory testing to determine the extent of physical damage and mechanical property change to the geotextiles. Soil samples were taken from the subgrade.

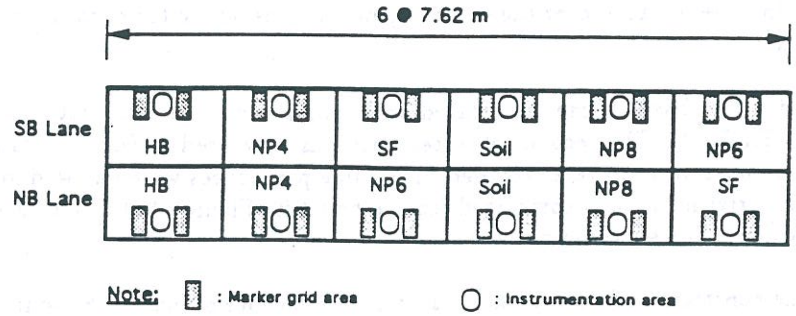

Figure 1: Locations of Geotextile and Instrumentation.

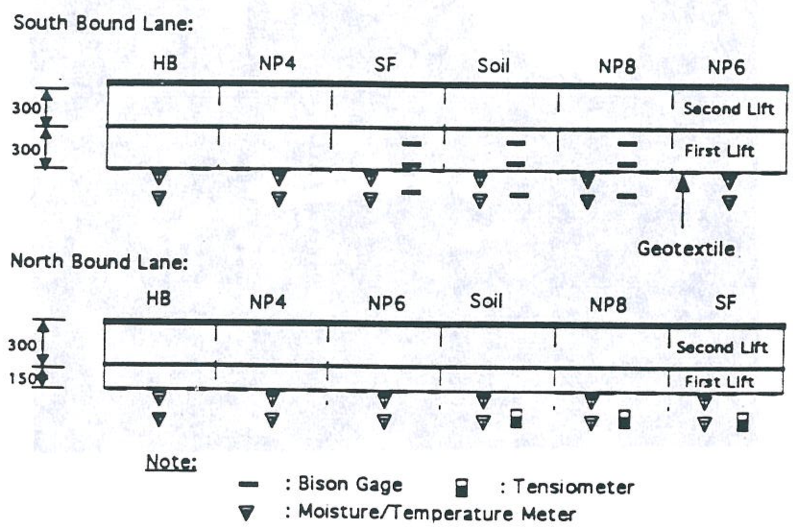

Figure 2: Cross Section Showing Instrumentation Placement (dimensions in mm).

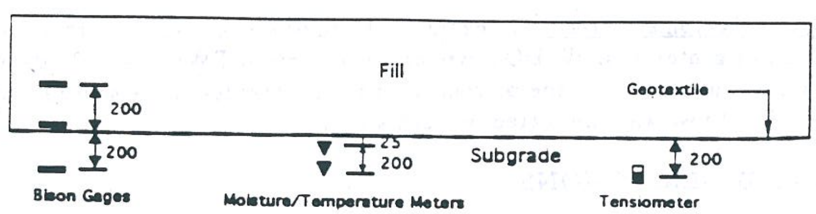

Figure 3: Vertical spacing of instruments (dimensions in mm).

Geotextile patches were placed over the sample removal areas before the excavations were backfilled and compacted.

The second lift of base course was placed and compacted. A traffic test was also performed (referred to as Traffic 2). The second set of test pits was excavated (referred to as Excav 2) to the fabric depth and observations were recorded. The same procedures were followed for the second lift and associated activities as was completed for the first lift. Figure 4 shows a general view of the second excavation in the southbound lane.

Due to time constraints, Excav 1 and Traffic 2 were not performed in the southbound lane.

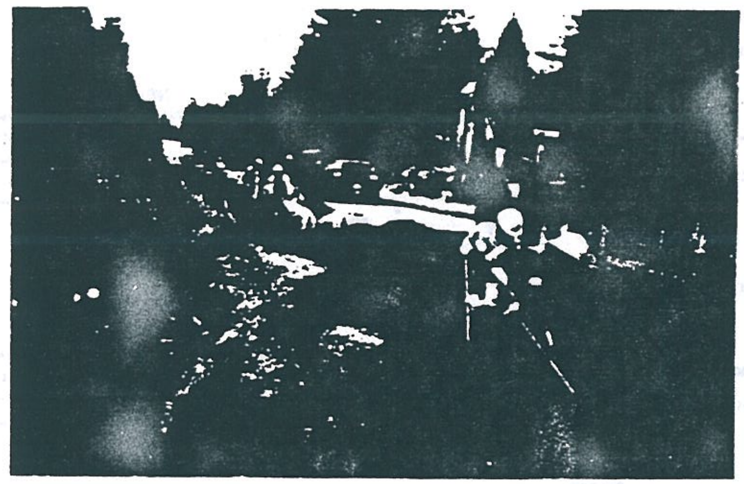

Figure 4: General View of Field Test during Excav 2 in Southbound Lane.

Falling Weight Deflectometer Tests. To examine the improvement in the stiffness of pavement due to the inclusion of geotextiles, WSDOT personnel performed FWD tests, 37 days before, and 49 days and 173 days subsequent to the placement of the geotextiles in the southbound lane. On each test date, one FWD test was conducted on each section.

RESULTS AND DISCUSSIONS

Only a portion of the study results are presented and discussed herein. Additional study findings will be reported in separate publications as additional data is obtained and analyzed.

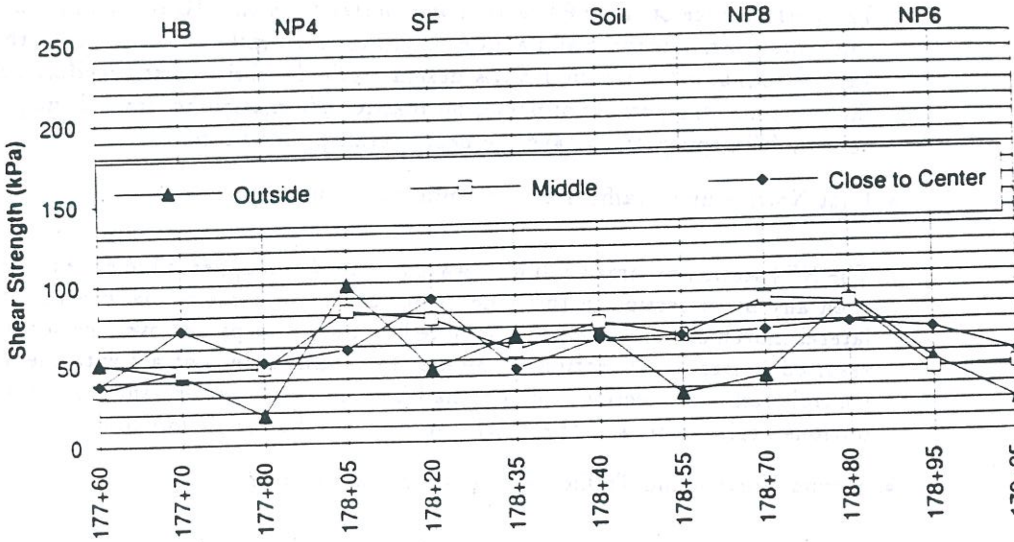

Figure 5: Shear Strength of Subgrade in the Southbound Lane using Hand Vane Tester.

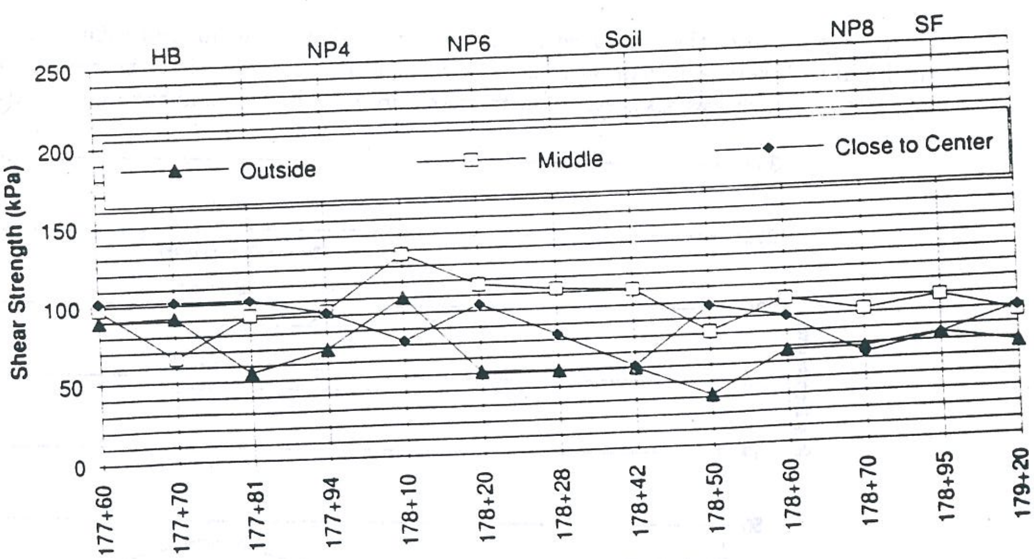

Figure 6: Shear Strength of Subgrade in the Northbound Lane using Hand Vane Tester.

- First Southbound Traffic Test (300 mm base course)

  The performance of the NP4 section was better than the HB section in that the NP4 section had more elastic response and a lower magnitude of elastic deflection than the HB section. As anticipated, based upon the FHWA design method (Christopher and Holtz, 1989), for this lift thickness and the number of passes no plastic deformation occurred during any of the passes. Section NP8 appeared to have the best overall performance.

- First Northbound Traffic Test (150 mm base course)

  The NP4 section became a full mud wave at pass 7 and appeared to have the worst performance than any other section in this lane. Due to the closeness of the wheel path to the fill edge, lateral movement of aggregate was noted as the truck passed over the section having SF and resulted in significant rutting in the first four passes. In contrast with the other sections, the control (soil only) section and NP8 had better overall performance. At this time, there is no obvious explanation why the control section had better performance.

- Second Northbound Traffic Test (450 mm base course)

  In this test, all sections had better performance than in the first traffic test in the same lane. Section HB and Section NP4 had very similar behavior and had the worst performance: after pass 5 both sections began undulating and waving. NP8 and the control section had the best overall performance. Again, there is no obvious reason why the control section performed better.

Rut Depth. All of the measured rut depths in Traffic 1 southbound (300 mm base course) shown in Figure 7 were less than 40 mm. Figure 7 also illustrates that the control section had largest rut depth, which was also less uniform than those in the sections having geotextiles.

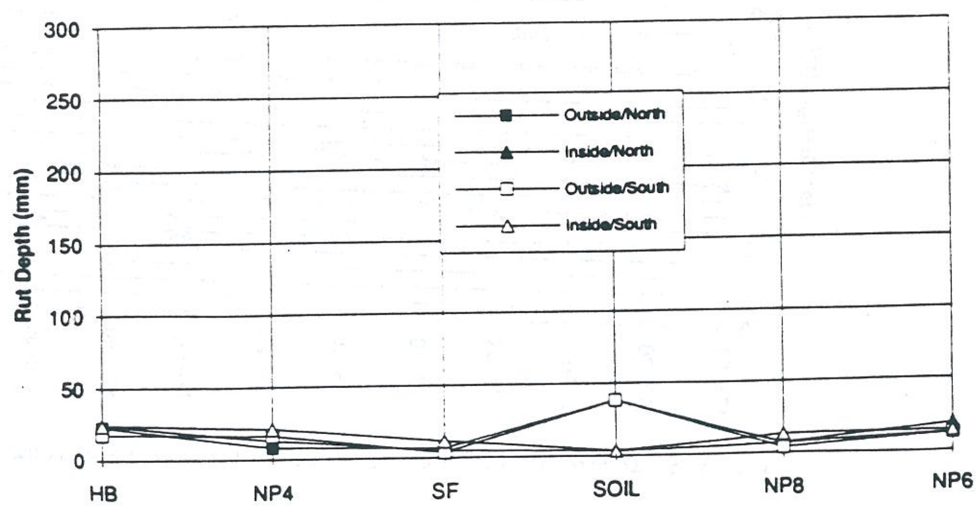

Figure 7: Rut Depth after the Tenth Pass in Traffic 1 in the Southbound Lane.

Figure 8 shows the measured rut depths in each section of the northbound lane in Traffic 1 (150 mm base course). The measured rut depths were relatively low, in the range of 19 to 87 mm, with the exception of NP4. Rut depths in the northbound lane were greater than those in the southbound lane, despite the fact that the sections in the northbound lane had higher average shear strengths. This difference is attributed to the thinner base course in the northbound lane, which was 150 mm less in thickness. Section NP4 had the greatest rut depth (264 mm) in the outside wheel path. This section was found to have failed after the first traffic test (Traffic 1). The thicknesses of the base layer in sections HB and NP4 were found to be less than in any other four sections. The large rut depths observed in Section SF may not reflect its true performance, since these rut depths may have been influenced by the lateral movement of the base course aggregates in the outer wheel path, which was observed during trafficking. Overall, NP8 resulted in the smallest rut depth for this traffic test.

Figure 9 indicates that the rut depths in Traffic 2, northbound, (450 mm thick base course) were very small (less than 25 mm), except in Sections HB and NP4, which had larger rut depths, up to 64 mm. The subgrade of both these sections contained organic materials.

Figures 7 through 9 indicate that geotextiles did not reduce rut depths in comparison with the control sections, probably due to the higher strengths of the involved subgrades: thus the reinforcing effect due to the presence of geotextiles was likely negligible. Hence, the contribution of the geotextile to the reduction of rut depth is very limited if the subgrade has a modest shear strength. In this case, geotextiles are expected to act as separators and drainage media only.

Strains in Subgrade and in Base. Figure 10 shows the induced final strains after traffic tests and the incremental strains during the traffic tests in the subgrade and in first lift in Sections SF and NP8 and the control (soil only) section. The strains in the base were very small; therefore the contribution of the geotextiles with respect to strain reduction could not be evaluated for the first lifts of the base layer. A majority of the strains in the subgrade were measured during placement and compaction of the first lift with much lower strains measured during the traffic tests. The control (soil only) section had the highest final strains, 11% in subgrade and 1% in the base. During the traffic tests, a strain increment of 1.1% was observed in the subgrade. The final measured strains in the section having NP8 were 10% in subgrade and −1% in base. The negative strain in the base may be due to the horizontal movement or a slight rotation of the Bison coils. A strain increment of 2.2% was observed in NP8 during the traffic tests (Figure 10). It should be noted that rut depths were not measured at the exact locations of the Bison coils.

SF had the lowest final strains in the subgrade (1%) and in the base (1%). Thus, the reduction of strain in the subgrade of Section SF was greater than in Section NP8. This may be due to the relatively low modulus of NP8. The low strains in the SF section may have been the result of a combination of high modulus and or poor drainage observed in that section. Since the subgrade had a lack of uniformity in water content and in shear strength, the differences in the induced strains cannot be directly attributed to the presence of different geotextiles.

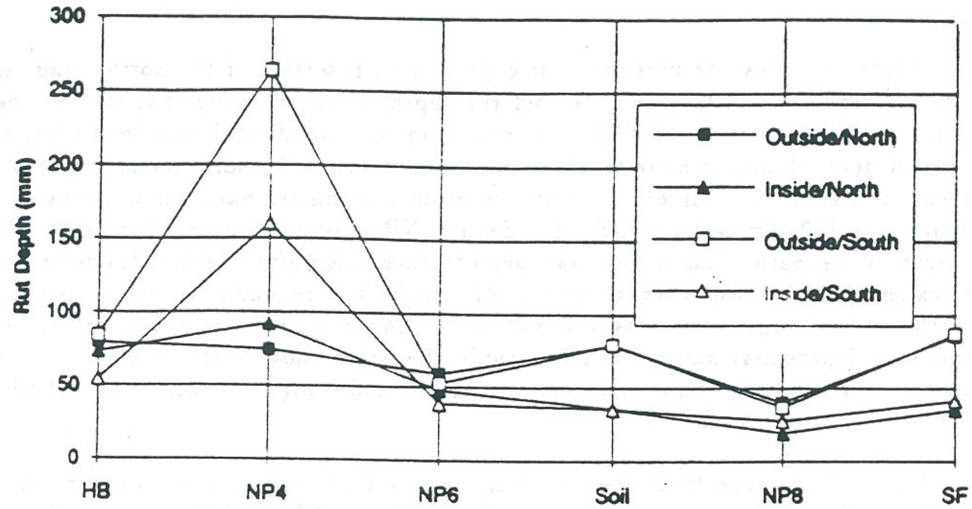

Figure 8: Rut Depth after the Tenth Pass in Traffic 1 in the Northbound Lane.

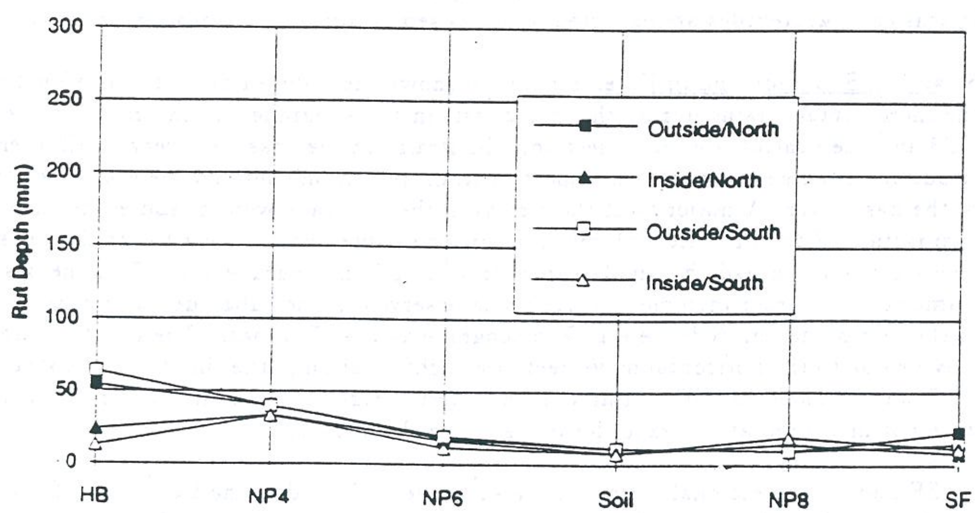

Figure 9: Rut Depth after the Tenth Pass in Traffic 2 in the Northbound Lane.

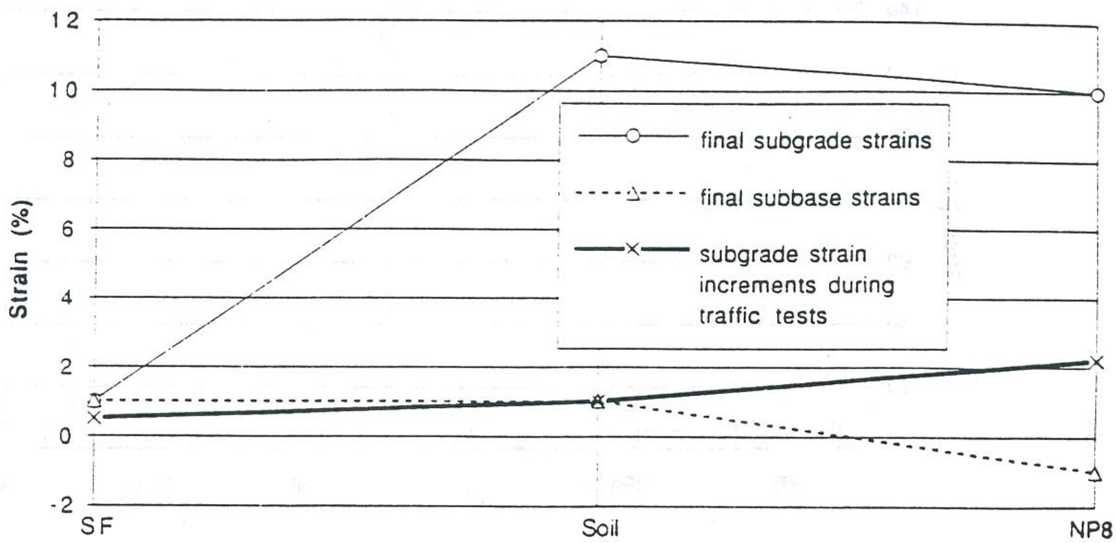

Figure 10: Strains in Subgrade and Base in the Southbound Lane.

Strains in Geotextiles. Figures 11 and 12 summarize the measured strains found in the geotextile surfaces when excavated. The results show that the induced strains in the cross lane direction in SF and NP8 relatively low, about 2% for SF and 4% for NP8. No geotextiles had strains greater than 8% except NP4 in the northbound lane, which had a strain of 136%. The strains in the geotextiles agree well with the measured rut depths; i.e. larger rut depths cause larger strains in the geotextiles.

Visual Observations after Excavations. In the second excavation (southbound lane), all geotextiles performed well. A high ground water table was observed in the test pits during this set of excavations. The designed thickness of fill was 600 mm but the measured thicknesses were not uniform in each section varying as much as 150 mm. SF was not flat and had some ripples (about 50 to 80 mm high) parallel to the lane direction. HB was not in tension and the subgrade was moist and pliable, which is consistent with saturated soft clay conditions. Water ponding under HB existed. NP6 was in tension and wet. NP8 appeared to have less strain. The soil under NP8 was relatively dry compared with the other sections even though the original natural moisture content of the soil was higher in this section indicating a possible influence from lateral drainage potential.

In the control (soil only) section, mixing of subgrade soil and aggregate occurred to a thickness of about 130 mm. However, the intermixture was not observed in the sections containing geotextiles.

In the first northbound lane excavation, SF was in tension but not stretched tightly. Under SF, the subgrade surface was saturated and ponding appeared to be developing. Similarly, NP8 experienced some tension, but was not tight. The soil below NP8 appeared to be relatively dry.

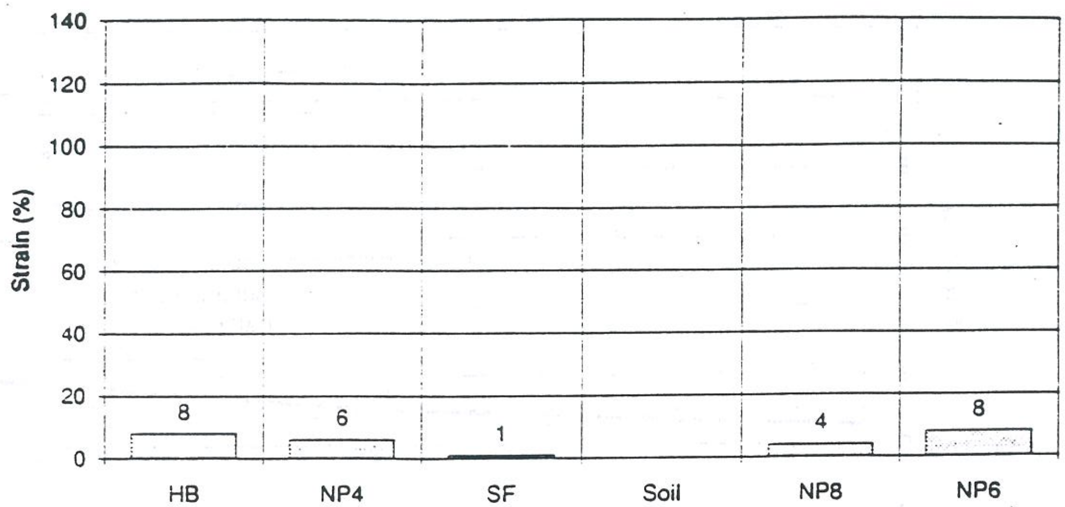

Figure 11: Strains in Geotextiles at Excav 2 in the Southbound Lane.

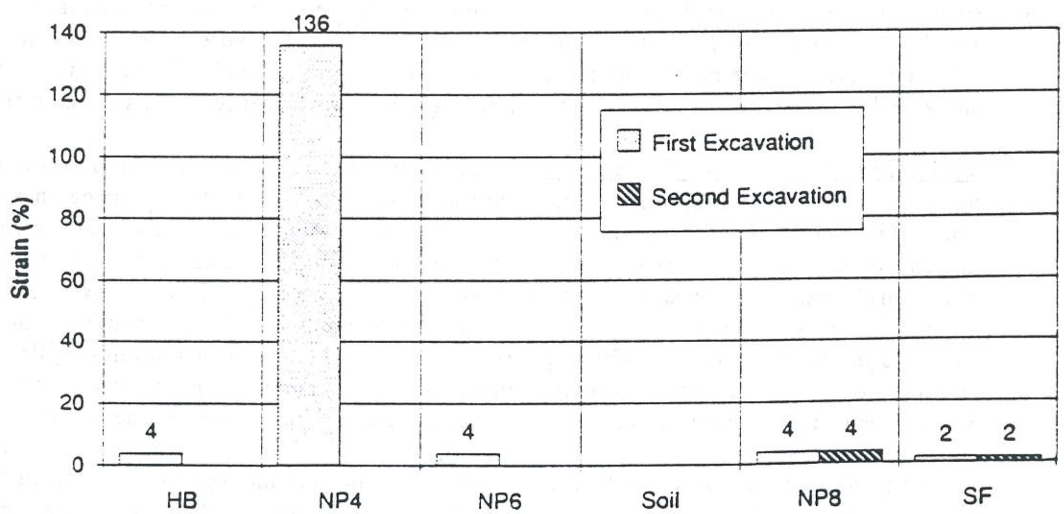

Figure 12: Strains in Geotextiles at Excav 1 and Excav 2 in the Northbound Lane.

NP4 was the only geotextile which did not survive construction. Several holes, which were punched by stones, were found in NP4. This was not surprising considering the subgrade condition, the minimal lift thickness, the amount of rutting observed and the relatively low survivability characteristics of the geotextile. Clay below NP4 appeared wet and slippery. HB was loose as it spanned over discontinuities. A mixture of aggregate and subgrade clay was observed in the control (soil only) section.

In the second excavation (northbound lane), the thickness of fill was less than the design thickness of 460 mm (330 mm for SF and 360 mm for NP8). Soil below NP8 was relatively dry and NP8 appeared tight. Some soil migration was found on the top of the SF, and the surface of the subgrade soil beneath was wet and slightly ponded.

SUMMARY AND CONCLUSIONS

This full scale road test was performed to evaluate the ability of different types of geotextiles to stabilize a soft subgrade for a highway construction. Based on the results of the study, a number of conclusions were drawn:

- The use of a geotextile was in all cases found to eliminate base/subgrade intermixing, if the geotextile survives the installation and placement operations.
- The presence of a geotextile can result in more uniform rut depths, if the geotextile survives the installation and placement operations.
- Rut depth cannot be reduced by geotextiles, if the subgrade has a modest shear strength.
- Compared with the other geotextiles used in this study, NP8 had the best overall performance based on visual observations and rut depths.
- Strains in the subgrade soil appear to be reduced by the SF geotextile; however some pumping of the subgrade may have influenced these results.
- The observations indicate that during construction the needle-punched nonwoven geotextiles allowed unrestricted drainage of the subgrade while the other types tended to retard drainage. The heavier weight needle-punched nonwoven geotextile appeared to enhance drainage.

This paper presents only the initial results of a planned long term monitoring plan. Although the initial results primarily indicate an improvement, the actual benefits of using geotextiles as separators in pavement systems can only be determined after long term monitoring and evaluation.

ACKNOWLEDGEMENTS

Financial support for the instrumentation and field test observations was provided by the Washington State DOT and Polyfelt, Inc. All geotextiles were supplied by Polyfelt, Inc. A special thanks to Mark Wayne for his diligent participation in the program.

REFERENCES

Christopher, B., and Holtz, R. D. (1989) Geotextile Design and Guidelines, National Highway Institute, U.S. Federal Highway Administration, Washington D.C., Report FHWA-HI-90-001.

Steward, J.E., Williamson, R., and Mohney, J., (1977) Guidelines for Use of Fabrics in Construction and Maintenance of Low Volume Roads, U.S. Forest Service, Portland, OR..

APPENDIX B

SOIL TEST RESULTS AND GRAIN SIZE DISTRIBUTION CURVES

APPENDIX B

SOIL TEST RESULTS AND GRAIN SIZE DISTRIBUTION CURVES

The soil testing methods are discussed in Section 7.1.2, and a summary of some of the results are presented in Section 7.2.2. The results of the grain size distribution tests are presented in Figures B.1 through B.13. The figures also contain the results of the water content and Atterberg limit tests. The following abbreviations are used in Figures B.1 through B.13:

LL	- Liquid Limit
PI	- Plastic Limit
USCS	- Unified Soil Classification System
WC	- Water Content
SB	- Southbound Lane
NB	- Northbound Lane
-300	- Sample within top 300 mm of fill
+150	- Sample approximately 150 mm above geotextile
+0-100	- Sample within 0 to 100 mm above fill/subgrade interface
+100-200	- Sample within 100 to 200 mm above fill/subgrade interface

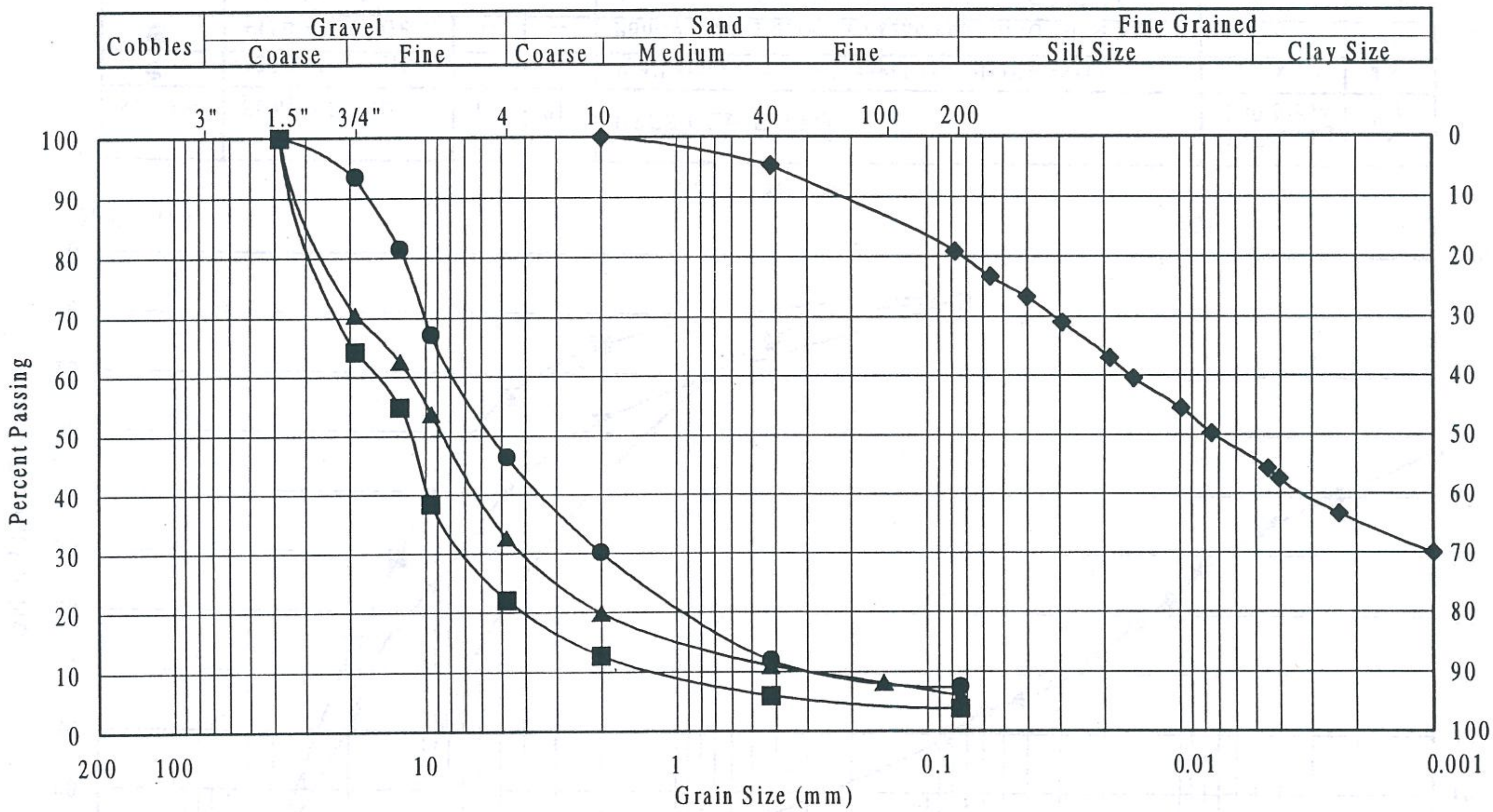

Symbol	Sample Location	LL	PI	USCS Classification	% Passing 200 Sieve	WC (%)
●	-300 Below Surface	--	--	Well graded gravel w/ sand and silt (GW-GM)	7.4	4.6
■	+150 Above Geot.	--	--	Well graded gravel w/ sand (GW)	3.8	3.3
▲	"Mudcake"	--	--	Well graded gravel w/ sand and silt (GW-GM)	5.9	4.4
◆	Nat. Subgrade	58	30	Fat clay with sand (CH)	81	30.5

Figure B.1 - Grain Size Distribution for HB - NB.

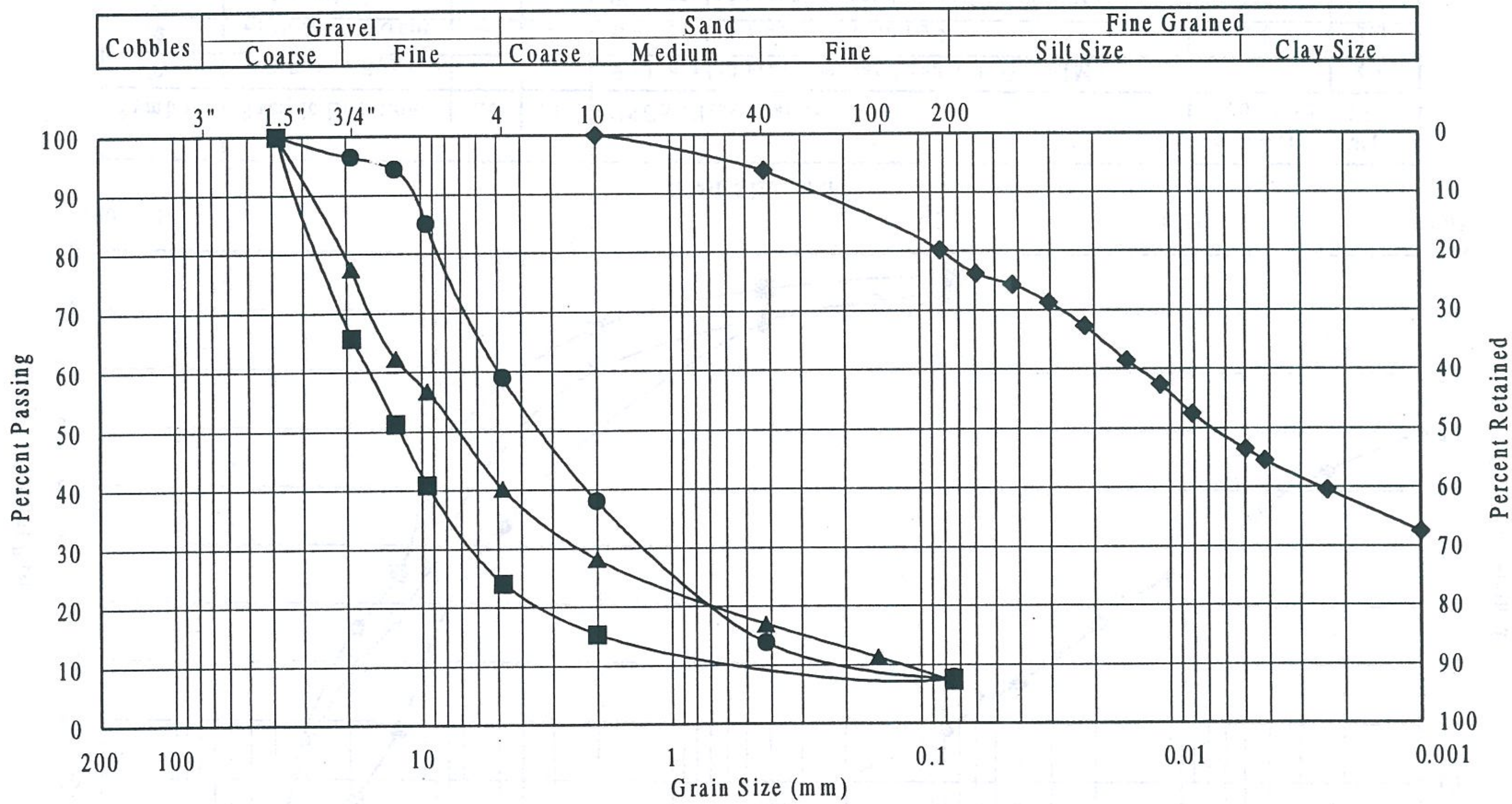

Symbol	Sample Location	LL	PI	USCS Classification	% Passing 200 Sieve	WC (%)
●	-300 Below Surface	--	--	Well graded sand w/ gravel and silt (SW-SM)	7.8	4.9
■	+150 Above Geot.	--	--	Poorly graded gravel w/ sand and silt (GP-GM)	7.6	5.2
▲	"Mudcake"	--	--	Poorly graded gravel w/ sand and silt (GP-GM)	7.1	5.0
◆	Nat. Subgrade	47	24	Lean clay with sand (CL)	78	28.2

Figure B.2 - Grain Size Distribution for NP4 - NB.

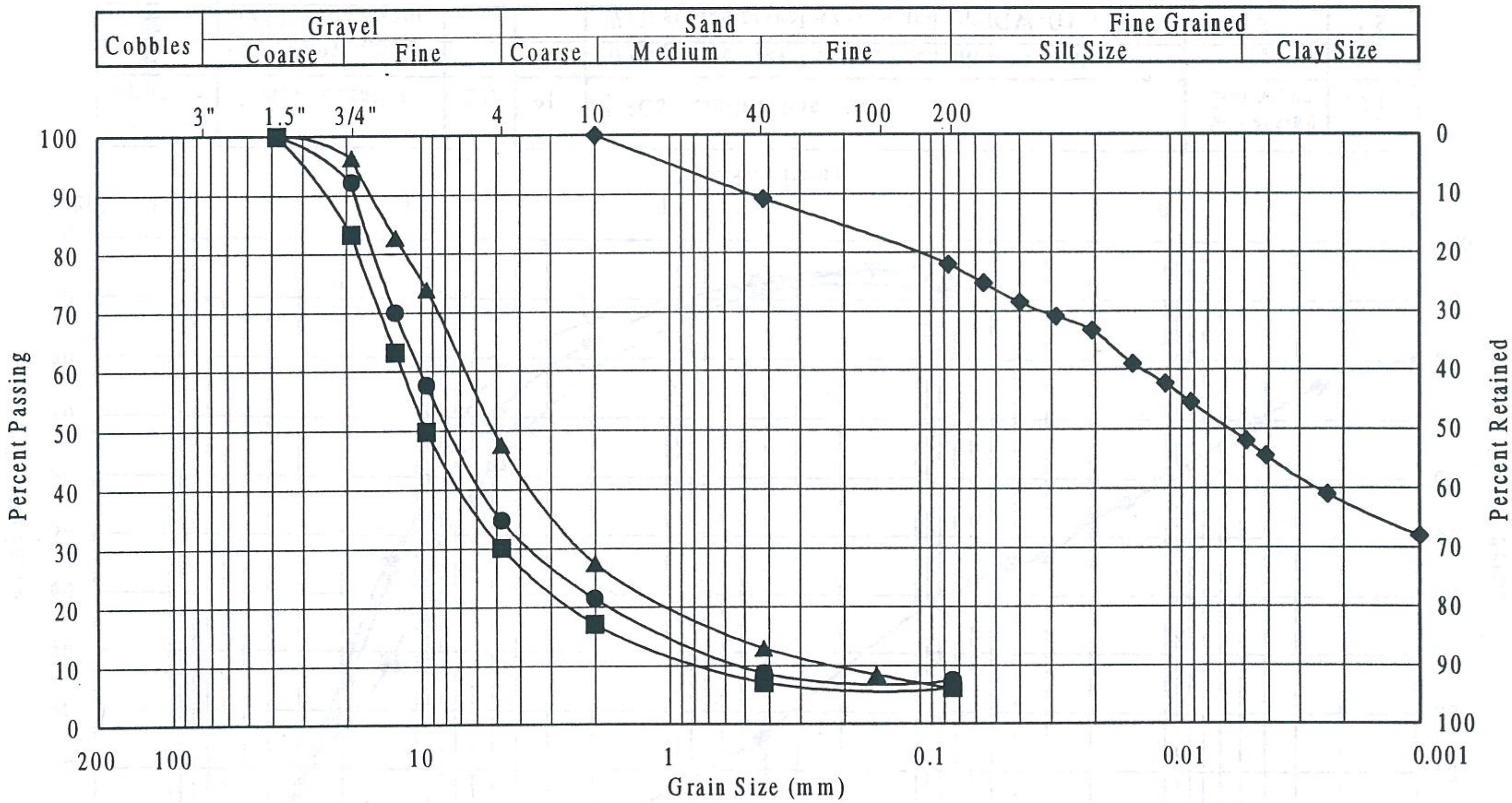

Symbol	Sample Location	LL	PI	USCS Classification	% Passing 200 Sieve	WC (%)
●	-300 Below Surface	--	--	Well graded gravel w/ sand and silt (GW-GM)	7.4	4.1
■	+150 Above Geot.	--	--	Well graded gravel w/ sand and silt (GW-GM)	6.1	6.4
▲	"Mudcake"	--	--	Poorly graded gravel w/ sand and silt (GP-GM)	6.0	5.4
◆	Nat. Subgrade	58	25	Elastic silt with sand (MH)	78	32.7

Figure B.3 - Grain Size Distribution for NP6 - NB.

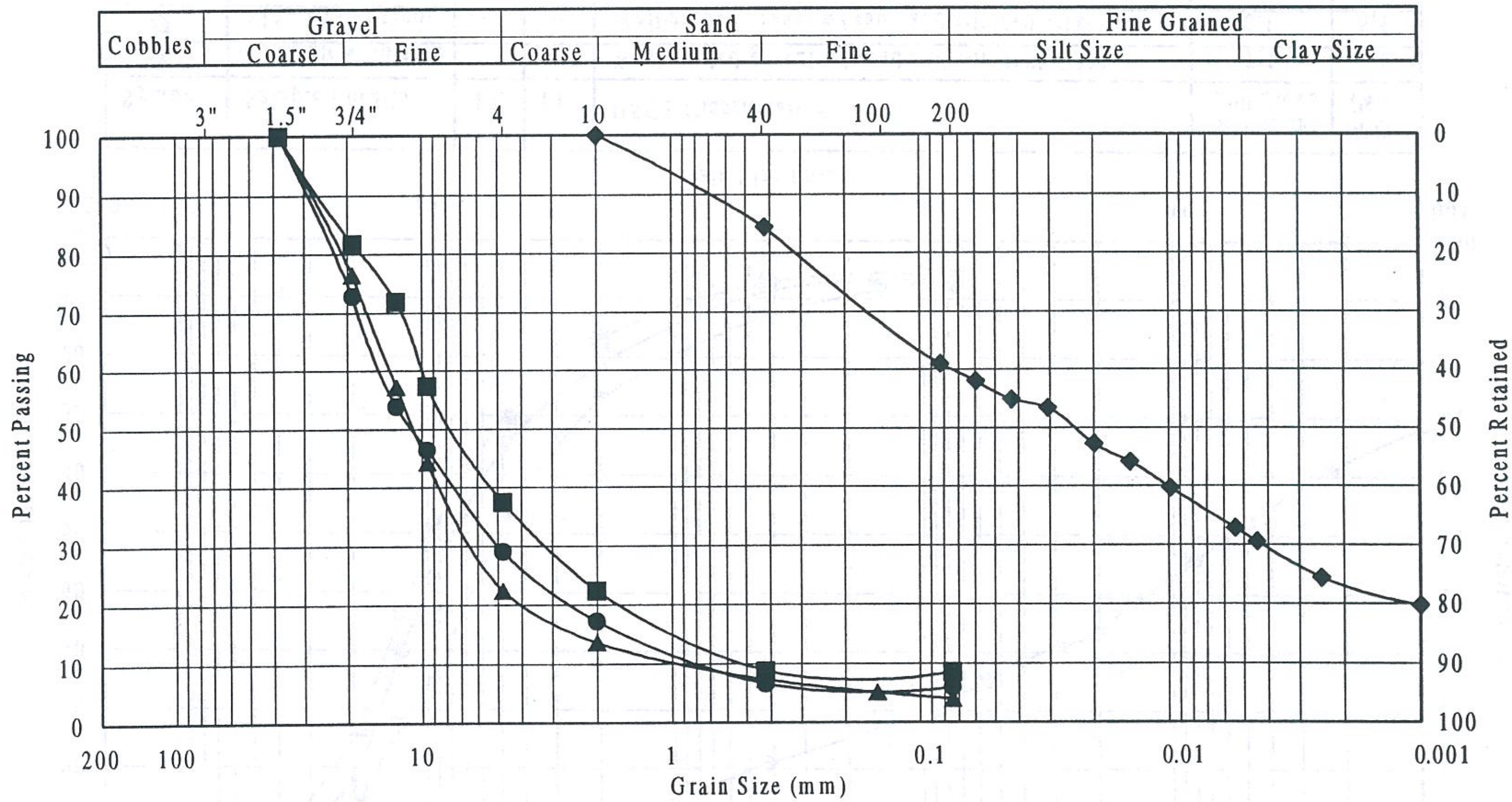

Symbol	Sample Location	LL	PI	USCS Classification	% Passing 200 Sieve	WC (%)
●	-300 Below Surface	--	--	Well graded gravel w/ sand and silt (GW-GM)	6.0	3.8
■	+150 Above Geot.	--	--	Well graded gravel w/ sand and silt (GW-GM)	8.6	4.8
▲	"Mudcake"	--	--	Poorly graded gravel w/ sand (GP)	4.0	4.6
◆	Nat. Subgrade	59	22	Sandy elastic silt (MH)	60	41.8

Figure B.4 - Grain Size Distribution for NP8 - NB.

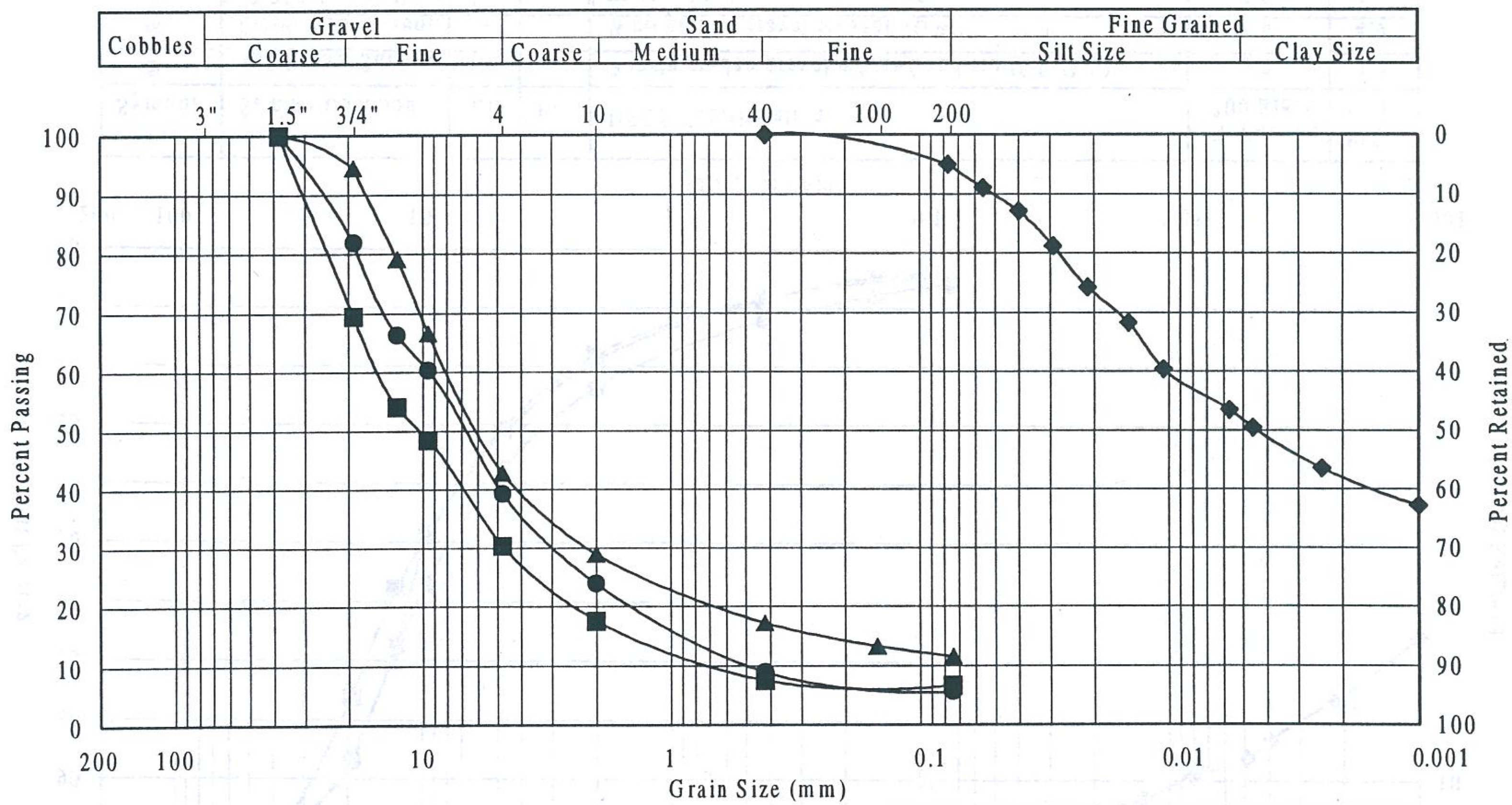

Symbol	Sample Location	LL	PI	USCS Classification	% Passing 200 Sieve	WC (%)
●	-300 Below Surface	--	--	Well graded gravel w/ sand and silt (GW-GM)	5.6	3.8
■	+150 Above Geot.	--	--	Well graded gravel w/ sand and silt (GW-GM)	6.7	4.2
▲	"Mudcake"	--	--	Poorly graded gravel w/ sand and silt (GP-GM)	11.6	7.7
◆	Nat. Subgrade	71	43	Fat clay (CH)	95	38.5

Figure B.5 - Grain Size Distribution for SF - NB.

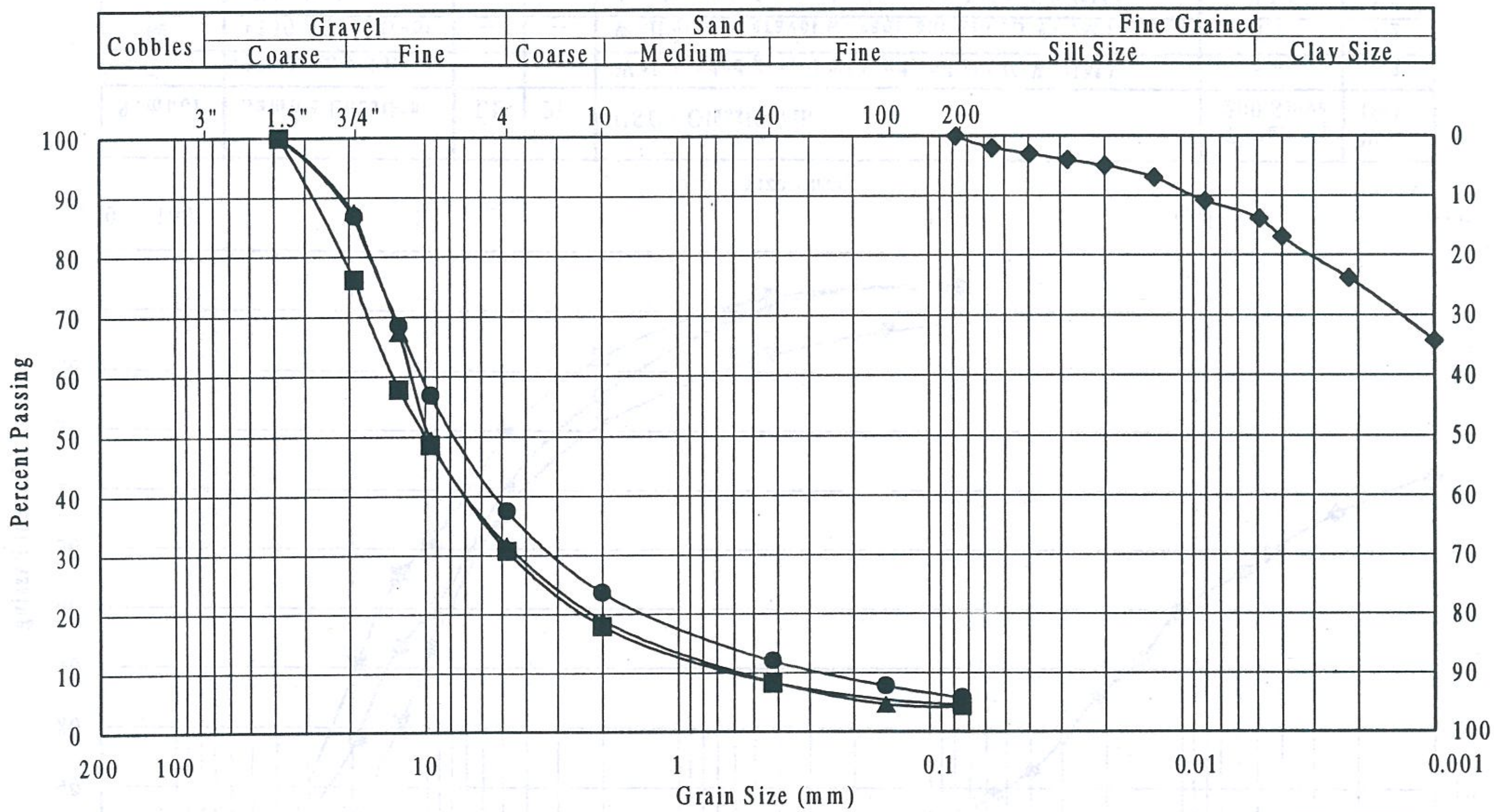

Symbol	Sample Location	LL	PI	USCS Classification	% Passing 200 Sieve	WC (%)
●	-300 Below Surface	--	--	Poorly graded gravel w/ sand and silt (GP-GM)	5.7	3.8
■	0-100 Above Geot.	--	--	Well graded gravel w/ sand (GW)	4.6	4.9
▲	100-200 Above Geot.	--	--	Well graded gravel w/ sand (GW)	4.2	4.1
◆	Nat. Subgrade	109	75	Fat clay (CH)	100	59.0

Figure B.6 - Grain Size Distribution for Soil - NB.

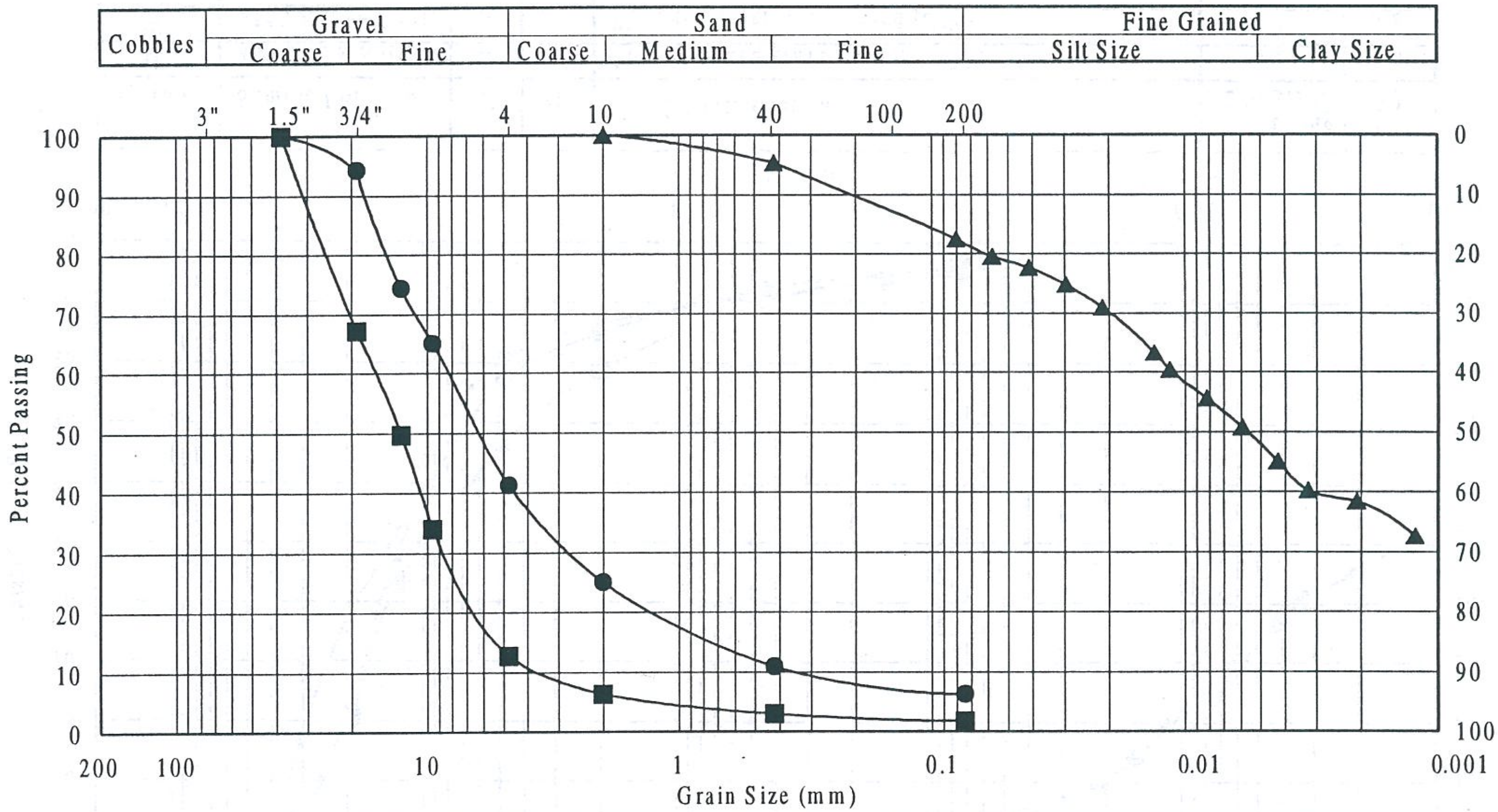

Symbol	Sample Location	LL	PI	USCS Classification	% Passing 200 Sieve	WC (%)
●	-300 Below Surface	--	--	Well graded gravel w/ sand and silt (GW-GM)	6.3	3.6
■	+150 Above Geot.	--	--	Well graded gravel (GW)	1.8	4.2
▲	Nat. Subgrade	35	14	Lean clay with sand (CL)	82	22.2

Figure B.7 - Grain Size Distribution for HB - SB.

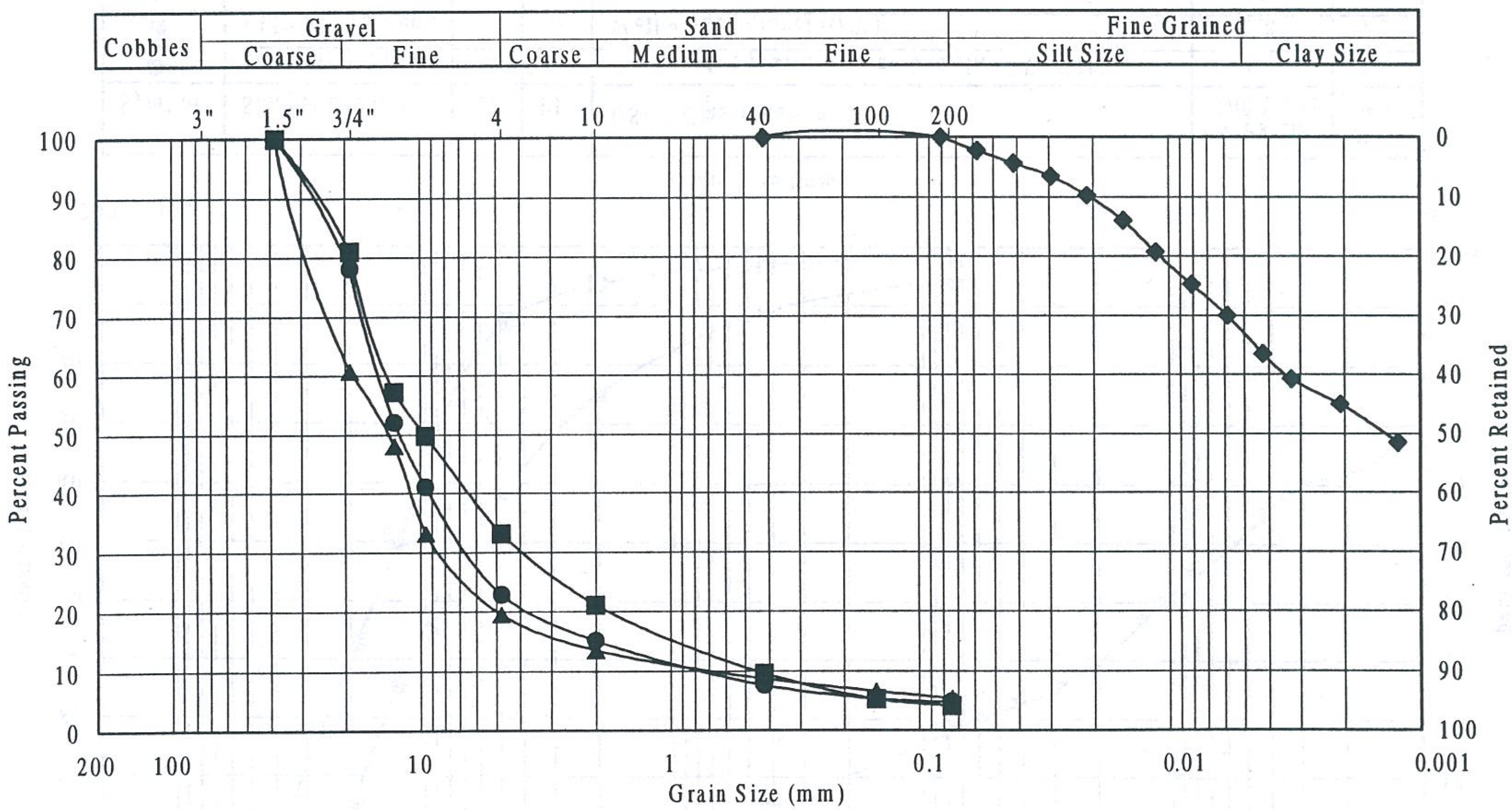

Symbol	Sample Location	LL	PI	USCS Classification	% Passing 200 Sieve	WC (%)
●	-300 Below Surface	--	--	Poorly graded gravel w/ sand (GP)	4.8	3.6
■	+150 Above Geot.	--	--	Well graded gravel w/ sand (GW)	4.2	3.8
▲	"Mudcake"	--	--	Poorly graded gravel w/ sand and silt (GP-GM)	5.4	6.3
◆	Nat. Subgrade	86	56	Fat clay (CH)	99	48.2

Figure B.8 - Grain Size Distribution for NP4 - SB.

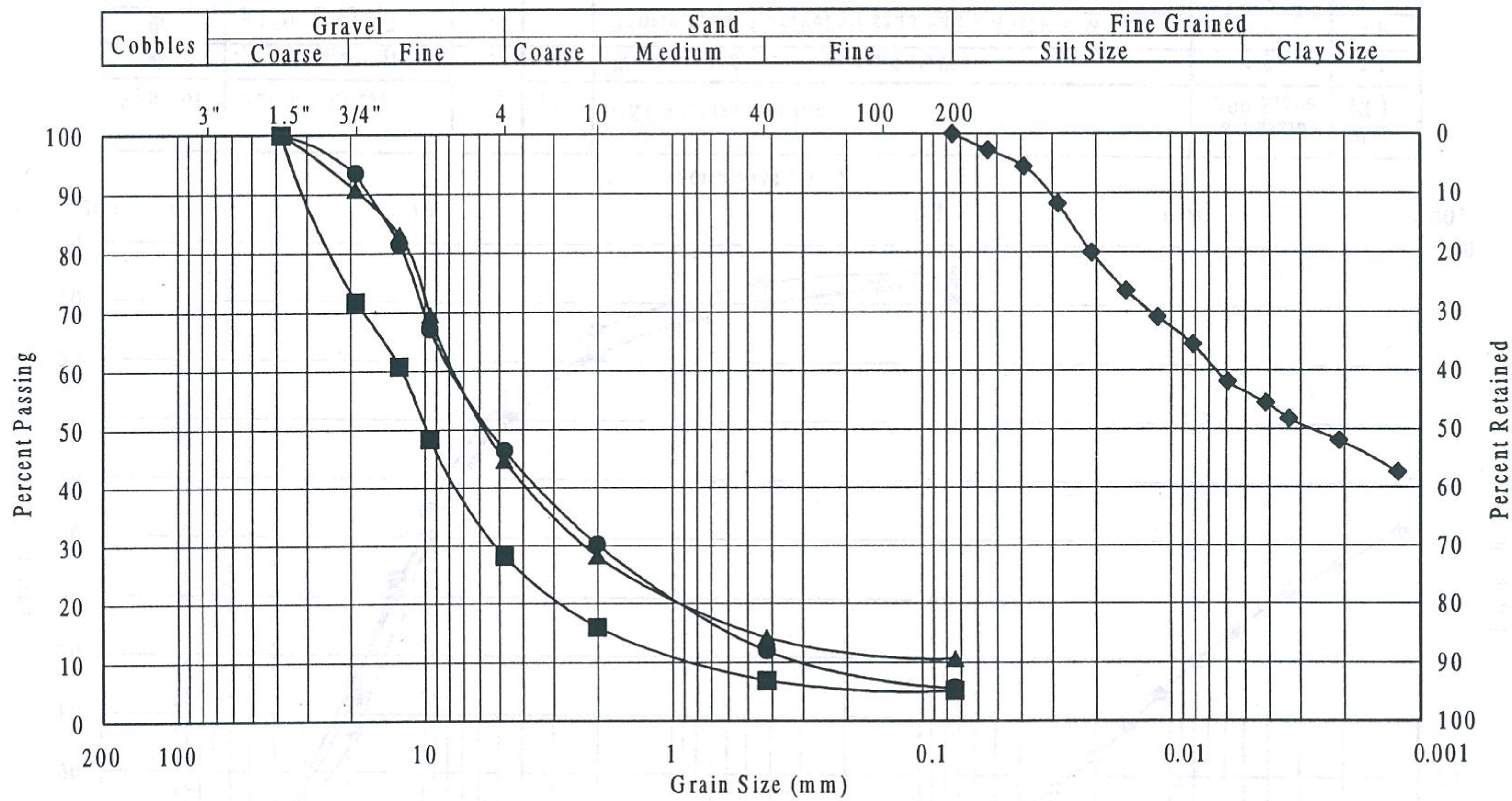

Symbol	Sample Location	LL	PI	USCS Classification	% Passing 200 Sieve	WC (%)
●	-300 Below Surface	--	--	Well graded gravel w/ sand and silt (GW-GM)	5.6	3.9
■	+150 Above Geot.	--	--	Well graded gravel w/ sand and silt (GW-GM)	5.2	5.0
▲	"Mudcake"	--	--	Poorly graded gravel w/ sand and silt (GP-GM)	10.6	9.8
◆	Nat. Subgrade	71	43	Fat clay (CH)	100	40.3

Figure B.9 - Grain Size Distribution for NP6 - SB.

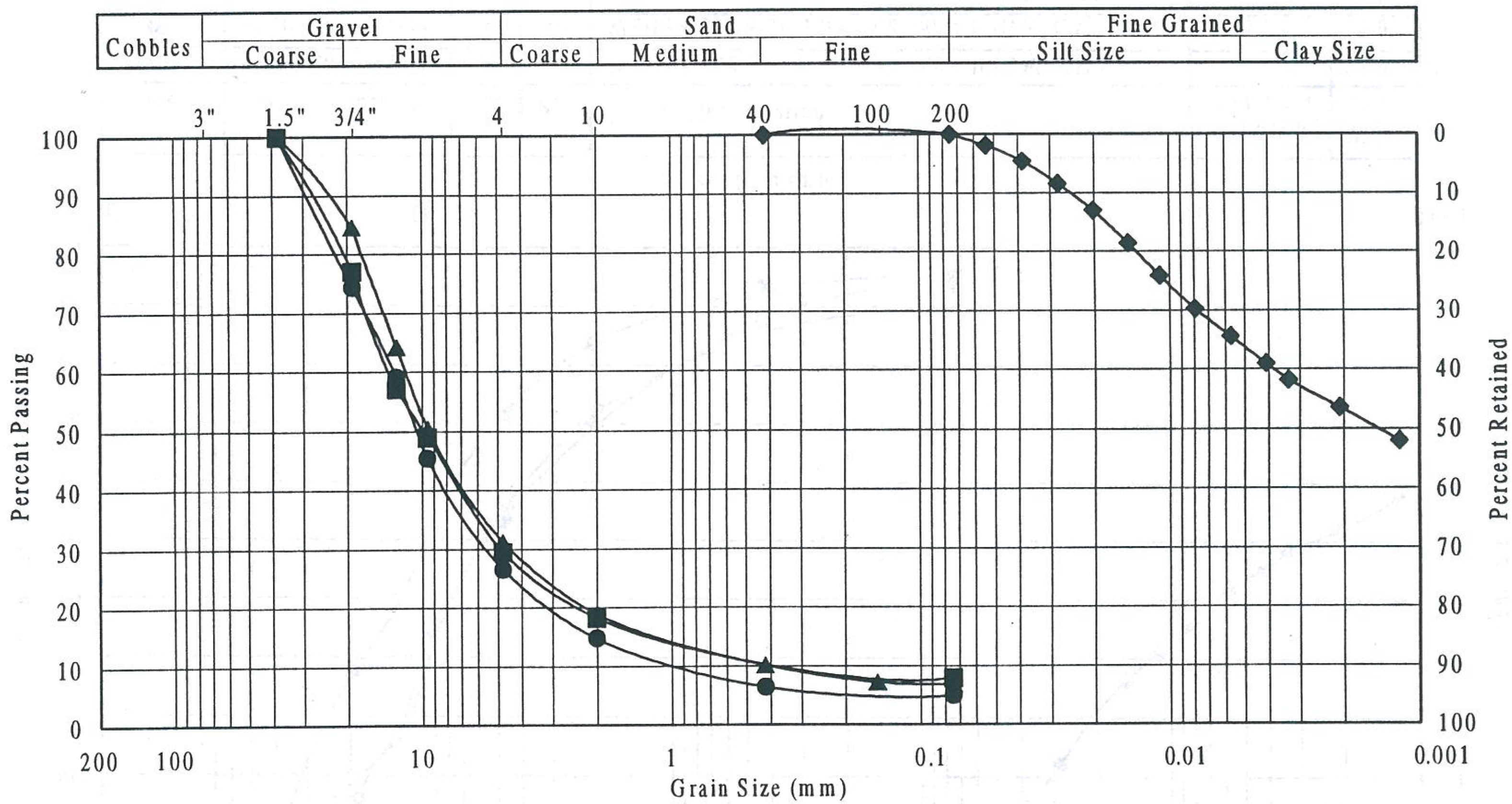

Symbol	Sample Location	LL	PI	USCS Classification	% Passing 200 Sieve	WC (%)
●	-300 Below Surface	--	--	Well graded gravel w/ sand (GW)	4.9	3.1
■	+150 Above Geot.	--	--	Poorly graded gravel w/ sand and silt (GP-GM)	7.9	9.6
▲	"Mudcake"	--	--	Poorly graded gravel w/ sand and silt (GP-GM)	6.8	8.1
◆	Nat. Subgrade	82	54	Fat clay (CH)	100	43.8

Figure B.10 - Grain Size Distribution for NP8 - SB.

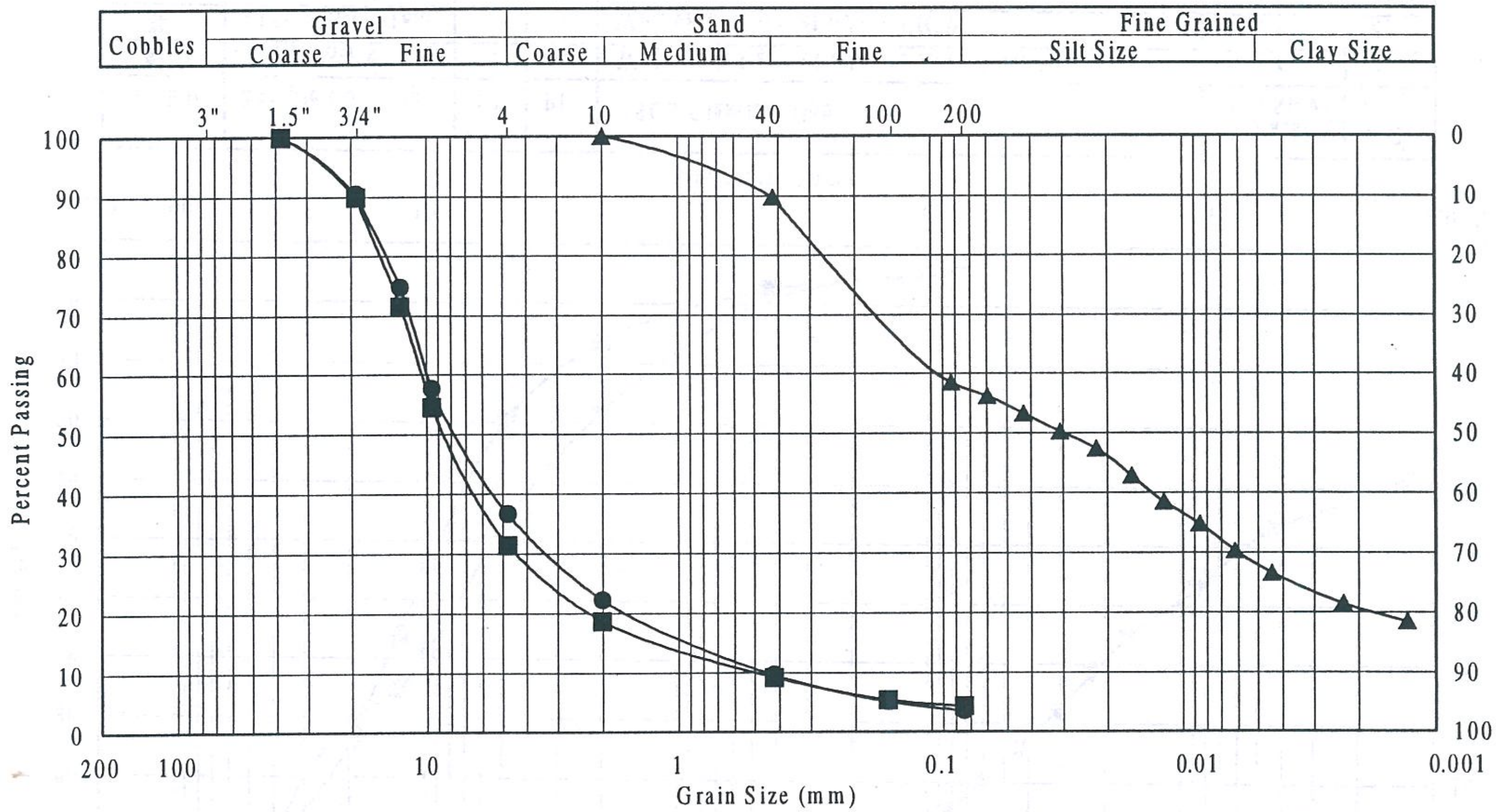

Symbol	Sample Location	LL	PI	USCS Classification	% Passing 200 Sieve	WC (%)
●	-300 Below Surface	--	--	Well graded gravel w/ sand (GW)	3.6	3.7
■	+150 Above Geot.	--	--	Poorly graded gravel w/ sand (GP)	4.4	4.9
▲	Nat. Subgrade	48	16	Sandy silt (ML)	57	30.0

Figure B.11 - Grain Size Distribution for SF - SB.

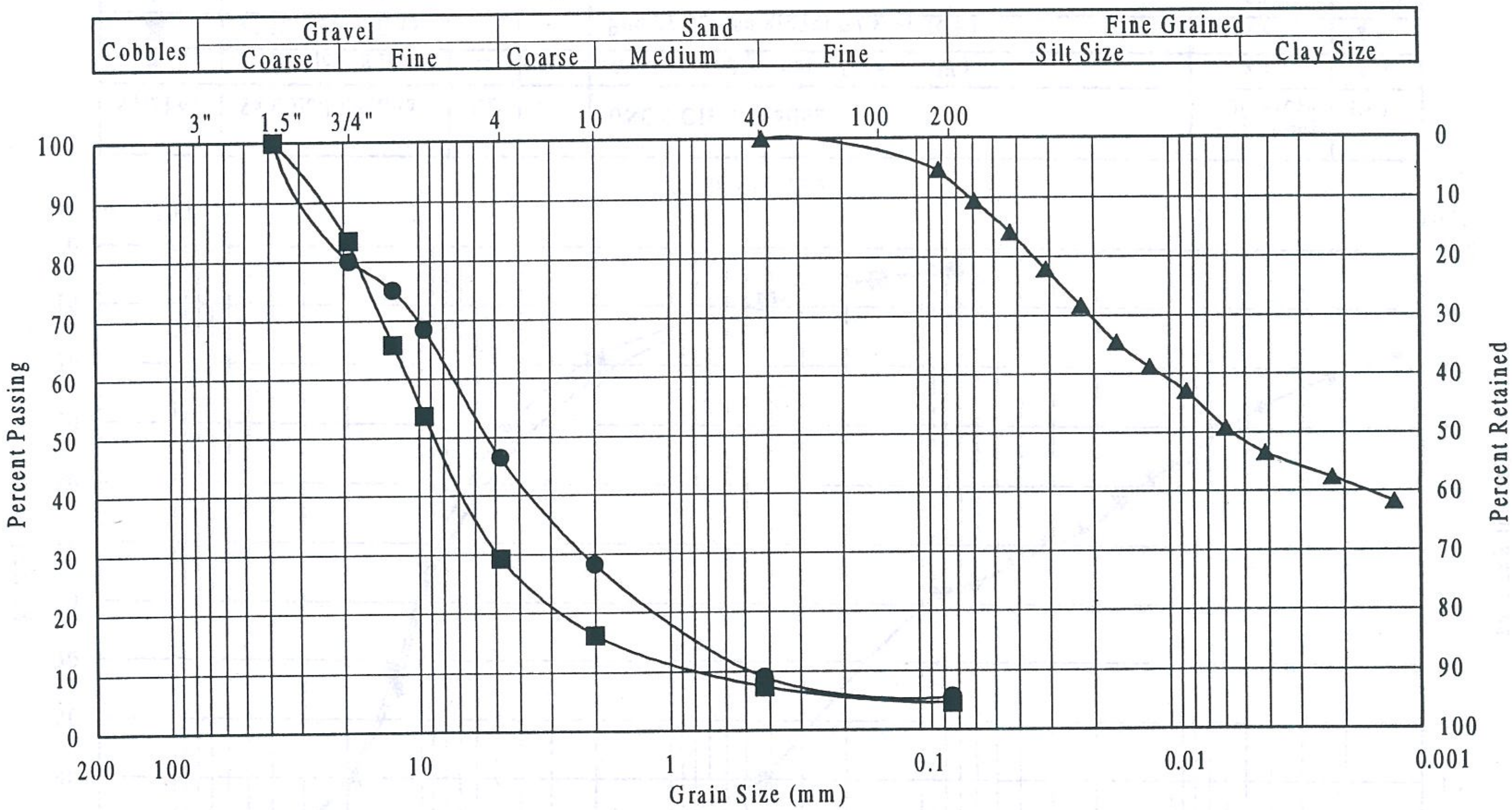

Symbol	Sample Location	LL	PI	USCS Classification	% Passing 200 Sieve	WC (%)
●	-300 Below Surface	--	--	Well graded gravel w/ sand and silt (GW-GM)	5.6	3.8
■	+150 Above Geot.	--	--	Well graded gravel w/ sand (GW)	4.6	4.7
▲	Nat. Subgrade	61	35	Fat clay (CH)	94	40.6

Figure B.12 - Grain Size Distribution for Soil - SB.

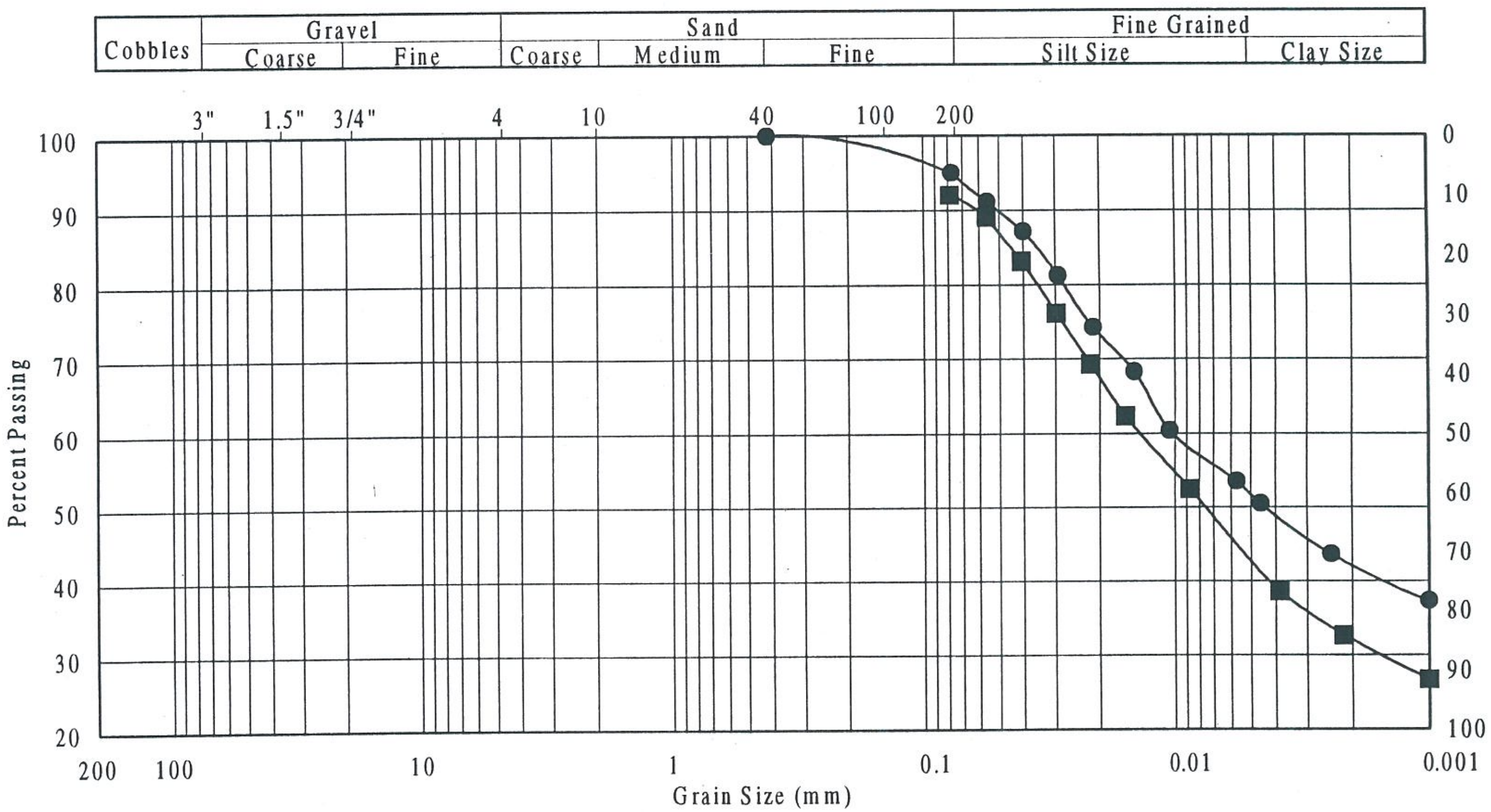

Symbol	Sample Location	LL	PI	USCS Classification	% Passing 200 Sieve	W C (%)
●	Nat. Subgrade	71	43	Fat clay (CH)	95	38.5
■	"Mudcake"	--	--	Fines washed from base aggregate	--	--

Figure B.13 - Grain Size Distribution for SF - NB, subgrade soil and mudcake.

APPENDIX C

PERMITTIVITY TEST PROCEDURES AND RESULTS

APPENDIX C

PERMITTIVITY TEST PROCEDURES AND RESULTS

The permittivity test procedures are discussed in Section 7.1.4, and a summary of the results is presented in Section 7.2.4. The results of the permittivity tests performed on the exhumed specimens are presented in Tables C.1 through C.10, and the tests performed on the control specimens are presented in Tables C.11 through C.15. The geotextile thicknesses used in calculating the permeability values are presented in Table 2.1 (values reported by the manufacturers).

The permittivity test procedures used were largely based on the procedures described by Metcalfe and Holtz (1994). The tests were generally performed as follows:

1. Four specimens were selected from each exhumed sample. In selecting the specimens, the exhumed sample was held up to a light so that specimens representative of the average degree of blinding and clogging could be taken. If the exhumed sample contained areas with notably different types or varying degrees of iron staining, clogging, or blinding, the specimens were collected so that the overall sample was fairly represented.

2. The specimens were cut approximately 55 mm in diameter, and inundated with deaired water in a sealed container for at least 24 hrs. The deaired water used throughout the testing procedures was obtained from a tank which filled with misted water while under a vacuum of approximately 75 cm mercury (Hg).

3. When a specimen was ready for testing, the lower portion of the permeameter was filled with deaired water until the water level reached the top of the union joint. The specimen was then placed between two rubber gaskets in the union joint, and

the joint was tightened. The bottom face of the specimen was in the upright position to simulate the field flow conditions. Deaired water was then added to the outlet port until the water level was at the top of the outlet port.

4. The temperature of the water at the outlet port was recorded. A stopper was carefully inserted into the outlet port so that the unwashed specimen was not disturbed.

5. The standpipe was then filled by keeping the end of the water supply tube immersed to minimize intrusion of air bubbles. The stopper with the air supply tube was inserted. A finger was placed over the top of the air supply tube, and the stopper at the outlet port was removed.

6. By slight finger movements, a small amount of air was allowed down the air supply tube so that atmospheric pressure acted at the bottom of the air supply tube. The water level was recorded. The test was started by simultaneously starting the stopwatch and removing the finger from the air supply tube to initiate flow. Before stopping the test, the water level in the standpipe was allowed to drop at least 300 mm or allowed to drop for at least 60 sec.

7. Steps 4 through 6 were repeated until 5 runs were complete. The apparatus was then disassembled and the specimen was washed by gently massaging it under swiftly moving water until nearly all the soil particles had washed from the specimen. Careful attempts were made to keep the structure of the geotextile intact during the washing process.

8. Steps 3 through 6 were repeated until 5 runs were complete on the washed specimen.

Table C.1 - Permittivity Test Results, HB - NB.

Specimen No.	Run No.	Water Level Drop (cm)	Time For Drop (sec)	Temp. (C)	Permittivity (sec^{-1})	Flow Rate (cc/s)	Permeability (cm/sec)
1 Unwashed	1	31.6	51.36	16	0.14	7.2	0.006
	2	37.4	33.32	16	0.25	13.1	0.010
	3	36.1	28.10	16	0.29	15.0	0.012
	4	36.5	24.79	16	0.33	17.2	0.013
	5	42.6	26.82	16	0.36	18.6	0.014
				Average	0.28	14.2	0.011
1 Washed	1	42.9	4.54	16	2.14	110.4	0.086
	2	40.1	4.17	16	2.18	112.3	0.087
	3	38.8	4.05	16	2.17	111.9	0.087
	4	37.0	3.77	16	2.22	114.6	0.089
	5	40.6	4.29	16	2.14	110.5	0.086
				Average	2.17	112.0	0.087
2 Unwashed	1	34.5	8.30	16	0.94	48.5	0.038
	2	34.9	7.70	16	1.03	52.9	0.041
	3	36.8	6.92	16	1.20	62.1	0.048
	4	33.6	6.10	16	1.25	64.3	0.050
	5	34.8	6.26	16	1.26	64.9	0.050
				Average	1.13	58.6	0.045
2 Washed	1	49.5	3.23	16	3.47	179.0	0.139
	2	38.9	2.64	16	3.33	172.1	0.133
	3	41.7	2.71	16	3.48	179.7	0.139
	4	42.6	2.82	16	3.42	176.4	0.137
	5	47.1	3.05	16	3.49	180.4	0.140
				Average	3.44	177.5	0.138
3 Unwashed	1	32.9	48.69	16	0.15	7.9	0.006
	2	32.8	30.96	16	0.24	12.4	0.010
	3	32.1	26.41	16	0.28	14.2	0.011
	4	33.5	23.26	16	0.33	16.8	0.013
	5	41.1	26.82	16	0.35	17.9	0.014
				Average	0.27	13.8	0.011
3 Washed	1	38.1	3.92	16	2.20	113.5	0.088
	2	35.2	3.64	16	2.19	112.9	0.088
	3	41.0	4.23	16	2.19	113.2	0.088
	4	38.6	3.95	16	2.21	114.1	0.088
	5	42.2	4.44	16	2.15	111.0	0.086
				Average	2.19	113.0	0.088
4 Unwashed	1	32.9	24.92	16	0.30	15.4	0.012
	2	32.3	19.80	16	0.37	19.1	0.015
	3	32.8	17.52	16	0.42	21.9	0.017
	4	33.6	16.47	16	0.46	23.8	0.018
	5	39.5	18.48	16	0.48	25.0	0.019
				Average	0.41	21.0	0.016
4 Washed	1	36.9	3.35	16	2.49	128.7	0.100
	2	38.3	3.57	16	2.43	125.3	0.097
	3	40.7	3.66	16	2.52	129.9	0.101
	4	42.6	3.80	16	2.54	130.9	0.101
	5	43.0	3.93	16	2.48	127.8	0.099
				Average	2.49	128.5	0.100

Table C.2 - Permittivity Test Results, NP4 - NB.

Specimen No.	Run No.	Water Level Drop (cm)	Time For Drop (sec)	Temp. (C)	Permittivity (sec^{-1})	Flow Rate (cc/s)	Permeability (cm/sec)
1	1	32.2	5.42	16	1.34	69.4	0.202
Unwashed	2	36.4	5.57	16	1.48	76.3	0.222
	3	35.6	5.26	16	1.53	79.1	0.230
	4	33.3	4.60	16	1.64	84.6	0.246
	5	39.6	5.23	16	1.71	88.4	0.257
				Average	1.54	79.6	0.231
1	1	45.0	3.70	16	2.75	142.1	0.413
Washed	2	44.9	3.60	16	2.82	145.7	0.423
	3	41.1	3.11	16	2.99	154.4	0.449
	4	34.7	2.76	16	2.85	146.8	0.427
	5	37.3	2.92	16	2.89	149.2	0.434
				Average	2.86	147.6	0.429
2	1	35.4	9.01	16	0.89	45.9	0.133
Unwashed	2	35.1	7.57	16	1.05	54.2	0.157
	3	38.8	7.41	16	1.19	61.2	0.178
	4	34.6	6.22	16	1.26	65.0	0.189
	5	34.1	5.74	16	1.34	69.4	0.202
				Average	1.15	59.1	0.172
2	1	36.8	3.60	16	2.31	119.4	0.347
Washed	2	37.2	3.55	16	2.37	122.4	0.356
	3	35.4	3.33	16	2.41	124.2	0.361
	4	35.8	3.45	16	2.35	121.2	0.352
	5	38.3	3.73	16	2.32	119.9	0.349
				Average	2.35	121.4	0.353
3	1	40.1	4.40	16	2.06	106.4	0.309
Unwashed	2	45.2	4.43	16	2.31	119.2	0.346
	3	38.7	3.69	16	2.37	122.5	0.356
	4	41.8	3.69	16	2.56	132.3	0.385
	5	49.3	4.29	16	2.60	134.2	0.390
				Average	2.38	122.9	0.357
3	1	56.4	3.57	16	3.58	184.5	0.536
Washed	2	53.4	2.80	16	4.32	222.8	0.647
	3	40.5	2.32	16	3.95	203.9	0.593
	4	42.7	2.60	16	3.72	191.8	0.558
	5	48.9	2.64	16	4.19	216.3	0.629
				Average	3.95	203.9	0.593
4	1	40.2	5.67	17	1.57	82.8	0.235
Unwashed	2	38.1	4.83	17	1.74	92.1	0.261
	3	36.9	4.33	17	1.88	99.5	0.282
	4	34.3	4.05	17	1.87	98.9	0.280
	5	34.9	3.99	17	1.93	102.2	0.290
				Average	1.80	95.1	0.270
4	1	31.2	2.64	17	2.61	138.0	0.391
Washed	2	33.2	2.69	17	2.72	144.2	0.409
	3	33.9	2.88	17	2.60	137.5	0.390
	4	35.0	2.82	17	2.74	145.0	0.411
	5	35.6	2.89	17	2.72	143.9	0.408
				Average	2.68	141.7	0.402

Table C.3 - Permittivity Test Results, NP6 - NB.

Specimen No.	Run No.	Water Level Drop (cm)	Time For Drop (sec)	Temp. (C)	Permittivity (sec^{-1})	Flow Rate (cc/s)	Permeability (cm/sec)
1	1	41.5	4.13	17	2.22	117.4	0.444
Unwashed	2	38.8	3.58	17	2.39	126.6	0.479
	3	40.7	3.64	17	2.47	130.6	0.494
	4	39.0	3.27	17	2.63	139.3	0.527
	5	39.4	3.57	17	2.44	128.9	0.487
				Average	2.43	128.6	0.486
1	1	42.0	3.01	17	3.08	163.0	0.616
Washed	2	37.4	2.79	17	2.96	156.6	0.592
	3	39.6	2.76	17	3.17	167.6	0.634
	4	34.7	2.60	17	2.95	155.9	0.589
	5	39.8	2.85	17	3.08	163.1	0.617
				Average	3.05	161.2	0.610
2	1	32.3	3.26	17	2.19	115.7	0.438
Unwashed	2	32.3	3.07	17	2.32	122.9	0.465
	3	33.8	2.94	17	2.54	134.3	0.508
	4	35.4	3.04	17	2.57	136.0	0.514
	5	40.7	3.21	17	2.80	148.1	0.560
				Average	2.48	131.4	0.497
2	1	35.4	2.64	17	2.96	156.6	0.592
Washed	2	37.5	2.83	17	2.93	154.8	0.585
	3	35.5	2.70	17	2.90	153.6	0.581
	4	36.5	2.77	17	2.91	153.9	0.582
	5	41.4	2.98	17	3.07	162.3	0.613
				Average	2.95	156.2	0.591
3	1	37.5	4.41	17	1.88	99.3	0.375
Unwashed	2	32.2	3.38	17	2.10	111.3	0.421
	3	37.7	3.62	17	2.30	121.6	0.460
	4	38.7	3.71	17	2.30	121.8	0.461
	5	44.4	4.16	17	2.36	124.7	0.471
				Average	2.19	115.7	0.438
3	1	35.8	2.71	17	2.92	154.3	0.583
Washed	2	37.8	2.61	17	3.20	169.2	0.640
	3	42.2	3.10	17	3.01	159.0	0.601
	4	36.5	2.73	17	2.95	156.2	0.590
	5	42.0	3.07	17	3.02	159.8	0.604
				Average	3.02	159.7	0.604
4	1	43.2	6.20	17	1.54	81.4	0.308
Unwashed	2	38.4	4.42	17	1.92	101.5	0.384
	3	39.9	4.17	17	2.11	111.8	0.423
	4	43.8	4.15	17	2.33	123.3	0.466
	5	41.7	4.01	17	2.30	121.5	0.459
				Average	2.04	107.9	0.408
4	1	44.8	3.21	17	3.08	163.0	0.616
Washed	2	34.4	2.51	17	3.03	160.1	0.605
	3	40.9	2.75	17	3.28	173.7	0.657
	4	35.4	2.46	17	3.18	168.1	0.635
	5	39.8	2.66	17	3.30	174.8	0.661
				Average	3.17	167.9	0.635

Table C.4 - Permittivity Test Results, NP8 - NB.

Specimen No.	Run No.	Water Level Drop (cm)	Time For Drop (sec)	Temp. (C)	Permittivity (sec^{-1})	Flow Rate (cc/s)	Permeability (cm/sec)
1	1	33.5	4.73	16	1.60	82.7	0.417
Unwashed	2	36.3	4.82	16	1.70	88.0	0.443
	3	32.7	4.32	16	1.71	88.4	0.445
	4	39.8	4.94	16	1.82	94.1	0.474
	5	43.6	5.29	16	1.87	96.3	0.485
				Average	1.74	89.9	0.453
1	1	43.0	4.25	16	2.29	118.2	0.595
Washed	2	43.6	4.32	16	2.28	117.9	0.594
	3	42.5	4.13	16	2.33	120.2	0.606
	4	39.4	3.92	16	2.27	117.4	0.591
	5	43.6	4.32	16	2.28	117.9	0.594
				Average	2.29	118.3	0.596
2	1	39.9	9.32	16	0.97	50.0	0.252
Unwashed	2	38.2	6.98	16	1.24	63.9	0.322
	3	36.9	6.29	16	1.33	68.5	0.345
	4	37.7	6.13	16	1.39	71.8	0.362
	5	37.3	5.86	16	1.44	74.3	0.375
				Average	1.27	65.7	0.331
2	1	40.1	4.88	16	1.86	96.0	0.484
Washed	2	36.4	4.30	16	1.92	98.9	0.498
	3	39.8	4.60	16	1.96	101.1	0.509
	4	35.7	4.14	16	1.95	100.7	0.507
	5	37.5	4.54	16	1.87	96.5	0.486
				Average	1.91	98.6	0.497
3	1	35.0	6.38	16	1.24	64.1	0.323
Unwashed	2	38.0	5.67	16	1.52	78.3	0.394
	3	36.3	4.98	16	1.65	85.1	0.429
	4	39.4	5.02	16	1.78	91.7	0.462
	5	43.8	5.33	16	1.86	96.0	0.484
				Average	1.61	83.0	0.418
3	1	42.8	4.01	16	2.42	124.7	0.628
Washed	2	42.2	3.55	16	2.69	138.8	0.699
	3	43.7	4.04	16	2.45	126.3	0.636
	4	43.5	4.01	16	2.46	126.7	0.638
	5	48.8	4.48	16	2.47	127.2	0.641
				Average	2.49	128.8	0.649
4	1	45.6	5.06	16	2.04	105.3	0.530
Unwashed	2	44.0	4.60	16	2.16	111.7	0.563
	3	37.3	3.85	16	2.19	113.2	0.570
	4	44.0	4.36	16	2.28	117.9	0.594
	5	43.6	4.32	16	2.28	117.9	0.594
				Average	2.19	113.2	0.570
4	1	44.0	3.58	16	2.78	143.6	0.723
Washed	2	42.9	3.41	16	2.85	146.9	0.740
	3	43.0	3.54	16	2.75	141.9	0.715
	4	43.4	3.45	16	2.85	146.9	0.740
	5	42.5	3.30	16	2.91	150.4	0.758
				Average	2.83	145.9	0.735

Table C.5 - Permittivity Test Results, SF - NB.

Specimen No.	Run No.	Water Level Drop (cm)	Time For Drop (sec)	Temp. (C)	Permittivity (sec^{-1})	Flow Rate (cc/s)	Permeability (cm/sec)
1	1	35.8	48.13	16	0.17	8.7	0.008
Unwashed	2	33.0	38.14	16	0.20	10.1	0.010
	3	32.7	35.41	16	0.21	10.8	0.010
	4	34.9	34.18	16	0.23	11.9	0.012
	5	32.8	31.39	16	0.24	12.2	0.012
				Average	0.21	10.7	0.010
1	1	32.2	27.16	16	0.27	13.8	0.013
Washed	2	32.9	27.48	16	0.27	14.0	0.014
	3	35.9	29.57	16	0.27	14.2	0.014
	4	33.0	27.04	16	0.28	14.3	0.014
	5	32.3	26.14	16	0.28	14.4	0.014
				Average	0.27	14.1	0.014
2	1	31.5	59.48	16	0.12	6.2	0.006
Unwashed	2	31.4	51.30	16	0.14	7.1	0.007
	3	31.8	47.35	16	0.15	7.8	0.008
	4	31.5	47.20	16	0.15	7.8	0.008
	5	32.2	47.30	16	0.15	8.0	0.008
				Average	0.14	7.4	0.007
2	1	32.4	37.36	16	0.20	10.1	0.010
Washed	2	31.7	35.83	16	0.20	10.3	0.010
	3	31.6	36.58	16	0.20	10.1	0.010
	4	32.3	37.27	16	0.20	10.1	0.010
	5	32.4	36.84	16	0.20	10.3	0.010
				Average	0.20	10.2	0.010
3	1	31.7	62.20	16	0.12	6.0	0.006
Unwashed	2	32.6	51.63	16	0.14	7.4	0.007
	3	32.0	47.64	16	0.15	7.8	0.008
	4	32.0	46.75	16	0.15	8.0	0.008
	5	38.1	52.92	16	0.16	8.4	0.008
				Average	0.15	7.5	0.007
3	1	31.8	39.35	16	0.18	9.4	0.009
Washed	2	33.1	40.35	16	0.19	9.6	0.009
	3	31.7	38.04	16	0.19	9.7	0.009
	4	32.3	39.23	16	0.19	9.6	0.009
	5	35.7	43.38	16	0.19	9.6	0.009
				Average	0.19	9.6	0.009
4	1	31.9	50.48	16	0.14	7.4	0.007
Unwashed	2	31.9	46.48	16	0.16	8.0	0.008
	3	33.0	46.04	16	0.16	8.4	0.008
	4	32.1	41.41	16	0.18	9.1	0.009
	5	33.9	42.57	16	0.18	9.3	0.009
				Average	0.16	8.4	0.008
4	1	32.8	32.33	16	0.23	11.8	0.011
Washed	2	32.1	31.10	16	0.23	12.1	0.012
	3	32.5	32.00	16	0.23	11.9	0.011
	4	32.6	31.56	16	0.23	12.1	0.012
	5	36.2	34.75	16	0.24	12.2	0.012
				Average	0.23	12.0	0.012

Table C.6 - Permittivity Test Results, HB - SB.

Specimen No.	Run No.	Water Level Drop (cm)	Time For Drop (sec)	Temp. (C)	Permittivity (sec^{-1})	Flow Rate (cc/s)	Permeability (cm/sec)
1	1	19.2	121.01	15	0.04	1.9	0.001
Unwashed	2	31.0	98.01	15	0.07	3.7	0.003
	3	33.8	65.38	15	0.12	6.0	0.005
	4	32.3	41.42	15	0.18	9.1	0.007
	5	31.7	34.64	15	0.21	10.7	0.009
				Average	0.13	6.3	0.005
1	1	37.6	4.25	15	2.06	103.3	0.082
Washed	2	34.2	3.94	15	2.02	101.4	0.081
	3	34.6	3.96	15	2.03	102.1	0.081
	4	31.0	3.57	15	2.02	101.4	0.081
	5	34.3	3.75	15	2.13	106.8	0.085
				Average	2.05	103.0	0.082
2	1	31.2	18.51	15	0.39	19.7	0.016
Unwashed	2	33.5	14.45	15	0.54	27.1	0.022
	3	34.1	13.41	15	0.59	29.7	0.024
	4	32.8	12.24	15	0.62	31.3	0.025
	5	40.7	13.92	15	0.68	34.2	0.027
				Average	0.57	28.4	0.023
2	1	37.4	4.58	15	1.90	95.4	0.076
Washed	2	36.0	4.39	15	1.91	95.8	0.076
	3	32.6	3.98	15	1.91	95.7	0.076
	4	33.3	3.96	15	1.96	98.2	0.078
	5	38.6	4.71	15	1.91	95.7	0.076
				Average	1.92	96.2	0.077
3	1	32.3	11.35	15	0.66	33.2	0.027
Unwashed	2	31.9	7.33	15	1.01	50.8	0.041
	3	35.8	7.64	15	1.09	54.7	0.044
	4	36.5	7.48	15	1.14	57.0	0.045
	5	37.4	7.23	15	1.20	60.4	0.048
				Average	1.02	51.2	0.041
3	1	42.9	3.36	15	2.97	149.1	0.119
Washed	2	39.2	2.95	15	3.09	155.2	0.124
	3	38.7	2.94	15	3.07	153.7	0.123
	4	38.8	2.76	15	3.27	164.2	0.131
	5	39.0	2.70	15	3.36	168.7	0.135
				Average	3.15	158.2	0.126
4	1	30.2	53.35	15	0.13	6.6	0.005
Unwashed	2	33.6	27.02	15	0.29	14.5	0.012
	3	31.2	24.05	15	0.30	15.2	0.012
	4	33.2	16.71	15	0.46	23.2	0.019
	5	34.7	16.23	15	0.50	25.0	0.020
				Average	0.34	16.9	0.013
4	1	34.2	2.94	15	2.71	135.9	0.108
Washed	2	32.5	2.83	15	2.67	134.1	0.107
	3	35.7	3.14	15	2.65	132.8	0.106
	4	36.9	3.14	15	2.74	137.3	0.109
	5	36.6	3.17	15	2.69	134.9	0.108
				Average	2.69	135.0	0.108

Table C.7 - Permittivity Test Results, NP4 - SB.

Specimen No.	Run No.	Water Level Drop (cm)	Time For Drop (sec)	Temp. (C)	Permittivity (sec^{-1})	Flow Rate (cc/s)	Permeability (cm/sec)
1	1	33.0	3.88	18	1.83	99.3	0.275
Unwashed	2	37.3	4.26	18	1.88	102.3	0.283
	3	38.0	4.11	18	1.99	108.0	0.299
	4	37.2	3.76	18	2.13	115.6	0.319
	5	43.2	4.48	18	2.08	112.6	0.311
				Average	1.98	107.6	0.297
1	1	34.4	3.33	18	2.22	120.7	0.334
Washed	2	32.6	3.01	18	2.33	126.5	0.350
	3	33.1	3.27	18	2.18	118.2	0.327
	4	32.6	3.13	18	2.24	121.7	0.336
	5	36.0	3.51	18	2.21	119.8	0.331
				Average	2.24	121.4	0.335
2	1	35.0	3.51	18	2.15	116.5	0.322
Unwashed	2	33.4	3.09	18	2.33	126.2	0.349
	3	38.0	3.40	18	2.41	130.5	0.361
	4	39.5	3.51	18	2.42	131.4	0.363
	5	44.8	3.77	18	2.56	138.8	0.384
				Average	2.37	128.7	0.356
2	1	40.1	3.15	18	2.74	148.7	0.411
Washed	2	36.8	2.86	18	2.77	150.3	0.415
	3	38.8	2.77	18	3.02	163.6	0.452
	4	40.4	2.85	18	3.05	165.6	0.458
	5	38.4	2.94	18	2.81	152.6	0.422
				Average	2.88	156.1	0.432
3	1	36.9	4.07	18	1.95	105.9	0.293
Unwashed	2	36.8	3.59	18	2.21	119.7	0.331
	3	38.6	3.64	18	2.28	123.9	0.342
	4	33.6	3.04	18	2.38	129.1	0.357
	5	37.9	3.58	18	2.28	123.7	0.342
				Average	2.22	120.4	0.333
3	1	34.7	2.52	18	2.96	160.8	0.445
Washed	2	34.8	2.76	18	2.71	147.3	0.407
	3	35.3	2.85	18	2.67	144.7	0.400
	4	35.5	2.84	18	2.69	146.0	0.404
	5	40.5	3.04	18	2.87	155.6	0.430
				Average	2.78	150.9	0.417
4	1	36.4	4.47	18	1.75	95.1	0.263
Unwashed	2	36.4	4.21	18	1.86	101.0	0.279
	3	38.2	3.94	18	2.09	113.2	0.313
	4	35.4	3.63	18	2.10	113.9	0.315
	5	42.5	4.45	18	2.06	111.6	0.308
				Average	1.97	107.0	0.296
4	1	45.0	3.58	18	2.71	146.8	0.406
Washed	2	38.7	3.10	18	2.69	145.8	0.403
	3	37.0	2.64	18	3.02	163.7	0.453
	4	35.1	2.85	18	2.65	143.8	0.398
	5	42.9	3.26	18	2.83	153.7	0.425
				Average	2.78	150.8	0.417

Table C.8 - Permittivity Test Results, NP6 - SB.

Specimen No.	Run No.	Water Level Drop (cm)	Time For Drop (sec)	Temp. (C)	Permittivity (sec^{-1})	Flow Rate (cc/s)	Permeability (cm/sec)
1	1	37.9	4.70	16	1.83	94.2	0.365
Unwashed	2	35.6	3.92	16	2.06	106.1	0.411
	3	35.9	3.60	16	2.26	116.5	0.451
	4	35.7	3.48	16	2.32	119.8	0.464
	5	36.9	3.46	16	2.41	124.6	0.483
				Average	2.17	112.2	0.435
1	1	37.7	3.01	16	2.83	146.3	0.567
Washed	2	37.5	3.01	16	2.82	145.5	0.564
	3	35.7	2.89	16	2.80	144.3	0.559
	4	37.6	3.01	16	2.83	145.9	0.565
	5	38.0	3.02	16	2.85	147.0	0.570
				Average	2.82	145.8	0.565
2	1	34.6	3.92	16	2.00	103.1	0.400
Unwashed	2	37.2	3.64	16	2.31	119.4	0.463
	3	37.8	3.45	16	2.48	128.0	0.496
	4	40.8	3.45	16	2.68	138.1	0.535
	5	43.0	3.36	16	2.90	149.5	0.579
				Average	2.47	127.6	0.495
2	1	46.8	3.51	16	3.02	155.7	0.604
Washed	2	44.0	3.07	16	3.24	167.4	0.649
	3	39.0	2.78	16	3.17	163.9	0.635
	4	41.9	2.89	16	3.28	169.3	0.656
	5	41.5	2.76	16	3.40	175.6	0.681
				Average	3.22	166.4	0.645
3	1	34.0	4.10	16	1.88	96.9	0.375
Unwashed	2	35.0	3.82	16	2.07	107.0	0.415
	3	30.6	3.05	16	2.27	117.2	0.454
	4	39.1	3.78	16	2.34	120.8	0.468
	5	39.6	3.83	16	2.34	120.8	0.468
				Average	2.18	112.5	0.436
3	1	41.6	2.77	16	3.40	175.4	0.680
Washed	2	44.5	3.04	16	3.31	170.8	0.662
	3	38.0	2.79	16	3.08	159.1	0.616
	4	38.1	2.73	16	3.16	163.0	0.632
	5	39.4	2.88	16	3.10	159.8	0.619
				Average	3.21	165.6	0.642
4	1	34.0	5.86	16	1.31	67.8	0.263
Unwashed	2	38.6	5.29	16	1.65	85.2	0.330
	3	34.6	4.25	16	1.84	95.1	0.369
	4	34.3	4.08	16	1.90	98.2	0.381
	5	46.6	5.41	16	1.95	100.6	0.390
				Average	1.73	89.4	0.346
4	1	34.4	3.33	16	2.34	120.7	0.468
Washed	2	30.2	2.83	16	2.42	124.6	0.483
	3	35.9	3.37	16	2.41	124.4	0.482
	4	40.3	3.83	16	2.38	122.9	0.476
	5	41.2	3.89	16	2.40	123.7	0.479
				Average	2.39	123.3	0.478

Table C.9 - Permittivity Test Results, NP8 - SB.

Specimen No.	Run No.	Water Level Drop (cm)	Time For Drop (sec)	Temp. (C)	Permittivity (sec^{-1})	Flow Rate (cc/s)	Permeability (cm/sec)
1 Unwashed	1	35.0	6.91	16	1.15	59.2	0.298
	2	37.1	6.19	16	1.36	70.0	0.353
	3	36.6	4.85	16	1.71	88.1	0.444
	4	36.9	4.76	16	1.75	90.5	0.456
	5	41.0	5.10	16	1.82	93.9	0.473
				Average	1.56	80.3	0.405
1 Washed	1	31.0	2.88	16	2.44	125.7	0.633
	2	33.7	3.17	16	2.41	124.2	0.626
	3	40.5	3.79	16	2.42	124.8	0.629
	4	38.0	3.68	16	2.34	120.6	0.608
	5	38.6	3.69	16	2.37	122.1	0.615
				Average	2.39	123.5	0.622
2 Unwashed	1	38.0	7.66	16	1.12	57.9	0.292
	2	34.6	5.69	16	1.38	71.0	0.358
	3	36.6	5.16	16	1.61	82.8	0.417
	4	41.5	5.19	16	1.81	93.4	0.471
	5	40.4	4.91	16	1.86	96.1	0.484
				Average	1.56	80.3	0.404
2 Washed	1	37.8	3.69	16	2.32	119.6	0.603
	2	31.5	3.05	16	2.34	120.6	0.608
	3	35.8	3.40	16	2.38	123.0	0.620
	4	33.5	3.08	16	2.46	127.0	0.640
	5	41.9	4.02	16	2.36	121.6	0.613
				Average	2.37	122.4	0.617
3 Unwashed	1	34.8	11.17	16	0.71	36.4	0.183
	2	35.0	8.20	16	0.97	49.9	0.251
	3	36.4	7.17	16	1.15	59.3	0.299
	4	32.5	5.68	16	1.29	66.8	0.337
	5	40.5	6.80	16	1.35	69.6	0.350
				Average	1.09	56.4	0.284
3 Washed	1	40.2	3.50	16	2.60	134.2	0.676
	2	32.6	2.94	16	2.51	129.5	0.652
	3	31.8	2.97	16	2.42	125.1	0.630
	4	34.4	3.11	16	2.50	129.2	0.651
	5	40.2	3.60	16	2.53	130.4	0.657
				Average	2.51	129.7	0.653
4 Unwashed	1	35.2	7.80	16	1.02	52.7	0.266
	2	38.7	6.52	16	1.34	69.3	0.349
	3	36.8	5.84	16	1.43	73.6	0.371
	4	36.1	5.51	16	1.48	76.5	0.386
	5	42.6	6.33	16	1.52	78.6	0.396
				Average	1.36	70.2	0.353
4 Washed	1	39.6	4.03	16	2.22	114.8	0.578
	2	35.9	3.60	16	2.26	116.5	0.587
	3	34.3	3.31	16	2.35	121.0	0.610
	4	37.1	3.61	16	2.33	120.0	0.605
	5	39.4	3.89	16	2.29	118.3	0.596
				Average	2.29	118.1	0.595

Table C.10 - Permittivity Test Results, SF - SB.

Specimen No.	Run No.	Water Level Drop (cm)	Time For Drop (sec)	Temp. (C)	Permittivity (sec^{-1})	Flow Rate (cc/s)	Permeability (cm/sec)
1	1	30.8	91.92	15	0.08	3.9	0.004
Unwashed	2	31.6	83.26	15	0.09	4.4	0.004
	3	30.9	81.76	15	0.09	4.4	0.004
	4	32.1	83.92	15	0.09	4.5	0.004
	5	31.1	81.45	15	0.09	4.5	0.004
				Average	0.09	4.3	0.004
1	1	31.1	50.93	15	0.14	7.1	0.007
Washed	2	32.4	53.63	15	0.14	7.1	0.007
	3	32.0	51.98	15	0.14	7.2	0.007
	4	31.9	52.43	15	0.14	7.1	0.007
	5	32.3	52.39	15	0.14	7.2	0.007
				Average	0.14	7.1	0.007
2	1	32.4	81.86	15	0.09	4.6	0.005
Unwashed	2	32.5	69.74	15	0.11	5.4	0.005
	3	31.9	60.92	15	0.12	6.1	0.006
	4	32.2	58.01	15	0.13	6.5	0.006
	5	32.4	58.26	15	0.13	6.5	0.006
				Average	0.12	5.8	0.006
2	1	32.4	40.58	15	0.19	9.3	0.009
Washed	2	32.2	40.28	15	0.19	9.3	0.009
	3	32.4	40.07	15	0.19	9.4	0.009
	4	34.3	42.91	15	0.19	9.3	0.009
	5	35.1	43.64	15	0.19	9.4	0.009
				Average	0.19	9.4	0.009
3	1	31.1	77.92	16	0.09	4.7	0.005
Unwashed	2	30.4	64.23	16	0.11	5.5	0.005
	3	32.2	62.79	16	0.12	6.0	0.006
	4	31.1	59.14	16	0.12	6.1	0.006
	5	31.0	53.78	16	0.13	6.7	0.007
				Average	0.11	5.8	0.006
3	1	32.0	40.27	16	0.18	9.3	0.009
Washed	2	31.2	40.07	16	0.18	9.1	0.009
	3	31.5	38.86	16	0.18	9.5	0.009
	4	31.1	39.07	16	0.18	9.3	0.009
	5	32.2	39.94	16	0.18	9.4	0.009
				Average	0.18	9.3	0.009
4	1	31.8	65.05	16	0.11	5.7	0.006
Unwashed	2	32.0	55.60	16	0.13	6.7	0.007
	3	31.4	48.07	16	0.15	7.6	0.007
	4	32.0	46.70	16	0.16	8.0	0.008
	5	34.3	51.08	16	0.15	7.8	0.008
				Average	0.14	7.2	0.007
4	1	31.4	32.01	16	0.22	11.5	0.011
Washed	2	32.9	33.87	16	0.22	11.3	0.011
	3	33.5	34.58	16	0.22	11.3	0.011
	4	33.8	34.56	16	0.22	11.4	0.011
	5	34.0	34.52	16	0.22	11.5	0.011
				Average	0.22	11.4	0.011

Table C.11 - Permittivity Test Results, HB - Control.

Specimen No.	Run No.	Water Level Drop (cm)	Time For Drop (sec)	Temp. (C)	Permittivity (sec^{-1})	Flow Rate (cc/s)	Permeability (cm/sec)
1	1	29.1	4.67	18	1.34	72.8	0.054
Unwashed	2	31.8	5.16	18	1.33	72.0	0.053
	3	34.6	5.60	18	1.33	72.2	0.053
	4	31.6	5.04	18	1.35	73.2	0.054
	5	35.5	5.66	18	1.35	73.3	0.054
				Average	1.34	72.7	0.054
1	1	32.1	5.04	18	1.37	74.4	0.055
Washed	2	33.0	5.32	18	1.34	72.5	0.053
	3	35.5	5.86	18	1.30	70.8	0.052
	4	30.4	4.88	18	1.34	72.8	0.054
	5	37.4	6.07	18	1.33	72.0	0.053
				Average	1.34	72.5	0.053
2	1	36.1	4.79	18	1.62	88.0	0.065
Unwashed	2	38.6	4.95	18	1.68	91.1	0.067
	3	40.3	4.85	18	1.79	97.1	0.072
	4	42.1	5.24	18	1.73	93.8	0.069
	5	44.0	5.44	18	1.74	94.5	0.070
				Average	1.71	92.9	0.068
2	1	46.6	5.60	18	1.79	97.2	0.072
Washed	2	44.3	5.44	18	1.75	95.1	0.070
	3	34.9	4.12	18	1.82	98.9	0.073
	4	43.1	5.22	18	1.78	96.4	0.071
	5	48.0	5.61	18	1.84	99.9	0.074
				Average	1.80	97.5	0.072
3	1	38.8	6.83	18	1.22	66.4	0.049
Unwashed	2	36.4	6.38	18	1.23	66.6	0.049
	3	43.7	7.67	18	1.23	66.5	0.049
	4	37.0	6.46	18	1.23	66.9	0.049
	5	46.5	8.19	18	1.22	66.3	0.049
				Average	1.23	66.6	0.049
3	1	35.4	6.33	18	1.20	65.3	0.048
Washed	2	37.5	6.51	18	1.24	67.3	0.050
	3	40.5	6.86	18	1.27	69.0	0.051
	4	37.4	6.42	18	1.25	68.0	0.050
	5	41.7	6.82	18	1.32	71.4	0.053
				Average	1.26	68.2	0.050
4	1	37.2	5.10	18	1.57	85.2	0.063
Unwashed	2	39.1	5.12	18	1.64	89.2	0.066
	3	38.9	5.27	18	1.59	86.2	0.064
	4	40.7	5.49	18	1.60	86.6	0.064
	5	36.7	5.07	18	1.56	84.5	0.062
				Average	1.59	86.3	0.064
4	1	38.9	4.63	18	1.81	98.1	0.072
Washed	2	39.5	4.83	18	1.76	95.5	0.070
	3	37.0	4.39	18	1.81	98.4	0.073
	4	39.4	4.73	18	1.79	97.3	0.072
	5	51.2	6.09	18	1.81	98.2	0.072
				Average	1.80	97.5	0.072

Table C.12 - Permittivity Test Results, NP4 - Control.

Specimen No.	Run No.	Water Level Drop (cm)	Time For Drop (sec)	Temp. (C)	Permittivity (sec^{-1})	Flow Rate (cc/s)	Permeability (cm/sec)
1	1	49.2	3.14	17	3.46	183.0	0.519
Unwashed	2	50.8	3.23	17	3.47	183.7	0.521
	3	45.9	3.01	17	3.37	178.1	0.505
	4	48.3	3.23	17	3.30	174.7	0.495
	5	52.3	3.38	17	3.42	180.7	0.512
				Average	3.40	180.0	0.510
1	1	44.3	2.98	17	3.28	173.6	0.492
Washed	2	48.8	3.14	17	3.43	181.5	0.515
	3	57.3	3.26	17	3.88	205.3	0.582
	4	47.9	2.89	17	3.66	193.6	0.549
	5	46.4	2.73	17	3.75	198.5	0.563
				Average	3.60	190.5	0.540
2	1	36.1	2.63	17	3.03	160.3	0.455
Unwashed	2	38.1	2.70	17	3.12	164.8	0.467
	3	37.3	2.60	17	3.17	167.6	0.475
	4	37.8	2.58	17	3.23	171.1	0.485
	5	37.1	2.61	17	3.14	166.0	0.471
				Average	3.14	166.0	0.471
2	1	41.6	2.77	17	3.32	175.4	0.497
Washed	2	38.6	2.58	17	3.30	174.7	0.495
	3	41.0	2.58	17	3.51	185.6	0.526
	4	41.6	2.82	17	3.26	172.3	0.489
	5	39.1	2.64	17	3.27	173.0	0.490
				Average	3.33	176.2	0.500
3	1	40.9	2.60	17	3.47	183.7	0.521
Unwashed	2	41.3	2.52	17	3.62	191.4	0.543
	3	39.1	2.49	17	3.47	183.4	0.520
	4	38.5	2.49	17	3.41	180.6	0.512
	5	39.8	2.58	17	3.41	180.2	0.511
				Average	3.48	183.9	0.521
3	1	35.1	2.32	17	3.34	176.7	0.501
Washed	2	46.1	2.61	17	3.90	206.3	0.585
	3	40.8	2.42	17	3.72	196.9	0.558
	4	38.6	2.42	17	3.52	186.3	0.528
	5	41.7	2.48	17	3.71	196.4	0.557
				Average	3.64	192.5	0.546
4	1	35.6	2.38	17	3.30	174.7	0.495
Unwashed	2	36.6	2.38	17	3.40	179.6	0.509
	3	37.6	2.38	17	3.49	184.5	0.523
	4	35.6	2.43	17	3.23	171.1	0.485
	5	35.5	2.36	17	3.32	175.7	0.498
				Average	3.35	177.1	0.502
4	1	33.1	2.08	17	3.51	185.9	0.527
Washed	2	34.5	2.22	17	3.43	181.5	0.515
	3	36.0	2.32	17	3.43	181.2	0.514
	4	38.4	2.48	17	3.42	180.9	0.513
	5	35.1	2.24	17	3.46	183.0	0.519
				Average	3.45	182.5	0.517

Table C.13 - Permittivity Test Results, NP6 - Control.

Specimen No.	Run No.	Water Level Drop (cm)	Time For Drop (sec)	Temp. (C)	Permittivity (sec^{-1})	Flow Rate (cc/s)	Permeability (cm/sec)
1	1	49.1	4.55	18	2.32	126.0	0.465
Unwashed	2	53.2	4.73	18	2.42	131.4	0.484
	3	44.7	3.99	18	2.41	130.9	0.482
	4	45.5	3.88	18	2.52	137.0	0.505
	5	51.5	4.45	18	2.49	135.2	0.498
				Average	2.43	132.1	0.487
1	1	48.5	4.26	18	2.45	133.0	0.490
Washed	2	45.4	4.04	18	2.42	131.3	0.484
	3	42.4	3.79	18	2.41	130.7	0.482
	4	50.0	4.30	18	2.50	135.8	0.501
	5	48.5	4.26	18	2.45	133.0	0.490
				Average	2.45	132.7	0.489
2	1	44.8	3.98	17	2.49	131.5	0.497
Unwashed	2	47.2	4.14	17	2.52	133.2	0.503
	3	46.7	4.10	17	2.51	133.0	0.503
	4	46.7	4.14	17	2.49	131.8	0.498
	5	46.6	4.29	17	2.40	126.9	0.480
				Average	2.48	131.3	0.496
2	1	48.5	4.55	17	2.35	124.5	0.471
Washed	2	52.7	4.59	17	2.53	134.1	0.507
	3	43.4	3.80	17	2.52	133.4	0.504
	4	48.0	4.32	17	2.45	129.8	0.491
	5	42.6	3.80	17	2.48	130.9	0.495
				Average	2.47	130.5	0.494
3	1	47.7	4.17	17	2.53	133.6	0.505
Unwashed	2	50.0	4.32	17	2.56	135.2	0.511
	3	47.1	4.15	17	2.51	132.6	0.501
	4	42.6	3.73	17	2.52	133.4	0.504
	5	46.8	4.05	17	2.55	135.0	0.510
				Average	2.53	133.9	0.506
3	1	44.4	3.95	17	2.48	131.3	0.496
Washed	2	44.4	3.90	17	2.51	133.0	0.503
	3	46.3	3.86	17	2.65	140.1	0.530
	4	44.6	3.80	17	2.59	137.1	0.518
	5	45.5	3.82	17	2.63	139.1	0.526
				Average	2.57	136.1	0.515
4	1	50.3	3.67	17	3.03	160.1	0.605
Unwashed	2	47.0	3.41	17	3.04	161.0	0.609
	3	50.3	3.45	17	3.22	170.3	0.644
	4	52.3	3.51	17	3.29	174.0	0.658
	5	48.2	3.41	17	3.12	165.1	0.624
				Average	3.14	166.1	0.628
4	1	48.6	3.41	17	3.15	166.5	0.629
Washed	2	51.8	3.27	17	3.50	185.0	0.699
	3	44.8	3.07	17	3.22	170.4	0.644
	4	46.2	3.05	17	3.34	176.9	0.669
	5	44.2	2.94	17	3.32	175.6	0.664
				Average	3.31	174.9	0.661

Table C.14 - Permittivity Test Results, NP8 - Control.

Specimen No.	Run No.	Water Level Drop (cm)	Time For Drop (sec)	Temp. (C)	Permittivity (sec^{-1})	Flow Rate (cc/s)	Permeability (cm/sec)
1 Unwashed	1	41.2	4.57	18	1.94	105.3	0.505
	2	42.5	4.76	18	1.92	104.3	0.500
	3	40.7	4.49	18	1.95	105.9	0.507
	4	39.8	4.33	18	1.98	107.4	0.514
	5	40.8	4.42	18	1.99	107.8	0.517
				Average	1.96	106.1	0.509
1 Washed	1	40.3	4.64	18	1.87	101.4	0.486
	2	41.4	4.57	18	1.95	105.8	0.507
	3	44.1	4.64	18	2.05	111.0	0.532
	4	43.1	4.73	18	1.96	106.4	0.510
	5	45.3	4.89	18	1.99	108.2	0.518
				Average	1.96	106.6	0.511
2 Unwashed	1	36.0	4.39	18	1.77	95.8	0.459
	2	41.5	4.89	18	1.83	99.1	0.475
	3	40.6	5.07	18	1.72	93.5	0.448
	4	40.1	4.88	18	1.77	96.0	0.460
	5	40.3	4.89	18	1.77	96.3	0.461
				Average	1.77	96.1	0.461
2 Washed	1	39.3	5.14	18	1.65	89.3	0.428
	2	38.6	4.85	18	1.71	93.0	0.445
	3	39.8	5.13	18	1.67	90.6	0.434
	4	37.8	4.73	18	1.72	93.3	0.447
	5	39.9	5.00	18	1.72	93.2	0.447
				Average	1.69	91.9	0.440
3 Unwashed	1	43.8	4.44	18	2.12	115.2	0.552
	2	41.6	4.26	18	2.10	114.1	0.547
	3	43.5	4.44	18	2.11	114.4	0.548
	4	43.1	4.30	18	2.16	117.1	0.561
	5	42.7	4.23	18	2.17	117.9	0.565
				Average	2.13	115.7	0.555
3 Washed	1	39.7	4.07	18	2.10	113.9	0.546
	2	42.8	4.26	18	2.16	117.3	0.562
	3	45.2	4.48	18	2.17	117.8	0.565
	4	47.5	4.51	18	2.27	123.0	0.589
	5	44.4	4.26	18	2.24	121.7	0.583
				Average	2.19	118.8	0.569
4 Unwashed	1	41.5	4.86	18	1.84	99.7	0.478
	2	41.7	4.82	18	1.86	101.0	0.484
	3	40.3	4.70	18	1.85	100.1	0.480
	4	47.2	5.79	18	1.75	95.2	0.456
	5	44.1	5.39	18	1.76	95.6	0.458
				Average	1.81	98.3	0.471
4 Washed	1	40.9	4.94	18	1.78	96.7	0.463
	2	39.1	4.76	18	1.77	95.9	0.460
	3	40.9	4.94	18	1.78	96.7	0.463
	4	43.7	5.14	18	1.83	99.3	0.476
	5	48.3	5.73	18	1.81	98.5	0.472
				Average	1.80	97.4	0.467

Table C.15 - Permittivity Test Results, SF - Control.

Specimen No.	Run No.	Water Level Drop (cm)	Time For Drop (sec)	Temp. (C)	Permittivity (sec^{-1})	Flow Rate (cc/s)	Permeability (cm/sec)
1	1	33.8	64.73	18	0.11	6.1	0.006
Unwashed	2	33.6	66.49	18	0.11	5.9	0.005
	3	34.3	67.39	18	0.11	5.9	0.005
	4	32.6	63.90	18	0.11	6.0	0.005
	5	34.0	68.05	18	0.11	5.8	0.005
				Average	0.11	5.9	0.005
1	1	30.3	55.61	18	0.12	6.4	0.006
Washed	2	33.2	61.84	18	0.12	6.3	0.006
	3	35.0	67.04	18	0.11	6.1	0.006
	4	35.8	67.42	18	0.11	6.2	0.006
	5	33.2	63.81	18	0.11	6.1	0.006
				Average	0.11	6.2	0.006
2	1	33.9	40.77	18	0.18	9.7	0.009
Unwashed	2	33.5	40.23	18	0.18	9.7	0.009
	3	32.9	39.67	18	0.18	9.7	0.009
	4	33.9	41.30	18	0.18	9.6	0.009
	5	35.2	42.96	18	0.18	9.6	0.009
				Average	0.18	9.7	0.009
2	1	31.8	40.54	18	0.17	9.2	0.008
Washed	2	34.0	43.58	18	0.17	9.1	0.008
	3	30.2	38.25	18	0.17	9.2	0.008
	4	32.8	42.20	18	0.17	9.1	0.008
	5	34.2	44.21	18	0.17	9.0	0.008
				Average	0.17	9.1	0.008
3	1	30.4	74.89	18	0.09	4.7	0.004
Unwashed	2	31.7	76.77	18	0.09	4.8	0.004
	3	32.8	82.39	18	0.09	4.6	0.004
	4	31.1	76.26	18	0.09	4.8	0.004
	5	31.6	77.64	18	0.09	4.8	0.004
				Average	0.09	4.7	0.004
3	1	29.9	69.53	18	0.09	5.0	0.005
Washed	2	33.1	79.39	18	0.09	4.9	0.004
	3	34.4	81.76	18	0.09	4.9	0.005
	4	32.0	76.79	18	0.09	4.9	0.004
	5	39.8	95.41	18	0.09	4.9	0.004
				Average	0.09	4.9	0.005
4	1	32.4	93.96	18	0.07	4.0	0.004
Unwashed	2	33.1	95.01	18	0.07	4.1	0.004
	3	29.9	84.07	18	0.08	4.2	0.004
	4	32.7	91.68	18	0.08	4.2	0.004
	5	32.1	87.96	18	0.08	4.3	0.004
				Average	0.08	4.1	0.004
4	1	32.8	78.50	18	0.09	4.9	0.004
Washed	2	31.9	78.04	18	0.09	4.8	0.004
	3	32.0	78.55	18	0.09	4.8	0.004
	4	32.3	80.92	18	0.09	4.7	0.004
	5	33.6	87.11	18	0.08	4.5	0.004
				Average	0.09	4.7	0.004

APPENDIX D

WIDE WIDTH STRENGTH TEST PROCEDURES AND RESULTS

APPENDIX D

WIDE WIDTH STRENGTH TEST PROCEDURES AND RESULTS

The wide width test procedures are discussed in Section 7.1.5, and a summary of the results is presented in Section 7.2.5. The results of the wide width tests performed on the exhumed specimens are presented in Tables D.1 and D.2, the tests performed on the control specimens are presented in Tables D.3 and D.4. Tables D.1 and D.2 also note any holes observed greater than or equal to 2 mm in size.

The wide width strength tests were performed in accordance with ASTM D 4595 and were generally conducted as follows:

1. Six representative specimens were selected from each exhumed sample. Areas of the geotextile that were damaged by the exploration procedures were avoided.

2. Nonwoven specimens were cut to the ASTM specified test dimensions of 203 by 203 mm (8 by 8 in.). Woven specimens were cut approximately 10 to 20 mm larger in the cross-machine direction so that individual tapes could be pulled away to obtain the required specimens dimensions. A felt pen was used to mark the edges of the clamping locations which were 51 mm (2 in.) from the edges of the specimen. The clamped ends of the woven geotextile specimens were protected with duct tape, as discussed in Section 7.2.5.

3. The specimens were inundated at least 24 hrs prior to testing. The number and size of any holes lying between the testing grips were also recorded.

4. The specimens were placed into the clamping apparatus so that the length of the specimen between the testing grips was 102 mm (4 in.). The specimens were stressed in the machine direction which was taken to be parallel to the roadway center line. The specimens were strained at a constant rate of 10 percent per minute.

5. Values of load and deformation were recorded during the test using an automatic data acquisition system, which employed the Labtech Notebook computer software. A voltmeter was also used to manually determine the maximum value of load during the test. The reported elongation represents the displacement of the specimen between the clamps.

Table D.1 - Wide width test results, northbound lane.

Geotextile	Specimen Number	Wide Width Strength kN/m (lb/in)	Elongation (%)	Geotextile Damage (Greater than 2 mm in size)
HB - NB	1	6.0 (34)	26	
	2	7.0 (40)	28	
	3	6.1 (35)	29	
	4	6.3 (36)	31	
	5	5.3 (30)	29	
	6	3.9 (22)	16	5 mm diameter hole
	Average	5.7 (33)	27	
	Std. Dev.	1.1 (6.2)	5.4	
NP4 - NB	1	7.5 (43)	22	
	2	7.7 (44)	22	
	3	7.2 (41)	24	
	4	6.7 (38)	20	
	5	7.5 (43)	22	
	6	7.4 (42)	21	
	Average	7.3 (42)	22	
	Std. Dev.	0.4 (2.1)	1.3	
NP6 - NB	1	10.2 (58)	22	3 mm diameter hole
	2	9.6 (55)	25	
	3	10.5 (60)	24	
	4	7.7 (44)	20	
	5	9.6 (55)	27	
	6	10.7 (61)	28	
	Average	9.7 (56)	24	
	Std. Dev.	1.1 (6.2)	3.0	
NP8 - NB	1	13.5 (77)	27	
	2	13.1 (75)	29	19 mm tear
	3	13.1 (75)	27	
	4	13.0 (74)	27	
	5	12.8 (73)	29	29 mm tear
	6	12.4 (71)	28	
	Average	13.0 (74)	28	
	Std. Dev.	0.4 (2.0)	1.0	
SF - NB	1	28.7 (164)	12	
	2	29.1 (166)	12	
	3	28.9 (165)	12	
	4	29.1 (166)	12	
	5	28.7 (164)	12	
	6	29.4 (168)	12	
	Average	29.0 (166)	12	
	Std. Dev.	0.3 (1.5)	0.0	

Table D.2 - Wide width test results, southbound lane.

Geotextile	Specimen Number	Wide Width Strength kN/m (lb/in)	Elongation (%)	Geotextile Damage (Greater than 2 mm in size)
HB - SB	1	6.5 (37)	31	
	2	7.0 (40)	30	
	3	7.7 (44)	35	
	4	7.4 (42)	33	
	5	8.2 (47)	43	
	6	7.4 (42)	37	
	Average	7.4 (42)	35	
	Std. Dev.	0.6 (3.4)	4.8	
NP4 - SB	1	9.8 (56)	30	
	2	9.3 (53)	26	
	3	9.3 (53)	28	
	4	8.1 (46)	27	
	5	8.6 (49)	28	
	6	9.3 (53)	28	
	Average	9.0 (52)	28	
	Std. Dev.	0.6 (3.6)	1.3	
NP6 - SB	1	12.6 (72)	30	
	2	11.6 (66)	32	
	3	12.4 (71)	30	
	4	11. 0 (63)	28	
	5	11.6 (66)	29	4 mm tear
	6	12.1 (69)	60	
	Average	11.9 (68)	35	
	Std. Dev.	0.6 (3.4)	12.4	
NP8 - SB	1	14.7 (84)	29	
	2	15.9 (91)	38	
	3	12.8 (73)	30	
	4	13.8 (79)	28	
	5	14.7 (84)	31	
	6	14.4 (82)	30	
	Average	14.4 (82)	31	
	Std. Dev.	1.0 (6.0)	3.6	
SF - SB	1	30.1 (172)	13	
	2	29.1 (166)	12	
	3	31.5 (180)	13	
	4	33.6 (192)	15	
	5	33.3 (190)	15	
	6	32.4 (185)	13	
	Average	31.7 (181)	14	
	Std. Dev.	1.8 (10.2)	1.2	

Table D.3 - Wide width test results, control specimens.

Geotextile	Specimen Number	Wide Width Strength kN/m (lb/in)	Elongation (%)	Geotextile Damage (Greater than 2 mm in size)
HB - Control Diamond Face Jaws	1	6.7 (38)	59	
	2	5.8 (33)	55	
	3	6.3 (36)	57	
	4	5.6 (32)	55	
	5	6.1 (35)	55	
	6	6.5 (37)	50	
	Average	6.1 (35)	55	
	Std. Dev.	0.4 (2.3)	3.0	
HB - Control Roughened Face Jaws	1	5.8 (33)	62	
	2	5.4 (31)	62	
	3	5.1 (29)	65	
	4	6.0 (34)	87	
	Average	5.6 (32)	69	
	Std. Dev.	0.4 (2.2)	12.1	
NP4 - Control Diamond Face Jaws	1	7.7 (44)	82	
	2	7.4 (42)	79	
	3	8.6 (49)	80	
	4	7.4 (42)	71	
	5	7.2 (41)	80	
	6	7.2 (41)	82	
	Average	7.5 (43)	79	
	Std. Dev.	0.5 (3.1)	4.1	
NP4 - Control Roughened	1	8.6 (49)	99	
	2	7.9 (45)	91	
	Average	8.2 (47)	95	
	Std. Dev.	0.5 (2.8)	5.7	
NP6 - Control Diamond Face Jaws	1	11.0 (63)	89	
	2	10.5 (60)	76	
	3	11.4 (65)	87	
	4	11.6 (66)	90	
	5	9.6 (55)	78	
	6	11.2 (64)	85	
	Average	10.9 (62)	84	
	Std. Dev.	0.7 (4.1)	5.8	
NP6 - Control Roughened Face Jaws	1	12.6 (72)	126	
	2	11.4 (65)	103	
	3	12.4 (71)	110	
	Average	12.1 (69)	113	
	Std. Dev.	0.6 (3.8)	11.8	

Table D.4 - Wide width test results, control specimens.

Geotextile	Specimen Number	Wide Width Strength kN/m (lb/in)	Elongation (%)	Geotextile Damage (Greater than 2 mm in size)
NP8 - Control	1	15.6 (89)	92	
Diamond Face	2	15.2 (87)	89	
Jaws	3	15.9 (91)	90	
	4	15.2 (87)	94	
	5	15.1 (86)	100	
	6	16.1 (92)	111	
	Average	15.6 (89)	96	
	Std. Dev.	0.4 (2.4)	8.3	
SF - Control	1	35.2 (201)	18	
Diamond;	2	34.0 (194)	19	
No Protection	3	34.7 (198)	17	
	Average	34.7 (198)	18	
	Std. Dev.	0.6 (3.5)	1.0	
SF - Control	1	39.1 (223)	22	
Diamond;	2	36.2 (207)	20	
Duct Tape	3	38.4 (219)	23	
Protection	4	37.1 (212)	19	
	5	38.5 (220)	21	
	6	36.2 (207)	18	
	Average	37.6 (215)	21	
	Std. Dev.	1.3 (6.9)	1.9	
SF - Control	1	38.9 (222)	24	
Diamond;	2	38.7 (221)	22	
Epoxy Prot.	3	39.8 (227)	25	
	Average	39.1 (223)	24	
	Std. Dev.	0.6 (3.2)	1.5	